

LANDSAT-4 Science Investigations Summary

Including December 1983 Workshop Results

Volume I

*Proceedings of the Landsat-4 Early
Results Symposium, February 22-24, 1983,
and the Landsat Science Characterization
Workshop, December 6, 1983, and held at
NASA Goddard Space Flight Center
Greenbelt, Maryland*

FOR SERVICE

100 10 11

NASA

NASA Conference Publication 2326

LANDSAT-4 Science Investigations Summary

Including December 1983 Workshop Results

Volume I

John Barker, *Editor*
NASA Goddard Space Flight Center

Proceedings of the Landsat-4 Early
Results Symposium, February 22-24, 1983,
and the Landsat Science Characterization
Workshop, December 6, 1983, and held at
NASA Goddard Space Flight Center
Greenbelt, Maryland

NASA
National Aeronautics
and Space Administration

**Scientific and Technical
Information Branch**

1984

Page intentionally left blank

FOREWORD

The Landsat Science Office at Goddard Space Flight Center (GSFC) is charged with the responsibility of characterizing the quality of Landsat-4 image data and, through data analysis, the performance of the Landsat system. It has enlisted the participation of recognized and experienced members of the Landsat community (private, academic and government, U.S. and International) in investigating various aspects of this multifaceted topic. The Landsat Science Investigations Program provides the framework within which the individual investigations are taking place. One feature of the Program is to provide in-progress exchange of observations and findings among individual investigators, especially through an ongoing series of Investigations Workshops. Release of information resulting from the investigations is via public symposia. The Landsat-4 Early Results Symposium (so named since most investigators had had access to Landsat data for only a brief period) was held on February 22-24, 1983. A second public symposium is planned for late 1984.

The present document is the first to be published containing collected results of the Investigations Program. It was originally intended as an Executive Summary companion volume to the Proceedings of the Landsat-4 Early Results Symposium, presenting abstracts of papers included in the proceedings. However, since publication has been delayed, it was decided that this summary volume should encompass results reached during post-symposium investigations wherever possible. Thus, results summarized herein range in date reported from February 22, 1983 (in a few cases) to December 6, 1983 (in most cases) on which date was held the most recent Investigations Workshop.

This document is arranged to follow the organization of the Early Results Symposium. It includes introductory papers (Landsat program and system descriptions) in their entirety followed by summaries of results of each individual investigation in the order in which they were reported at the symposium (even though most contain more recent data). The symposium proceedings,

to be published in the near future, will contain investigations papers in this same order.

The papers delivered at the symposium were divided into three major sessions: one on Multispectral Scanner (MSS) Investigations, one on Thematic Mapper (TM) Investigations and one on Applications Investigations. The MSS and TM sessions progressed topically from radiometry to geometry; the Applications session progressed through the various disciplines of application. Although the focus of some investigations shifted from one topic to another during the period since the symposium, the summaries of results of such investigations are, nonetheless, retained in the original presentation order in these summary volumes.

LANDSAT-4 INVESTIGATION SUMMARY
VOLUME I

	PAGE
FOREWORD	iii
THE LANDSAT-4 PROGRAM: AN OVERVIEW William Webb NASA/Goddard Space Flight Center	1
LANDSAT-4 SYSTEM DESCRIPTION Theodore C. Aeppli General Electric Company	15
MSS INSTRUMENT DESCRIPTION EXERPTED FROM LANDSAT-D INVESTIGATIONS WORKSHOPS, MAY 13-14, 1982	31
THEMATIC MAPPER (TM) INSTRUMENT DESCRIPTION Jack Engel Santa Barbara Research Center	41
AN OVERVIEW OF LANDSAT-4 AND THE THEMATIC MAPPER James R. Irons NASA/Goddard Space Flight Center	62
THEMATIC MAPPER SENSOR CHARACTERISTICS Jack Engel Santa Barbara Research Center	65
RADIOMETRIC CALIBRATION AND PROCESSING PROCEDURE FOR REFLECTIVE BANDS ON LANDSAT-4 PROTOFLIGHT THEMATIC MAPPER John L. Barker NASA/Goddard Space Flight Center R. B. Abrams, D. L. Ball and K. C. Leung Computer Sciences Corporation	90
AN OVERVIEW OF THE THEMATIC MAPPER GEOMETRIC CORRECTION SYSTEM Eric P. Beyer General Electric Company	92
THEMATIC MAPPER IMAGE PROCESSING SYSTEM (TIPS) PROCESSING STATUS Joan Brooks General Electric Space Division	101

THEMATIC MAPPER IMAGE PRODUCTION IN THE ENGINEERING
CHECK-OUT PHASE

David Fische1
NASA/Goddard Space Flight Center

John C. Lyon
Systems and Applied Sciences Corporation 106

LANDSAT-4 RADIOMETRIC AND GEOMETRIC CORRECTION
AND IMAGE ENHANCEMENT RESULTS

Ralph Bernstein and Jeffrey B. Lotspiech
IBM Corporation
Palo Alto Scientific Center 108

TM DIGITAL IMAGE PRODUCTS FOR APPLICATIONS

John L. Barker
NASA/Goddard Space Flight Center

Fred J. Gunther, Rochelle B. Abrams and Dave Ball
Computer Sciences Corporation 116

CCRS EVALUATION OF LANDSAT-4 DATA INVESTIGATION UPDATE

W. Murray Strome
Canada Centre For Remote Sensing 120

SPECTRAL CHARACTERIZATION OF THE LANDSAT THEMATIC MAPPER SENSORS

Brian L. Markham and John L. Barker
NASA/Goddard Space Flight Center 127

PRE-LAUNCH ABSOLUTE RADIOMETRIC CALIBRATION
OF LANDSAT-4 PROTOFLIGHT THEMATIC MAPPER

John L. Barker
NASA/Goddard Space Flight Center

D. L. Ball and K. C. Leung
Computer Sciences Corporation

J. A. Walker
Santa Barbara Research Center 130

RELATIVE RADIOMETRIC CALIBRATION OF LANDSAT
TM REFLECTIVE BANDS

John L. Barker
NASA/Goddard Space Flight Center 140

EVALUATION OF THE RADIOMETRIC INTEGRITY OF LANDSAT-4
THEMATIC MAPPER BAND 6 DATA

John R. Schott
Rochester Institute of Technology 181

THERMAL BAND CHARACTERIZATION OF LANDSAT-4 THEMATIC MAPPER

Jack C. Lansing
Santa Barbara Research Center

John L. Barker
NASA/Goddard Space Flight Center 186

A PRELIMINARY ASSESSMENT OF LANDSAT-4 THEMATIC MAPPER DATA D. G. Goodenough, E. A. Fleming and K. Dickinson Department of Energy, Mines and Resources, Canada	189
REVISED RADIOMETRIC CALIBRATION TECHNIQUE FOR LANDSAT-4 THEMATIC MAPPER DATA BY THE CANADA CENTRE FOR REMOTE SENSING J. Murphy, T. Butlin, P. Duff and A. Fitzgerald Canada Centre For Remote Sensing	190
A PRELIMINARY ANALYSIS OF LANDSAT-4 THEMATIC MAPPER RADIOMETRIC PERFORMANCE C. Justice and L. Fusco European Space Agency/Earthnet Programme Office W. Mehl Commission of The European Communities/Joint Research Centre . . .	199

LANDSAT-4 INVESTIGATION SUMMARY
VOLUME II

LANDSAT-4 MSS AND TM SPECTRAL CLASS COMPARISON AND COHERENT NOISE ANALYSIS P. Anuta, L. Bartolucci, E. Dean, F. Lozano E. Malaret, C. McGillem, J. Valdes, and C. Valenzuela Purdue University	1
TM FAILED DETECTORS DATA REPLACEMENT L. Fusco and D. Trevese European Space Agency/EPO	7
IN-FLIGHT ABSOLUTE RADIOMETRIC CALIBRATION OF THE THEMATIC MAPPER K. R. Castle, R. G. Holm, C. J. Kastner, J. M. Palmer and P. N. Slater University of Arizona M. Dinguirard Centre D'Etudes Et De Recherches De Toulouse C. E. Ezra and R. D. Jackson U. S. Department of Agriculture R. K. Savage Atmospheric Sciences Laboratory	15
LANDSAT-4 THEMATIC MAPPER CALIBRATION AND ATMOSPHERIC CORRECTION Warren A. Hovis NOAA/National Environmental Satellite, Data, and Information Service	20

CALIBRATION OF TM DATA FROM GROUND-BASED MEASUREMENTS	
S. I. Rasool	
Laboratoire de Meteorologie Dynamique, Paris	
P. Y. Deschamps	21
Department Etudes Thematiques, CNES, Toulouse	
SCAN-ANGLE AND DETECTOR EFFECTS IN THEMATIC	
MAPPER RADIOMETRY	
Michael D. Metzler and William A. Malila	
Environmental Research Institute of Michigan	23
THEMATIC MAPPER SPECTRAL DIMENSIONALITY AND DATA STRUCTURE	
E. P. Crist and R. C. Cicone	
Environmental Research Institute of Michigan	28
MTF ANALYSIS OF LANDSAT-4 THEMATIC MAPPER	
Robert Schowengerdt	
University of Arizona	32
INTRABAND RADIOMETRIC PERFORMANCE OF THE LANDSAT-4	
THEMATIC MAPPER	
Hugh H. Kieffer, Eric M. Eliason and Pat S. Chavez, Jr.	
U. S. Geological Survey, Flagstaff	33
ANALYSIS OF LANDSAT-4 TM DATA FOR LITHOLOGIC AND	
IMAGE MAPPING PURPOSES	
M. H. Podwysocki, J. W. Salisbury, L. V. Bender, O. D. Jones and	
D. L. Mimms	
U. S. Geological Survey, Reston	35
STATUS OF THE ESA-EARTHNET LANDSAT-4 TM GROUND PROCESSING CHAIN	
L. Fusco	
European Space Agency/EPO	40
AN ANALYSIS OF LANDSAT-4 THEMATIC MAPPER	
GEOMETRIC PROPERTIES*	
R. E. Walker, A. L. Zobrist, N. A. Bryant,	
B. Gokhman, S. Z. Friedman, and T. L. Logan	
	46
THE USE OF LINEAR FEATURE DETECTION TO INVESTIGATE	
THEMATIC MAPPER DATA PERFORMANCE AND PROCESSING	
Charlotte M. Gurney	
Systems and Applied Sciences Corporation	50
SPATIAL RESOLUTION ESTIMATION OF LANDSAT-4 TM DATA	
Clare D. McGillem, Paul E. Anuta and Erick Malaret	
Purdue University	
Kai-Bor YU	
Virginia Polytechnic Institute	53
AN ANALYSIS OF THE HIGH FREQUENCY VIBRATIONS	
IN EARLY THEMATIC MAPPER SCENES	
John Kogut and Elaine Larduinat	
Research and Data Systems, Inc.	54

ASSESSMENT OF THEMATIC MAPPER BAND-TO-BAND REGISTRATION BY THE BLOCK CORRELATION METHOD Don H. Card and Robert C. Wrigley NASA/Ames Research Center	
Frederick C. Mertz and Jeff R. Hall Technicolor Government Services, Inc. Ames Research Center	55
TESTS OF LOW-FREQUENCY GEOMETRIC DISTORTIONS IN LANDSAT-4 IMAGES R. M. Batson and W. T. Borgeson U. S. Geological Survey, Flagstaff	59
INVESTIGATION OF TM BAND-TO-BAND REGISTRATION USING THE JSC REGISTRATION PROCESSOR S. S. Yao and M. L. Amis Lockheed Engineering and Management Services Company, Inc.	60
GEODETIC ACCURACY OF LANDSAT-4 MULTISPECTRAL SCANNER AND THEMATIC MAPPER DATA J. M. Thormodsgard and D. J. Devries U. S. Geological Survey, EROS Data Center	62
THE EFFECT OF POINT-SPREAD FUNCTION INTERACTION WITH RADIANCE FROM HETEROGENEOUS SCENES ON MULTITEMPORAL SIGNATURE ANALYSIS M. J. Duggin and L. B. Schoch State University of New York/Syracuse	64
RADIOMETRIC ACCURACY ASSESSMENT OF LANDSAT-4 MULTISPECTRAL SCANNER (MSS) DATA William L. Alford and Marc L. Imhoff NASA/Goddard Space Flight Center	69
SPECTRAL CHARACTERIZATION OF THE LANDSAT-4 MSS SENSORS Brian L. Markham and John L. Barker NASA/Goddard Space Flight Center	73
INVESTIGATION OF RADIOMETRIC PROPERTIES OF LANDSAT-4 MSS Daniel R. Rice and William A. Malila Environmental Research Institute of Michigan	76
RADIOMETRIC CALIBRATION AND GEOCODED PRECISION PROCESSING OF LANDSAT-4 MULTISPECTRAL SCANNER PRODUCTS BY THE CANADA CENTRE FOR REMOTE SENSING J. Murphy, D. Bennett and F. Guertin Canada Centre For Remote Sensing	81
LANDSAT SCENE-TO-SCENE REGISTRATION ACCURACY ASSESSMENT James E. Anderson NASA/National Space Technology Laboratories	82

GEOMETRIC ACCURACY OF LANDSAT-4 MSS IMAGE DATA R. Welch and E. Lynn Usery University of Georgia, Athens.	83
GEOMETRIC ACCURACY ASSESSMENT OF LANDSAT-4 MULTISPECTRAL SCANNER (MSS) Marc L. Imhoff and William L. Alford NASA/Goddard Space Flight Center	85
IMPACT OF LANDSAT MSS SENSOR DIFFERENCES ON CHANGE DETECTION ANALYSIS William C. Likens and Robert C. Wrigley NASA/Ames Research Center	87
LANDSAT-4 MSS GEOMETRIC CORRECTION: METHODS AND RESULTS J. Brooks, E. Kimmer and J. Su General Electric Space Division	91
IMPACT OF THEMATIC MAPPER SENSOR CHARACTERISTICS ON CLASSIFICATION ACCURACY Darrel L. Williams, James R. Irons, Brian L. Markham, Ross F. Nelson and David L. Toll NASA/Goddard Space Flight Center Richard S. Latty University of Maryland Mark L. Stauffer Computer Sciences Corporation	93
CHARACTERIZATION OF LANDSAT-4 TM AND MSS IMAGE QUALITY FOR INTERPRETATION OF AGRICULTURAL AND FOREST RESOURCES S. D. DeGloria and R. N. Colwell University of California/Berkeley	98
EVALUATION OF LANDSAT-4 THEMATIC MAPPER DATA AS APPLIED TO GEOLOGIC EXPLORATION: SUMMARY OF RESULTS Jon D. Dykstra, Charles A. Sheffield, and John R. Everett Earth Satellite Corporation	103
PRELIMINARY GEOLOGIC/SPECTRAL ANALYSIS OF LANDSAT-4 THEMATIC MAPPER DATA, WIND RIVER/BIGHORN BASIN AREA, WYOMING Harold R. Lang, James E. Cone and Earnest D. Paylor Jet Propulsion Laboratory	109
AN INITIAL ANALYSIS OF LANDSAT-4 THEMATIC MAPPER DATA FOR THE DISCRIMINATION OF AGRICULTURAL, FORESTED WETLAND, AND URBAN LAND COVERS Dale A. Quattrochi NASA/National Space Technology Laboratories	111

PRELIMINARY EVALUATION OF THEMATIC MAPPER
IMAGE DATA QUALITY
R. B. MacDonald, F. G. Hall, D. E. Pitts and R. M. Bizzell
NASA/Lyndon B. Johnson Space Center

S. Yao, C. Sorensen, E. Reyna and J. Carnes
Lockheed Engineering and Management Services Company, Inc. 113

ASSESSMENT OF COMPUTER-BASED GEOLOGIC MAPPING OF ROCK UNITS IN THE
LANDSAT-4 SCENE OF NORTHERN DEATH VALLEY, CALIFORNIA
Nicholas M. Short
NASA/Goddard Space Flight Center 114

A CONCEPT FOR THE PROCESSING AND DISPLAY OF
THEMATIC MAPPER DATA
Rupert Haydn
University of Munich 116

QUICK LOOK ANALYSIS OF TM DATA OF THE WASHINGTON, D.C. AREA
Darrel L. Williams, James R. Irons, Brian L. Markham,
Ross F. Nelson and David L. Toll
NASA/Goddard Space Flight Center

Richard S. Latty
University of Maryland

Mark L. Stauffer
Computer Sciences Corporation 119

ABOVEGROUND BIOMASS ESTIMATION IN A TIDAL BRACKISH MARSH
USING SIMULATED THEMATIC MAPPER SPECTRAL DATA
Michael Hardisky and V. Klemas
University of Delaware 121

COMPARISON OF THE INFORMATION CONTENT OF DATA FROM THE LANDSAT-4
THEMATIC MAPPER AND THE MULTISPECTRAL SCANNER
John C. Price
USDA Hydrology Laboratory 128

STUDY OF THEMATIC MAPPER AND MULTISPECTRAL SCANNER
DATA APPLICATIONS
F. G. Sadowski, R. H. Haas, J. A. Sturdevant, W. H. Anderson,
P. M. Seevers, J. W. Feuquay, L. K. Balick and F. A. Waltz
Technicolor Government Services, Inc./EROS Data Center

D. T. Lauer
U.S. Geological Survey/EROS Data Center 129

THEMATIC MAPPER DATA QUALITY AND PERFORMANCE ASSESSMENT
IN RENEWABLE RESOURCES/AGRICULTURE REMOTE SENSING
Robert M. Bizzell and Harold L. Prior
NASA/Lyndon B. Johnson Space Center 133

PRELIMINARY COMPARISONS OF THE INFORMATION CONTENT AND UTILITY OF TM VERSUS MSS DATA Brian L. Markham NASA/Goddard Space Flight Center	135
PARAMETRIC AND NONPARAMETRIC ANALYSIS OF LANDSAT TM AND MSS IMAGERY FOR DETECTING SUBMERGED PLANT COMMUNITIES Steven G. Ackleson and Vytautas Klemas University of Delaware	137
A FIRST EVALUATION OF LANDSAT TM DATA TO MONITOR SUSPENDED SEDIMENTS IN LAKES F. R. Schiebe, J. C. Ritchie and G. O. Boatwright U.S. Department of Agriculture	141
SNOW REFLECTANCE FROM LANDSAT-4 THEMATIC MAPPER Jeff Dozier University of California/Santa Barbara	142
PRELIMINARY EVALUATION OF TM FOR SOILS INFORMATION David R. Thompson, Keith E. Henderson, A. Glen Houston and David E. Pitts NASA/Lyndon B. Johnson Space Center	148
THE USE OF THEMATIC MAPPER DATA FOR LAND COVER DISCRIMINATION -- PRELIMINARY RESULTS FROM THE UK SATMaP PROGRAMME M. J. Jackson and J. R. Baker Natural Environment Research Council, UK J. R. G. Townshend, J. E. Gayler and J. R. Hardy Reading University, UK	149
LANDSAT-4 THEMATIC MAPPER SCENE CHARACTERISTICS FOR A SUBURBAN AND REGIONAL TEST SITE D. L. Toll	153
NASA/Goddard Space Flight Center	
FINAL COMPARISON OF TM AND MSS DATA FOR SURFACE MINE ASSESSMENT IN LOGAN COUNTY, WEST VIRGINIA R. G. Witt and H. W. Blodget NASA/Goddard Space Flight Center R. M. Marcell Scientific Applications Research	160
COMPARISON OF LAND COVER INFORMATION FROM LANDSAT MULTISPECTRAL SCANNER (MSS) AND AIRBORNE THEMATIC MAPPER SIMULATION (TMS) DATA FOR HYDROLOGIC APPLICATIONS J. C. Gervin NASA/Goddard Space Flight Center Y. C. Lu and R. F. Marcell Computer Sciences Corporation	167

RELATIVE ACCURACY ASSESSMENT OF LANDSAT-4 MSS AND TM DATA
FOR LEVEL I LAND COVER INVENTORY

E. M. Middleton, R. G. Witt
NASA/Goddard Space Flight Center

Y.C. Lu and R. S. Sekhon Computer Sciences Corporation	171
LIST OF AFFILIATIONS	173

THE LANDSAT-4 PROGRAM: AN OVERVIEW

WILLIAM WEBB

NASA/GODDARD SPACE FLIGHT CENTER

INTRODUCTION

Landsat-4 was launched aboard a Delta 3920 launch vehicle from the Western Test Range (Vandenberg Air Force Base, California) on July 22, 1982. This is the latest in a series of NASA Earth-observation satellites and the first to carry the newly-developed high resolution, high data rate Thematic Mapper (TM). The purpose of this paper is to present an overview of the Landsat-4 Program in terms of the program plan, accomplishments and future events, the transition of operational responsibility to National Oceanic and Atmospheric Administration (NOAA) management and the challenges remaining to both NASA personnel and Landsat-4 Investigations Program participants.

PROGRAM PLAN

The Landsat series of satellites began in July of 1972 with the launch of the Earth Resources Technology Satellite (ERTS)-1. The first of the series (later termed Landsat-1) bore two imaging systems, the Multispectral Scanner (MSS) and the Return Beam Vidicon (RBV) camera. With the MSS and the RBV, Landsat-1 also carried a Data Collection System (DCS) for the monitoring and recording of data from a number of Earth-stationed collection platforms. Figure 1 depicts the series of Landsat satellites and places Landsat-4 (with its MSS and the new TM) in the continuum of NASA Earth observing and resource monitoring satellites.

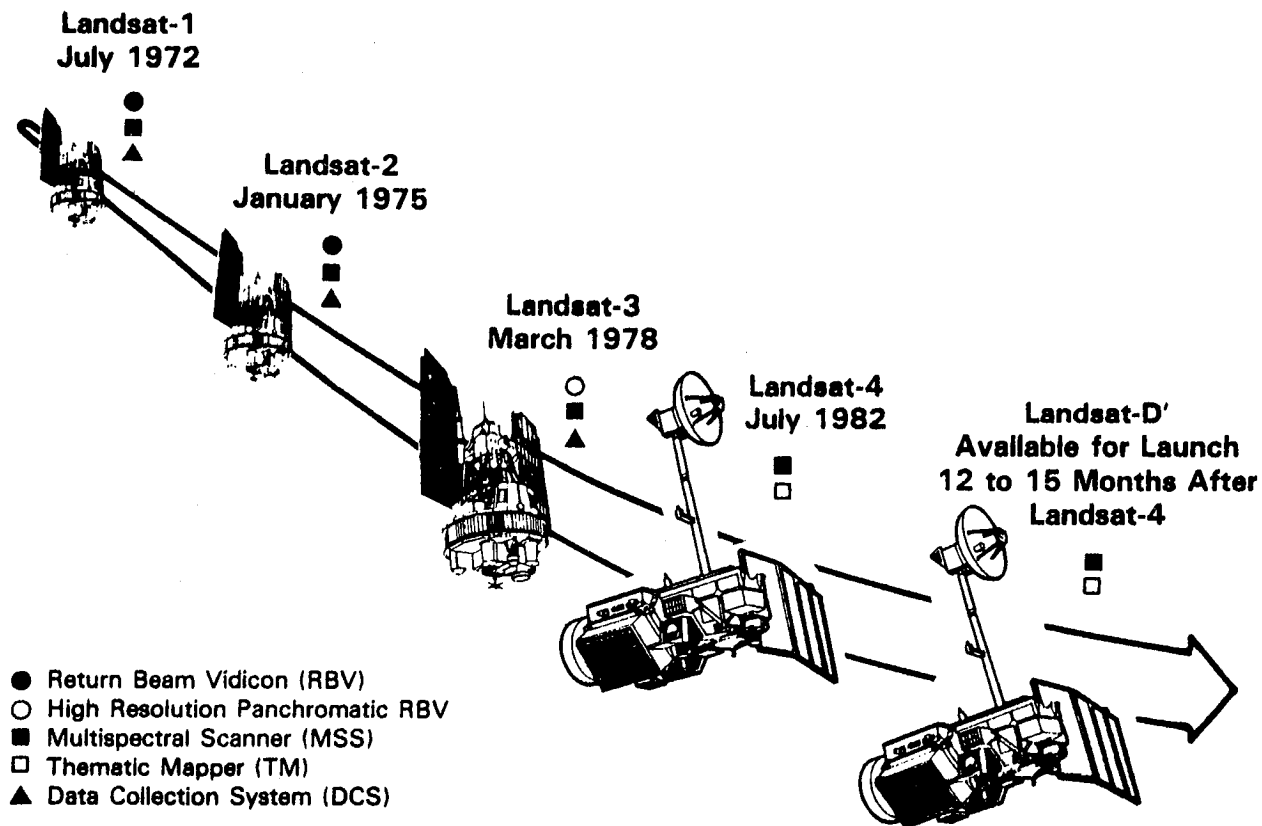


FIGURE 1. HISTORICAL PERSPECTIVE: THE LANDSAT SERIES

Based on experience gained from Landsats 1, 2 and 3 and the expressed desire of Landsat imagery users for higher resolution data across a broader range of the electromagnetic spectrum, the Landsat-4 Project Office formulated the major mission objectives presented in Table 1 and the system requirements outlined in Table 2.

TABLE 1. MAJOR OBJECTIVES OF THE LANDSAT-4 MISSION

- To Provide for System-Level Feasibility Demonstrations in Concert with NOAA and User Agencies to Define the Characteristics of an Operational System
- To Assess the Capability of the Thematic Mapper (TM) and Associated Systems to Provide Improved Information for Earth Resources Management
- To Provide for Continued Availability of Multispectral Scanner (MSS) Data
- To Provide a Transition for Both Domestic and Foreign Users from MSS Data to the Higher Resolution and Data Rate of the TM
- To Permit Continued Foreign Participation in the Program

TABLE 2. SYSTEM REQUIREMENTS

- | | |
|---|--|
| <ul style="list-style-type: none"> ● Orbit <ul style="list-style-type: none"> - Altitude: 705.3 km - Descending Node: 9:30-10:00 a.m. ● Launch Vehicle <ul style="list-style-type: none"> - Delta 3920 (Shuttle Retrievable) ● Instruments <ul style="list-style-type: none"> - Multispectral Scanner <ul style="list-style-type: none"> -- 4 Band -- 83 Meter IFOV - Thematic Mapper <ul style="list-style-type: none"> -- 7 Band -- 30 Meter IFOV ● Flight Segment <ul style="list-style-type: none"> - Uses Multi-Mission Modular Spacecraft ● Ground Segment <ul style="list-style-type: none"> - Controls Spacecraft - Receives & Records Data - Processes & Distributes Data ● Mission Life <ul style="list-style-type: none"> - 3 Years (Goal) | <ul style="list-style-type: none"> ● Coverage <ul style="list-style-type: none"> - Ground Station Tracking and Data Network (GSTDN) Initially - Tracking and Data Relay Satellite System (TDRSS) When Available ● Scenes/Day - Flight Segment Capacity <ul style="list-style-type: none"> - NASA (200 MSS; 100 TM) - Foreign (337 MSS; 150 TM) ● Data Quantity - Ground Segment Capacity <ul style="list-style-type: none"> - MSS <ul style="list-style-type: none"> -- 200 Scenes/Day - TM <ul style="list-style-type: none"> -- 1 Scene/Day - Begins July 1, 1982 -- 12 Scenes/Day - Begins July 31, 1983 -- 50 Scenes/Day - Begins January 31, 1985 ● Products Through Ground System Within 48 Hours <ul style="list-style-type: none"> - High Density Tapes - Computer Compatible - TM Film |
|---|--|

The system design, both in flight and ground segments, was developed in direct response to the requirements shown above.

Figure 2 depicts the overall configuration of the flight and communications portions of the Landsat-4 system. Initially, the spacecraft will be controlled and image data received via NASA's Ground Station Tracking Data Network (GSTDN) augmented by a Transportable Ground Station (TGS) located at the Goddard Space Flight Center (GSFC). In addition, a series of foreign ground stations will receive image and associated telemetry data, each according to its defined acquisition requirements. When available, NASA's Tracking and Data Relay Satellite System (TDRSS) will be employed as the primary command/control/image data acquisition link, with data being routed through the TDRSS Ground Station at White Sands, New Mexico.

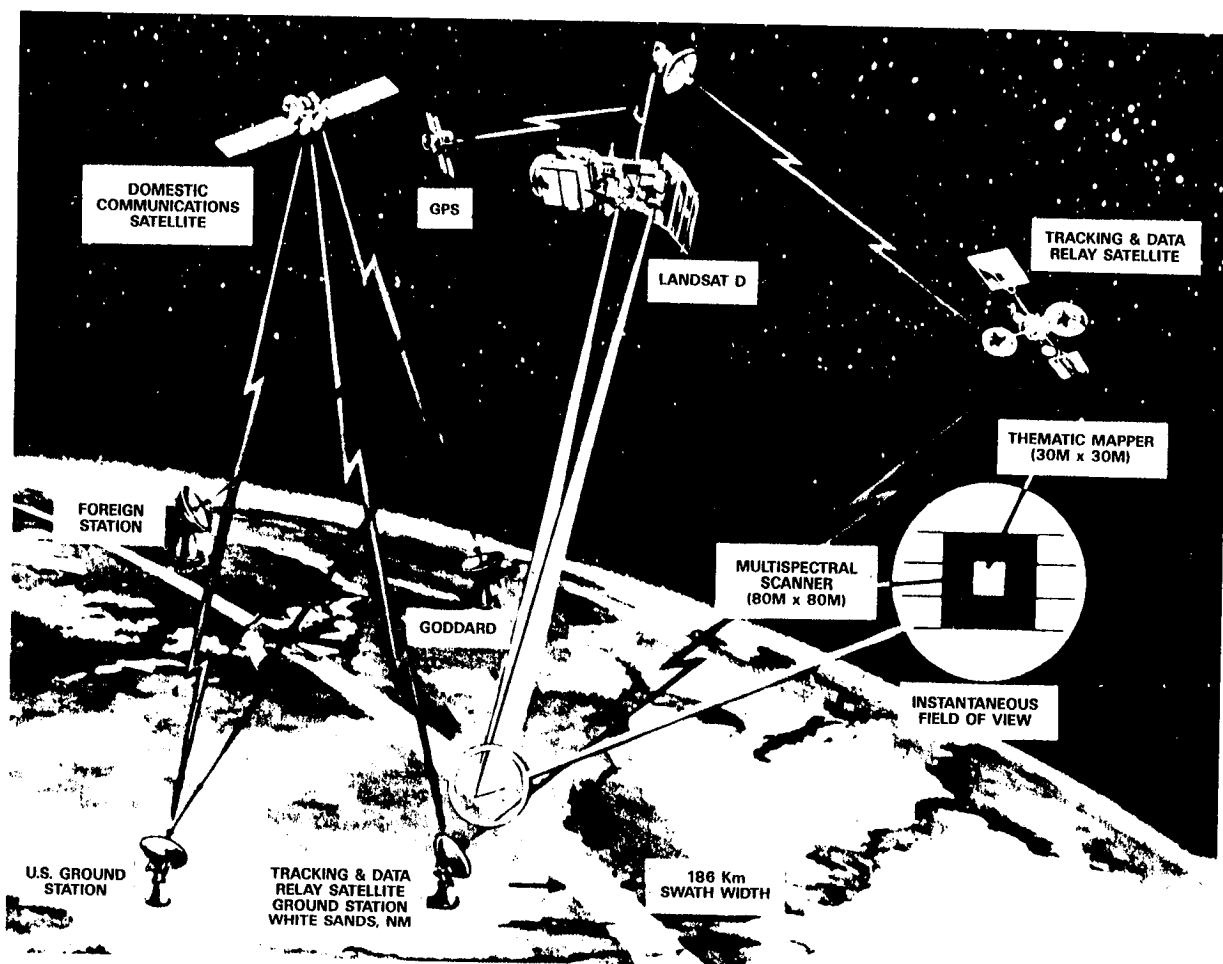


FIGURE 2. SYSTEM DESIGN: FLIGHT SEGMENT AND COMMUNICATIONS LINKS

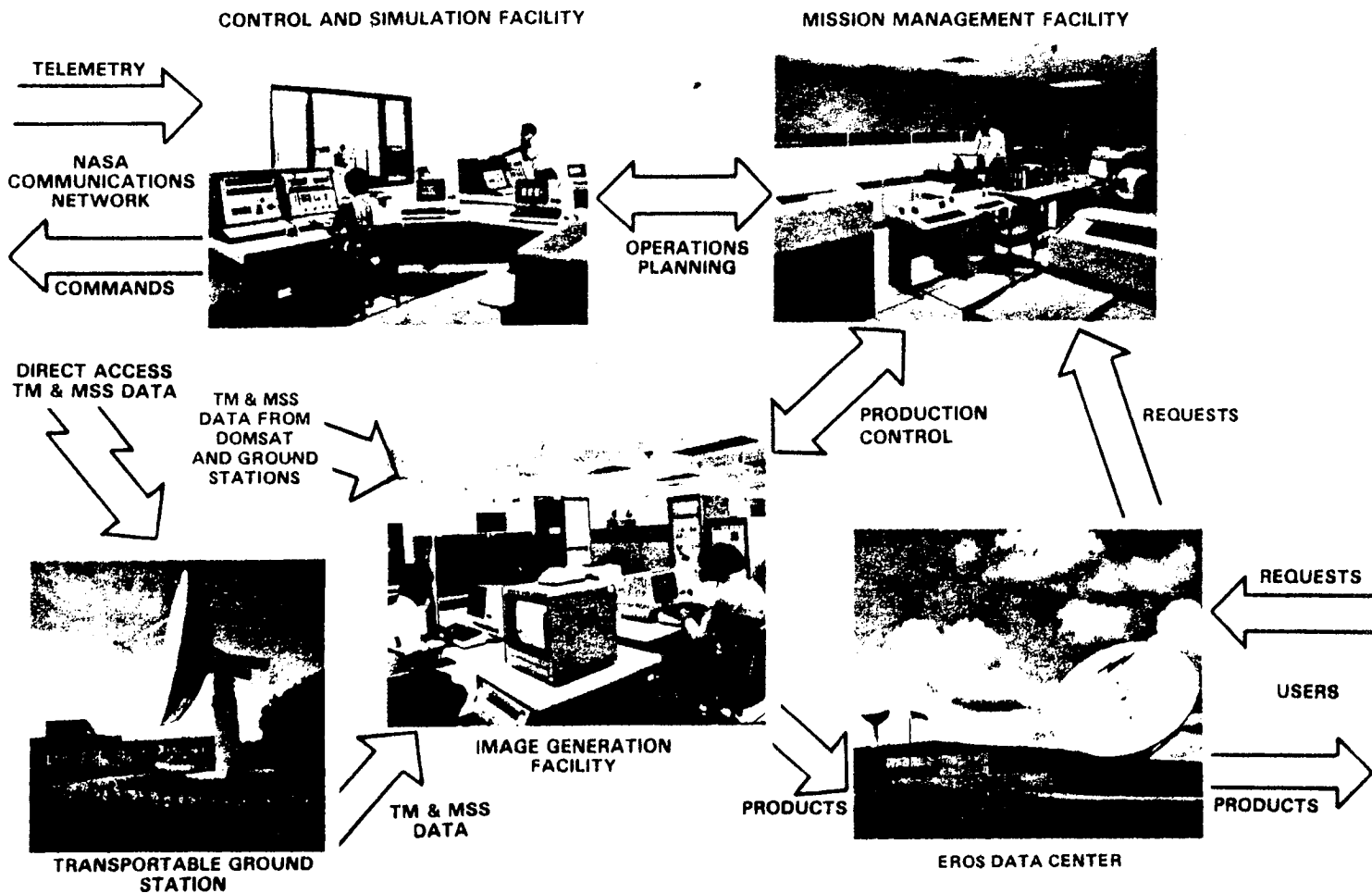


FIGURE 3. SYSTEM DESIGN: GROUND SEGMENT

Figure 3 presents the high level Ground Segment design. As shown, the end-to-end Ground Segment consists of five elements: the Mission Management Facility (MMF), the Control and Simulation Facility (CSF), the Image Generation Facility (IGF), the Transportable Ground Station (TGS) and the EROS Data Center (EDC). The first four of these elements are located at GSFC while EDC is located in Sioux Falls, South Dakota. Briefly stated, the Ground Segment works in the following manner: user requests for image data acquisition are received at EDC and forwarded to the MMF (in fact, there exist two MMFs, one each for MSS and TM mission management) wherein they are sorted according to date and priority before being sent via computer-to-computer data link to the CSF. Based on these prioritized requests, the CSF schedules and commands the spacecraft accordingly. In addition, the CSF receives

housekeeping telemetry data for monitoring the spacecraft's health as well as telemetry data to be reformatted for later use in image processing.

Image data are then received directly via the TGS or via domestic communications satellite (DOMSAT) from GSTDN stations or the TDRSS Ground Station. MSS foreign data required by U.S. users are also recorded on High Density Tapes at the Japan, Australia, Sweden and Brazil Stations and mailed to the Ground Segment for processing. After receipt of image data and under the control of the appropriate MMF, the IGF (either MSS or, when operational, TM) processes these data into user products that are either shipped or transmitted via DOMSAT to EDC for distribution.

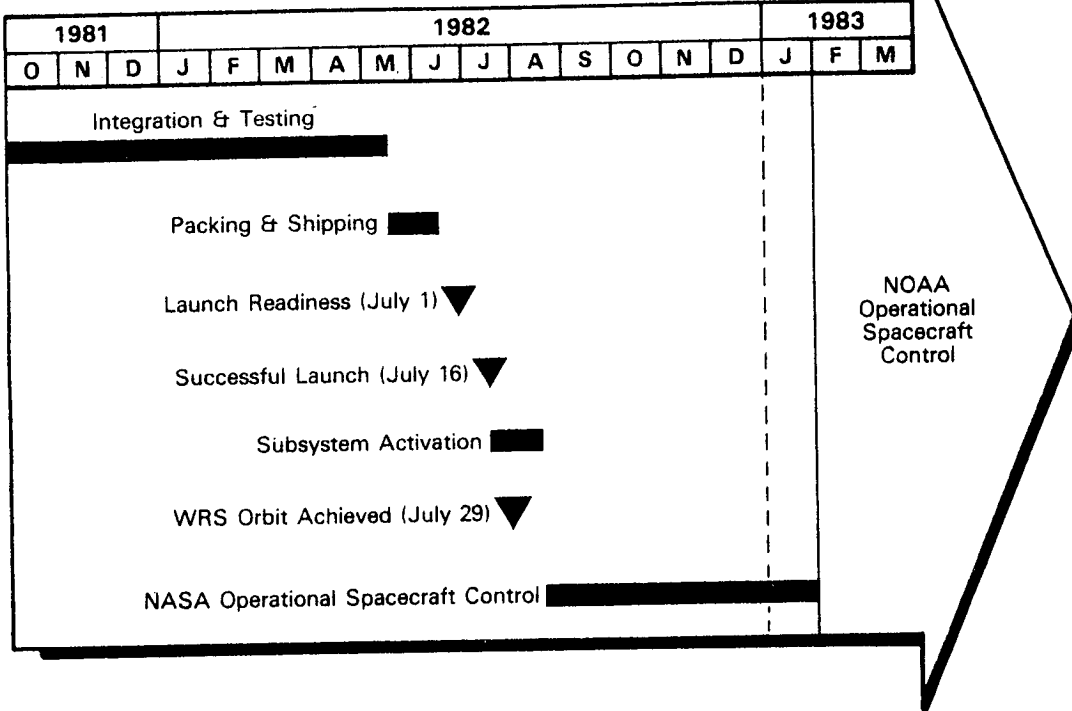
ACCOMPLISHMENTS AND FUTURE EVENTS

This section describes Landsat Program accomplishments and future events with respect to Flight Segment milestones, image data acquisition capabilities and Ground Segment milestones.

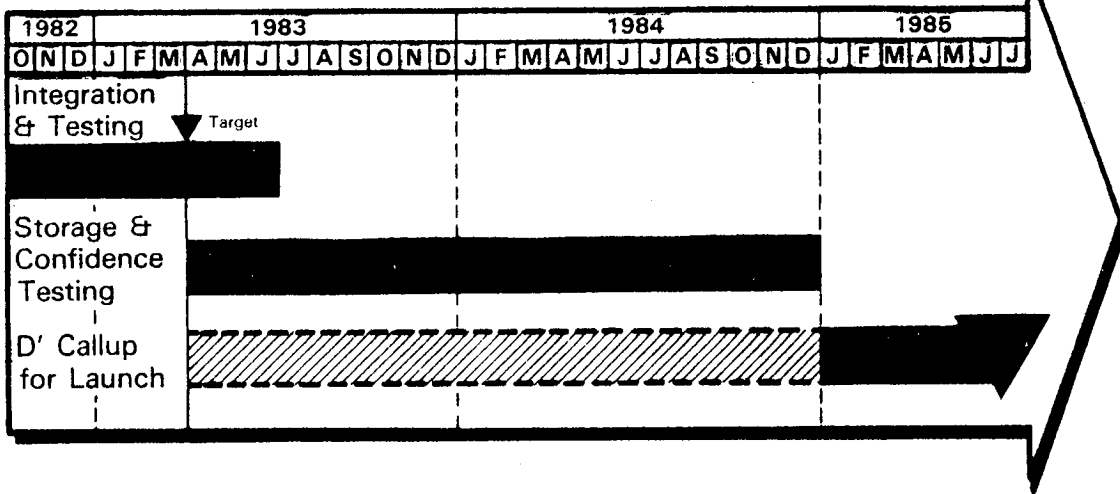
Figure 4 (top) depicts significant events in the history of the Landsat-4 spacecraft. All milestones having been successfully achieved, NASA anticipates turning over operational control of Landsat-4 to NOAA management on January 31, 1983. Figure 4 (bottom) recounts the integration and testing of the Landsat-D' spacecraft with the completion of this activity scheduled to take place in April of this year (1983). Storage and confidence testing is scheduled to occupy a maximum of 1-3/4 years, but the spacecraft will be available for early launch at any time after storage begins. Launch of Landsat-D' is currently scheduled for mid-1985.

Figure 5 presents the growth of acquisition capability (in satisfaction of United States user requirements) from the pre-TDRSS era (TGS, GSTDN and selected foreign sites) through limited use of the TDRS-East in May of 1983 to use of TDRS-East and -West in December 1983 (projected use of TDRSS is based on the current schedule). As Figure 5 indicates, "full-up" use of the TDRSS will allow near-total global coverage (a small portion of the Soviet Union is the only land mass area remaining unavailable during the Landsat/TDRSS era).

Landsat-4



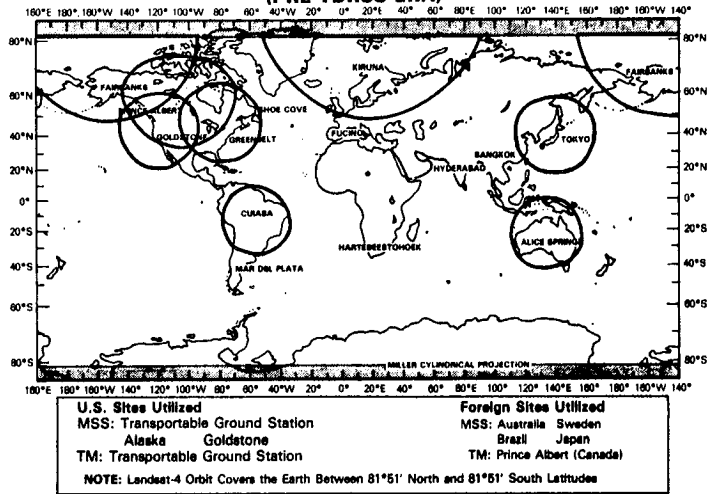
Landsat D'



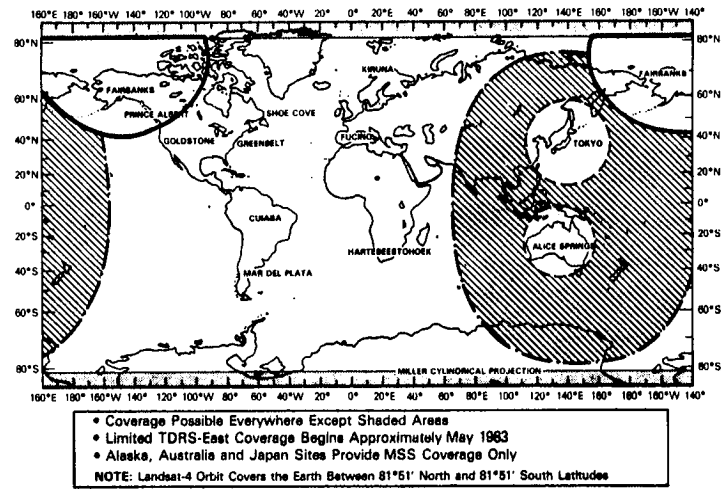
NASA TO SUPPORT NOAA FOR D' STORAGE, CONFIDENCE TESTING & LAUNCH

FIGURE 4
FLIGHT SEGMENT ACCOMPLISHMENTS AND FUTURE EVENTS

Acquisition Capabilities: UNITED STATES USER REQUIREMENTS (PRE-TDRS ERA)



(USING TDRS-EAST)



(USING TDRS-EAST AND -WEST)

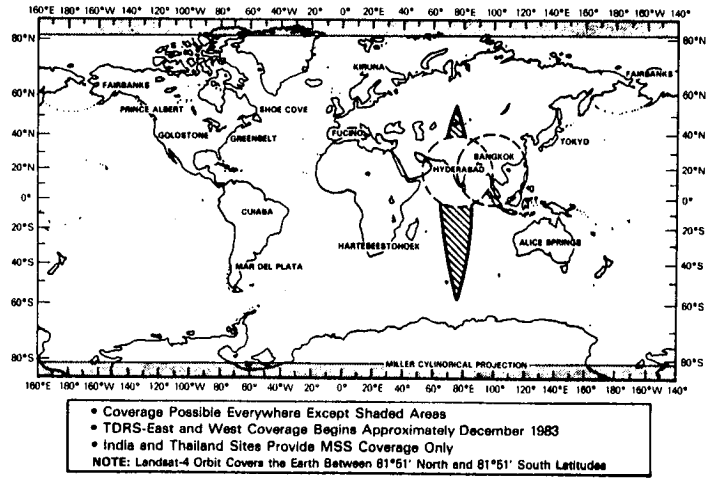


FIGURE 5. GROWTH OF ACQUISITION CAPABILITY IN SATISFACTION
OF U.S. USER REQUIREMENTS

Figure 6 depicts non-U.S. ground stations currently active in support of satisfying foreign Landsat data user requirements.

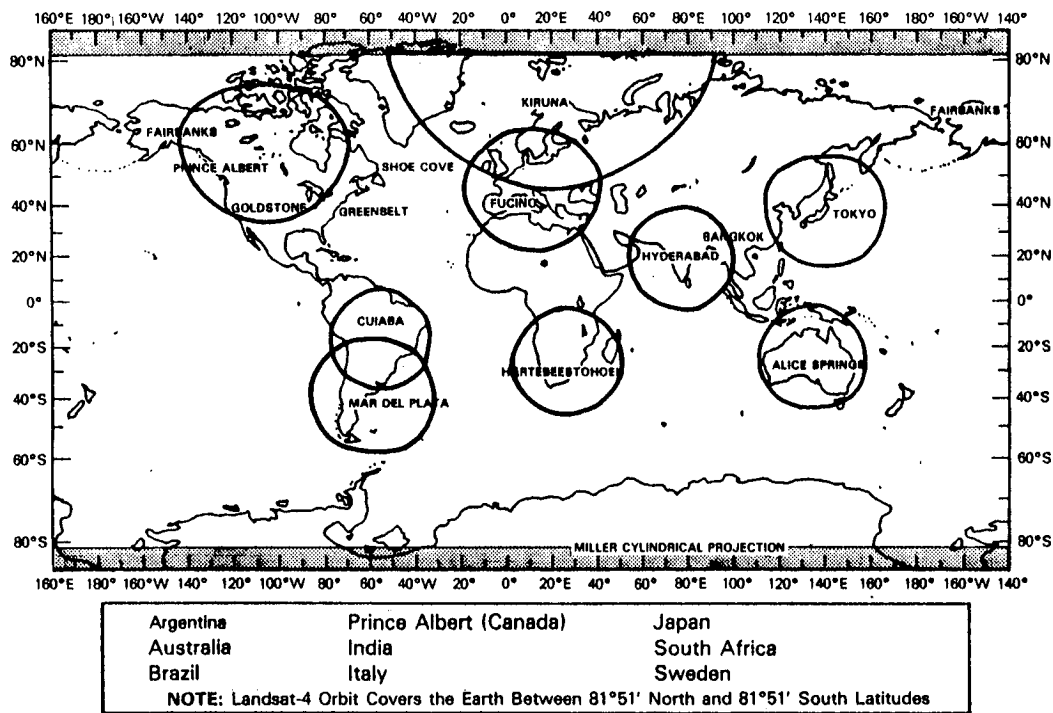
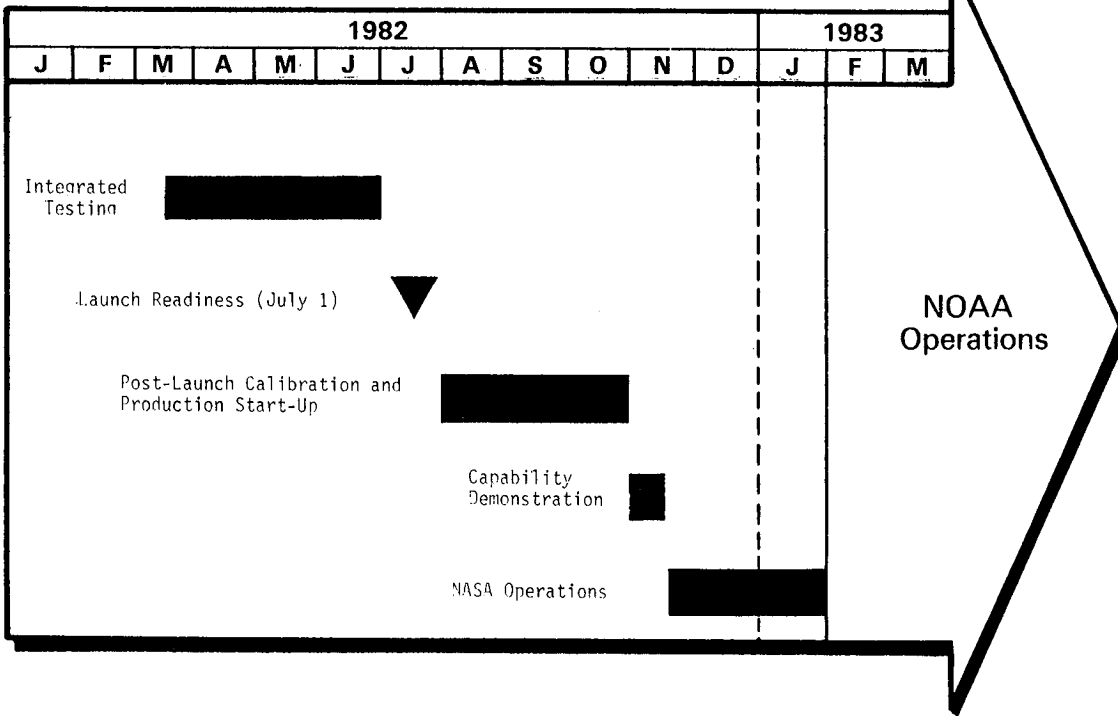


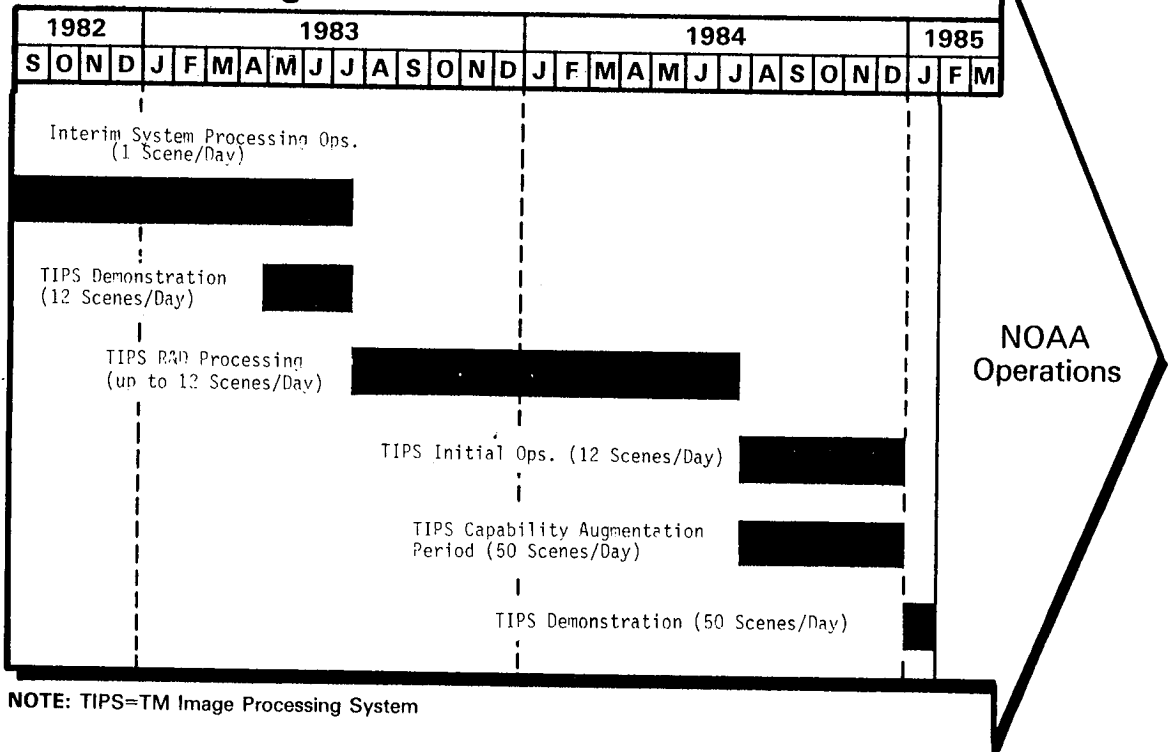
FIGURE 6. ACTIVE FOREIGN GROUND STATIONS

The Landsat-4 Ground Segment is designed to process MSS and TM image data separately. Figure 7 (top) presents significant historical events in NASA's development of the MSS processing capability. NOAA operation of the system began on January 31 of this year. Figure 7 (bottom) depicts the TM processing capability development. TM data are currently being processed by an interim system consisting of a variety of elements located at GSFC. This temporary system (termed the "Scrounge System") will process TM data at the one scene per day level until the TM Image Processing System enters its research and development phase on July 31 of this year. TM processing will ultimately be turned over to NOAA management on January 31 of 1985.

MSS Processing



TM Processing



NOTE: TIPS=TM Image Processing System

FIGURE 7. GROUND SEGMENT PROCESSING DEVELOPMENT

TRANSFER OF LANDSAT-4 OPERATIONS TO NOAA MANAGEMENT

Presidential Directive 54 (November 16, 1979) assigned management responsibility for all civil operational remote sensing satellites to NOAA. All aspects of Landsat-4/D' operations will, accordingly, be transferred to NOAA management. Table 3 presents salient points of the Landsat transfer from NASA to NOAA, while Figure 8 presents a schedule of events with respect to this transfer.

TABLE 3. TRANSFER OF LANDSAT-4 OPERATIONS
TO NOAA MANAGEMENT

- Presidential Directive 54, Dated November 16, 1979, Assigns Management Responsibility for all Civil Operational Remote Sensing Satellite Systems to NOAA
- NASA Retains Responsibility to Design, Develop, Test, Integrate and Initially Operate the Landsat-4 System
- NASA to Transfer All Phases of the Landsat-4 System Incrementally to NOAA Management During the Period January 1983 Through January 1985
- EROS Data Center to Serve as Data Distribution Center
- All Aspects of Landsat-4/D' Operations, Including Product Distribution, Under NOAA Management After January 1985

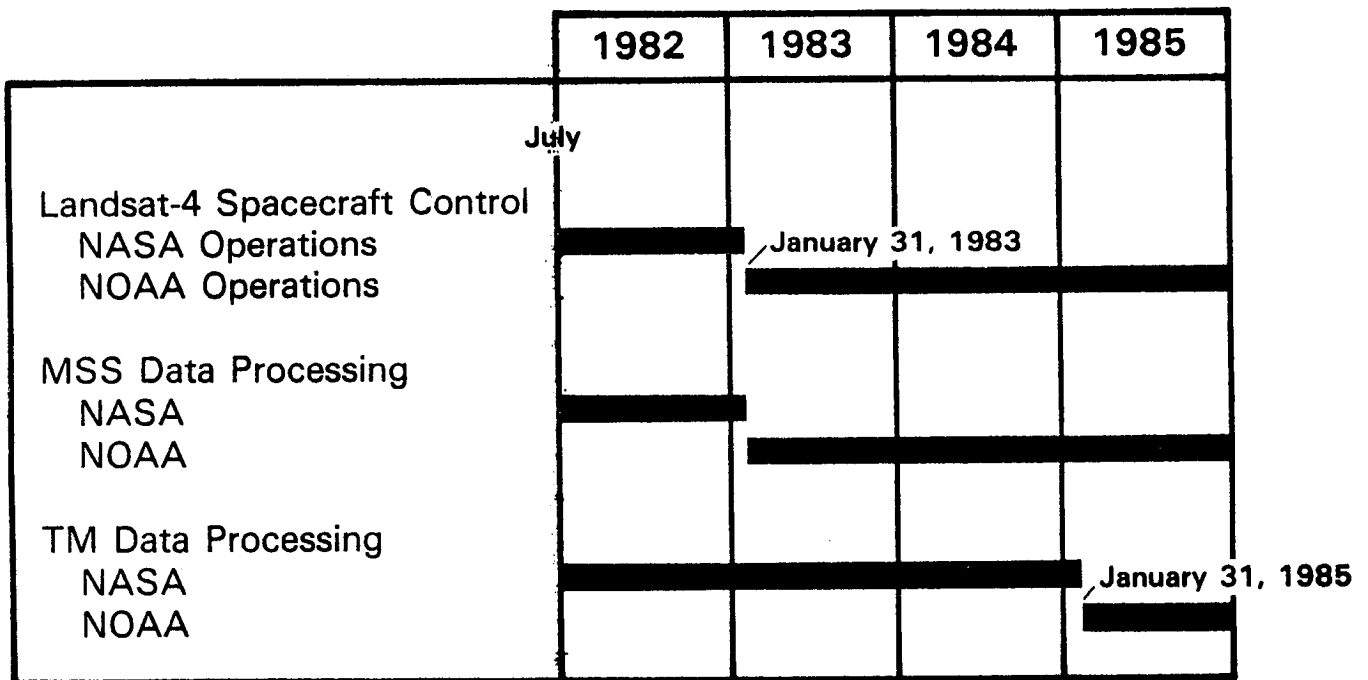


FIGURE 8. LANDSAT-4/D' TRANSITION TO NOAA: SCHEDULE OF EVENTS

REMAINING CHALLENGES

After the successful launch of Landsat-4 and activation of its imaging systems, several challenges remain both to NASA personnel and Investigations Program participants. Table 4 summarizes these challenges.

TABLE 4. CHALLENGES REMAINING TO NASA PERSONNEL
AND INVESTIGATIONS PROGRAM PARTICIPANTS

<p>NASA</p>	<ul style="list-style-type: none"> ● Complete TM Image Processing Development, thus making an Increased Number of Higher Quality Products Available to the User Community ● Achieve Transition to TDRSS, thereby Providing Near Global MSS and TM Coverage Available to the User Community
<p>INVESTIGATORS</p>	<ul style="list-style-type: none"> ● Carry Out Research with MSS and TM Imagery in Your Various Application Areas ● Promote the Routine and Practical Use of these Data for the Betterment of Mankind

LANDSAT-4 SYSTEM DESCRIPTION

THEODORE C. AEPLI
GENERAL ELECTRIC COMPANY

The Landsat-4 Flight Segment is shown in its orbital configuration in Figure 1. It consists of two major sections. The Multimission Modular Spacecraft at the aft end is a standard set of subsystems originally designed by Goddard Space Flight Center a few years ago. It's first flight was on the Solar Maximum Mission; Landsat-4 is the second satellite program to use the Multimission Modular Spacecraft. The forward end of the satellite is new and contains the mission unique equipment for Landsat-4; it is called the Instrument Module.

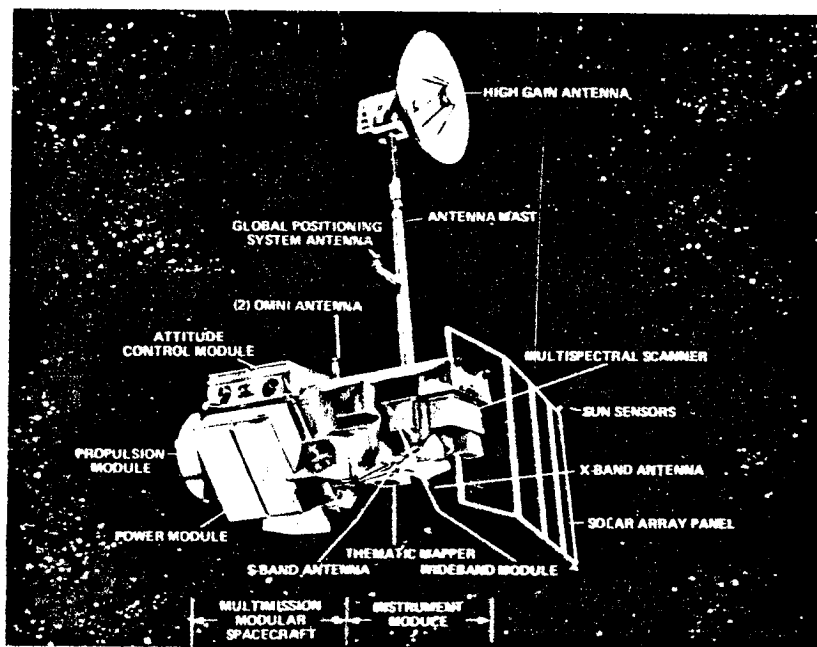


Figure 1. Landsat-4 Flight Segment

The Multimission Modular Spacecraft contains the standard service subsystems for the satellite. The attitude control subsystem is the module on top. A power module is on the second side of the triangular structure. The communications and data handling subsystem, not visible in this view, is mounted on the third side of the structure. This subsystem is used for low

data rate telemetry and commanding of the satellite. It includes an on-board computer that is used for a variety of satellite functions such as detailed ephemeris and attitude control computations, the pointing of the large antenna, and internal satellite monitoring. Also on the Multimission Modular Spacecraft at the very aft end is a propulsion module which provides the capability to trim the orbit following launch, and is used for periodic adjustments to the orbit to maintain a repeating ground coverage pattern.

The aft end of the Multimission Modular Spacecraft structure also provides the interface to the Delta launch vehicle. In the Delta configuration the satellite is launched vertically. When the spacecraft is retrieved by the shuttle it sits in the shuttle cargo bay horizontally, attached via three mounting points at each corner of the triangular structure.

The forward end of the spacecraft, the instrument module, contains the Thematic Mapper, mounted right in the middle of the satellite. The earth pointing aperture faces down in the figure, with the cooler for the upper three bands of the Thematic Mapper facing out of the figure. The Multispectral Scanner is at the forward end of the satellite. The wideband module, containing the X-band electronics, is between the two instruments. The upper structure of the instrument module contains various other electronic modules.

The solar array extends out one side only and is approximately 20 feet long by 7-1/2 feet high. The old Landsat configuration had two solar arrays. However, Landsat-4 can have the array on one side only so that it does not obstruct the field of view of the Thematic Mapper cooler.

The antenna mast is 13 feet high. It has three joints so that it can fold and fit into the Delta launch vehicle shroud. The first joint is at the base of the mast where it joins the satellite center body. The second joint is in the middle of the mast and the two axis gimbal, an azimuth over elevation gimbal that is mounted inside the compartment at the top, is used as a third joint. Once in orbit the solar array deploys first, then the mast and finally the antenna gimbal. The two access gimbal system permits the antenna to view slightly more than hemispherical coverage allowing communication with

either of the two Tracking and Data Relay Satellites. The antenna must have full field-of-view coverage to the Tracking and Data Relay Satellite and, since there are positions in orbit where it has to look directly over the outer edge of the solar array, it requires a mast high enough to see over that edge for all Landsat/TDRSS orbital geometries. One of the design challenges in building the satellite was to make a folding mast rigid enough so it did not vibrate in orbit.

Figure 2 is a photograph of the satellite during tests at Valley Forge; the view is from the earth facing side. The Multimission Modular Spacecraft is at the bottom. The Thematic Mapper is located midway up the satellite; this view is into the optical aperture. Above the Thematic Mapper is the X-band antenna, with the wideband S-band antenna just to the left. The wideband S-band system is used for transmitting MSS data in the same way that MSS data has been transmitted from Landsats 1, 2 and 3 over the last 10 years. The wideband module is behind the antennas. The MSS is just above the wideband module and has a cover over its aperture. The 6-foot diameter high-gain antenna is positioned at the top with the antenna mast stowed in its launch configuration.

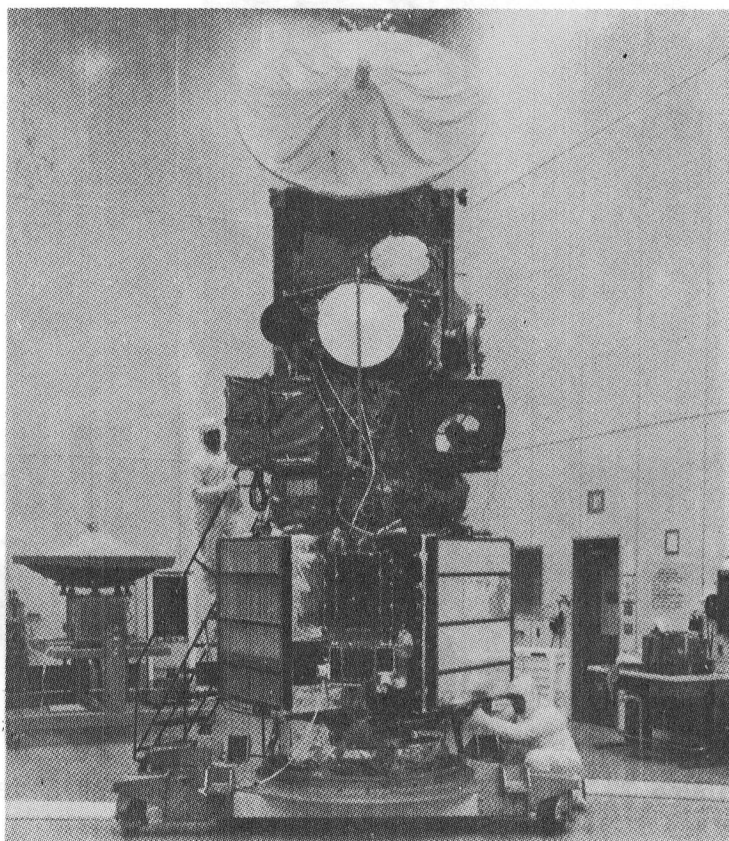


Figure 2. Landsat-4 During Test - Earth Facing Side

Figure 3 is a photograph of the satellite from the reverse side with the solar array as the most pronounced feature. It has four panels folded accordion style in the launch configuration. Four bolts fit through the solar array and are released in orbit. The array extends and rotates about a hinge mechanism on the left. Once deployed it rotates around a single axis once per orbit.

The antenna mast is behind the array; it mounts to the main body of the satellite through a motor driven hinge behind the wideband module. It extends to the top of the photograph where a second motor drive hinge is located. It folds back against itself to a point approximately halfway down the lower section of the mast. The RF compartment is latched against the lower section of the mast to keep the antenna in position during launch.

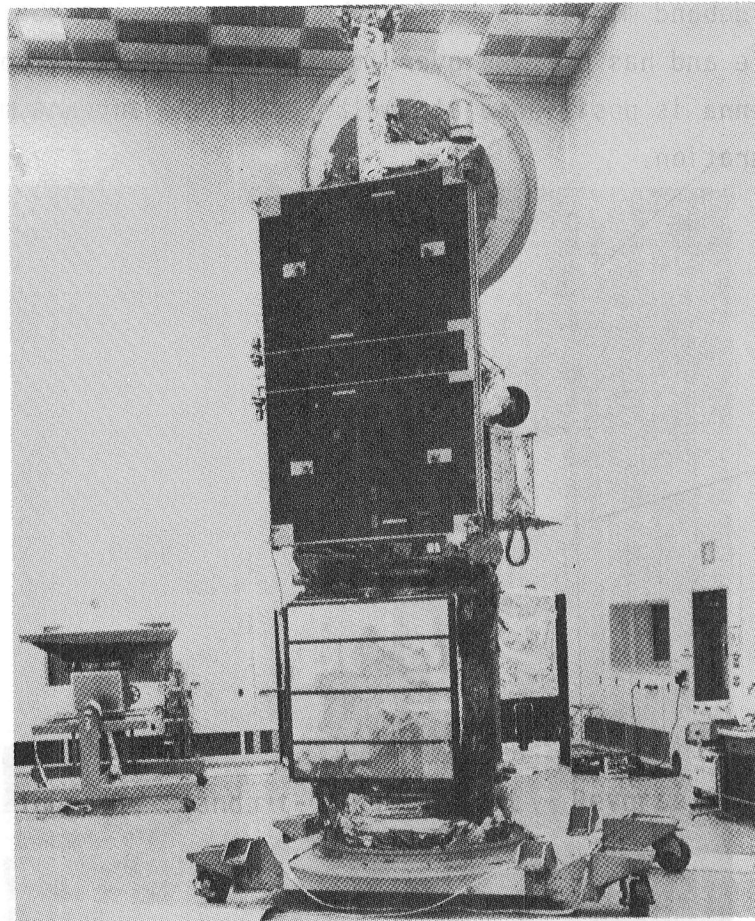


Figure 3. Landsat-4 During Test - Reverse Side

The Landsat-D orbital parameters, shown on Figure 4, are different from those of Landsats 1, 2 and 3. Most significant is the nominal altitude which is 705 kilometers as opposed to the nominal 900 kilometer altitude of Landsats 1, 2 and 3. It has approximately the same time of day equatorial crossing or descending node time, is within a few minutes of the same period and approximately the same inclination.

The different orbit results in a ground track coverage pattern that is different for Landsat-4 than for the earlier Landsats (Figure 5). Previously the satellite progressed westerly every day; its immediate adjacent ground track was always one swath to the west. Landsat-4 does not progress the same way. It has a 7-day skip pattern. Given any ground track, the immediately adjacent orbit to the west is 7 days later, the immediately adjacent orbit to the east is 7 days prior. Landsat-4 has a 16-day repeat cycle as opposed to the 18-day repeat cycle for earlier Landsats.

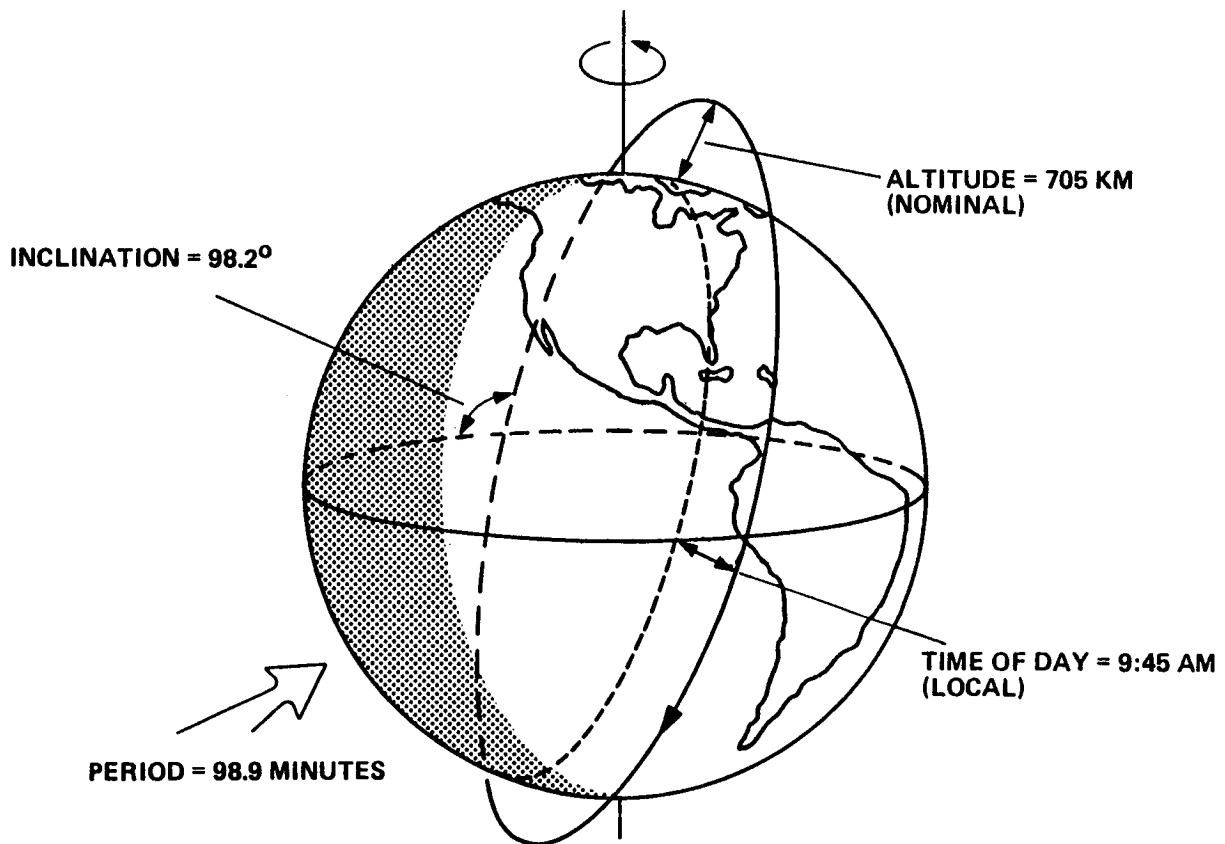


Figure 4. Orbital Parameters

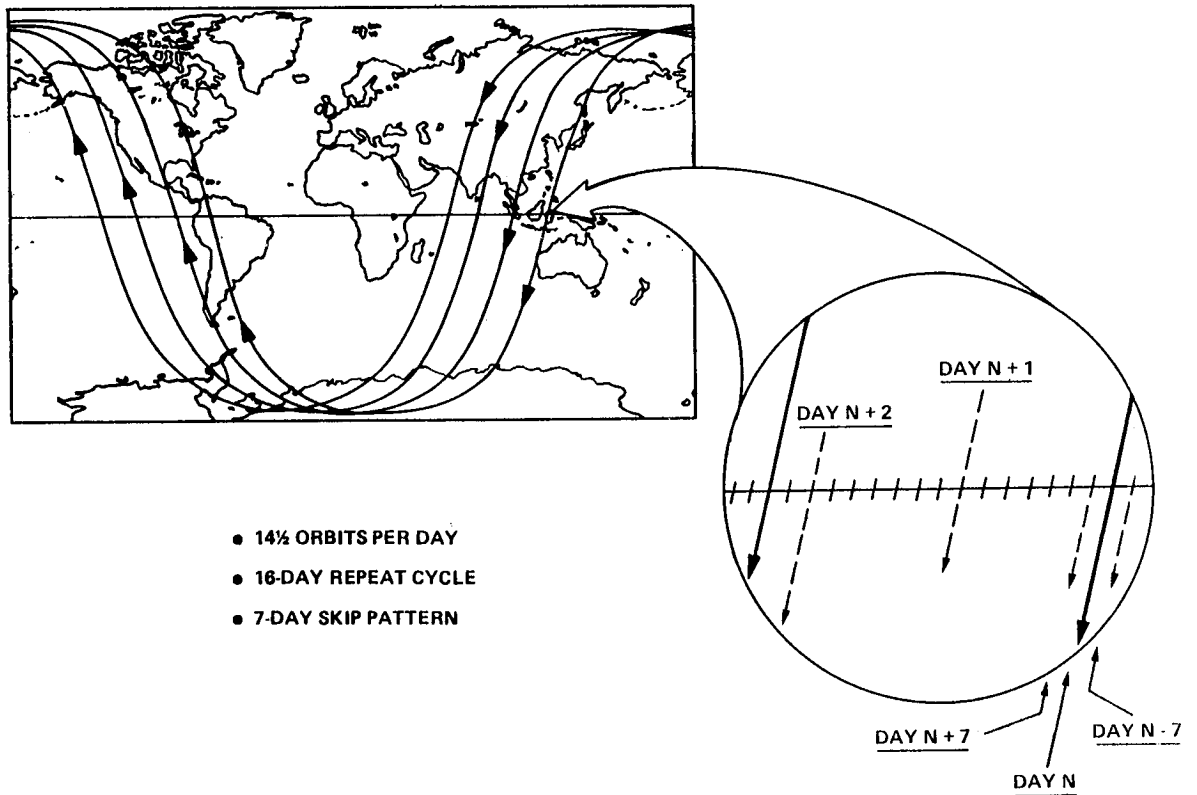


Figure 5. Ground Track Coverage Pattern

Figure 6 shows an overview of the ground segment. Requests for MSS data are consolidated at the EROS Data Center in Sioux Falls, South Dakota. The consolidated requests are forwarded to the Mission Management Facility at GSFC periodically. In the Mission Management Facility the requests are sorted by day and transferred via computer link to the Control and Simulation Facility.

The Control and Simulation Facility is that portion of the ground segment that operates the satellite. Here user requests for data are converted to specific satellite activities lists considering current status of the flight segment, availability of communications links and predicted cloud cover. Once or twice a day a set of commands is uplinked to the satellite and operate the satellite for the next 12-24 hours. Included in those commands are those to turn on the instruments and data links over the United States and all foreign ground stations.

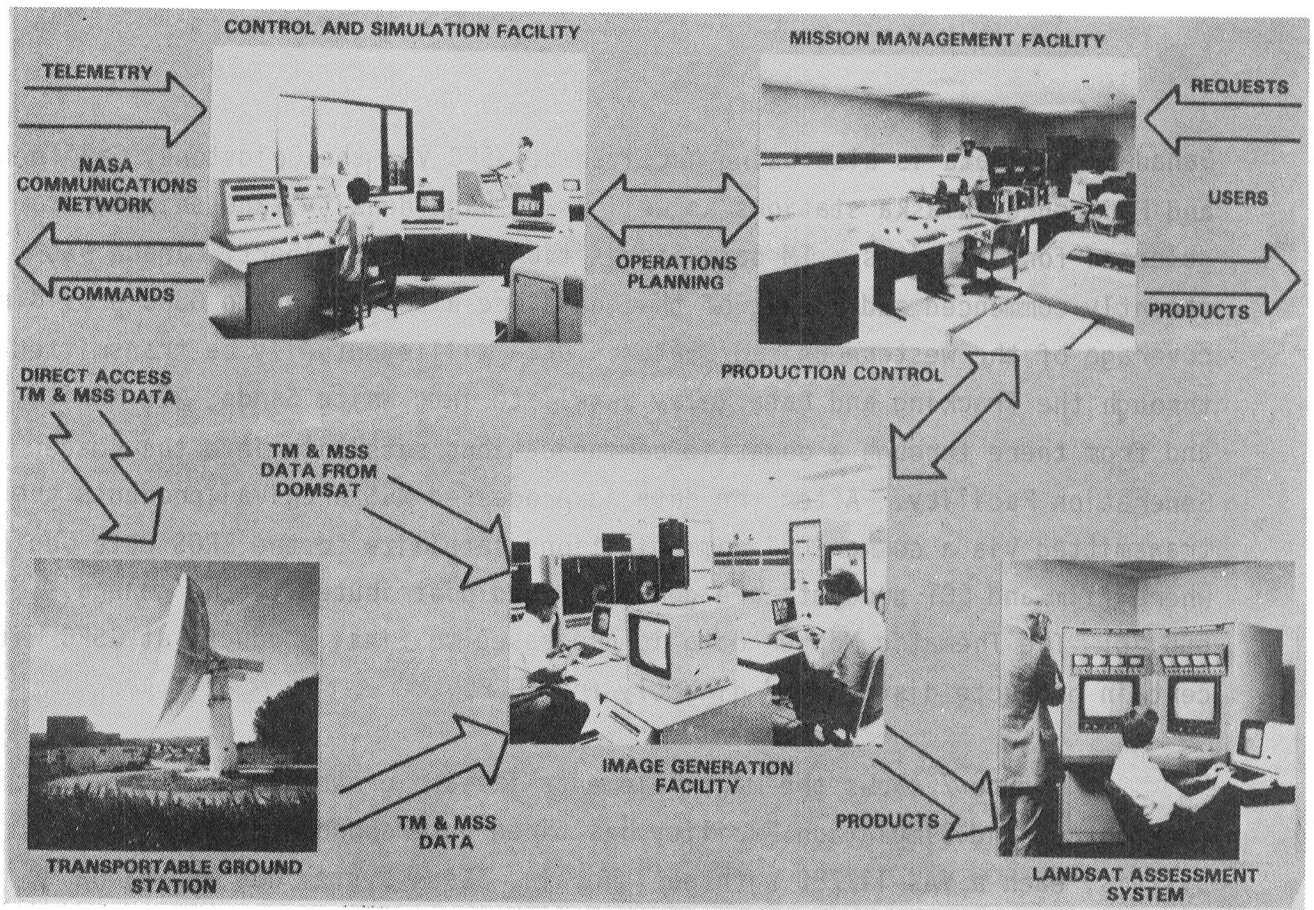


Figure 6. Overview of Ground Segment

The Control and Simulation Facility also serves to receive 8 and 32 kilobit per second telemetry data from the satellite. A portion of the 8 kilobit per second telemetry data is called housekeeping or health and safety data allowing the ground to monitor satellite performance. Other data such as ephemeris and attitude also are included in the telemetry stream and are used for subsequent processing of MSS imagery.

In addition, higher frequency attitude displacement data, often called jitter data, plus the attitude and ephemeris data are transmitted in the 32 kilobit per second data stream and are used in processing TM imagery. The data used for image correction is stripped out in the Control and Simulation Facility and routed via the Mission Management Facility to the Image Generation Facility where it is used in subsequent processing.

MSS and Thematic Mapper image data is received directly at GSFC through the Transportable Ground Station providing coverage of the eastern half of the United States, a portion of the Caribbean and the eastern part of

Canada. MSS data is also being received at GSFC via the Goldstone, California and Fairbanks, Alaska stations as well as on high-density tape shipped from selected foreign sites. TM data acquisition at Prince Albert, Canada has recently commenced and copies of that data are also shipped to GSFC providing coverage of the western United States. Data will eventually be transmitted through the Tracking and Data Relay Satellite into White Sands, New Mexico, and from there through a domestic communications satellite into the Image Generation Facility. After the data is processed MSS archival products are transmitted via a commercial communications satellite to the EROS Data Center where film and CCT products are generated and distributed to the general public. The Thematic Mapper data is processed to final products at GSFC with certain products distributed directly from GSFC.

Figure 7 shows the major elements in each ground segment facility. The Control and Simulation Facility has three interconnected major computer systems, each a VAX 11/780 with peripherals. Each system has additional communications equipment, some of it standard purchased and some of it specially built, to allow any of the computers to interconnect to the NASA communications network for commanding and telemetry acquisition. The normal configuration is one system prime, a second as a backup and the third off-line doing the next days scheduling and reducing data from previous acquisitions. They are all connected to the Mission Management Facility by computer to computer links. It is through these data links that information on user requests is passed from the Mission Management Facility into the Control and Simulation Facility and the reduced telemetry information is passed back for use in subsequent image processing. There are two Mission Management Facilities in the ground segment. Each includes a DEC 20 computer and standard peripherals. One is allocated to MSS data processing control and a separate one for Thematic Mapper data processing control.

There are three MSS processing strings, all configured identically. Together, the three provide the capacity to process 200 MSS scenes per day. Each string includes a VAX 11/780 and a standard set of peripherals, some special purpose high-speed hardware and an AP-180V array processor. Typically only one or two strings are used for processing the data load since the system currently is not operating to its full input capacity. The processing load

is expected to increase later this year when global earth coverage is achieved following launch of the two Tracking and Data Relay Satellites.

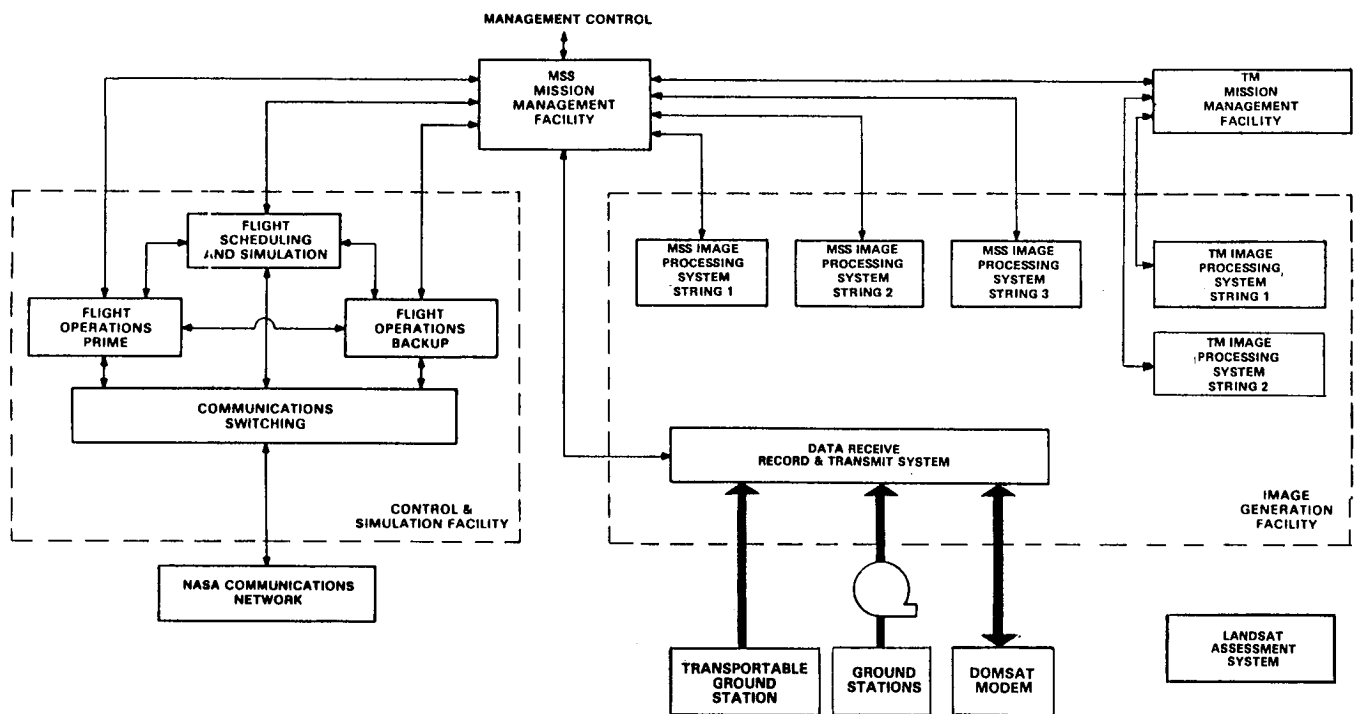


Figure 7. Major Elements in Each Ground Segment Facility

The Image Generation Facility also includes a Data Receive, Record and Transmit Subsystem. This subsystem consists of a PDP 11/34 computer with peripherals and a bank of high-density digital recorders. It receives and records all of the high-data rate TM and MSS data, either directly from the Transportable Ground Station, from White Sands via a domestic communications satellite or on tape originally generated at the foreign ground stations. During recording, selected information is stripped out and transferred via computer to computer link to the Mission Management Facility for use in subsequent image processing.

Each of the two TM image processing strings include a VAX 11/780 computer and peripherals, a General Electric produced Federation of Functional Processors array processor with imbedded special purposed hardware for geometric correction at high throughput rates, plus other assorted special purpose high-speed hardware that are uniquely tailored to handle the high-speed

TM data. There is considerably more special purpose hardware in the TM strings than in the MSS strings where existing designs could be used. At the present time one TM image processing string is completely built and installed, the other is nearing completion. Final tests of this system will start in April. By the end of July, one string will be operating one shift a day to produce twelve TM scenes in a production mode. The second string will be available shortly thereafter, and will be used for continued development work throughout the year.

Figure 8 summarizes the flow of data for MSS processing. Data from the various sources is recorded in the Data Receive, Record and Transmit System on a tape called the raw high-density tape, or HDT-R. This tape is stored in an archive area and is retrieved at the proper time for processing on any of the three MSS processing strings. During processing, the data is stripped off the raw data tape and stored on disks. Eight image disks are used and are capable of storing up to 30 scenes of MSS data. The attitude and ephemeris information originally received via the eight kilobit satellite downlink in the control center is used, along with other MSS unique data such as scan mirror profile and detector placements, to generate geometric correction matrices. Radiometric correction functions are also generated along with various annotation data. Radiometric corrections are applied as the image data is read off of disk onto the output high-density tape, and the annotation data and the geometric correction matrices are appended. The output tape is called the archival high-density tape or HDT-A.

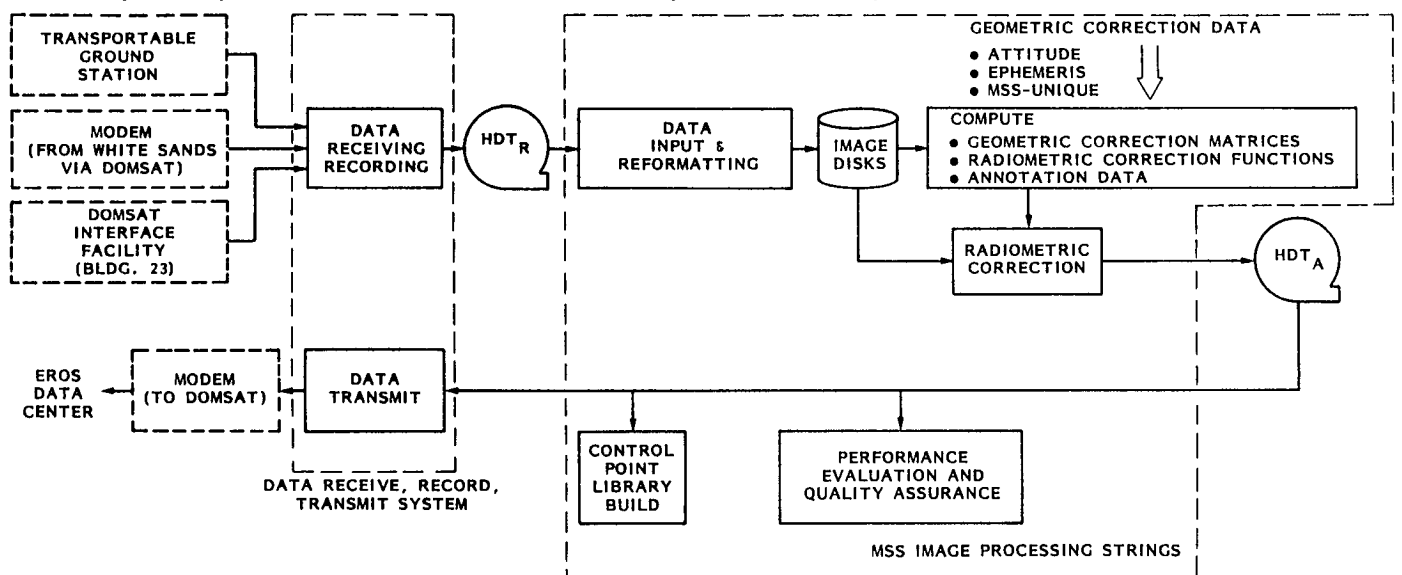


Figure 8. Multispectral Scanner Image Process Flow

Following quality assurance inspection, the tape is carried to the Data Receive, Record and Transmit System and the data is sent to the EROS Data Center via a domestic communications satellite. At the EROS Data Center the geometric corrections are applied, products are generated and shipped to users. There is a basic difference between the MSS processing system and the Thematic Mapper processing system. The data that is sent to the EROS Data Center is in archival format for MSS in that it is radiometrically corrected but not geometrically corrected, with the EROS Data Center doing the geometric correction and product generation. The TM data is transferred to the EROS Data Center in a product format. It is both radiometrically and geometrically corrected.

Figure 9 is the first MSS scene acquired from Landsat-4 four days after launch. It covers the New York City area and the New Jersey coast.



Figure 9. Multispectral Scanner Image

A demonstration to measure ground segment performance against requirements was run in October 1982. The requirements on the Landsat-4 MSS processing system (Table 1) were considerably tighter than for previous Landsats. The demonstration was intended not only to show that the system met its requirements but also to measure its capacity. The system was designed to achieve a 200 scene per day throughput capacity; in fact, over a five day demonstration period the system averaged 226 scenes per day. The system was designed to have a 15 percent margin to insure adequate recovery time in case of anomalies, hence, a requirement for 85% or less utilization of equipment and people. The system averaged 226 scenes per day with only 74% utilization. The system is designed to process data, from the time the raw data is received at the ground segment until the archive product is ready for uplink over a communications satellite to the EROS Data Center, in less than 48 hours, substantially better than the earlier Landsat 1, 2 and 3 system. During the demonstration the turnaround time ranged between 7.5 and 31.6 hours with over 90% of the data turned around in less than 20 hours. So the system in terms of its throughput and capacity exceeds all its requirements.

Table 1. Ground Segment Performance

MEASUREABLE	REQUIREMENT	DEMONSTRATED PERFORMANCE
Throughput (Scenes Per Day)	200	226 (Average)
Utilization (Percent)	≤ 85	74 (Average)
Turnaround Time (Hours)	≤ 48	7.5 To 31.6
MSS Image Performance		
- Radiometric Accuracy (Quantum Level)	± 1 (of 128)	± 1
- Temporal Registration (Pixel)	≤ 0.3	≤ 0.3
- Geodetic Rectification (Pixel)	≤ 0.5	≤ 0.5

Image performance was also examined during the demonstration. The radiometric accuracy requirement was ± 1 quantum level out of 128 levels; the measured performance in October was slightly better than that. The geometric accuracy requirements are less than or equal to 0.3 pixel temporal registration and 0.5 pixel geodetic rectification to a map 90% of the time. Because it takes a long time to evaluate the system with sufficient control points, only limited data sets are available for assessment. However, it is clear that, by late 1982, the system was achieving these accuracies. The real challenge in the ground system was to build a system that could consistently process such a large quantity of data to very tight accuracies in a 48-hour period of time; everyone is pleased at the success.

Figure 10 illustrates the Thematic Mapper process flow using the Scrounge system. The Scrounge system bridges the gap between the Landsat-4 launch and the scheduled completion date of July, 1983 for the Thematic Mapper operational ground system described earlier. It is a composite of (1)

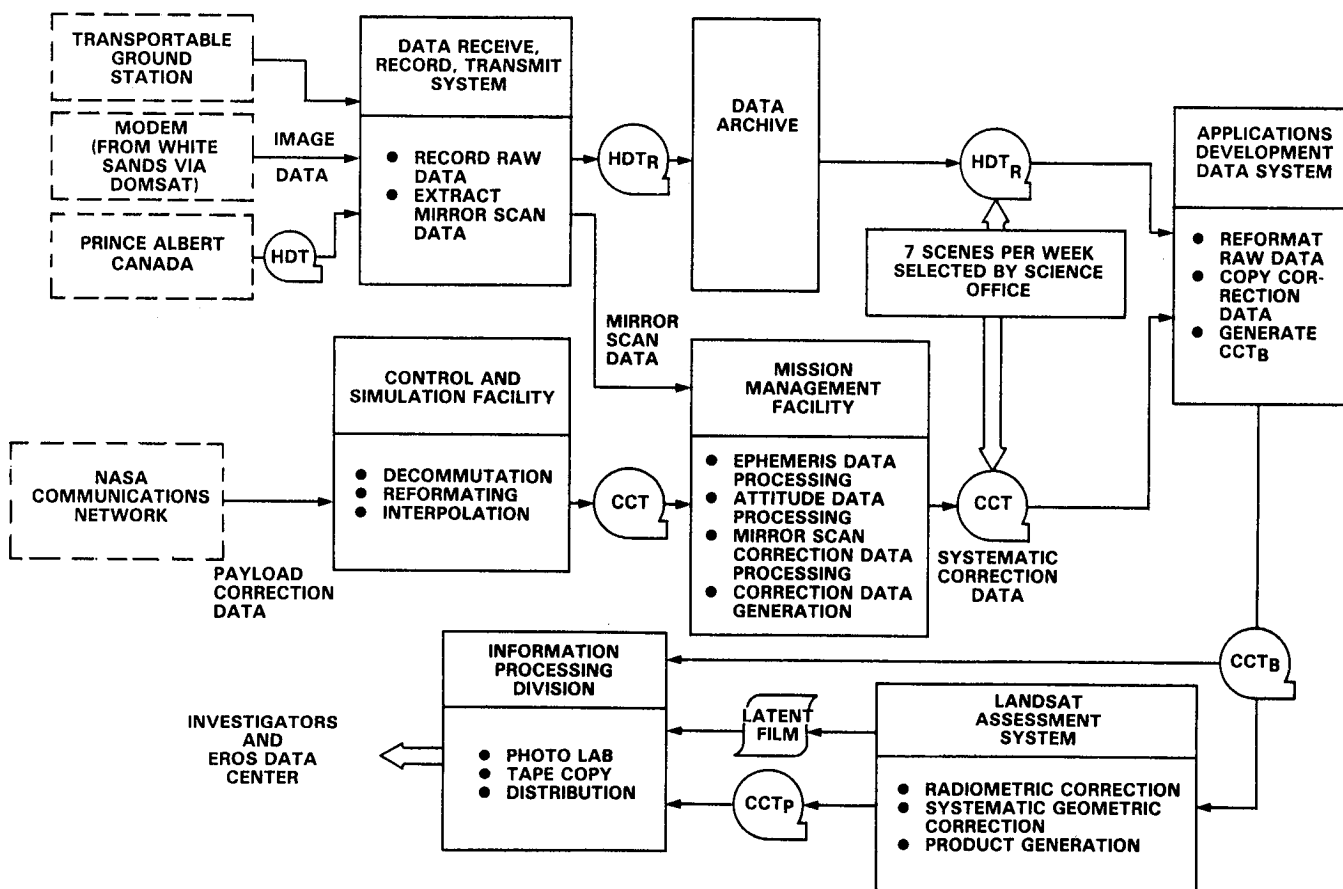


Figure 10. Scrounge Data Flow

portions of the Landsat-4 ground segment including the Data Receive, Record and Transmit System, the Control and Simulation Facility and the Thematic Mapper Mission Management Facility, (2) two R&D systems at Goddard Space Flight Center, the Landsat Assessment System built as part of the Landsat-4 development and the Applications Development Data System built as a separate facility for high speed image processing R&D, and (3) the Information Processing Division providing standard services for photo processing, tape copy and distribution functions.

Since launch Thematic Mapper data covering the eastern United States has been received via the Transportable Ground Station and, since November, via tapes from the Prince Albert, Canada station covering the western United States. Similar information to that for MSS is extracted in the Data Receive, Record and Transmit Subsystem with one noteworthy addition; mirror scan correction data is extracted from the image data and is later used to correct the TM data on a scan by scan basis. The extracted information is routed to the TM Mission Management Facility where it is merged with ephemeris and attitude information. For TM processing, attitude information includes both low frequency gyro data and higher frequency jitter data. Correction matrices, called systematic correction data, are generated and output to computer compatible tape. All TM data is archived; the Science Office nominally requests seven scenes per week, for processing. The principal users of that data are the Landsat Image Data Quality Analysis Program investigators although much of it now is being distributed by the EROS Data Center.

The correction data on a computer compatible tape and the raw data on a high-density tape are carried to the Applications Development Data System which has the capacity to read these tapes, reformat the image data, copy the correction data, and generate what is called a CCT-B. This is an intermediate tape (as opposed to the A or P tapes described earlier) and selected investigators are using this tape directly in their evaluations. The CCT-B is the input medium to the Landsat Assessment System which performs the radiometric correction, systematic geometric correction and master film and CCT product generation. The latent film is developed by the Information Processing Division in the photo lab. Copies of both tapes and film are generated and distributed to the investigators and are sent to the EROS Data Center.

The Landsat Assessment System uses correction algorithms very similar to those in the operational TM image processing system with one exception. No ground control points are used in the Scrounge processing hence the output products are systematically corrected but not registered to a map.

Figure 11 shows the now famous Detroit scene, acquired five days after launch. Considered in the context of a brand new satellite design, a brand new instrument, a brand new ground system and the many elements of the Scrounge System, a great appreciation develops for the contributions of the many hundreds of men and women in NASA and the various contractor organizations which allowed a fully corrected, high-quality scene to be available just 12 hours from the time it was acquired.

Many investigators will be reporting on this scene throughout the symposium. It represents the culmination of ten years of effort to bring the Landsat-D system to completion and the beginning of an entire new era in earth resources management applications.



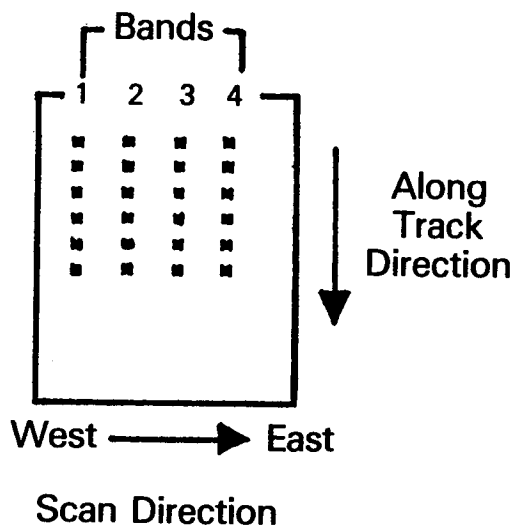
Figure 11. Thematic Mapper Image - Detroit Scene

MULTISPECTRAL SCANNER (MSS)
INSTRUMENT DESCRIPTION

[Exerpted from Landsat-D Investigations Workshop, May 13-14, 1982, John L. Barker, Gary Banks]

Multispectral Scanner (MSS) Sensor

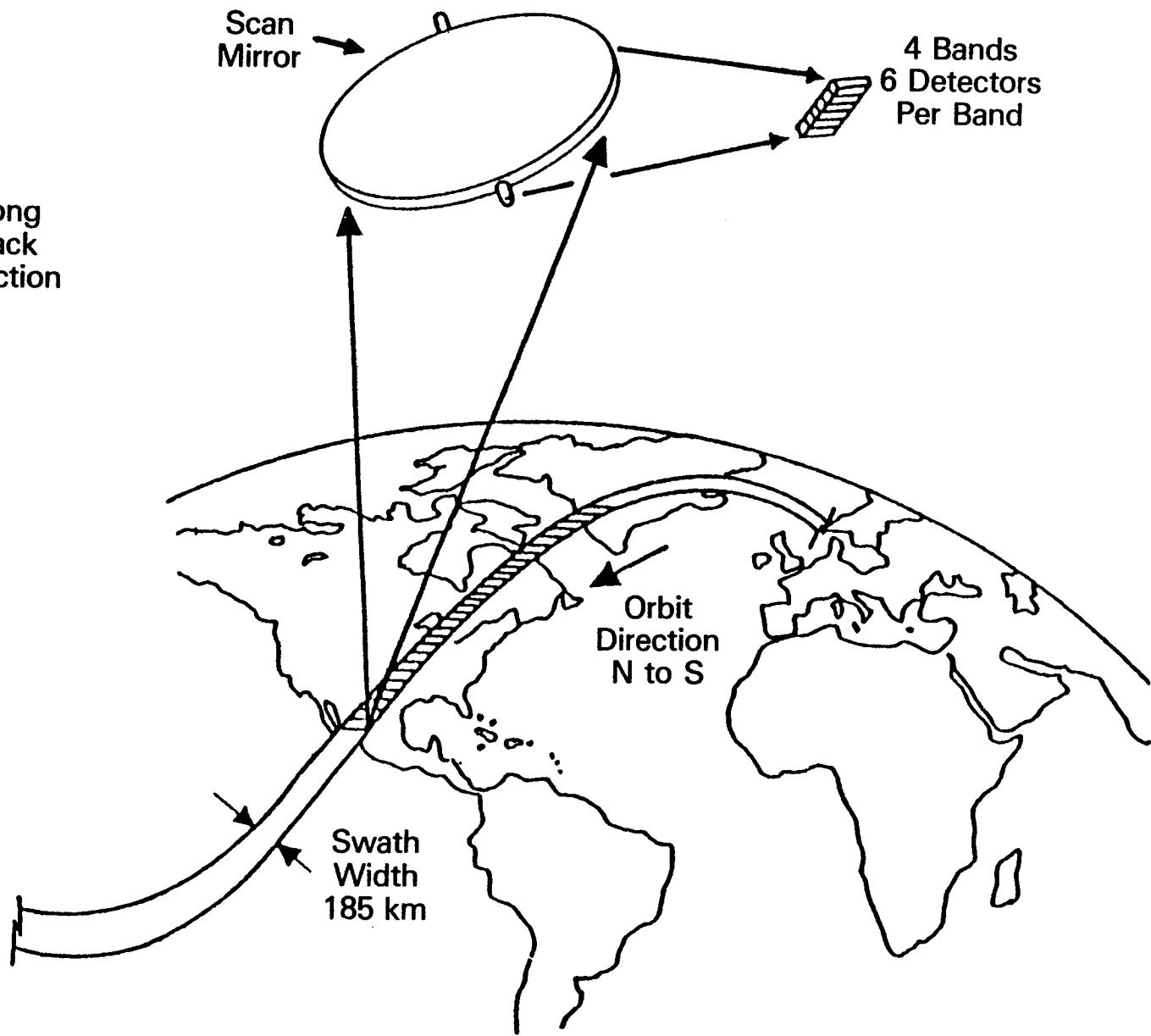
MSS Detector Details



32

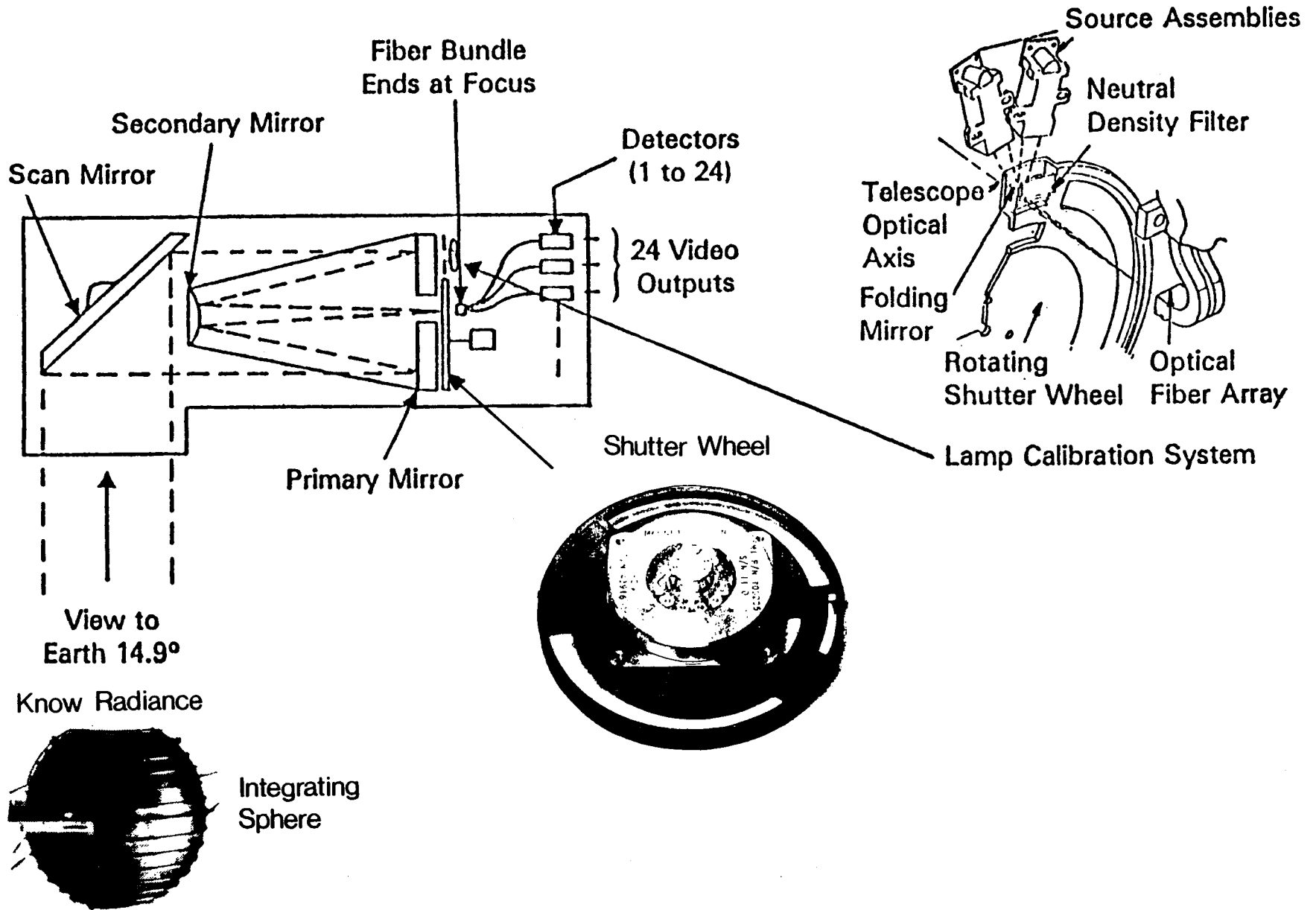
Band	Spectral Ranges μm
1	.5 - .6
2	.6 - .7
3	.7 - .8
4	.8 - 1.1

Ground IFOV
 All Bands — 83 Meters
 Data Rate — 15.06 Mbps
 Quantization Levels — 64

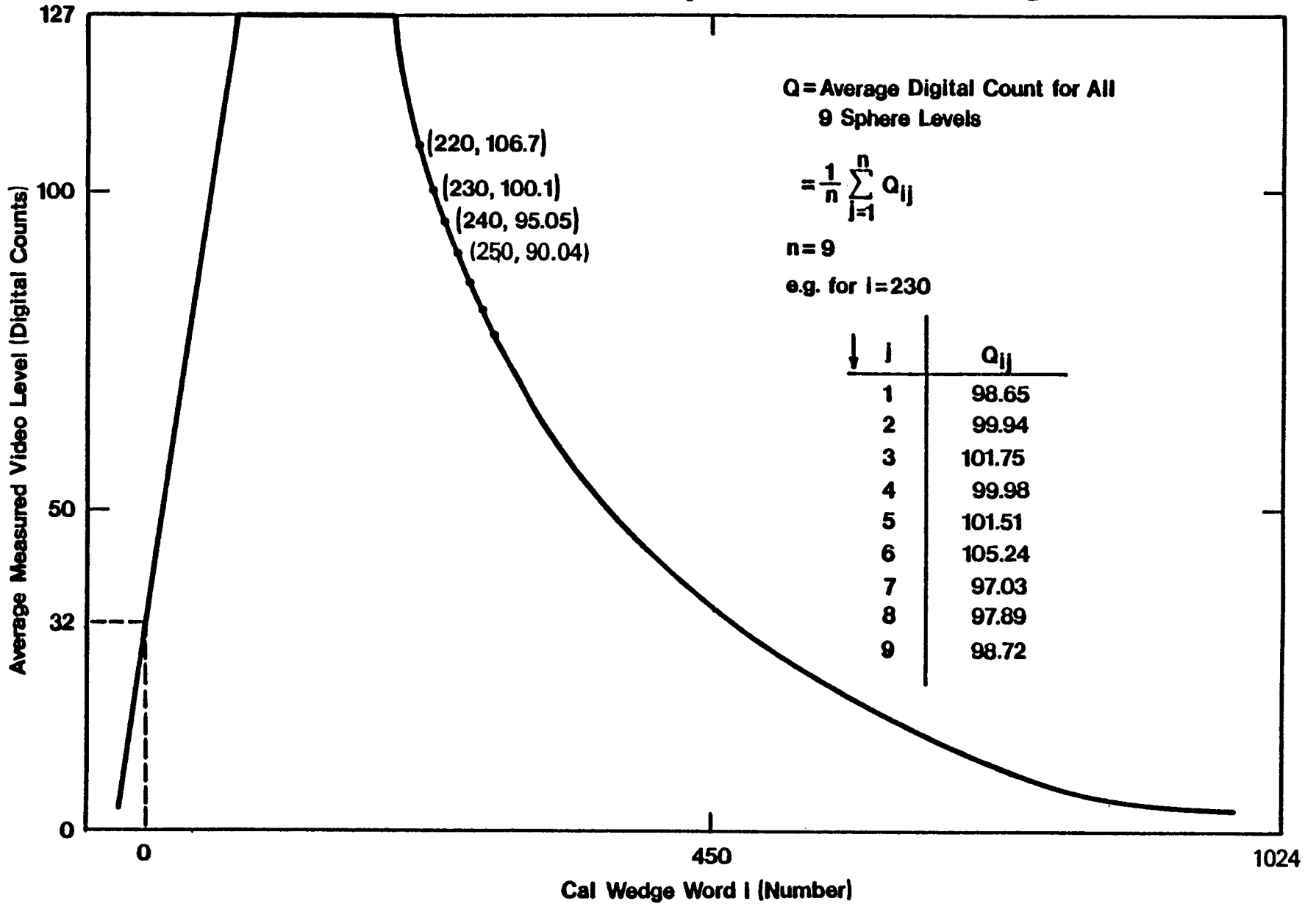


Landsat MSS Absolute Radiometric Calibration

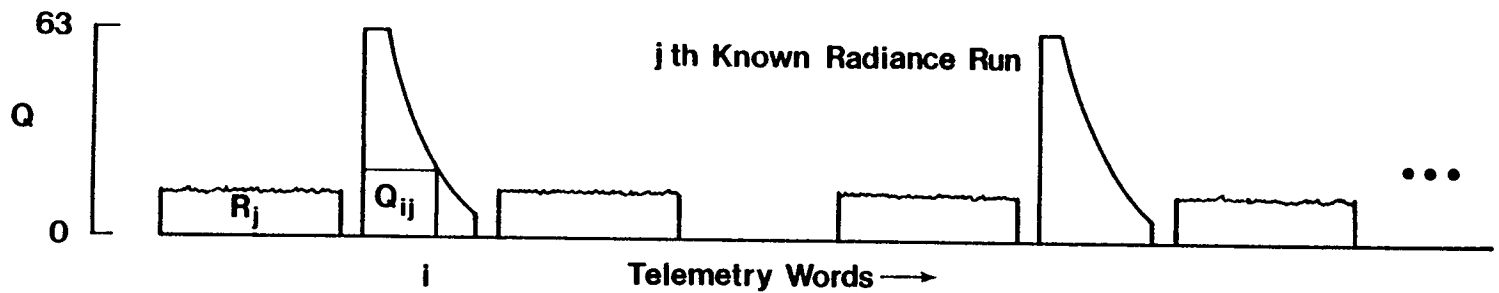
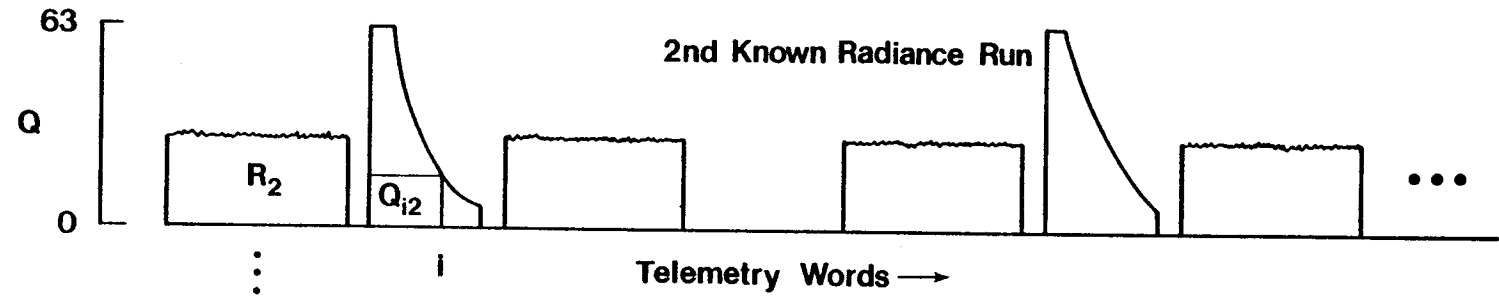
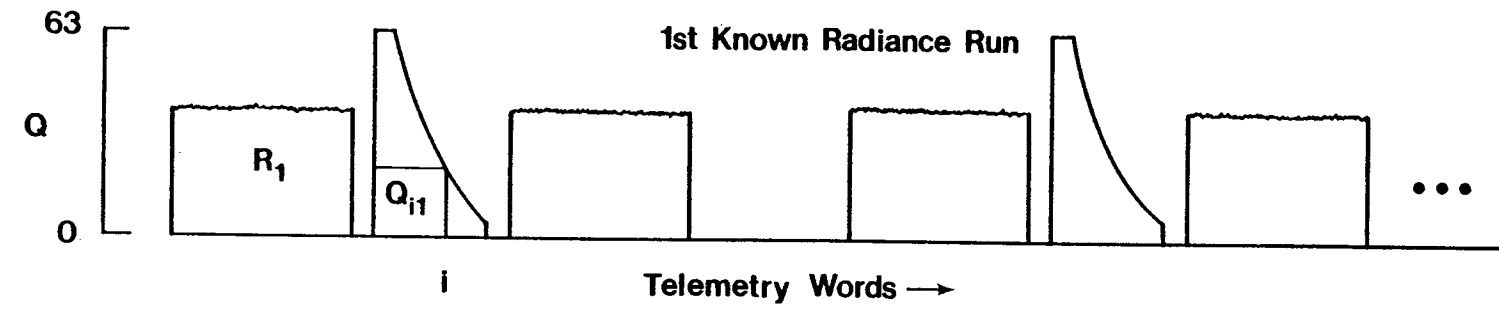
33



Illustrative MSS/PF Lamp Calibration Wedge



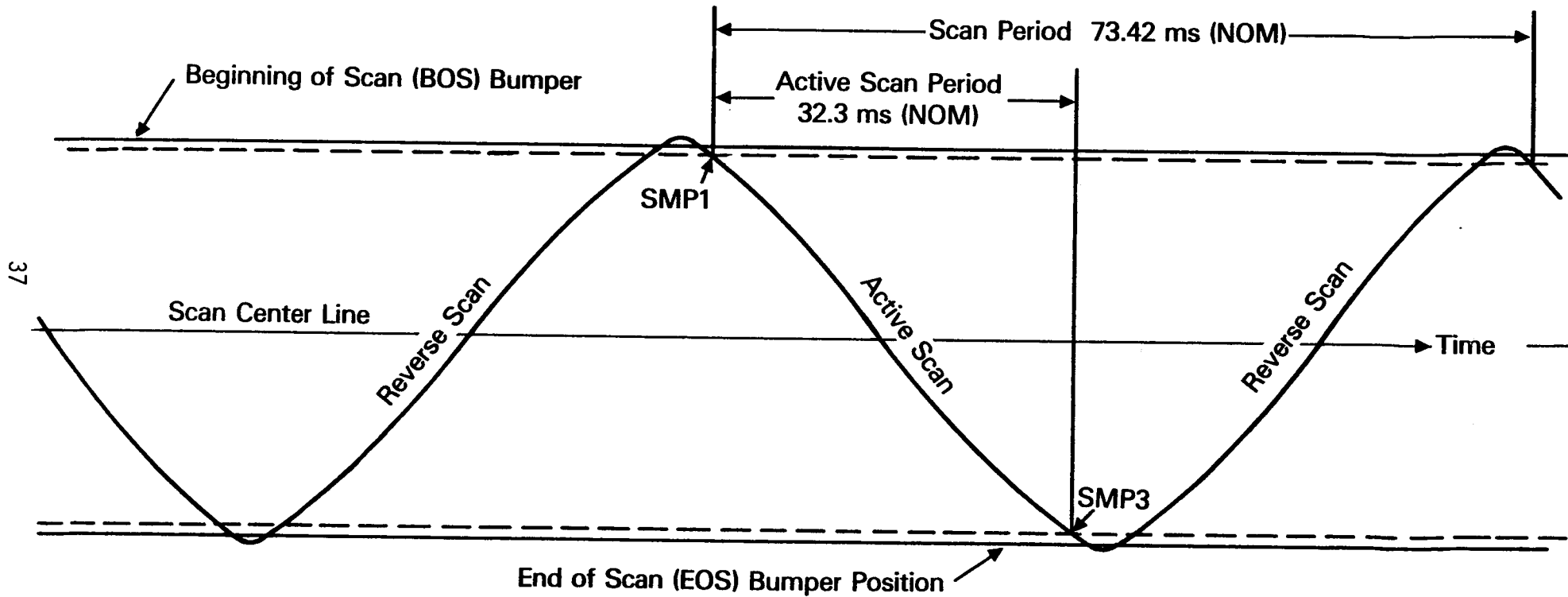
Systematic MSS Video and Wedge Level Timing Sequence



Protoflight MSS-D Geometric Performance Summary

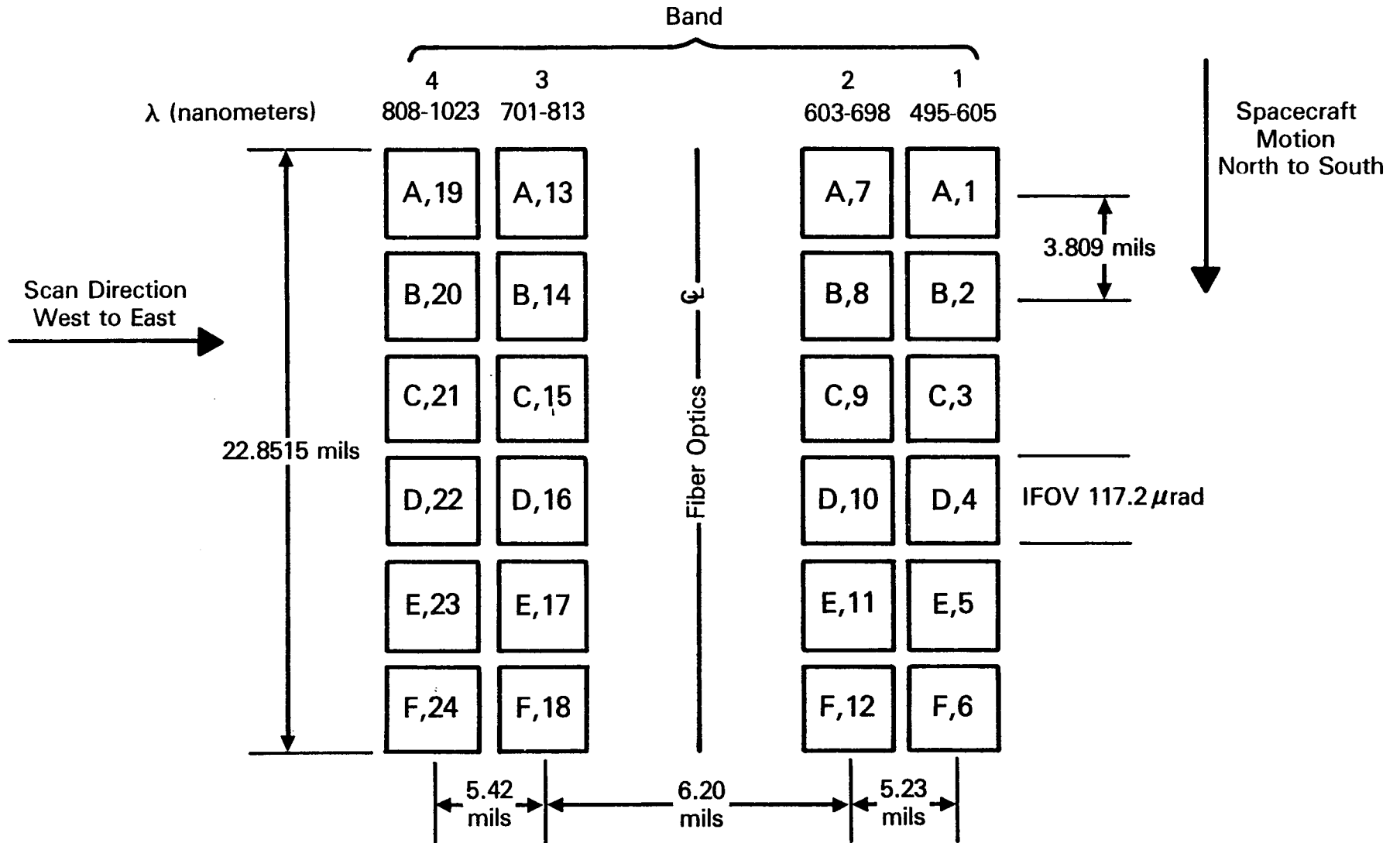
	SPEC	ACTUAL
Line Length Variation		
TM off	42 μ rad (rms)	12-19 μ rad (rms)
TM on	42 μ rad (rms)	109-113 μ rad (rms)
Line Length (Average)	31.5-34 ms	32.3 ms
Total Scan Angle	.26 \pm .001 rad	.2603 rad
Scan Repeatability		
TM off	24 μ rad (rms)	< 3 μ rad (rms)
TM on	24 μ rad (rms)	< 7 μ rad (rms)
Cross Scan		
Systematic	\pm 200 μ rad	< \pm 42 μ rad
Random	24 μ rad (1 σ)	< 3 μ rad
MTF (10]2 μ rad bars)		
Band 1	> .36	.49-.54
Band 2	> .36	.47-.54
Band 3	> .36	.47-.52
Band 4	> .36	.45-.48

Scan Mirror Angle vs. Time Trajectory



SMP = Scan Monitor Pulse

Landsat-D MSS/PF Focal Plane Dimensions

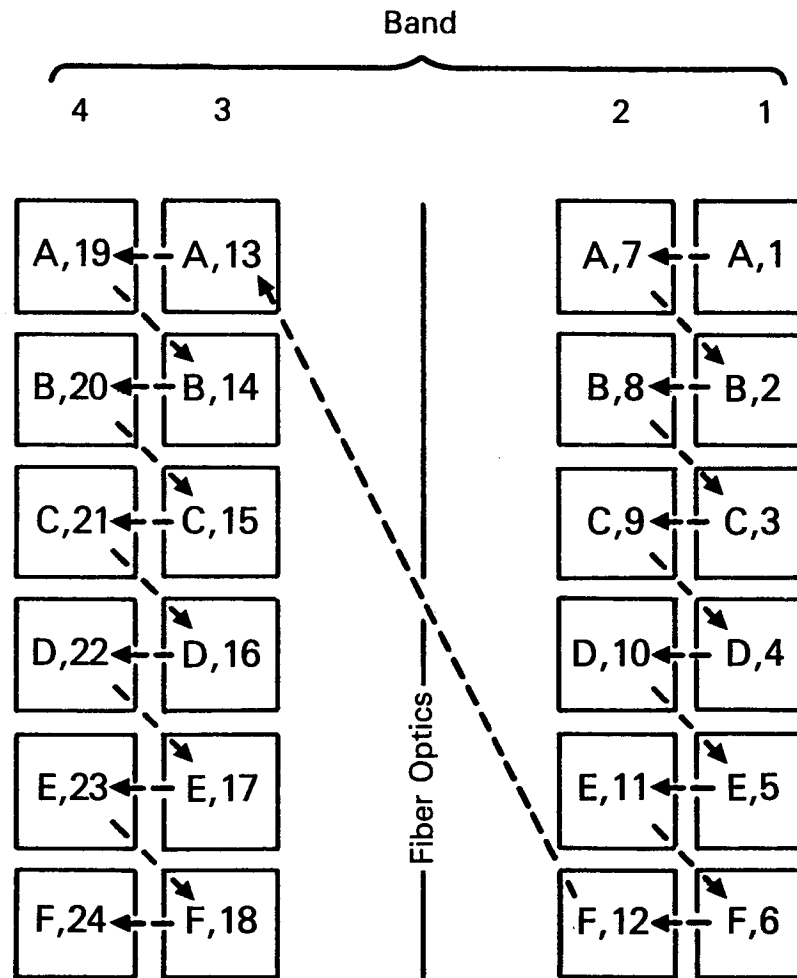


38

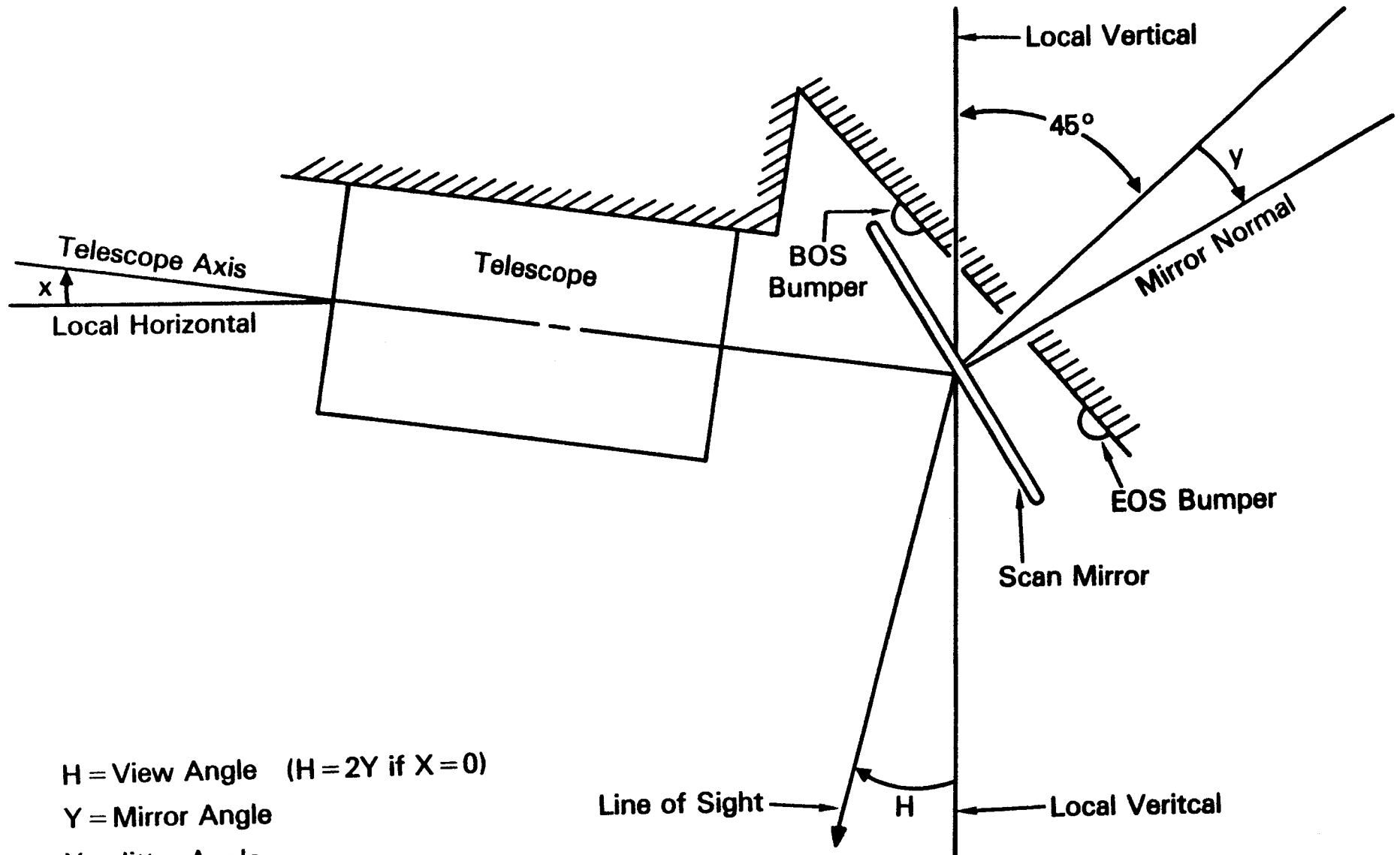
mils = 0.001 inch

Note: Telescope Focal Length = 32.289 inches

MSS Detector Sampling Sequence



MSS Scan Mirror Co-ordinate System



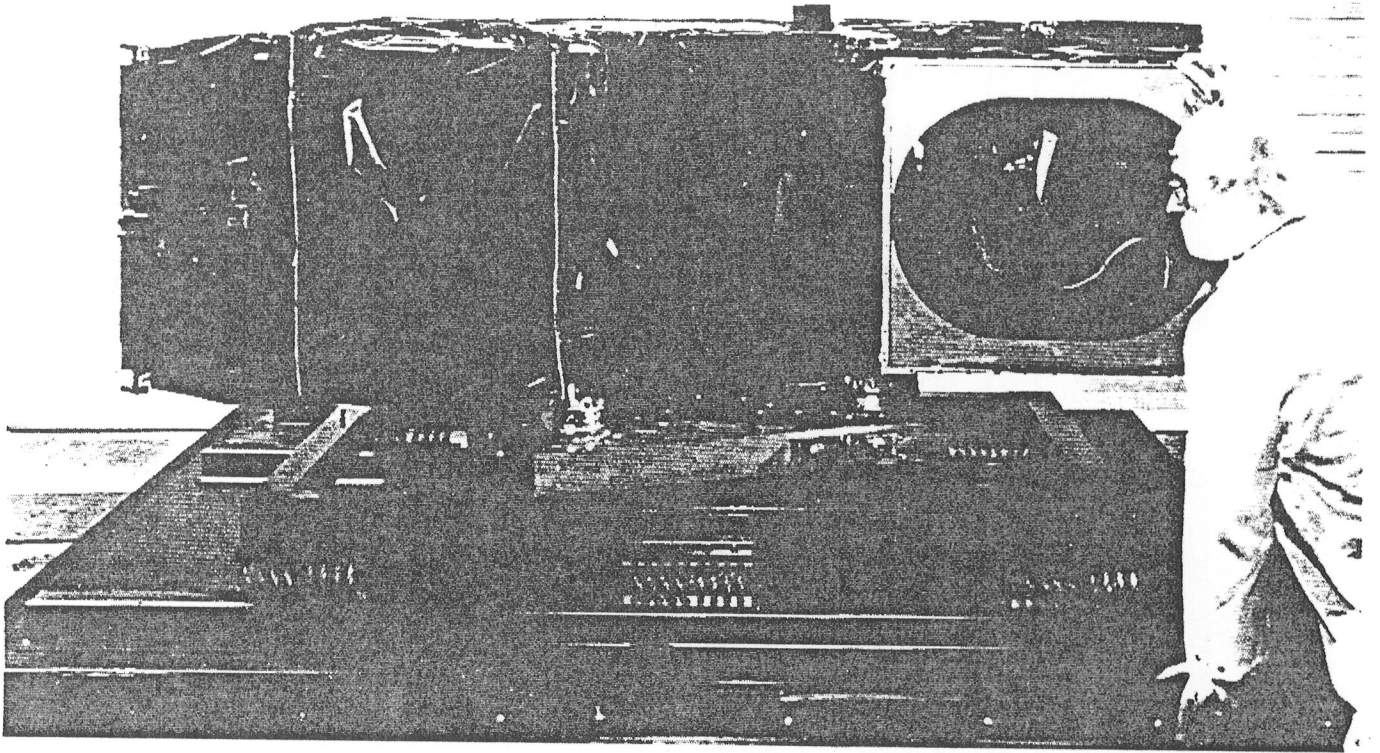
40

H = View Angle ($H = 2Y$ if $X = 0$)
 Y = Mirror Angle
 X = Jitter Angle

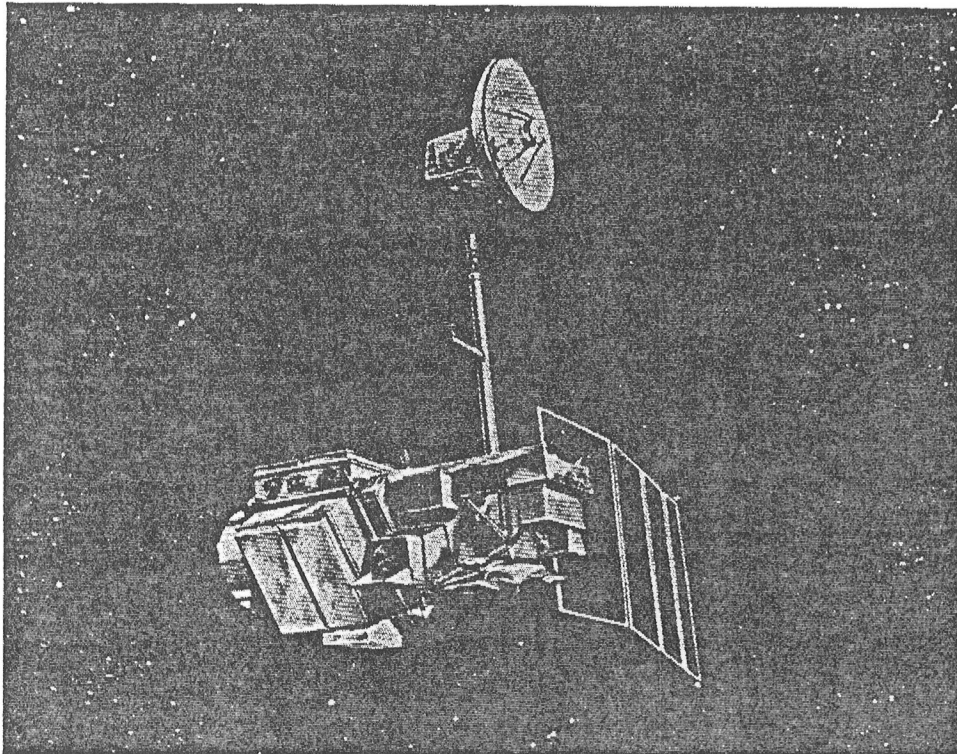
THEMATIC MAPPER (TM) INSTRUMENT DESCRIPTION

JACK ENGEL
SANTA BARBARA RESEARCH CENTER

PROTOFLIGHT THEMATIC MAPPER
ON SHIPPING CONTAINER BASE
(VIEW OF TELESCOPE APERTURE)



LANDSAT-D SPACECRAFT
WITH THEMATIC MAPPER AND MSS



THEMATIC MAPPER

SECOND GENERATION MULTISPECTRAL
EARTH RESOURCES SENSOR
LAUNCHED 16 JULY 1982
LANDSAT D SPACECRAFT

IMPROVED SPATIAL RESOLUTION
IMPROVED SPECTRAL RESOLUTION
IMPROVED RADIOMETRIC SENSITIVITY
IMPROVED SCAN GEOMETRY

DIMENSIONS	201 cm x 66 cm x 109 cm
WEIGHT	244.4 kgm
POWER DEMAND	330 watts
DATA RATE	85 Mbps
DESIGN LIFE	3 YEARS

TM IMPROVEMENTS OVER MSS

SPATIAL RESOLUTION

- TM - 30m
- MSS - 80m
- CLASSIFICATION OF 4-hectare FIELDS (TM)
VS 28.3-hectare FIELDS (MSS)

SPECTRAL RESOLUTION

- TM - 6 REFLECTED LIGHT BANDS (0.45-2.35 μm)
- MSS - 4 REFLECTED LIGHT BANDS (0.5-1.1 μm)
- ADDITION OF THERMAL BAND (10.4-12.5 μm)
- SPECTRAL BANDS ARE MORE OPTIMALLY SELECTED
TO ENHANCE CLASSIFICATION ACCURACY

RADIOMETRIC SENSITIVITY

- LOWER NOISE EQUIVALENT REFLECTANCE
- IMPROVED RADIOMETRIC RESOLUTION & ACCURACY
 - LARGER OPTICS (40.6 cm VS 22.9 cm)
 - IMPROVE SCAN EFFICIENCY (0.85 VS 0.45)
 - MORE DETECTORS PER BAND (16 VS 6)
 - GREATER ENCODING RESOLUTION (8 BITS
VS 6 BITS)

SCAN PROFILE LINEARITY

- TM PEAK NONLINEARITY < 40 μrad
- MSS PEAK NONLINEARITY \approx 500 μrad

THEMATIC MAPPER SPECTRAL
AND SPATIAL CHARACTERISTICS

BAND NO.	SPECTRAL INTERVAL (μm)	DETECTORS (TYPE AND QUANTITY)		IGFOV (μrad)	SPATIAL RESOLUTION (meters)
1	0.45 - 0.52	SIPD	(16)	42.5	30
2	0.52 - 0.60	SIPD	(16)	42.5	30
3	0.63 - 0.69	SIPD	(16)	42.5	30
4	0.76 - 0.90	SIPD	(16)	42.5	30
5	1.55 - 1.75	InSb	(16)	43.75	31
7	2.08 - 2.35	InSb	(16)	43.75	31
6	10.4 - 12.5	HgCdTe	(4)	170	120
		TOTAL	(100)		

SPECTRAL BAND APPLICATIONS

BAND	SPECTRAL RANGE	RADIOMETRIC RESOLUTION	PRINCIPAL APPLICATIONS
1	0.45-0.52 μm	0.8 NE ρ	COASTAL WATER MAPPING; SOIL/VEGETATION DIFFERENTIATION; DECIDUOUS/CONIFEROUS DIFFERENTIATION
2	0.52-0.60 μm	0.5% NE ρ	GREEN REFLECTANCE BY HEALTHY VEGETATION
3	0.63-0.69 μm	0.5% NE ρ	CHLOROPHYL ABSORPTION FOR PLANT SPECIES DIFFERENTIATION
4	0.76-0.90 μm	0.5% NE ρ	BIOMASS SURVEYS; WATER BODY DELINEATION
5	1.55-1.75 μm	1.0% NE ρ	VEGETATION MOISTURE MEASUREMENT; SNOW/CLOUD DIFFERENTIATION
6	10.4-12.5 μm	0.5K NETD	PLANT HEAT STRESS MEASUREMENT; OTHER THERMAL MAPPING
7	2.08-2.35 μm	2.4% NE ρ	HYDROTHERMAL MAPPING

4/82

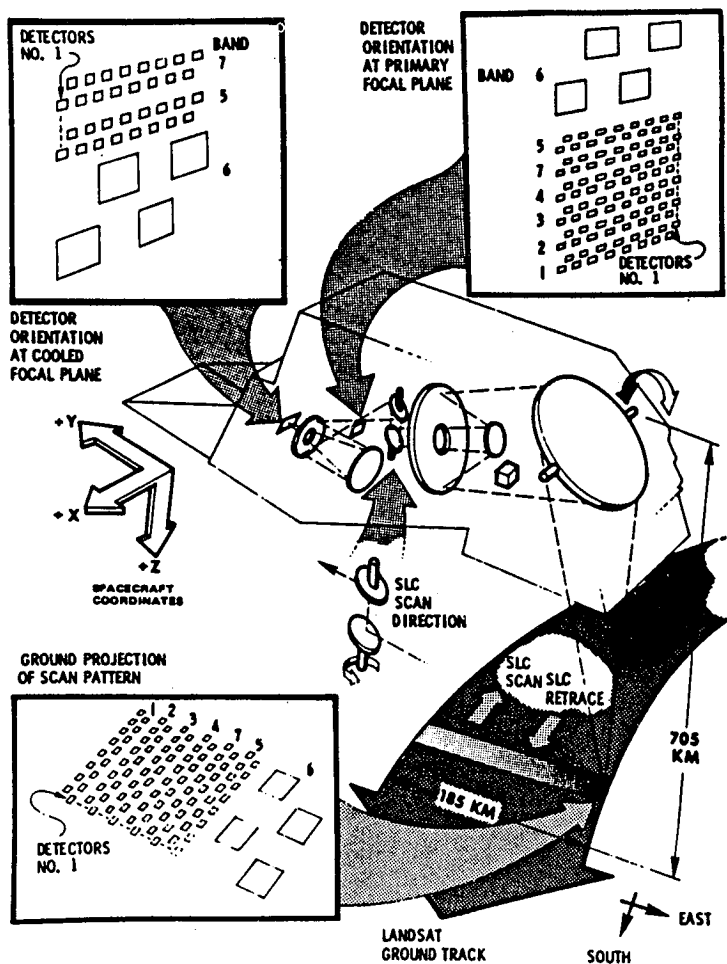
LANDSAT DATA HAVE DIVERSE APPLICATIONS

- AGRICULTURE CROP CLASSIFICATION, YIELD ASSESSMENT
- CARTOGRAPHY 1:96,000, 1:25,000
- ENVIRONMENTAL FOREST & RANGELAND INVENTORY, POLLUTION MONITORING
- GEOLOGY/MINERALOGY TECTONIC MAPPING, ROCK MAPPING, OIL & MINERAL IDENTIFICATION
- LAND USE CLASSIFICATION, PLANNING
- OCEAN/COASTAL MAPPING CURRENTS, WETLANDS INVENTORY, SEDIMENT, PLANKTON
- WATER RESOURCES SNOW/ICE COVER, FLOOD CONTROL, DRAINAGE MAPPING

ORBITAL PARAMETERS

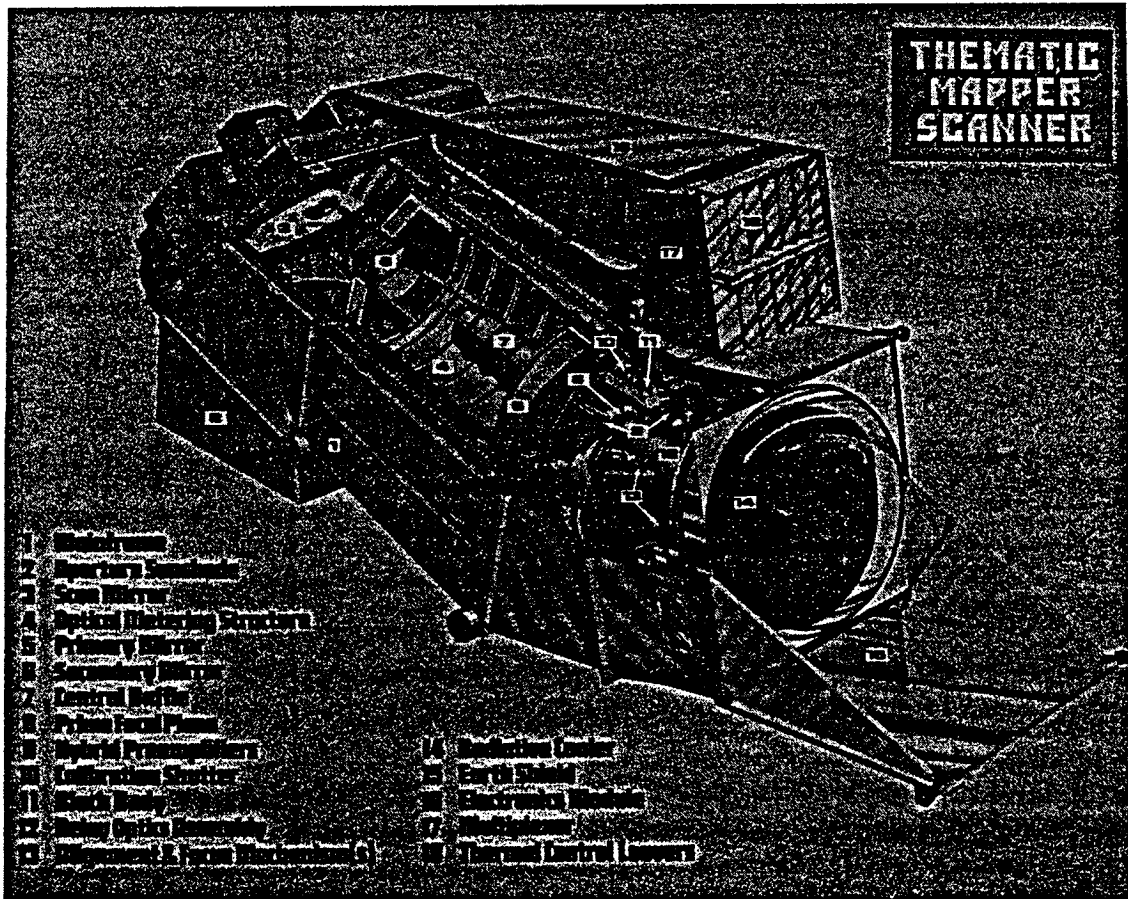
DESCRIPTION	SUN SYNCHRONOUS
TIME OF DAY	9:15 AM - 11:15 AM
LANDSAT D	9:45 AM
ALTITUDE AT 0°N	705.29 km
ALTITUDE AT 40°N	712.47 km
INCLINATION	98.21
ECCENTRICITY	0
REPEAT CYCLE	16 days
PERIOD	98.88 minutes

OPTICAL CONFIGURATION AND FOCAL PLANE PROJECTIONS ON GROUND TRACK



SUBSYSTEMS

CUTAWAY VIEW OF THEMATIC MAPPER SUBSYSTEMS

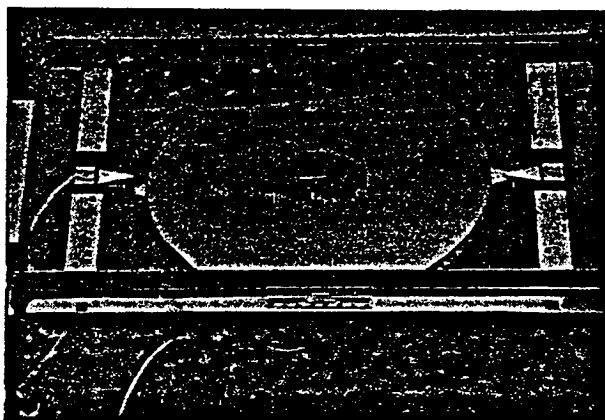


SCAN MIRROR ASSEMBLY

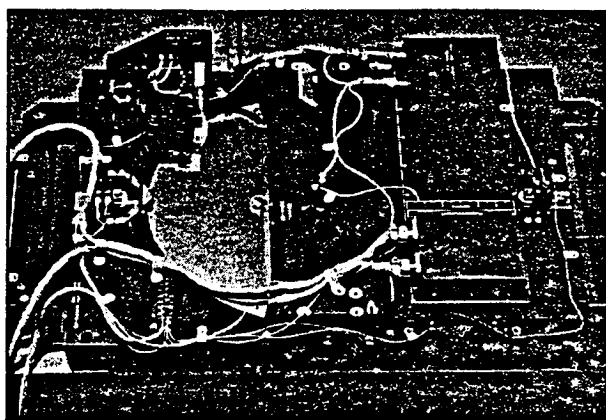
SWATH LENGTH	185 km
SCAN PERIOD	142.925 msec
SCAN FREQUENCY	6.9967 Hz
SCAN EFFICIENCY	0.85
ACTIVE SCAN TIME	60.743 msec
TURNAROUND TIME	10.719 msec
I FOV DWELL TIME	9.611 sec
LINE LENGTH	6320 IFOV
SIZE	21.050 x 16.250 in. (53.47 x 41.28 cm)
MATERIAL	NICKEL-PLATED BERYLLIUM (EGGCRATE) SILVER COATING WITH SiO_2 OVERCOAT

SCAN MIRROR ASSEMBLY

FRONTSIDE



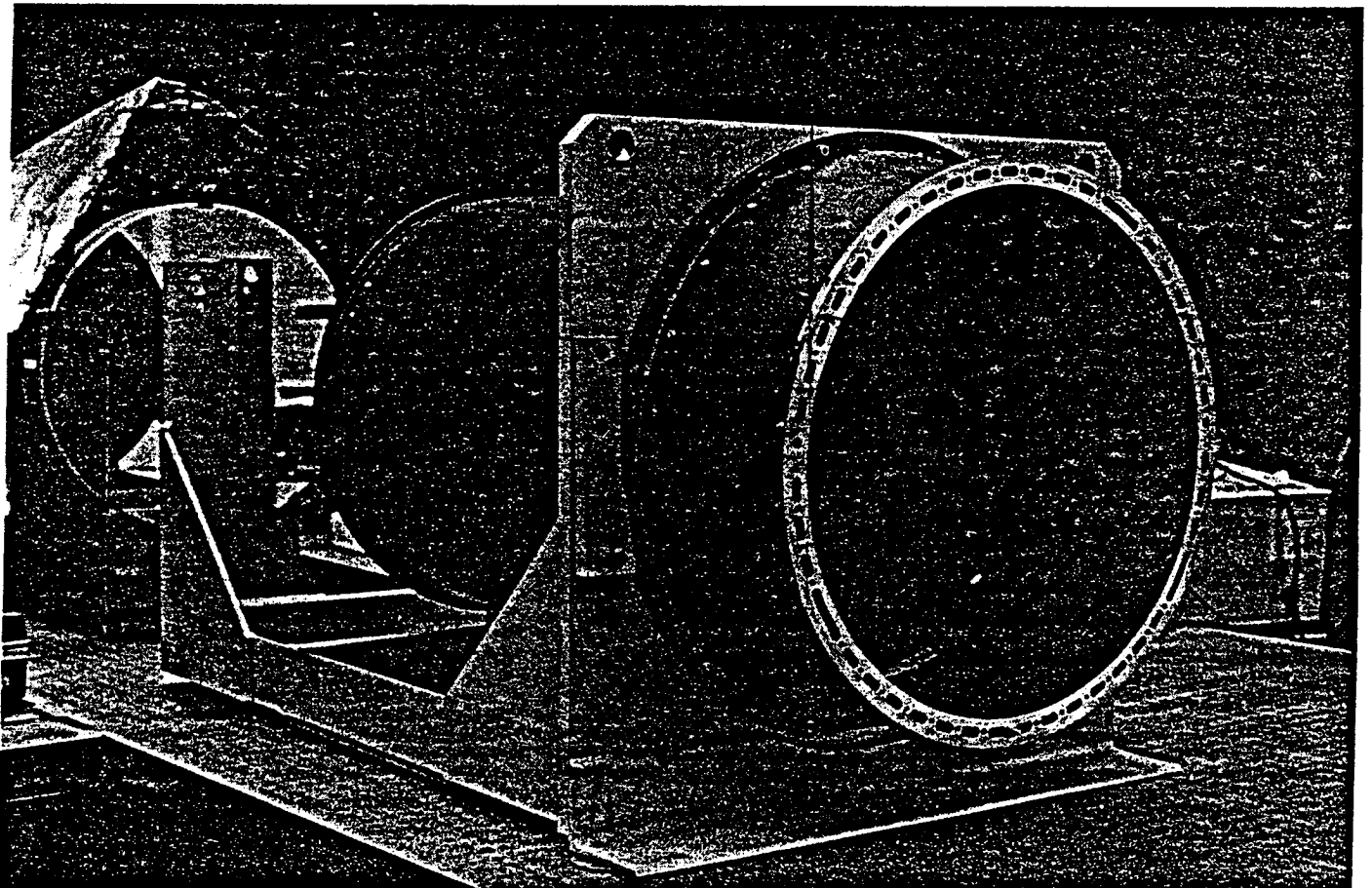
BACKSIDE



PRIMARY TELESCOPE

CONFIGURATION	RITCHY-CHRETIEN
f / NO.	6.0
MIRROR MATERIAL	ULE GLASS (TITANIUM SILICATE), EGGCRATE CONSTRUCTION, SILVER COATING WITH SiO ₂ OVERCOAT
PRIMARY MIRROR CLEAR APERTURE DIAMETER	16.20 in. (41.15 cm)
SECONDARY MIRROR BAFFLE DIAMETER (OBSCURATION)	6.173 in. (15.7 cm)
TELESCOPE CLEAR APERTURE	1056 cm ²
EFFECTIVE FOCAL LENGTH	96 in. (243.8 cm)

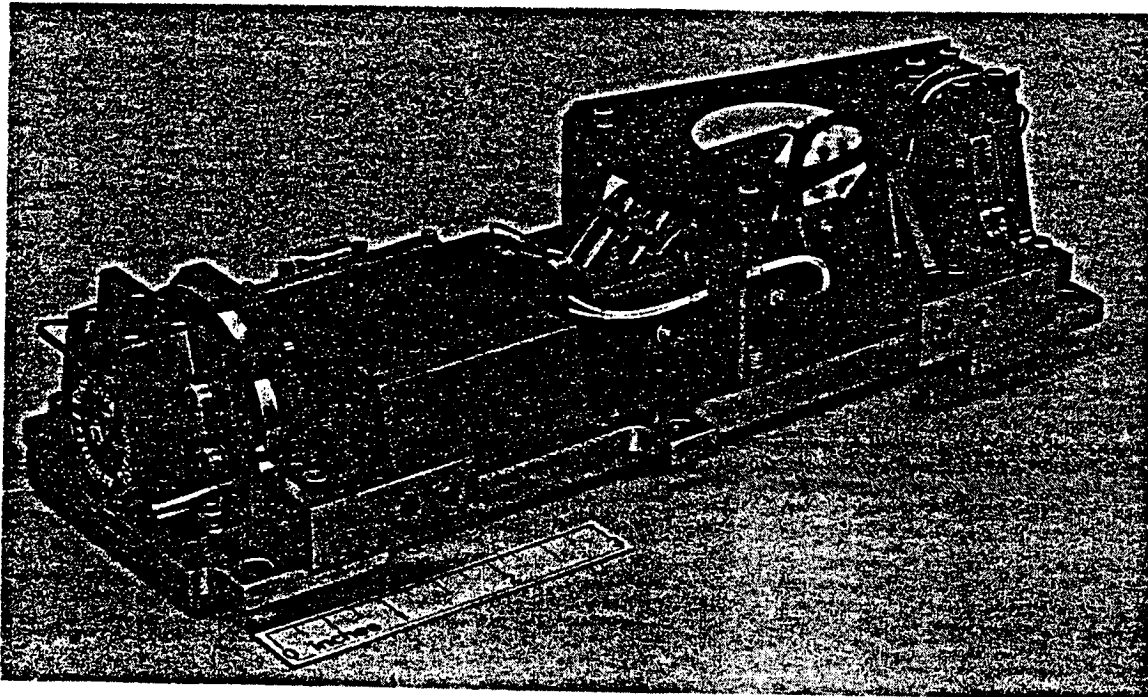
PRIMARY TELESCOPE ASSEMBLY



SCAN LINE CORRECTOR

SCAN FREQUENCY	13.9934 Hz
SCAN PERIOD	71.462 msec
SCAN RATE IN OBJECT SPACE	9.610 mrad/sec
SLC ROTATION RATE	576.6 mrad/sec
SLC LINEAR SCAN ANGLE	35.02 mrad
MIRROR SEPARATION	1.600 in. (4.064 cm)
LINEAR IMAGE DISPLACEMENT AMPLITUDE	0.056 in. (0.142 cm) (13.7 IFOV)
MIRROR MATERIAL	NICKEL-PLATED BERYLLIUM, SILVER COATING WITH SiO_2 OVERCOAT

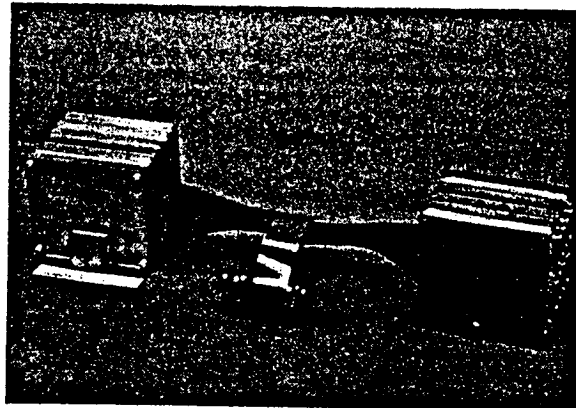
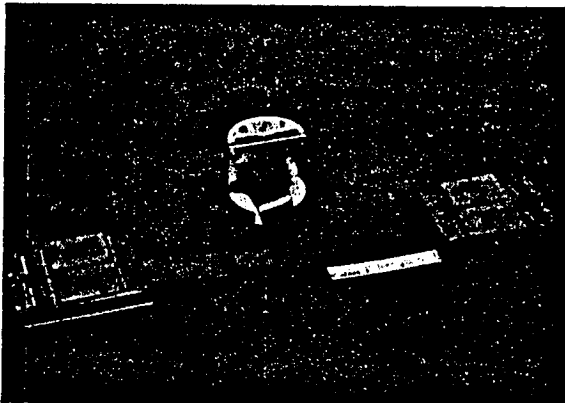
SCAN LINE CORRECTOR ASSEMBLY



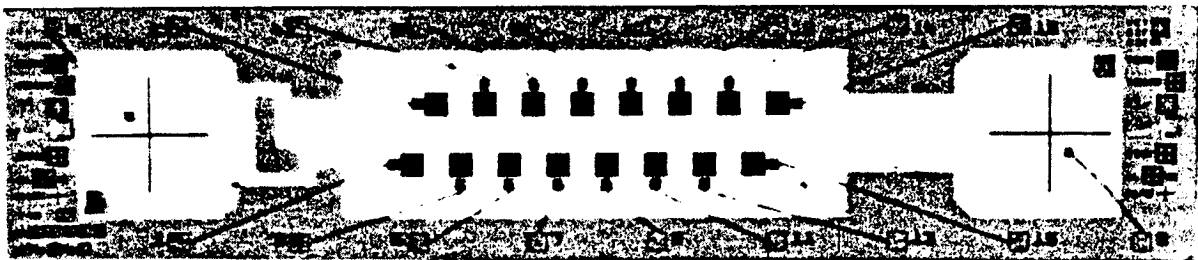
PRIME FOCAL PLANE

NUMBER OF BANDS	4
NUMBER OF DETECTORS (MONOLITHIC SILICON)	16 BANDS
DETECTOR SIZE	0.00408 in sq (0.01036 cm sq)
IFOV SIZE	42.5 μ rad
CENTER-TO-CENTER SPACING IN EACH ROW	0.00816 in (0.0207 cm) (2 IFOV)
CENTER-TO-CENTER SPACING BETWEEN ROWS	0.01020 in (0.0259 cm) (2.5 IFOV)
BAND-TO-BAND SPACING	0.102 in (0.259 cm) (25 IFOV)
OPERATING TEMPERATURE	10°C TO 25°C

PRIME FOCAL PLANE ASSEMBLY



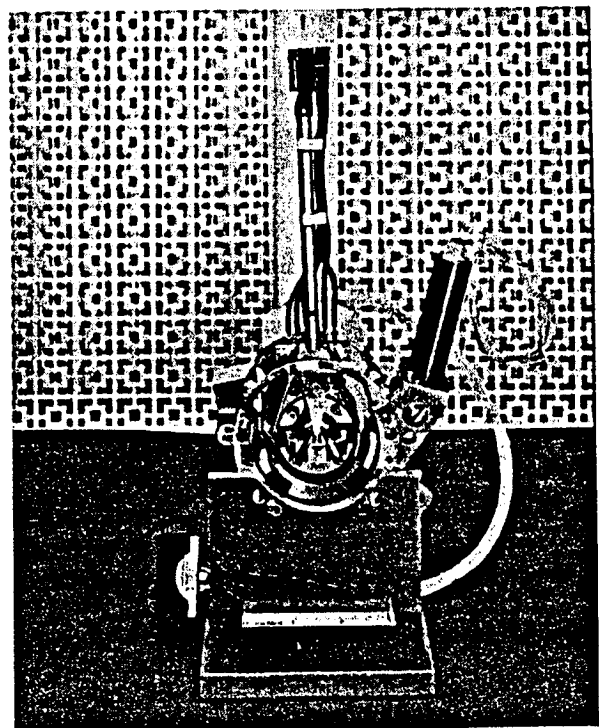
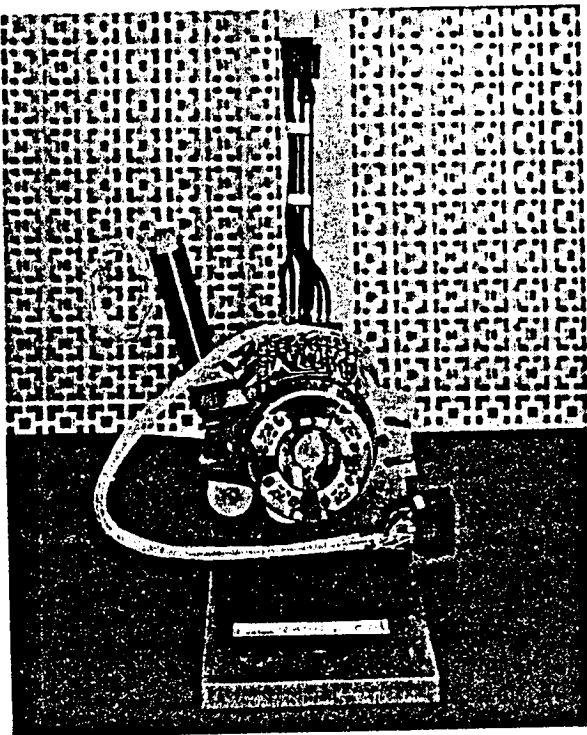
SILICON PHOTODIODE ARRAY (BANDS 1-4)



ON-BOARD CALIBRATOR (AND DC RESTORE SHUTTER)

CALIBRATION	13.9934 Hz (EACH SCAN MIRROR TURNAROUND)
CONFIGURATION	PIVOT MOUNTED SHUTTER
RESONANT FREQUENCY	6.9967 Hz
NUMBER OF CALIBRATION LEVELS BANDS 1 - 5 AND 7	7 + DARK - AUTOMATICALLY SEQUENCED
NUMBER OF SCANS AT EACH LEVEL	40 (APPROXIMATELY 3 sec)
NUMBER OF SAMPLES PER SCAN	APPROXIMATELY 90 SAMPLES
BAND 6 CALIBRATION	MIRROR ON SHUTTER REFLECTING BLACKBODY ENERGY. THREE CONTROLLABLE TEMPERATURES
DC RESTORE	EACH TURNAROUND (BEFORE CALIBRATION, AFTER FORWARD SCAN; AFTER CALIBRATION, AFTER REVERSE SCAN)

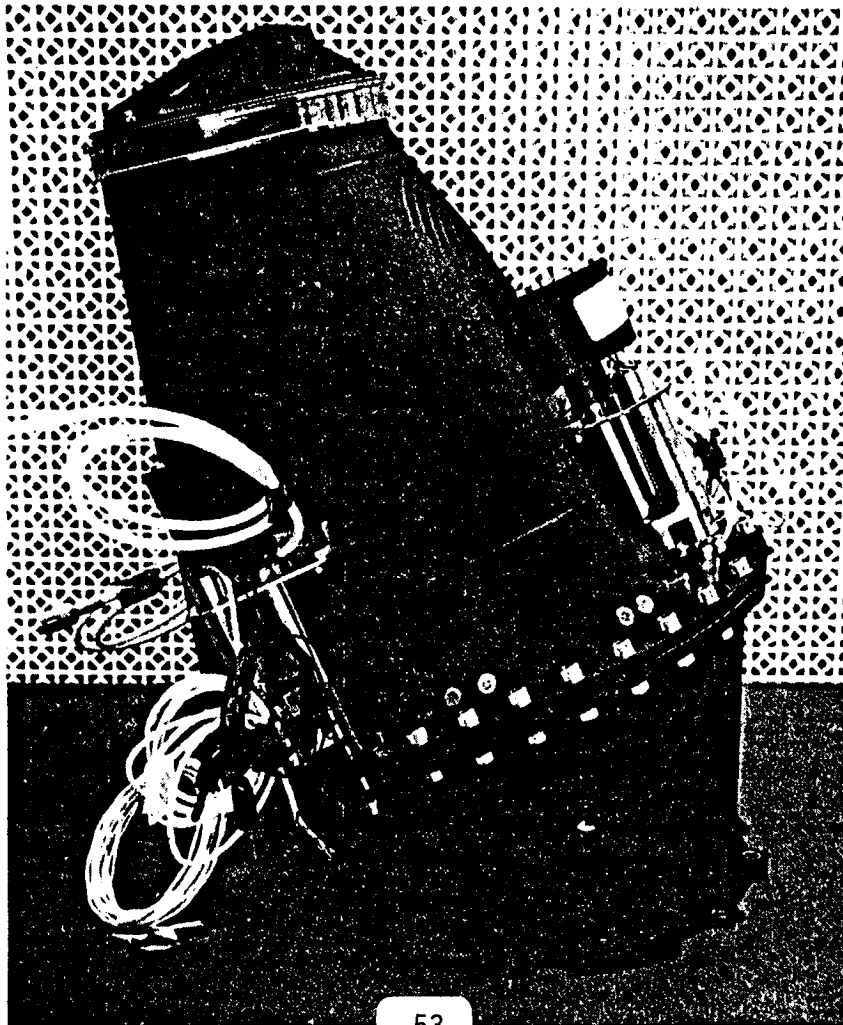
ON-BOARD CALIBRATOR



RELAY OPTICS

RELAY OPTICS ASSEMBLY

ALL REFLECTIVE	2 MIRRORS
OUTER DIAMETER OF FOLDING MIRROR CLEAR APERTURE	3.14 in. (7.98 cm)
INNER DIAMETER OF FOLDING MIRROR CLEAR APERTURE	0.537 in. (1.36 cm)
SPHERICAL MIRROR CLEAR APERTURE DIAMETER	5.538 in. (14.067 cm)
MAGNIFICATION	0.5
f/NO.	3.0
MATERIAL	ULE GLASS (TITANIUM SILICATE), ALUMINUM COATING WITH SiO ₂ OVERCOAT

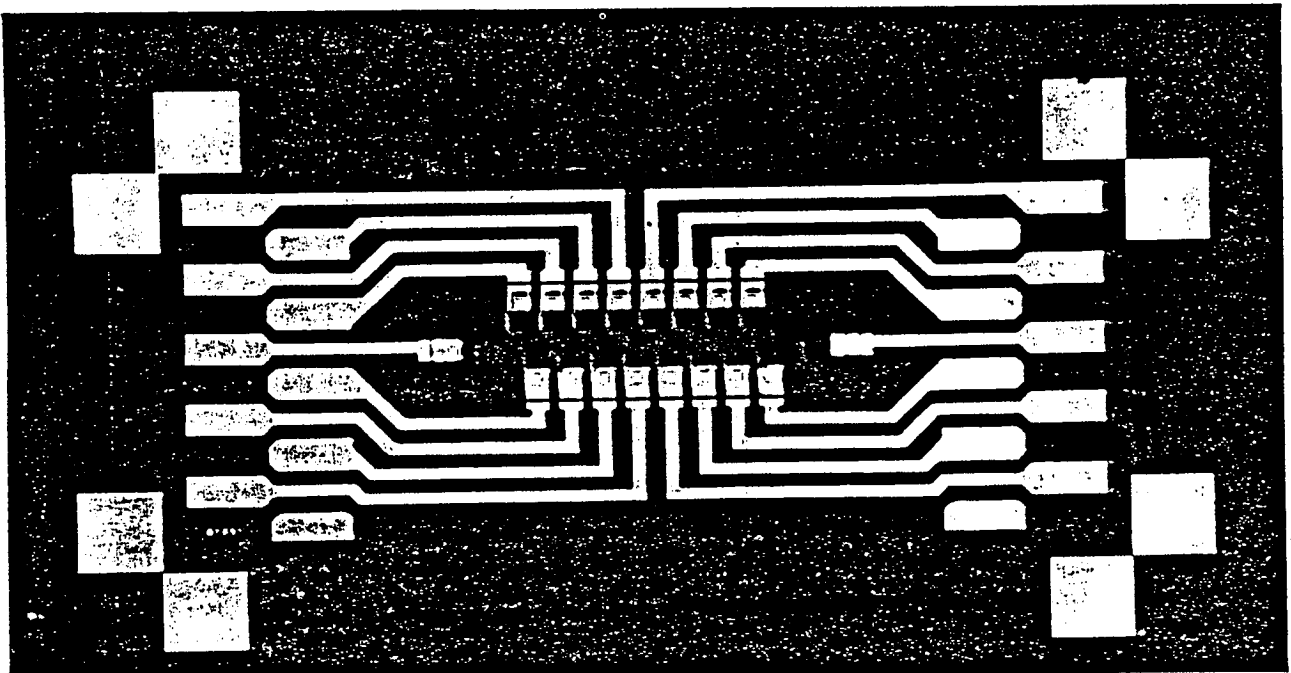


COOLED FOCAL PLANE

COOLED FOCAL PLANE ASSEMBLY

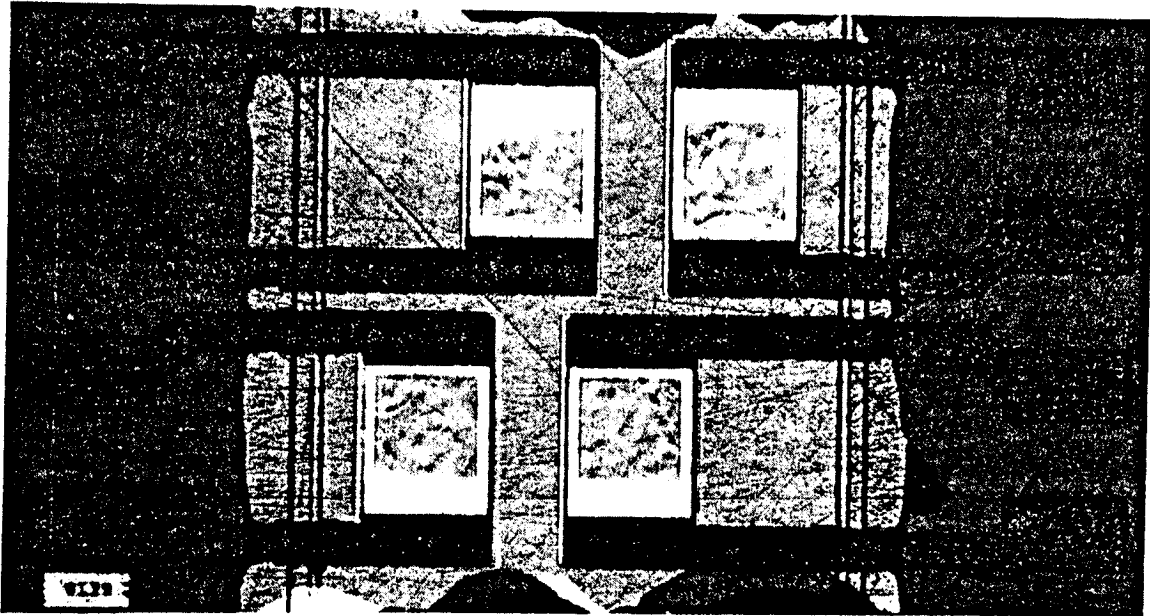
NUMBER OF BANDS	3
NUMBER OF DETECTORS	
BANDS 5, 7 (MONOLITHIC InSb)	16/BAND
BAND 6 (PHOTOCONDUCTIVE HgCdTe)	4
DETECTOR SIZE	
BANDS 5, 7	0.0021 in. sq (0.00533 cm sq)
BAND 6	0.00816 in. sq (0.0207 cm sq)
IFOV SIZE	
BANDS 5, 7	43.75 μ rad
BAND 6	170.0 μ rad
CENTER-TO-CENTER SPACING IN EACH ROW	
BANDS 5, 7	0.00408 in. (0.01036 cm) (2 IFOV)
BAND 6	0.01632 in. (0.04145 cm) (2 IFOV)
CENTER-TO-CENTER SPACING BETWEEN ROWS	
BANDS 5, 7	0.00510 in. (0.01295 cm) (2.5 IFOV)
BAND 6	0.02040 in. (0.0518 cm) (2.5 IFOV)
BAND 7 - 5 SPACING	0.053 in. (0.135 cm) (26 IFOV)
BAND 5 - 6 SPACING	0.071 in. (0.180 cm) (34.75 IFOV)
OPERATING TEMPERATURES	90K, 95K, 105K

INDIUM ANTIMONIDE (INSB) PHOTODIODE DETECTOR ARRAY (BANDS 5 AND 7)

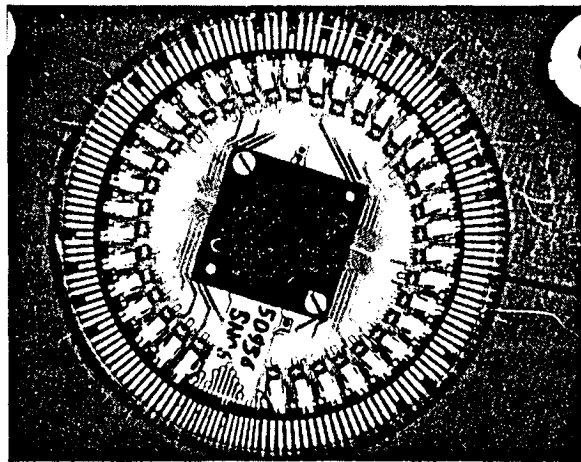
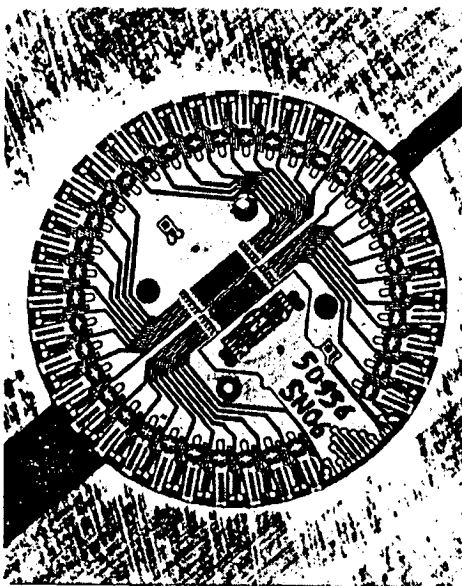


COOLED FOCAL PLANE

MERCURY CADMIUM TELLURIDE (HgCdTe)
DETECTOR ARRAY (BAND 6)



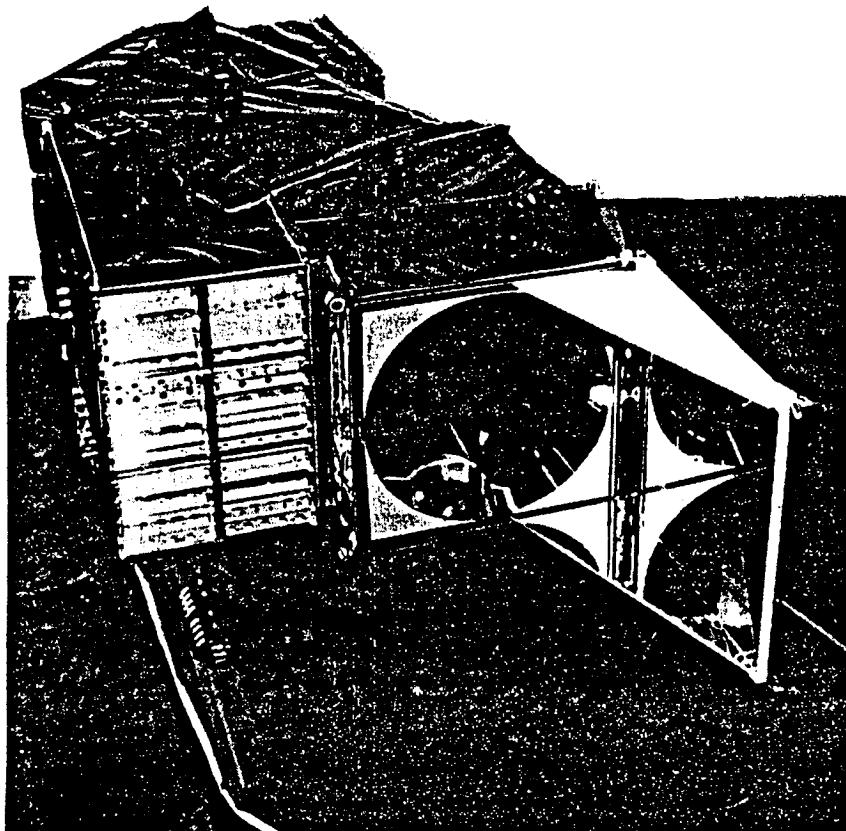
COOLED FOCAL PLANE SUBSTRATE
ASSEMBLY WITH AND WITHOUT
SPECTRAL FILTERS



RADIATIVE COOLER

HORIZONTAL FIELD OF VIEW	160°
VERTICAL FIELD OF VIEW	114°
INTERMEDIATE STAGE RADIATOR AREA	660 cm ²
COLD STAGE RADIATOR AREA	430 cm ²
COLD STAGE MINIMUM TEMPERATURE CAPABILITY (ALL BANDS ON)	84.4K
RADIATION SURFACE	BLACK PAINTED HONEYCOMB
INTERMEDIATE STAGE TEMPERATURE	≈ 147K
INTERMEDIATE STAGE HEAT LOAD	2.2 watts
COLD STAGE HEAT LOAD	117 mw

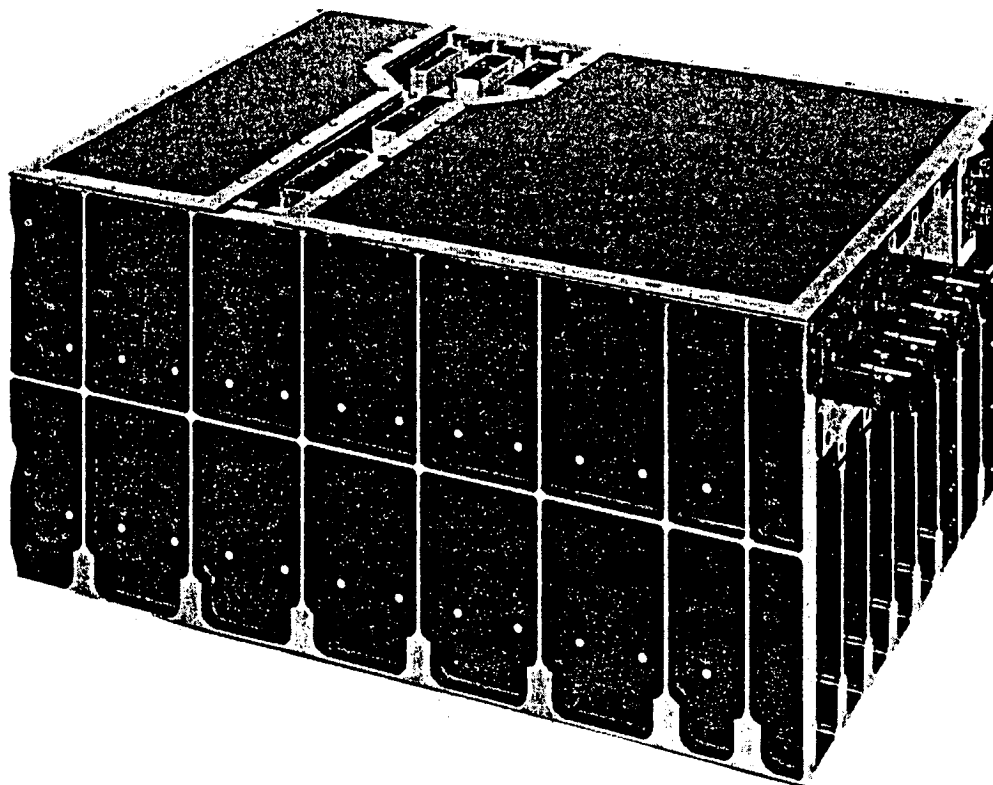
PROTOFLIGHT THEMATIC MAPPER ON BASE SHIPPING CONTAINER BASE (VIEW OF RADIATIVE COOLER)



MULTIPLEXER

BIT RATE	84.903 mbps (PN CODED)
ENCODING RESOLUTION	8 BITS (256 LEVELS)
THRESHOLD ACCURACY	$\pm \frac{1}{2}$ LSB
WORD RATE	10.613×10^6 words/sec
MINOR FRAME RATE	104.048×10^3 frames/sec
MINOR FRAME TIME	9.611 μ sec
WORDS / MINOR FRAME	102
POWER REQUIREMENT	120 watts

THEMATIC MAPPER MULTIPLEXER



SYSTEM PERFORMANCE

MEASURED THEMATIC MAPPER PERFORMANCE

- SPECTRAL COVERAGE
- RADIOMETRIC SENSITIVITY
- MODULATION TRANSFER FUNCTION
- BAND-TO-BAND REGISTRATION
- SCAN GEOMETRY

MEASURED SPECTRAL COVERAGE (μM)

BAND	REQUIREMENT		PF PERFORMANCE		FLT PERFORMANCE	
	50% RESPONSE BAND EDGE, μm	50% RESPONSE BAND EDGE, μm	50% RESPONSE BAND EDGE, μm	50% RESPONSE BAND EDGE, μm	LOWER	UPPER
	LOWER	UPPER	LOWER	UPPER		
1	0.45±0.01	0.52±0.01	0.45	0.52	0.45	0.52
2	0.52±0.01	0.60±0.01	0.53	0.61	0.53	0.61
3	0.63±0.02	0.69±0.01	0.62	0.69	0.61	0.69
4	0.76±0.02	0.90±0.01	0.78	0.91	0.77	0.89
5	1.55±0.02	1.75±0.02	1.57	1.78	1.56	1.76
6	10.4±0.10	12.5±0.10	10.42	11.61	10.45	12.43
7	2.08±0.03	2.35±0.03	2.10	2.35	2.08	2.35

SYSTEM PERFORMANCE

MEASURED PROTOFLIGHT RADIOMETRIC SENSITIVITY

BAND	SCENE RADIANCE (mW/cm ² SR)		SNR				NE _p (%)	
	MINIMUM SPECIFIED	MAXIMUM SPECIFIED	MINIMUM SCENE		MAXIMUM SCENE		MEASURED	SPECIFIED
			MEASURED	SPECIFIED	MEASURED	SPECIFIED		
1	0.28	1.00	52.0	32	143.0	85	0.16	0.8
2	0.24	2.33	60.0	35	279.0	170	0.18	0.5
3	0.13	1.35	48.0	26	248.0	143	0.20	0.5
4	0.19	3.00	35.0	32	342.0	240	0.19	0.5
5	0.08	0.60	40.0	13	194.0	75	0.23	1.0
6	300K	320K	NEΔT = 0.12K	NEΔT = 0.5K	NEΔT = 0.10K	NEΔT = 0.42K		
7	0.046	0.43	21.0	5	164.0	45	0.41	2.4

* BAND 5 CHANNEL 3 - BAD DETECTOR

BAND 2 CHANNEL 2 AND 4 - PPOR MTF

BAND 7 CHANNEL 7 - NOISIER THAN OTHERS BUT MEETS SNR REQUIREMENTS


96 CHANNELS FULLY FUNCTIONAL

MEASURED FLIGHT MODEL RADIOMETRIC SENSITIVITY

BAND	SCENE RADIANCE (mW/cm ² SR)		SNR				NE _p (%)	
	MINIMUM SPECIFIED	MAXIMUM SPECIFIED	MINIMUM SCENE		MAXIMUM SCENE		MEASURED	SPECIFIED
			MEASURED	SPECIFIED	MEASURED	SPECIFIED		
1	0.28	1.00	60.3	32	143.2	85	0.16	0.8
2	0.24	2.33	59.7	35	234.9	170	0.21	0.5
3	0.13	1.35	46.25	26	215.1	143	0.23	0.5
4	0.19	3.00	46.2	32	298.7	240	0.22	0.5
5	0.08	0.60	35.8	13	176.4	75	0.25	1.0
7	0.046	0.43	28.3	5	180.6	45	0.37	2.4
6	300K	320K	NEΔT = 0.13	NEΔT = 0.5K	NEΔT = 0.11	NEΔT = 0.42K		

SYSTEM PERFORMANCE

MTF REQUIREMENTS WERE MET WITH MARGIN

BAND	SQUARE-WAVE RESPONSE AT NYQUIST FREQUENCY		
	SPECIFIED	MEASURED PF	MEASURED FLT
1	0.35 	0.46	0.42
2		0.44	0.41
3		0.41	0.39
4		0.43	0.40
5		0.42	0.44
7		0.44	0.42
6		0.44	0.43

MEASURED PROTOFLIGHT DYNAMIC
BAND-TO-BAND REGISTRATION (BBR)

	<u>MEASURED</u>	<u>SPECIFIED</u>
ALONG SCAN REGISTRATION		
WITHIN PFPA	< 0.1 IFOV	≤ 0.2 IFOV (6 meters)
WITHIN CFPA	< 0.08 IFOV	≤ 0.2 IFOV (6 meters)
CFPA TO PFPA	< 0.19 IFOV	≤ 0.3 IFOV (9 meters)
CROSS SCAN REGISTRATION		
WITHIN PFPA	< 0.13 IFOV	≤ 0.2 IFOV (6 meters)
WITHIN CFPA	< 0.10 IFOV	≤ 0.2 IFOV (6 meters)
CFPA TO PFPA	< 0.27 IFOV	≤ 0.3 IFOV (9 meters)

SYSTEM PERFORMANCE

MEASURED PROTOFLIGHT GEOMETRIC ACCURACY

SCAN RATE

- AVERAGE RATE WITHIN 0.05% OF NOMINAL RATE

OVERLAP/UNDERLAP

- MISSION REQUIREMENTS WILL BE MET ON-ORBIT (LESS THAN 6 METERS NEGLECTING BOWTIE EFFECT)

SCAN LINE LENGTH

- 400 SCAN STATISTICS (TYPICAL)
 - AVERAGE = 60742.89 μ s
 - MAXIMUM = 60747.35 μ s
 - MINIMUM = 60738.30 μ s
 - σ = 1.71 μ s (ONE IFOV DWELL TIME = 9.61 μ s)

SCAN PROFILE LINEARITY

- PEAK NONLINEARITY < 25 μ rad FORWARD SCAN
< 40 μ rad REVERSE SCAN

SCAN PROFILE REPEATABILITY

- BOTH FORWARD AND REVERSE PROFILES ARE REPEATABLE TO WITHIN 3 μ rad AFTER APPLICATION OF MIDSCAN CORRECTION

AN OVERVIEW OF LANDSAT-4 AND THE THEMATIC MAPPER

JAMES R. IRONS
NASA/GODDARD SPACE FLIGHT CENTER

Knowledge of the Landsat-4 satellite, its orbit, and Thematic Mapper (TM) sensor design, and the ground processing of TM data is essential to the effective utilization of TM data for scientific research and applications. The first three Landsat satellites were quite similar in design and operation. The design of Landsat-4 incorporates several technological advancements which include a new sensor, the TM. The TM offers refinements over the familiar Multispectral Scanners (MSS's) aboard all of the Landsat satellites in terms of spatial, spectral, and radiometric resolutions. TM data undergo radiometric and geometric corrections on the ground to provide investigators with pictorial and digital image data products. Investigators have just begun to evaluate the quality and utility of TM data.

Landsat-4 is the first of the Landsat series to conform to NASA's Multimission Modular Spacecraft design. The new design permits three-axis control of attitude along with improved pointing accuracy (0.01 degree) and stability (10^{-6} degree/second). The first three Landsat-satellites allowed only one-axis control of attitude resulting in a 0.7 degree pointing accuracy and 0.01 degree/second stability.

Landsat-4 was launched into a circular, near-polar, sun-synchronous orbit on July 16, 1982. The orbit's inclination angle is 98.2 degrees and the satellite's altitude is 705 km. The satellite crosses the equator at approximately 9:45 a.m. local solar time during the descending (north-to-south) portion of each orbit. The TM will occasionally acquire night-time thermal data during the ascending portion (9:45 p.m. equatorial crossing) of each orbit.

The Landsat-4 instrument payload consists of a MSS and the TM. When compared to the MSS, the TM represents a refinement in sensor technology. The advanced design of the TM affords new remote sensing capabilities which include: additional and more optimally placed spectral bands when compared to the MSS bands; a finer spatial resolution (30m) than the MSS resolution (80m); and enhanced radiometric sensitivity permitting eight-bit data quantization in comparison to the six-bit quantization of MSS data.

The previous three Landsat satellites depended upon tape recorders to store MSS data until the satellites flew within the range of a ground receiving station. The recorders proved less reliable than the other components of the system and Landsat-4 does not carry recorders for either MSS or TM data. Instead, Landsat-4 will eventually use the Tracking and Data Relay Satellite (TDRS) system to transmit these data to a single receiving station in White Sands, New Mexico. The capability to transmit MSS and TM data directly to ground stations is also provided for the interim between the launch of Landsat-4 and the initiation of TDRS operations. Unfortunately, after transmitting approximately 6000 TM scenes, the transmitter for TM data failed and TM data will not often be received until routine TDRS operations begin after the autumn of 1983.

Available TM data are sent to facilities at NASA's Goddard Space Flight Center (GSFC) for ground processing. Processing begins with radiometric corrections to remove striping caused by slight differences in the radiometric response of the 16 detectors used to generate the data for each TM spectral band (four detectors are used for TM's thermal band). Geometric corrections are performed next to create nearly conformal representations of the earth's surface consisting of TM multispectral digital image data which are precisely registered from band-to-band. To this end, TM data from each band are registered to either the Space Oblique Mercator or the Universal Transverse Mercator cartographic projections. Corrected TM data are then shipped to the EROS Data Center for public dissemination.

Early analyses of TM data indicate that both the sensor and the ground data processing system are performing well. Slight band-to-band misregistration and indistinct detector-to-detector striping have been found

in TM data, but these findings have lead to adjustments in the geometric and radiometric correction procedures which should further improve data quality. Overall, most indicators of radiometric and geometric quality are comparable to or exceed prelaunch specifications.

THEMATIC MAPPER SENSOR CHARACTERISTICS

JACK ENGEL
SANTA BARBARA RESEARCH CENTER

DISCUSSION TOPICS

Instantaneous Field of View Size

Rise Time

Delay Time

MTF (Square Wave Response)

Bright Target Recovery

Altitude Effects

Band-to-Band Registration

Scan Profile Linearity

INSTANTANEOUS FIELD OF VIEW SIZE

SPATIAL COVERAGE PROTOFLIGHT MODEL
COOLED FOCAL PLANE

BAND	CHANNEL	LINE SPREAD FUNCTION WIDTH (μ rad)		
		TRACK	SCAN	SPECIFIED
5	2	47.5	42.6	≤ 46.35
5	16	46.9	42.5	
7	2	47.8	45.5	
7	16	49.6	44.8	
6	1	172.2	173.0	≤ 174.4
6	2	173.8	170.2	
6	3	177.5	178.3	
6	4	175.3	174.0	

PRIME FOCAL PLANE

BAND	CHANNEL	LINE SPREAD FUNCTION WIDTH (μ rad)		
		TRACK	SCAN	SPECIFIED
1	2	44.4	44.0	≤ 43.2
1	16	43.4	42.3	
2	1	44.8	44.9	
2	15	---	---	
3	2	45.5	45.1	
3	16	43.9	44.9	
4	2	44.0	44.1	
4	16	43.1	44.5	

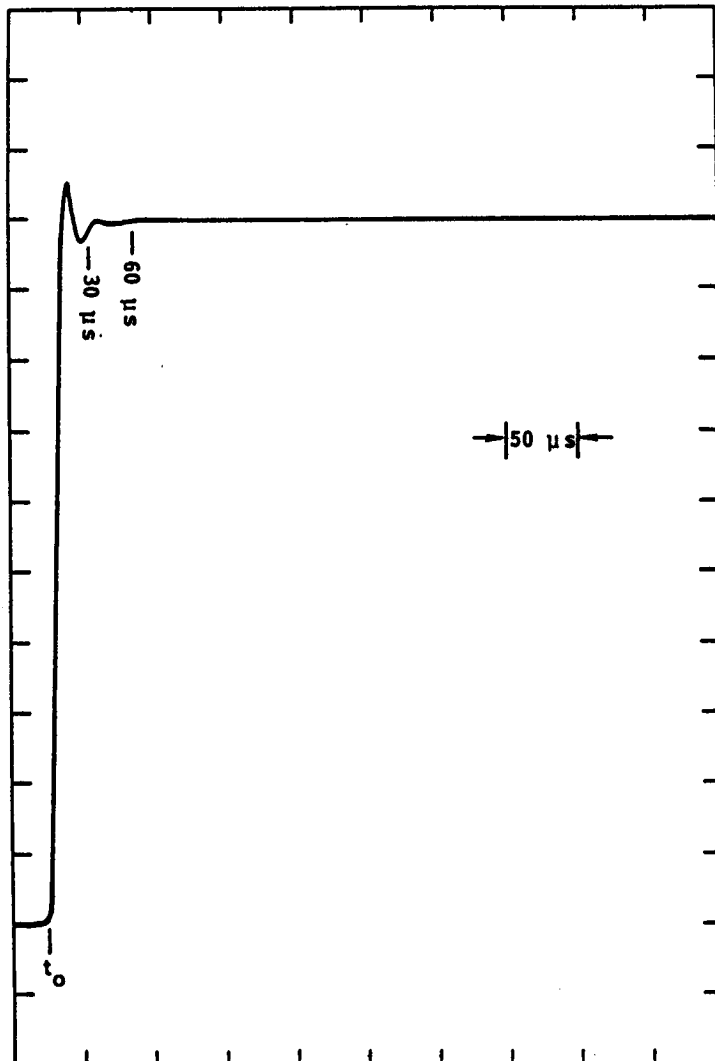
STEP RESPONSE CHARACTERISTICS

STEP RESPONSE BANDS 1 TO 5, & PROTOFLIGHT MODEL

PARAMETER	SPECIFICATION	PERFORMANCE
OVERSHOOT	<u><10%</u>	<u><10%</u> 3.5% TYP, BANDS 1-4 8.0% TYP, BANDS 5,7
SETTLING TIMES	<u><1.5% ERROR AFTER 30 μSEC</u> <u><1.0% ERROR AFTER 60 μSEC</u>	<u><1.5% AFTER 35 μSEC</u> EXCEPT BAND 2 CHAN 6 = 2.1% BAND 3 CHAN 2 = 1.8% <u><1.0% EXCEPT</u> BAND 2 CHAN 6 = 2.1% ≤ 1% IN 100 μs CHAN 8 = 1.1% ≤ 1% IN 100 μs BAND 3 CHAN 2 = 1.8% CHAN 8 = 1.1% CHAN 14 = 1.4%
RISETIME	<u><20 μSEC</u>	<u><17 μSEC</u>
DROOP	<u><0.5%</u>	NO DATA

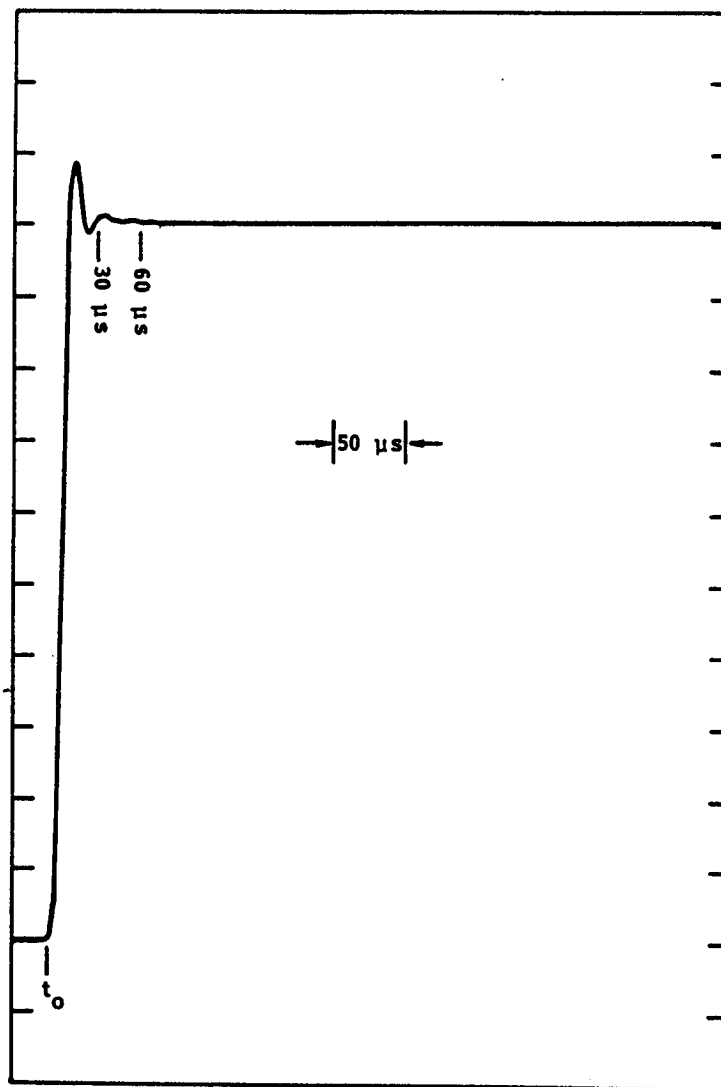
STEP RESPONSE CHARACTERISTICS

TYPICAL RESPONSE TO A STEP OF RADIANCE
(BANDS 1-4) (BAND 3 CHANNEL 7)



STEP RESPONSE CHARACTERISTICS

TYPICAL RESPONSE TO A STEP OF RADIANCE BANDS 5 & 7
(BAND 5 CHANNEL 5)



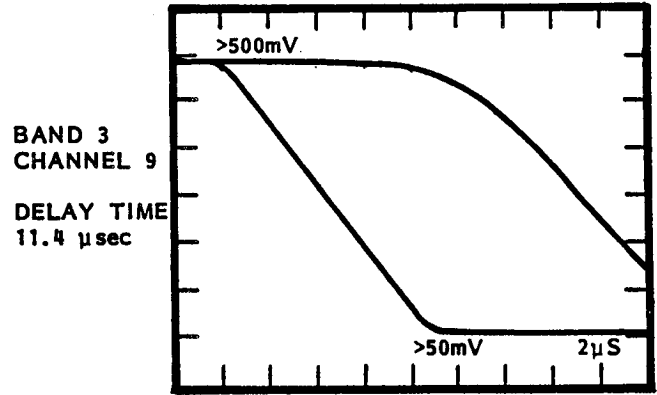
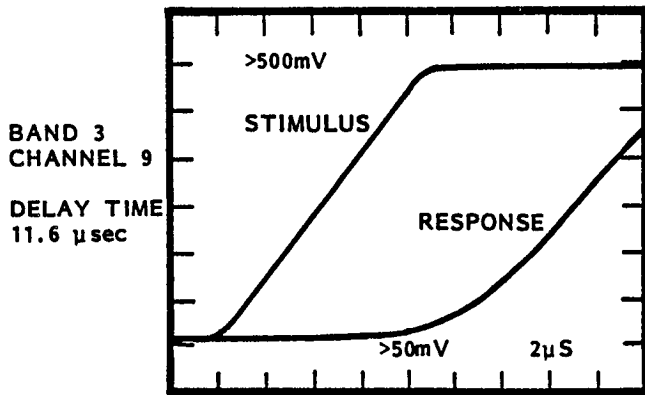
STEP RESPONSE CHARACTERISTICS

STEP RESPONSE BAND 6 PROTOFLIGHT MODEL

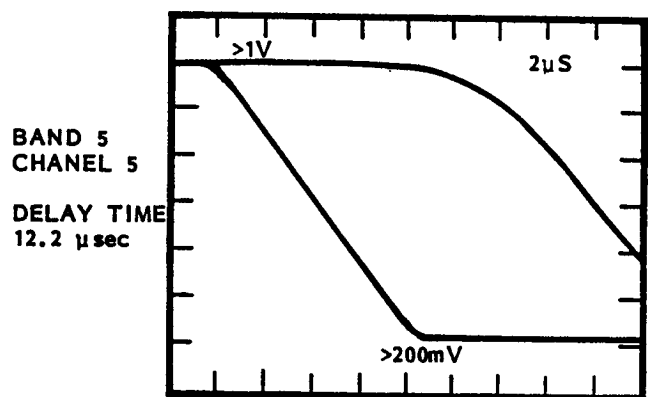
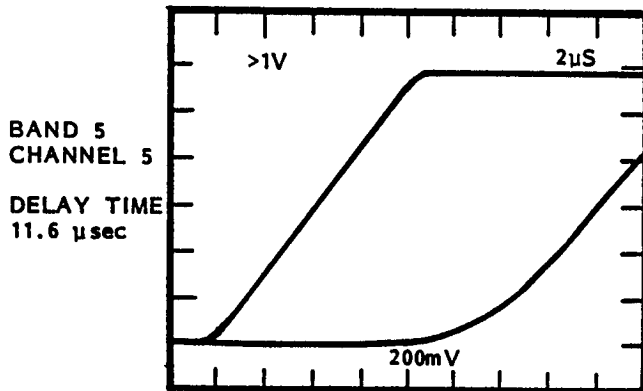
PARAMETER	SPECIFICATION	PERFORMANCE
OVERSHOOT	<u><10%</u>	<u><3.8%</u>
SETTLING TIMES	<u><1.5% ERROR</u> <u>AFTER 120 μSEC</u>	<u><1.5% ERROR</u> <u>AFTER 35 μSEC</u>
	<u><1.0% ERROR</u> <u>AFTER 240 μSEC</u>	<u><1.0% ERROR</u> <u>AFTER 65 μSEC</u>
RISETIME	<u><80 μSEC</u>	<u><70 μSEC</u>
DROOP	<u><0.5%</u>	NO DATA

RESPONSE DELAY

TYPICAL RESPONSE DELAY
BANDS 1-4



TYPICAL RESPONSE DELAY
BANDS 5 & 7



RESPONSE DELAY

DYNAMIC FORWARD SCAN
 CHANNEL-TO-CHANNEL OFFSETS
 (REFERRED TO B4D9)
 IFOV's

BAND CHANNEL	1	2	3	4	7	5
1	+0.08	+0.09	+0.02	-0.03	+0.11	+0.17
2	+0.02	*	-0.02	-0.07	-0.02	+0.02
3	+0.04	+0.05	0.00	-0.04	+0.08	*
4	+0.01	*	-0.03	-0.03	-0.03	0.00
5	+0.03	+0.08	+0.02	-0.04	+0.09	+0.09
6	+0.02	+0.01	+0.03	-0.05	-0.02	+0.08
7	+0.04	+0.05	+0.02	-0.04	*	+0.02
8	-0.02	-0.03	+0.03	-0.02	0.00	+0.15
9	+0.02	+0.06	-0.06	REF	+0.05	+0.09
10	0.00	-0.01	-0.03	-0.04	-0.03	+0.02
11	0.00	+0.04	-0.02	-0.03	+0.08	+0.10
12	0.00	+0.01	+0.02	-0.04	-0.08	0.00
13	+0.05	+0.09	+0.01	+0.02	+0.06	+0.09
14	-0.01	+0.03	+0.04	+0.01	-0.09	+0.05
15	+0.02	+0.09	+0.05	-0.01	+0.09	+0.04
16	+0.03	+0.04	+0.06	+0.01	-0.11	+0.03

* DETECTOR NOT FUNCTIONAL

RESPONSE DELAY



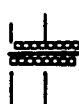


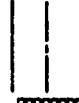


DYNAMIC REVERSE SCAN
 CHANNEL-TO-CHANNEL OFFSETS
 (REFERRED TO B4D9)
 IFOV's

BAND CHANNEL	1	2	3	4	7	5
1	+0.15	-0.01	+0.03	-0.02	-0.15	-0.08
2	+0.09	*	+0.01	-0.03	0.00	+0.05
3	+0.08	-0.04	-0.01	-0.03	-0.13	*
4	+0.09	*	-0.01	-0.01	-0.02	+0.02
5	+0.06	-0.01	+0.01	-0.04	-0.08	-0.07
6	+0.08	-0.05	+0.04	-0.03	-0.04	+0.11
7	**	-0.06	0.00	-0.04	*	-0.11
8	+0.07	-0.08	+0.04	0.00	+0.01	+0.20
9	+0.03	-0.04	-0.07	REF	-0.10	-0.02
10	+0.05	-0.07	-0.02	-0.02	-0.01	+0.09
11	+0.01	-0.05	-0.03	-0.03	-0.05	+0.02
12	+0.07	-0.06	+0.04	-0.02	-0.04	+0.10
13	+0.07	-0.05	-0.01	+0.02	-0.07	+0.02
14	+0.06	-0.04	+0.04	+0.02	0.00	+0.17
15	+0.03	-0.02	+0.02	-0.01	-0.05	-0.02
16	+0.09	-0.04	+0.07	+0.03	+0.03	+0.21

* DETECTOR NOT FUNCTIONAL

RESPONSE DELAY

NOMINAL BAND TO BAND SPACING

BAND		SEPARATION, IPOV	OFF-AXIS, DEGREES
6			0.2482
			0.2322
5		34.75	0.14788
		28	
7			0.08427
		46	
4			0.02631
		28	
3			0.08618
		28	
2			0.14706
		28	
1			0.30783
			0.21219

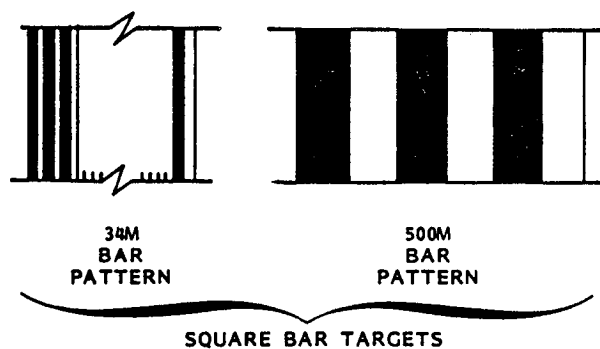
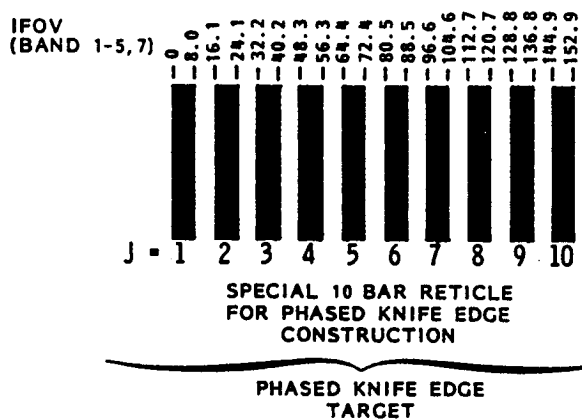
SQUARE WAVE MODULATION

SQUARE WAVE MODULATION WAS MEASURED USING TWO TECHNIQUES

- PHASED KNIFE EDGE
 - THE THEMATIC MAPPER SCANS 10 KNIFE EDGES EACH OF WHICH IS SPACED BY 16.1 IFOVs FROM THE PRECEDING EDGE
 - AN EDGE RESPONSE IS CONSTRUCTED FROM THE 10 SAMPLES AND THE SWR IS GENERATED BY PASSING COMPUTER GENERATED BARS OF VARYING SPATIAL EXTENT THROUGH THE RESPONSE EDGE AND COMPUTING THE MAGNITUDE OF THE MODULATION
- SQUARE BAR PATTERNS OF VARYING SPATIAL EXTENT
 - THE THEMATIC MAPPER SCANS BARS OF 34M AND 500M EXTENT
 - THE RESPONSES ARE RATIOED TO EVALUATE THE 34M SWR

SQUARE WAVE MODULATION

PHASED KNIFE EDGE AND SQUARE BAR PATTERNS

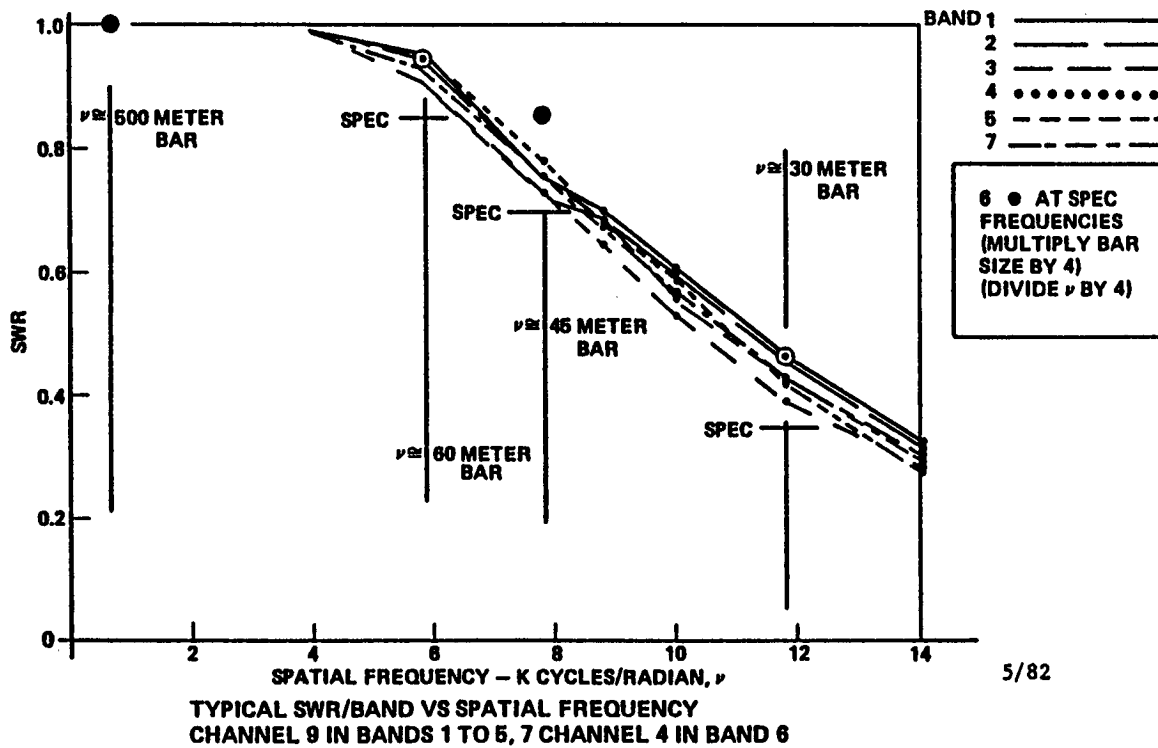


SQUARE WAVE MODULATION

MEASURED PROTOFLIGHT SQUARE WAVE RESPONSE (SWR) (BAND AVERAGE)

BAND	30 METER BAR		45 METER BAR		60 METER BAR		500 METER BAR	
	SWR	σ	SWR	σ	SWR	σ	SWR	σ
1	0.46	0.01	0.76	0.03	0.94	0.02	1.0	0.0
2	0.44	0.02	0.72	0.04	0.96	0.03	1.0	0.0
3	0.41	0.01	0.72	0.02	0.91	0.02	1.0	0.0
4	0.43	0.01	0.76	0.03	0.95	0.03	1.0	0.0
5	0.42	0.02	0.78	0.03	0.89	0.03	1.0	0.0
7	0.44	0.02	0.76	0.02	0.92	0.02	1.0	0.0
SPEC	0.35		0.70		0.85		1.0	
BAND	120 METER BAR		180 METER BAR		240 METER BAR		2000 METER BAR	
	SWR	σ	SWR	σ	SWR	σ	SWR	σ
6	0.44	0.04	0.78	0.01	0.94	0.00	1.0	0.0
SPEC	0.35		0.70		0.85		1.0	

TM PROTOFLIGHT/THERMAL VAC 9/15/81 COLLECTS



BRIGHT TARGET RECOVERY

BRIGHT TARGET RECOVERY

TABLE SHOWS IN BAND RADIANCES FOR WHICH A RECOVERY TIME OF LESS THAN 4 IFOV DWELL TIMES IS INSURED. RECOVERY FROM LARGER SIGNALS TAKES 10 IFOV DWELL TIMES (TYPICAL).

WORST CASE NUMBERS ARE BASED ON A THEORETICAL ANALYSIS OF THE PREAMPLIFIER ELECTRONICS.

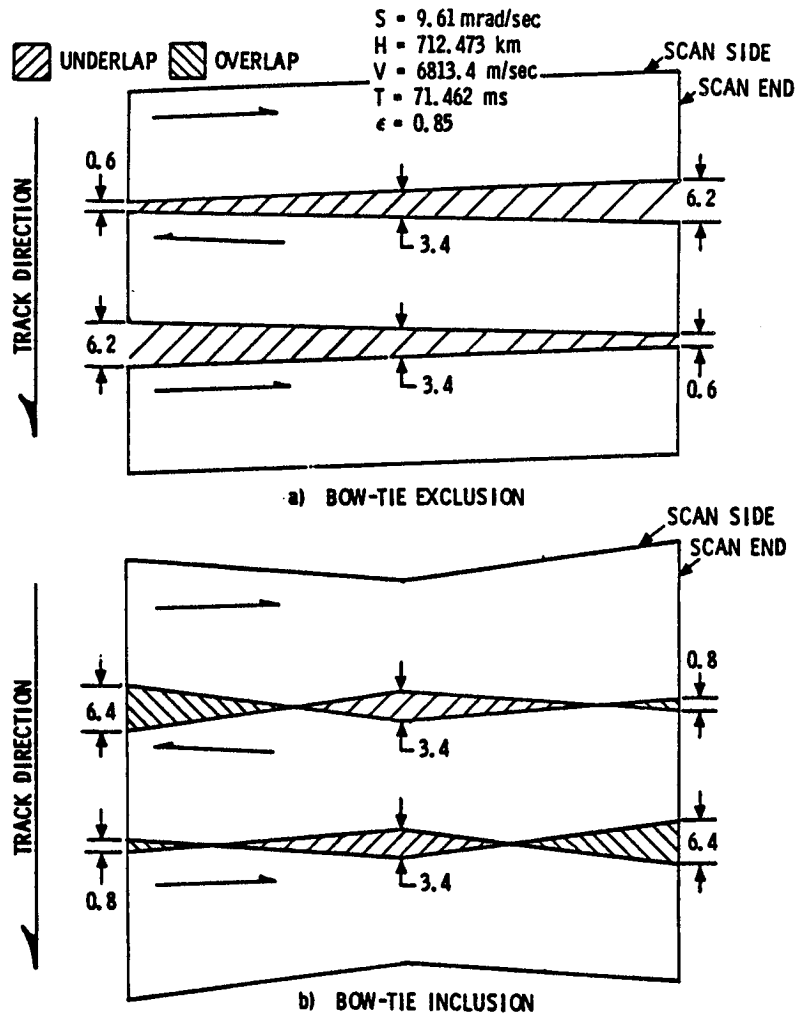
BAND	IN BAND BRIGHT TARGET RADIANCE (MW/CM ² /STER)		
	SPEC	TYPICAL AT 17°C	WORST CASE AT 12°C
1	2.0	7.9*	6.0
2	4.5	6.2	4.7
3	2.9	4.6	3.5
4	5.0	5.1*	3.5*
5	1.3	14.2	10.7
6	330 K	—	500°K
7	0.8	8.5	6.4

*BASED ON PROTOFLIGHT PREAMPLIFIER GAIN

5/82

ALTITUDE EFFECTS

GROUND TRACE OVERLAP/UNDERLAP
AT 40° N DESIGN POINT
 μ RAD



ALTITUDE EFFECTS

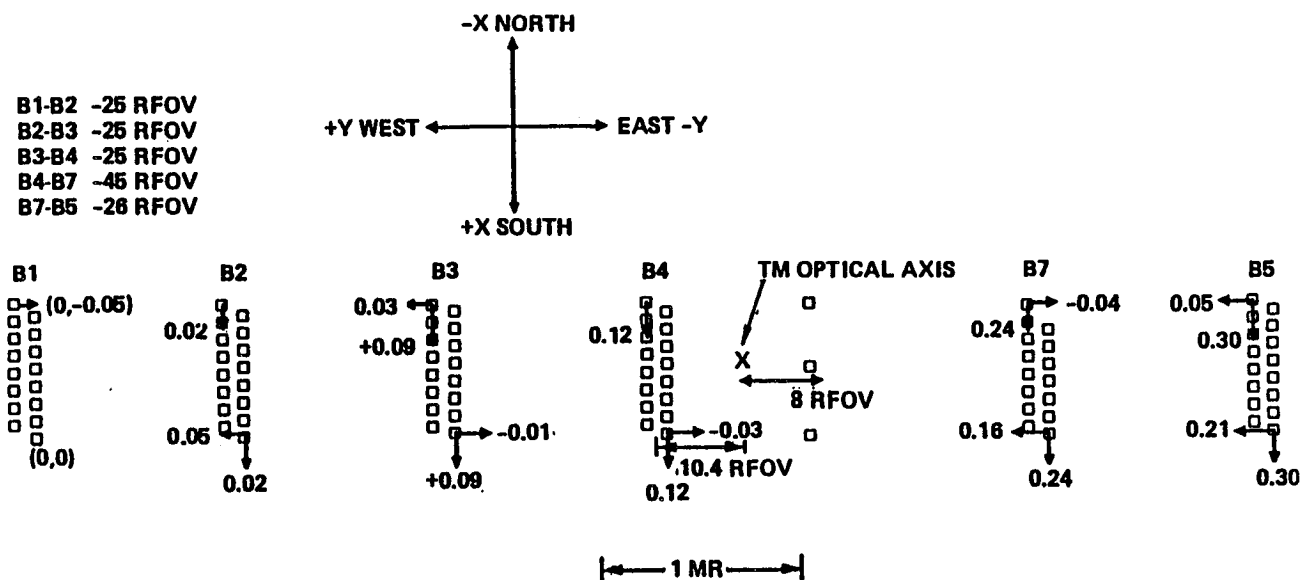
OVERLAP/UNDERLAP (μ RAD)

SOURCE	PROTOFLIGHT		
	UNDER	OVER	RANDOM*
NOMINAL ORBIT AND SCAN PARAMETERS**	3.4	-3.4	
BOW TIE EFFECT	0.0	6.5	
SMA			
SM CROSS AXIS MOTION	2.0	2.0	1.0†
SM PERIOD VARIATION	2.6	1.3	0.0
VIBRATION			0.5
RADIOMETER			
NON-IDEAL SLC SCAN	2.0	2.0†	0.2
EFL DEVIATION			
TELESCOPE	-1.0	1.0	
RELAY OPTICS	4.3‡	4.3‡	
DETECTOR IFOV SIZE	-5.4‡	+5.4‡	
VIBRATION	-1.7‡‡	+1.7‡‡	1.4
TOTAL			
PFPA	7.3	11.1	1.8
CFPA	7.9	10.5	
SPECIFICATION		8.5	
EFFECT OF ORBITAL ALTITUDE VARIATIONS BETWEEN 45°N AND 45°S LATITUDES	22.0	15.7	

*1 SIGMA
 **ALTITUDE = 712.5KM
 VELOCITY = 6821 KM/SEC
 SCAN PERIOD = 142.925 MSEC

† OVER FULL TEMPERATURE RANGE
 ‡ AFFECTS COOLED FOCAL PLANE ONLY
 ‡‡ AFFECTS PRIME FOCAL PLANE ONLY

MAP OF TM FOCAL PLANE
REGISTRATION BANDS (1 TO 5, AND 7)
AS PROJECTED ON GROUND



BAND TO BAND REGISTRATION - ALONG SCAN

FORWARD SCAN (UNITS ARE RFOV)
Data taken 18 September 1981

RT	B2-B1	B3-B1	B4-B1	B7-B1	B5-B1
30	24.99	50.02	75.05	120.00	146.04
29	24.96	49.99	75.03	119.93	145.95
28	24.98	50.01	75.04	119.93	145.95
27	24.99	50.03	75.05	119.93	145.98
26	24.97	50.02	75.05	119.95	145.96
25	24.96	50.00	75.03	119.93	145.95
24	24.95	50.00	75.02	119.91	145.91
23	24.95	49.99	75.01	119.89	145.88
22	24.94	50.00	75.02	119.91	145.91
21	24.96	50.03	75.06	119.94	145.95
20	24.97	50.04	75.08	119.96	145.98
19	24.96	50.02	75.04	119.93	145.95
18	24.95	50.02	75.05	119.92	145.94
17	24.95	50.01	75.04	119.90	145.91
16	24.96	50.02	75.04	119.93	145.93
15	24.97	50.03	75.05	119.94	145.96
14	24.96	50.03	75.06	119.94	145.95
13	24.96	50.03	75.05	119.93	145.95
12	24.95	50.02	75.03	119.89	145.91
11	24.96	50.02	75.04	119.89	145.90
10	24.96	50.02	75.04	119.89	145.92
9	24.96	50.01	75.04	119.85	145.88
8	24.96	50.01	75.03	119.85	145.88
7	24.97	50.01	75.03	119.82	145.85
6	24.96	50.01	75.02	119.82	145.82
5	24.97	50.04	75.05	119.84	145.86
4	24.97	50.04	75.05	119.84	145.88
3	24.98	50.06	75.08	119.88	145.90
2	24.99	50.07	75.10	119.85	145.93
NOMINAL	25.00	50.00	75.00	120.00	146.00
AVERAGE	24.96	50.02	75.04	119.90	145.92
STD. DEV.	0.01	0.02	0.02	0.04	0.05

BAND-TO-BAND REGISTRATION

REVERSE SCAN (UNITS ARE RFOV)
Data taken 18 September 1981

BAND TO BAND
REGISTRATION -
ALONG SCAN

RT	B2-B1	B3-B1	B4-B1	B7-B1	B5-B1
2	-24.96	-50.03	-75.10	-119.99	-146.11
3	-24.88	-49.95	-74.98	-119.86	-145.93
4	-24.91	-49.98	-74.95	-119.84	-145.91
5	-24.94	-49.98	-74.95	-119.63	-145.91
6	-24.89	-49.93	-74.92	-119.80	-145.88
7	-24.87	-49.94	-74.93	-119.79	-145.87
8	-24.88	-49.93	-74.92	-119.77	-145.86
9	-24.88	-49.93	-74.92	-119.79	-145.86
10	-24.88	-49.92	-74.90	-119.79	-145.85
11	-24.90	-49.94	-74.91	-119.80	-145.87
12	-24.92	-49.96	-74.95	-119.86	-145.93
13	-24.90	-49.94	-74.94	-119.85	-145.92
14	-24.89	-49.93	-74.92	-119.83	-145.89
15	-24.91	-49.95	-74.94	-119.86	-145.91
16	-24.88	-49.91	-74.90	-119.80	-145.87
17	-24.89	-49.92	-74.92	-119.83	-145.90
18	-24.91	-49.94	-74.92	-119.83	-145.90
19	-24.91	-49.93	-74.92	-119.83	-145.89
20	-24.89	-49.92	-74.90	-119.81	-145.86
21	-24.88	-49.91	-74.89	-119.79	-145.84
22	-24.89	-49.92	-74.90	-119.83	-145.88
23	-24.90	-49.92	-74.90	-119.82	-145.87
24	-24.85	-49.86	-74.85	-119.76	-145.81
25	-24.89	-49.92	-74.88	-119.81	-145.83
26	-24.88	-49.92	-74.88	-119.77	-145.81
27	-24.91	-49.92	-74.89	-119.78	-145.82
28	-24.87	-49.86	-74.86	-119.77	-145.80
29					
30	-24.91	-49.92	-74.91	-119.87	-145.90
NOMINAL	-25.00	-50.00	-75.00	-120.00	-146.00
AVERAGE	-24.89	-49.93	-74.92	-119.81	-145.88
STD. DEV.	0.02	0.03	0.04	0.06	0.06

FORWARD SCAN (UNITS ARE RFOV)
Data taken 18 September 1981

BAND TO BAND
REGISTRATION -
CROSS SCAN

RT	B2-B1	B3-B1	B4-B1	B7-B1	B5-B1
30	-0.01	-0.09	-0.13	-0.30	-0.22
29	-0.01	-0.06	-0.08	-0.14	-0.23
28	0.00	-0.07	-0.10	-0.16	-0.20
27	-0.01	-0.07	-0.09	-0.15	-0.19
26	-0.02	-0.08	-0.10	-0.15	-0.20
25	-0.02	-0.08	-0.11	-0.16	-0.23
24	-0.03	-0.10	-0.13	-0.16	-0.23
23	-0.01	-0.08	-0.10	-0.15	-0.22
22	-0.03	-0.10	-0.12	-0.20	-0.23
21	-0.01	-0.06	-0.10	-0.18	-0.24
20	-0.02	-0.08	-0.10	-0.14	-0.22
19	-0.03	-0.08	-0.11	-0.18	-0.25
18	0.00	-0.07	-0.10	-0.17	-0.20
17	-0.01	-0.08	-0.12	-0.22	-0.24
16	-0.01	-0.08	-0.11	-0.16	-0.22
15	-0.01	-0.08	-0.10	-0.16	-0.21
14	-0.01	-0.09	-0.12	-0.18	-0.25
13	-0.02	-0.09	-0.12	-0.18	-0.26
12	-0.03	-0.09	-0.11	-0.20	-0.26
11	-0.02	-0.09	-0.11	-0.21	-0.25
10	-0.03	-0.09	-0.11	-0.16	-0.20
9	-0.02	-0.08	-0.11	-0.19	-0.23
8	-0.03	-0.09	-0.13	-0.17	-0.25
7	0.00	-0.07	-0.09	-0.25	-0.22
6	-0.02	-0.07	-0.11	-0.20	-0.23
5	-0.01	-0.08	-0.10	-0.15	-0.21
4	-0.01	-0.08	-0.12	-0.18	-0.23
3	-0.02	-0.08	-0.12	0.00	-0.26
2	-0.02	-0.08	-0.11	-0.17	-0.23
NOMINAL	0.00	0.00	0.00	0.00	0.00
AVERAGE	-0.02	-0.08	-0.11	-0.18	-0.23
STD. DEV.	0.01	0.01	0.01	0.03	0.02

BAND-TO-BAND REGISTRATION

REVERSE SCAN (UNITS ARE RFOV)
Data taken 18 September 1981

	RT	B2-B1	B3-B1	B4-B1	B7-B1	B5-B1
BAND TO BAND	2	0.02	-0.09	-0.13	-0.34	-0.22
	3	0.01	-0.04	-0.07	-0.17	-0.20
REGISTRATION -	4	0.01	-0.06	-0.05	-0.16	-0.18
	5	0.00	-0.04	-0.08	-0.15	-0.19
CROSS SCAN	6	0.02	-0.04	-0.08	-0.17	-0.19
	7	-0.01	-0.07	-0.09	-0.24	-0.25
	8	-0.03	-0.11	-0.15	-0.22	-0.27
	9	-0.03	-0.09	-0.11	-0.12	-0.23
	10	-0.01	-0.07	-0.11	-0.17	-0.21
	11	-0.01	-0.08	-0.09	-0.17	-0.23
	12	-0.01	-0.06	-0.10	-0.18	-0.23
	13	0.01	-0.05	-0.08	-0.14	-0.23
	14	0.01	-0.06	-0.09	-0.15	-0.22
	15	-0.02	-0.09	-0.11	-0.16	-0.24
	16	0.01	-0.07	-0.09	-0.16	-0.20
	17	0.01	-0.06	-0.09	-0.15	-0.18
	18	0.03	-0.04	-0.06	-0.16	-0.18
	19	-0.01	-0.06	-0.09	-0.16	-0.23
	20	0.00	-0.06	-0.09	-0.16	-0.23
	21	0.00	-0.06	-0.09	-0.18	-0.24
	22	0.02	-0.04	-0.06	-0.14	-0.17
	23	0.01	-0.06	-0.09	-0.15	-0.19
	24	-0.01	-0.07	-0.10	-0.16	-0.21
	25	-0.02	-0.07	-0.10	-0.18	-0.21
	26	0.00	-0.04	-0.07	-0.13	-0.18
	27	0.02	-0.04	-0.06	-0.12	-0.17
	28	0.01	-0.05	-0.07	0.00	-0.18
	29					
	30	0.03	-0.02	-0.05	-0.16	-0.19
NOMINAL		0.00	0.00	0.00	0.00	0.00
AVERAGE		0.00	-0.06	-0.09	-0.17	-0.21
STD. DEV.		0.02	0.02	0.02	0.04	0.03

FORWARD SCAN (UNITS ARE RFOV)
Data taken 18 September 1981

	RT	B1	B2	B3	B4	B7	B5
BAND TO BAND	30	1.98	1.97	2.00	2.00	1.86	1.97
	29	1.97	1.94	2.01	2.00	1.86	1.95
REGISTRATION -	28	1.97	1.95	2.02	2.00	1.87	1.95
	27	1.98	1.96	2.01	2.00	1.86	1.96
EVEN TO ODD	26	1.98	1.96	2.01	1.99	1.88	1.96
CHANNEL	25	1.97	1.97	2.01	2.00	1.87	1.96
	24	1.97	1.97	2.01	2.00	1.86	1.96
	23	1.97	1.97	2.01	2.00	1.85	1.95
	22	1.97	1.96	2.01	1.99	1.87	1.95
	21	1.97	1.96	2.02	2.00	1.87	1.95
	20	1.96	1.98	2.01	2.00	1.86	1.96
	19	1.96	1.97	2.01	1.99	1.88	1.96
	18	1.96	1.98	2.01	2.00	1.87	1.96
	17	1.96	1.99	2.01	2.00	1.87	1.96
	16	1.96	1.97	2.01	2.00	1.86	1.96
	15	1.97	1.99	2.01	2.00	1.88	1.96
	14	1.97	1.98	2.01	2.00	1.87	1.96
	13	1.96	1.97	2.01	2.00	1.86	1.95
	12	1.96	1.96	2.01	1.99	1.87	1.96
	11	1.97	1.95	2.01	2.00	1.87	1.96
	10	1.97	1.97	2.01	2.00	1.87	1.96
	9	1.97	1.95	2.01	2.00	1.85	1.96
	8	1.97	1.95	2.01	2.00	1.86	1.96
	7	1.97	1.95	2.01	2.00	1.87	1.96
	6	1.98	1.95	2.01	2.00	1.88	1.96
	5	1.98	1.93	2.02	2.00	1.85	1.96
	4	1.98	1.95	2.02	2.00	1.90	1.96
	3	1.97	1.96	2.03	2.01	1.87	1.97
	2	1.98	1.95	2.03	2.00	1.80	1.96
NOMINAL		2.00	2.00	2.00	2.00	2.00	2.00
AVERAGE		1.97	1.96	2.01	2.00	1.87	1.96
STD. DEV.		0.01	0.01	0.01	0.00	0.02	0.00

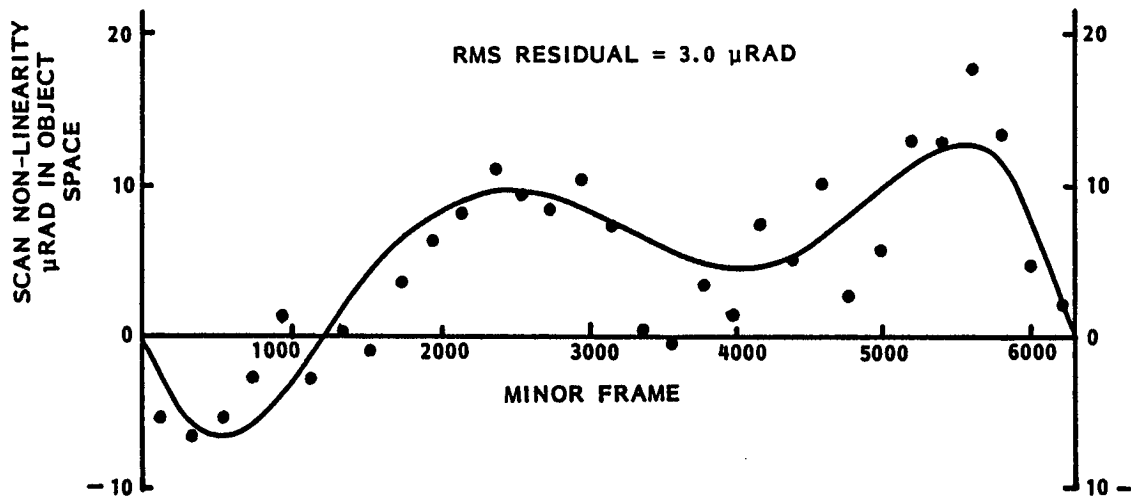
BAND-TO-BAND REGISTRATION

BAND TO BAND REGISTRATION - EVEN TO ODD CHANNEL REVERSE SCAN (UNITS ARE RFOV) Data taken 18 September 1981

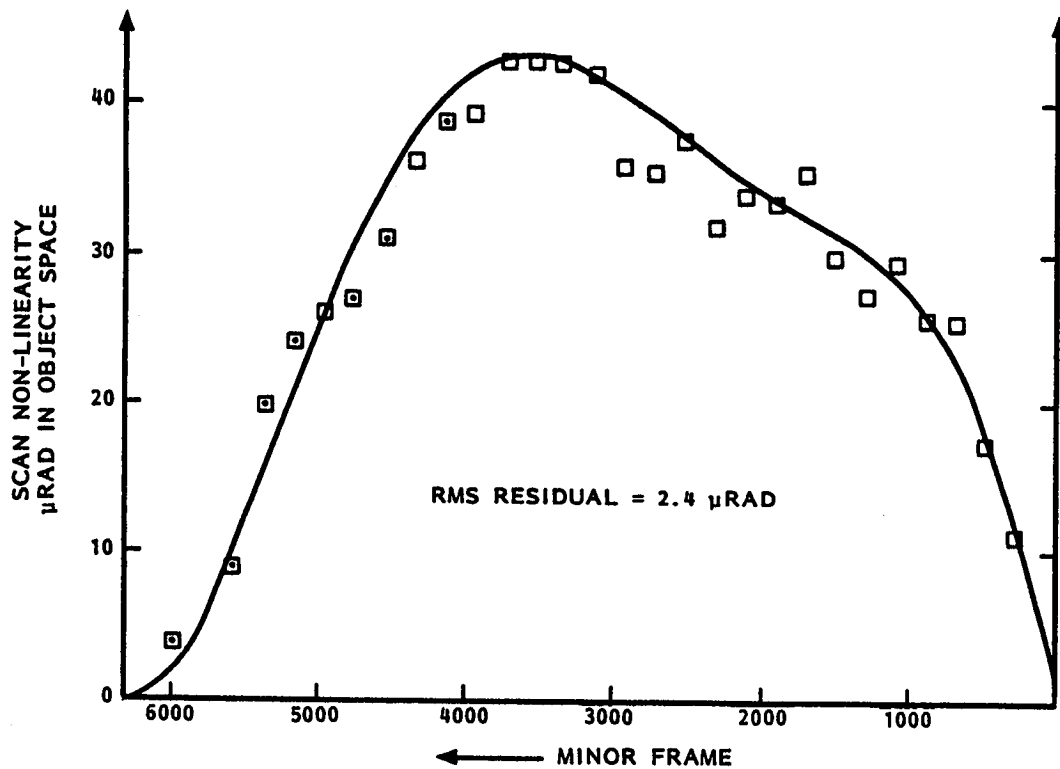
RT	B1	B2	B3	B4	B7	B5
2	-3.01	-3.02	-2.98	-2.99	-2.93	-2.83
3	-3.00	-3.01	-2.97	-2.98	-2.92	-2.84
4	-3.00	-3.02	-2.97	-2.98	-2.91	-2.85
5	-2.99	-3.00	-2.98	-3.00	-2.70	-2.85
6	-3.01	-3.02	-2.98	-2.99	-2.91	-2.85
7	-2.98	-3.01	-2.98	-2.99	-2.90	-2.84
8	-3.01	-3.02	-2.96	-2.99	-2.91	-2.84
9	-3.00	-3.01	-2.96	-2.99	-2.92	-2.84
10	-2.99	-3.02	-2.96	-2.98	-2.91	-2.83
11	-2.99	-3.02	-2.98	-2.99	-2.92	-2.84
12	-2.99	-3.02	-2.97	-2.99	-2.92	-2.85
13	-2.99	-3.00	-2.97	-2.99	-2.91	-2.84
14	-2.99	-3.01	-2.97	-2.99	-2.92	-2.84
15	-2.99	-3.01	-2.97	-2.99	-2.92	-2.85
16	-2.99	-3.02	-2.97	-2.99	-2.92	-2.84
17	-2.98	-3.01	-2.96	-2.99	-2.92	-2.84
18	-3.00	-3.01	-2.97	-2.99	-2.91	-2.85
19	-3.00	-3.01	-2.97	-2.99	-2.93	-2.85
20	-2.98	-3.00	-2.97	-2.99	-2.91	-2.83
21	-2.99	-3.01	-2.96	-2.99	-2.91	-2.84
22	-2.98	-3.00	-2.96	-2.98	-2.92	-2.84
23	-2.99	-3.01	-2.97	-2.99	-2.92	-2.84
24	-3.00	-3.02	-2.96	-2.99	-2.93	-2.83
25	-2.97	-3.01	-2.97	-2.99	-2.88	-2.84
26	-3.02	-3.01	-2.99	-3.00	-2.89	-2.85
27	-3.02	-3.03	-2.97	-2.99	-2.90	-2.86
28	-2.99	-3.04	-2.95	-2.99	-2.92	-2.84
29						
30	-3.01	-3.04	-2.99	-2.99	-2.93	-2.85
NOMINAL	-3.00	-3.00	-3.00	-3.00	-3.00	-3.00
AVERAGE	-3.00	-3.01	-2.97	-2.99	-2.91	-2.84
STD. DEV.	0.01	0.01	0.01	0.00	0.04	0.01

ALONG SCAN PROFILE

FORWARD SCAN PROFILE
SME-1 SAM MODE



REVERSE SCAN PROFILE
SME-1 SAM MODE



ALONG SCAN PROFILE

QUALITY OF ALONG SCAN DATA
FOR FULL BL19/20 COLLECT

- EACH DATA POINT IS THE AVERAGE OF FIVE SCANS
- SCAN TO SCAN REPEATABILITY (AFTER LINE LENGTH CORRECTION) IS $\pm 4 \mu\text{rad RMS}$
- SCAN TO SCAN REPEATABILITY DOES NOT DEPEND ON POSITION WITHIN THE SCAN
- RESIDUAL BETWEEN AVERAGED DATA POINTS AND COMPUTED PROFILE IS $\pm 3 \mu\text{rad RMS}$

PARAMETERS FOR COMPUTATION
OF THE ALONG SCAN PROFILE

	FORWARD SCAN								REVERSE SCAN								
	a_0	a_1	a_2	a_3	a_4	a_5	PHI_0^f	W_F	a_0	a_1	a_2	a_3	a_4	a_5	PHI_0^r	W_R	K'_0
SME-1 SAM MODE	0.0	-3.1507E-8	4.5738E-11	-2.0410E-14	3.6950E-18	-2.3511E-22	-4.4 E-6	42.5146E-6	3.28 E-5	5.6926E-8	-4.3551E-11	1.7302E-14	-3.1186E-18	1.9711E-22	34.6 E-6	42.5127E-6	0.499933
SME-2 SAM MODE	0.0	-3.6085E-8	4.5812E-11	-2.0071E-11	3.6306E-18	-2.3084E-22	-9.4 E-6	42.5196E-6	3.44 E-5	5.3268E-8	-4.4062E-11	1.7826E-14	-3.2106E-18	2.0287E-22	32.3 E-22	42.5187E-6	0.499911

UNITS:

- a_i IN $\text{rad}/(\text{mf})^i$
- $\text{PHI}_0^f, \text{PHI}_0^r$ IN rad
- W_F, W_R IN rad/mf
- K'_0 IS A PURE NUMBER
- a_0 IS CHOSEN SO THAT THE FORWARD AND REVERSE SCAN ANGLES ARE CONSISTENT FOR BAND 4 CHANNEL 9
- THE DESIGN SCAN RATE IS $42.50\text{E}-6 \text{ rad}/\text{MF}$

ALONG SCAN PROFILE

COMPUTATION OF THE ALONG SCAN PROFILE

FOR FORWARD SCANS

$$\theta(mf) = W_F \cdot mf^{**} + \sum_{i=0}^5 C_i (mf^{**})^i + 4 \cdot \phi_{mid} \frac{mf^{**} (6320 - mf^{**})}{6320^2}$$

FOR REVERSE SCANS

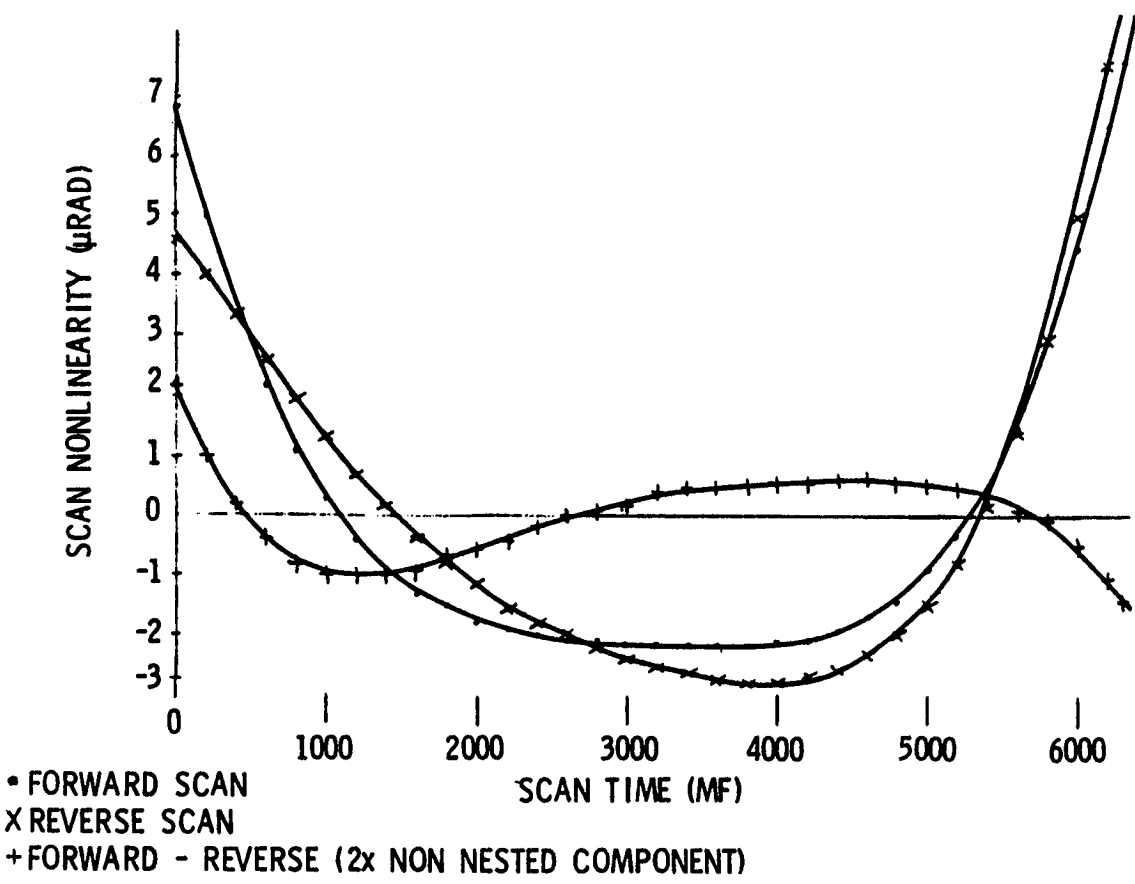
$$\theta(mf) = W_R \cdot (6320 - mf^{**}) + \sum_{i=0}^5 C_i (mf^{**})^i + 4 \cdot \phi_{mid} \frac{mf^{**} (6320 - mf^{**})}{6320^2}$$

WHERE

$$mf^{**} = \frac{mf}{1 + \frac{\Delta TSCAN}{TSCAN}}$$

CROSS SCAN PROFILE

NONLINEARITIES



CROSS SCAN PROFILE

5TH ORDER POLYNOMIAL COEFFICIENTS

	FORWARD SCAN	REVERSE SCAN
C ₀	-0.000287	-0.000276
C ₁	-1.014827E-8	-1.628688E-8
C ₂	4.295777E-12	8.563377E-12
C ₃	-7.930246E-16	-2.248363E-15
C ₄	4.174148E-20	2.998088E-19
C ₅	2.675552E-24	-1.531221E-23
W _C	9.286E-8	9.286E-8

$$\phi_{CS} = \sum_{i=0}^5 C(i) IMF^i \quad \phi_{CS} \text{ (radians)}$$

$$W_C = 9.287E-8 \text{ rad/MF} = 9.66E-3 \text{ rad/sec}$$

$$IMF = 9.611 \mu\text{sec}$$

RADIOMETRIC CALIBRATION AND PROCESSING PROCEDURE FOR
REFLECTIVE BANDS ON LANDSAT-4 PROTOFLIGHT
THEMATIC MAPPER

JOHN L. BARKER
NASA/GODDARD SPACE FLIGHT CENTER

R. B. ABRAMS, D. L. BALL, AND K. C. LEUNG
COMPUTER SCIENCES CORPORATION

KEYWORDS: Absolute Calibration, Relative Calibration, Band-to-Band
Calibration, Internal Calibration System, SCROUNGE, TIPS, Scan
Cycle Timeline, Thematic Mapper

ABSTRACT

This paper provides descriptive and procedural background material for understanding results that are given in the following papers by Barker et al. appearing in these Proceedings: "Prelaunch Absolute Radiometric Calibration of the Reflective Bands on the Landsat-4 Protoflight Thematic Mapper," "Characterization of Radiometric Calibration of Landsat-4 TM Reflective Bands," and "TM Digital Image Products for Applications."

The radiometric subsystems of NASA's Landsat-4 Thematic Mapper (TM) sensor is described. Special emphasis is placed on the internal calibrator (IC) pulse shapes and timing cycle. The procedures for the absolute radiometric calibration of the TM channels with a 122-centimeter integrating sphere and the transfer of radiometric calibration from the channels to the IC are reviewed.

The use of the IC to calibrate TM data in the ground processing system consists of pulse integration, pulse averaging, IC state identification, linear regression analysis, and histogram equalization. An

overview of the SCROUNGE-era (before August 1983) method is presented. Procedural differences between SCROUNGE and the TIPS-era (after July 1983) and the implications of these differences are discussed.

INTRODUCTION

Absolute calibration is essential for a variety of scientific studies and image analysis applications. Arithmetic spectral transformations, such as those used to determine path radiance for removal or normalization of atmospheric effects, require absolute radiometric data. To extend signatures, based on averages or moments, beyond a scene, to data collected in different scenes or at different times under different atmospheric conditions, or even to data collected by different satellites, requires both an absolute measure of radiance and correction for atmospheric efforts.

AN OVERVIEW OF THE
THEMATIC MAPPER GEOMETRIC CORRECTION SYSTEM

ERIC P. BEYER
GENERAL ELECTRIC COMPANY

INTRODUCTION

This paper summarizes the processing concepts which form the basis of the NASA Thematic Mapper (TM) Geometric Correction System.

TM geometric correction is a system process which includes both the Flight and Ground Segments. The principle Flight Segment subsystems are:

- Thematic Mapper
- Attitude Control
- Attitude Measurement
- On-Board Computer.

The principle Ground Segment processes are:

- Payload Correction
- Control Point Processing
- Geometric Correction (Resampling).

Purpose and Fundamental Concept of Geometric Correction

The overall purpose of Geometric Correction is to place TM image samples onto an output coordinate system which is related to a map projection. This output product simplifies the data processing for subsequent applications. Conceptually, the geometric correction is accomplished in two phases: First, correction data is generated and then the raw TM image data is resampled using the correction data.

Figure 1-1 illustrates correction data generation. The spacecraft position, TM frame attitude, position of the TM scanning mirrors and detector sampling are known as a function of time, through a combination of Flight Segment measurements, Ground Segment modeling and control point information. This information, along with an earth geoid model, is used to determine the geoid location for each TM image sample (geoid look point). Then, using map projections, correction data can be generated which defines the location of each TM sample on the output coordinate system.

As with previous Landsats, products will be provided on an output grid system known as a World Reference System (WRS). The WRS is defined by a nominal orbit path. Each of the nominal 233 orbit paths of the sun synchronous Landsat-D orbit is divided into 248 WRS scenes. Including overlap with adjacent scenes in the same orbit, a scene is approximately 170 km along-track by 185 km across-track. A WRS scene is identified by a scene center latitude and longitude and a map rotation angle for each map projection. Output products can be provided in either of two map projections:

1. Space Oblique Mercator (SOM).
2. Universal Transverse Mercator when scene center is between 65 degrees South latitude and 65 degrees North latitude or Polar Stereographic when scene center is below 65 degrees South latitude and above 65 degrees North latitude.

The output coordinate system for all satellite passes over the WRS scene is the map projection coordinate system rotated about the WRS scene center location by the map rotation angle.

Figure 1-2 illustrates the resampling concept. The correction data is used to locate TM detector samples on the output coordinate system, and TM detector samples are then interpolated to the desired output grid locations.

FIGURE 1-1
CORRECTION DATA GENERATION CONCEPT

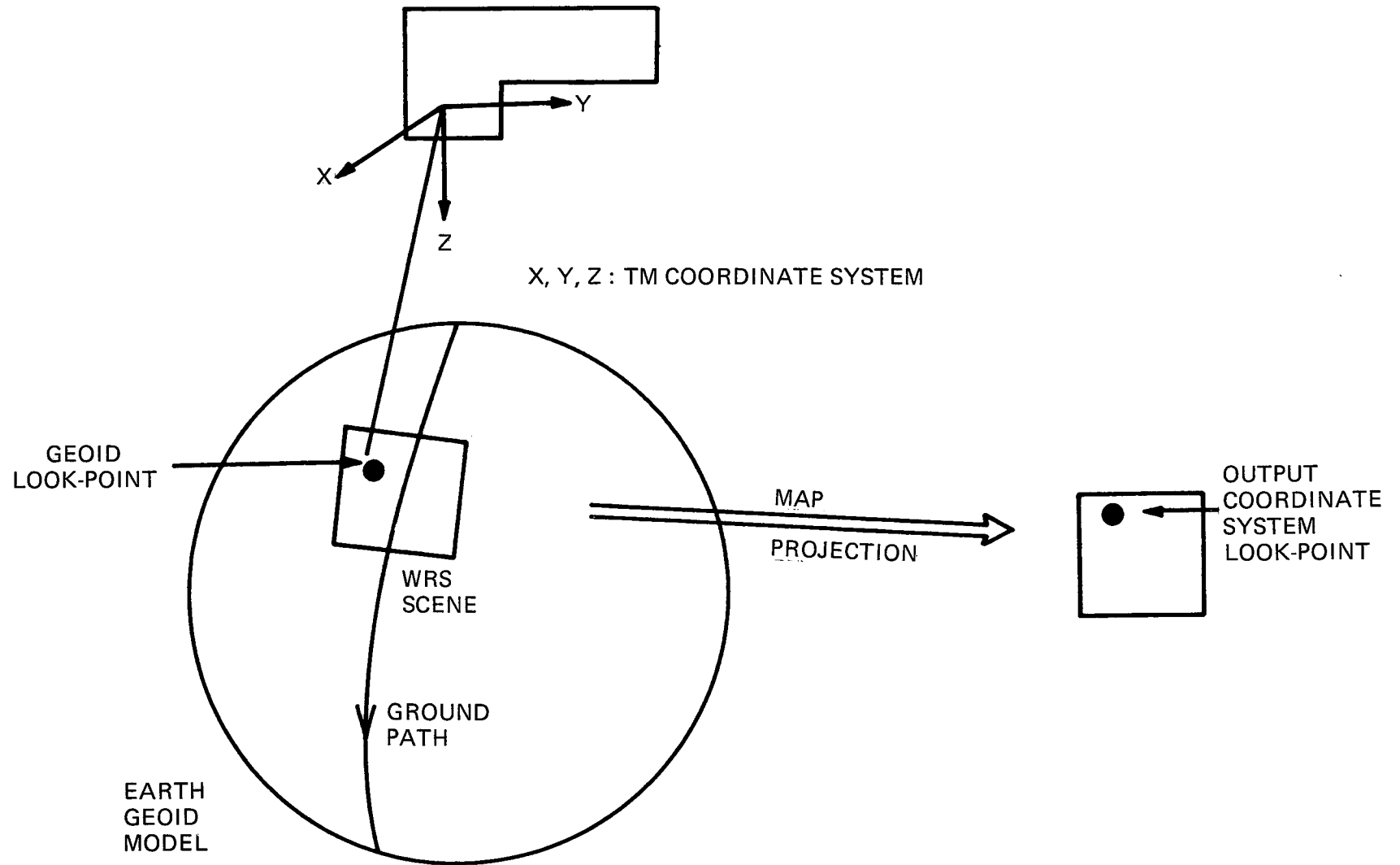
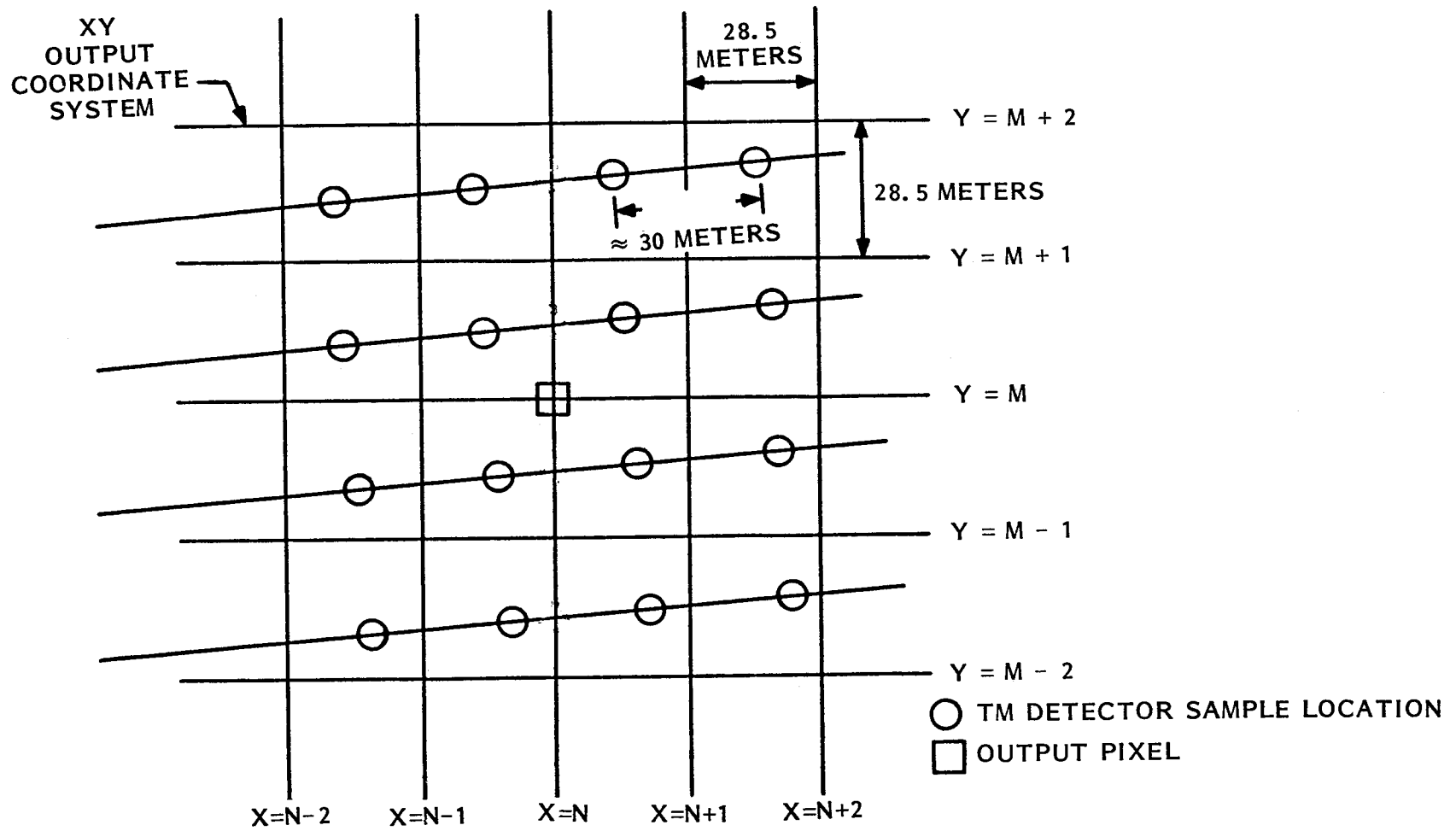


FIGURE 1-2
RESAMPLING CONCEPT



Geometric Accuracy

An overview of the Landsat-D geometric accuracy specifications are shown in Figure 1-3. Effectively, a reference interval (set of consecutively imaged scenes) is geodetically rectified to a set of maps. Registration control points are then extracted from the reference interval and stored in a control point library. Subsequently imaged intervals are registered to the reference interval using the control point library. There are three geometric accuracy requirements: Band-to-band registration, temporal registration and geodetic rectification.

Band-to-band registration is the ability to overlay spectral bands within a single scene. It is considered the most important accuracy requirement. The Thematic Mapper band-to-band requirements are 0.2 pixel (90% of the time) between spectral bands on the same focal plane and 0.3 pixel (90% of the time) between spectral bands on primary and cold focal planes. A TM pixel is 42.5 microradians. Bands 1 to 4 are on the primary focal plane and Bands 5 to 7 are on the cold focal plane. With ground processing, these band-to-band accuracy requirements are expected to be easily satisfied.

Temporal registration is the ability to overlay a band of the registrant scene with the corresponding band of the reference scene. The accuracy requirement is 0.3 pixel (90% of the time). The temporal registration requirement is the most challenging system accuracy requirement. The following simplified calculation illustrates this point:

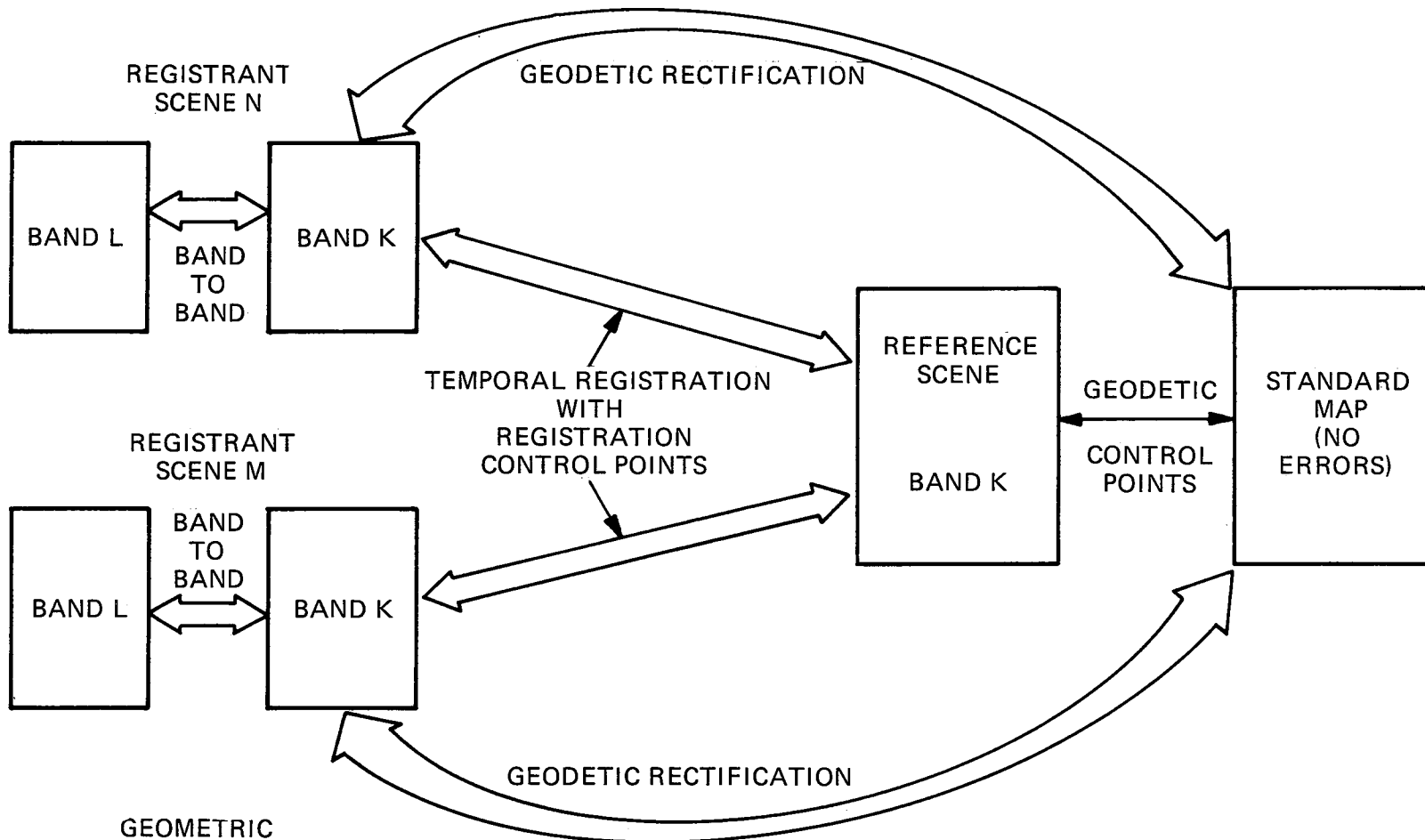
$$0.3 \text{ pixel temporal (90\%)} \times \frac{42.5 \text{ } \mu\text{rad}}{\text{pixel}} \times \frac{(1\sigma)}{1.645 (90\%)} \times \frac{\text{Single scene}}{\sqrt{2} \text{ temporal}}$$

$$= 5.48 \text{ } \mu\text{rad (1}\sigma\text{) single scene}$$

$$= 1.13 \text{ arc-sec (1}\sigma\text{) single scene}$$

$$= 3.87 \text{ meter (at 705.3 km) (1}\sigma\text{) single scene}$$

FIGURE 1-3
 GEOMETRIC ACCURACY SPECIFICATIONS



97

GEOMETRIC CORRECTION REQUIREMENTS
 90% OF THE TIME

GEODETIC	0.5 PIXEL
TEMPORAL	0.3 PIXEL (REGISTRANT TO REFERENCE)
BAND-TO-BAND	0.3 PIXEL (BETWEEN PRIMARY AND COLD FOCAL PLANES)
	0.2 PIXEL (WITHIN EACH FOCAL PLANE)

That is, the 0.3 pixel 90% of the time accuracy between two scenes allows no more than 3.87 meters (1σ) total system error for one scene. This simplified calculation assumes that the error is Gaussian (the factor of $1/1.645$ converts 90% to 1σ) and that the errors in the two scenes are uncorrelated (the factor of $1/\sqrt{2}$). The temporal registration accuracy requires an adequate number of ground control points. This may be as large as 18 control points when a single scene is processed, but can be reduced to 3 to 4 control points per scene when consecutive scenes from one orbit (an interval) are processed. This requirement excludes the error effects caused by interaction of earth topology and orbit non-repeatability. Geodetic rectification is the ability to overlay a band of the registrant scene with the original maps. The accuracy requirement is 0.5 pixel (90% of the time). This accuracy is to be met when the maps have no geometric errors, over regions without topological variations and given sufficient numbers of geodetic control points. To the extent that these conditions are not satisfied in actual operation, the geodetic accuracy of output products will degrade.

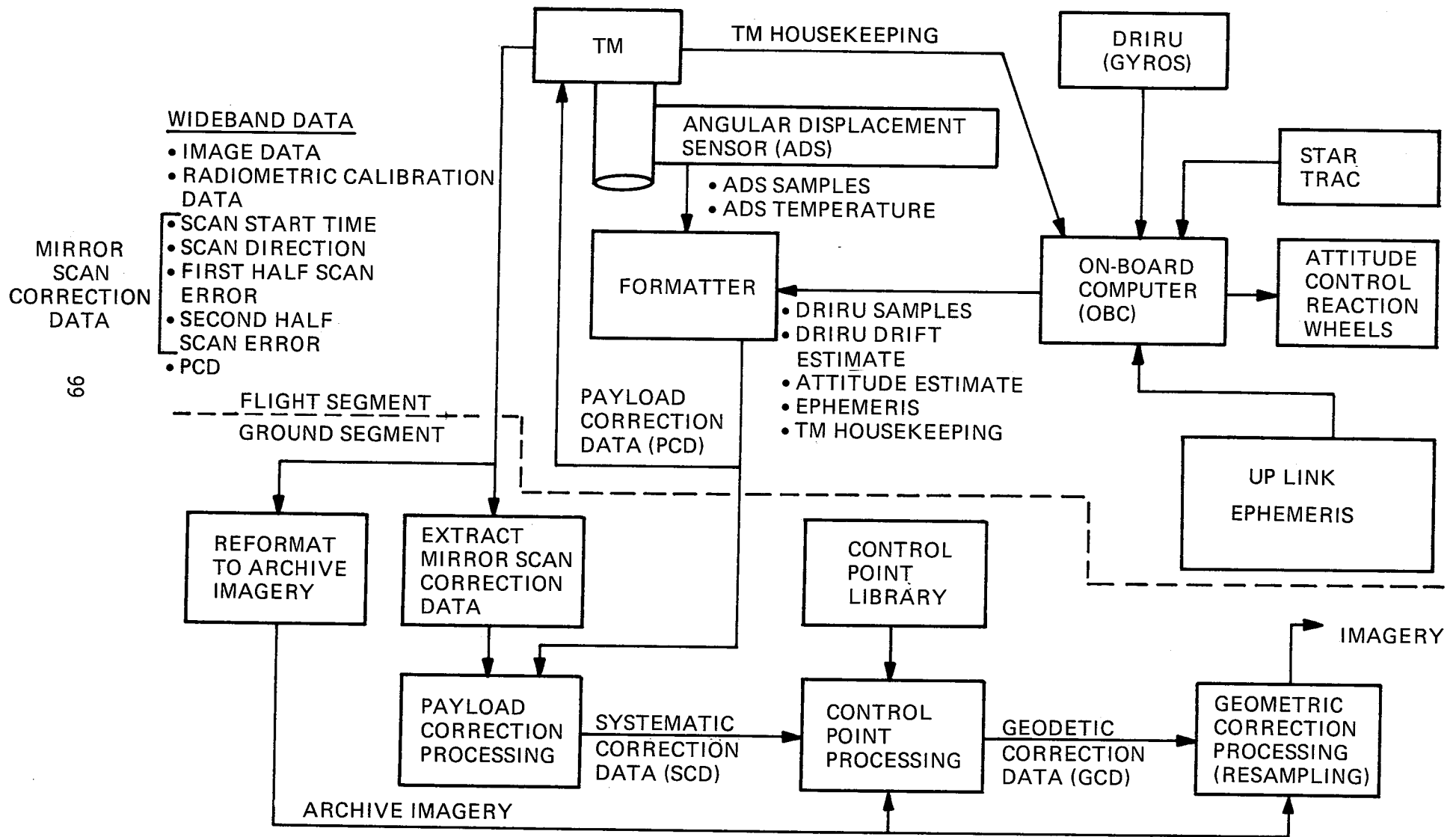
System Overview

An overview of NASA's Landsat-D TM Geometric Correction System is shown in Figure 1-4. The Flight Segment includes the TM instrument, attitude measurement devices, attitude control and ephemeris processing. The Flight Segment inertial attitude estimates are made using an extended Kalman Filter process, which corrects integrated gyro measurements using star tracker information. Attitude is controlled using reaction wheels. Ephemeris, used for attitude control and ground processing is uplinked from the ground or determined using the on-board Global Positioning System. Attitude control and ephemeris processing are implemented in the On-Board Computer.

The spacecraft attitude is downlinked for ground processing but at a rate of (4.096 seconds) that cannot follow all TM attitude deviations. Low frequency (0 to 2 Hz) attitude deviations are measured by gyro samples supplied every 0.064 seconds per axis. Higher frequency (2 to 125 Hz) attitude deviations are measured using Angular Displacement Sensors (ADS) which are sampled every 0.002 seconds per axis. The Angular Displacement Sensor is mounted directly on the Thematic Mapper.

FIGURE 1-4

LANDSAT D TM GEOMETRIC CORRECTION SYSTEM OVERVIEW



A spacecraft formatter combines the necessary On-Board Computer information and the ADS samples into a 32 kilobit per second telemetry stream called Payload Correction Data (PCD). PCD contains all Flight Segment information needed to perform TM data processing. It is both downlinked on a telemetry channel and included with the TM wideband data. Also imbedded into TM wideband data is Mirror Scan Correction Data (MSCD) from which the scan mirror position is determined as a function of time. This data includes scan start time, scan direction, first half scan time error, and second half scan time error.

The NASA TM ground processing extracts the Mirror Scan Correction Data (MSCD) from the TM wideband data. The PCD is received using the telemetry path. Payload Correction Processing then combines the MSCD and PCD to generate Systematic Correction Data (SCD). The Systematic Correction Data is a complete set of correction data except that large bias and slow drift errors exist due to time, ephemeris, gyro measurement, attitude control and TM alignment uncertainty. These bias and drift errors are removed by Control Point Processing. Control Point Processing uses the mislocation between features in reference interval and the same features in the registrant interval to estimate these SCD errors. The SCD is then modified to remove the error effects and the result is called Geodetic Correction Data.

The payload correction and control point processing are performed over an interval or number of consecutively imaged scenes in an orbit path. This results in improved accuracy and fewer control points than processes that operate on individual scenes.

The final steps in geometric correction system involve resampling the TM image samples to place them onto the output coordinate system. The TM wideband data is first reformatted into Archive imagery in which reverse scan data has been reordered to correspond to the forward scan data, and integer detector and band offsets have been removed. The Archive imagery is then resampled during Geometric Correction Processing. The resampling is performed using the Geodetic Correction Data and it results in product imagery.

[EXERPTED FROM EARLY RESULTS SYMPOSIUM PAPER]

THEMATIC MAPPER IMAGE PROCESSING SYSTEM (TIPS) PROCESSING STATUS

JOAN BROOKS
GENERAL ELECTRIC SPACE DIVISION

TIPS PROCESSING STATUS

- Radiometric Correction Performance
 - Present Status
 - Current and Planned Efforts

- Geometric Correction Performance
 - Methods and Problems of Measurement
 - Results
 - Current and Planned Efforts

RADIOMETRIC CORRECTION PERFORMANCE: PRESENT STATUS

- 1 Quantum Level Requirement Met in all Bands (Occasional Band 7 Exception)

- Problems Outside Present Capabilities
 - Noisy Detector 7 in Band 7 -- Sensor Striping
 - DC Restore Instability -- Sensor Striping
 - Hysteresis (Slow Recovery from Saturation) -- Sensor and Scan Striping
 - "Droop" Effect and DC Restore Asymmetry -- Scan Striping

- Initial Post Launch Calibration has Taken Place

- Absolute Radiometric Calibration in Progress

TABLE 1

WITHIN-SCAN DETECTOR RANGE FOR SEVEN BANDS.
 UNITS ARE QUANTUM LEVELS (QL). NUMBERS IN
 PARENTHESIS INDICATE THE NUMBER OF SCANS
 THAT EXCEEDED THE 2 QL LIMIT.

AREA	# of SCANS	BANDS						
		1	2	3	4	5	6	7
1	32	1.33	.60	.79	.38	.90	.23	3.95 (7)
2	26	1.21	.47	.79	.60	.61	.26	1.91 (6)
3	32	1.38	.65	.76	.35	.85	.22	3.60 (32)
4	32	1.30	.42	.64	.58	1.01	.24	.89
5	32	1.23	.45	.77	.54	.87	.30	1.33 (10)
6	32	1.21	.50	.79	.49	.85	.26	.97
7	32	1.21	.43	.70	.33	.69	.24	1.54 (2)
8	32	1.26	.52	.64	.33	.70	.23	.87
9	32	1.37	.65	.81	.37	.74	.31	.92

TIPS R/C PERFORMANCE: CURRENT/PLANNED EFFORTS

- Absolute Radiometric Calibration: New Radiance Range, All Bands
 - Impact Study in Progress
 - Plan for Initial and Three Downstream Updates
 - Coordinated with D' Instrument Calibration

- Investigation of Low Impact Solutions to Scan Striping Planned
 - Timelines Must be Preserved
 - Present R/C Processing is Detector/Multi-Scan Based
 - Geometric Correction Process is Scan-Segment Based - May Be Good Place for Filter

- Fine Tuning Band 6 Parameters

- Scene Content Limitation Algorithms

GEOMETRIC CORRECTION PERFORMANCE

- Methods of Measurement
 - System Outputs from Control Point Processing During A-Tape and Chip Generation
 - Estimate of Random Error From CP Residuals
 - Estimate of Modeling Error from Covariance Matrix

 - Direct Measurement
 - Temporal Registration by Correlation of Control Areas in Two Corrected Scenes

- Geodetic Rectification by Designation of Evaluation Points in Rectified Imagery - Zoom Transfer Scope
- Problems
 - Slow Acquisition of Usable Companion Intervals
 - Bands 2 & 5 Chips have Degraded Along Track Correlation
 - Seasonal Effects Degrade Correlation
- Performance Data
 - Temporal Registration
 - 3 3-Scene Intervals - <10 CP Per Scene
 - 3 Single Scene Direct Measurements - ~30 Eval. Pts. Per Scene
 - Geodetic Rectification
 - 3 5-Scene Intervals - <10 CP Per Scene
 - 1 5-Scene Interval Direct Measurement - 100 Eval. Pts.

TIPS GEOMETRIC CORRECTION PERFORMANCE

- Temporal Registration
 - Requirement is 0.30 Pixel, 90 Percent
 - Measurement Range in Pixels, 90 Percent
 - $0.20 \leq \text{Cross Track Error} \leq 0.36$
 - $0.28 \leq \text{Along Track Error} \leq 0.41$
 - Low End is Direct Measurement

- Geodetic Registration
 - Requirement is 0.50 Pixel, 90 Percent
 - Measurement Range in Pixels, 90 Percent
 - $0.43 \leq \text{Cross Track Error} \leq 0.67$
 - $0.37 \leq \text{Along Track Error} \leq 0.90$
 - Low End is Direct Measurement
- Modeling Error Budget
 - Budget is 0.165 Pixel, 90 Percent
 - Met with Less Than 10 CP Per Scene
 - Timelines Are Met With 20 or Fewer CP Per Scene

GEOMETRIC CORRECTION PERFORMANCE - CURRENT/PLANNED EFFORTS

- Eliminate Band 2, Band 5 Chips from Library
- Continue Performance Monitoring
- Pursue Calibration
 - Profile
 - Misalignment Angles
 - Filter Parameters
- Study Need for Seasonal Geodetic Control Points
- Improve Sub-Pixel Correlation Technique.

THEMATIC MAPPER IMAGE PRODUCTION
IN THE ENGINEERING CHECKOUT PHASE

DAVID FISCHER
NASA/GODDARD SPACE FLIGHT CENTER

JOHN C. LYON
SYSTEMS AND APPLIED SCIENCES CORPORATION

ABSTRACT

Thematic Mapper data processing during Landsat 4's first year was performed on an engineering evaluation basis. Fully corrected products were created for some 282 scenes during this period using software and systems based upon the intended full production systems to become operational following the evaluation period. The engineering systems included substantial software and procedures for assessing spacecraft, instrument and ground processing algorithmic behavior. The data systems are described here in terms of performance objectives, processing organization and data flow, quality assurance measurements and achievement of goals. The a priori implementation of TM radiometric and geometric corrections is described in some detail. Changes to processing suggested by or implemented on the basis of on-orbit data analysis are discussed. An evaluation of spacecraft, instrument and algorithmic performance is made.

INTRODUCTION AND BACKGROUND

The Landsat-D (now Landsat-4) program was initiated by the U.S. National Aeronautics and Space Administration (NASA) in the mid-1970's. The program and the spacecraft as ultimately defined include the fourth Multispectral Scanner (MSS) and the new higher-resolution Thematic Mapper (TM) in a 705.3km sun-synchronous circular orbit with a repeat observation cycle of 16 days. The spacecraft was launched July 16, 1982. It was recognized from the outset that the geometric and radiometric correction of the TM into useable form would require more stringent error budgets than for MSS. Sixteen detectors per spectral band for the six reflective bands and four in the

thermal band vs. six detectors in each of the four MSS bands accentuate the problems of radiometric correction for TM. Geometric correction to sub-pixel accuracies (both temporal and geodetic), similar to specifications for the larger-pixel MSS, carries with it a host of rigorous demands on the spacecraft and instrument systems in terms of stability and attitude measurement. These concerns are expressed equally in the ground processing, in which diligent concern has been given to error budgeting and the modelling of spacecraft and sensor performance to a high degree of precision.

The ultimate goal for the ground segment for TM is the production of some one hundred scenes per day to a radiometrically corrected form, with geometric corrections applied to half these scenes although the correction matrices are calculated and appended to the data as header information for the partially processed scenes. This level is to be achieved in early 1985, after an intensive R&D period and growing experience with the systems and the data.

At the outset of the program in 1976 and 1977, it was clear as well that the achievement of the engineering and scientific objectives of the mission on such a schedule was ambitious, and that substantial attention must be paid to 1) validating the precise spacecraft and instrument performance on-orbit, 2) seeking, as necessary, improvements or modifications to the ground processing procedures to accommodate experience, and 3) aggressively defining the quantitative measures of TM utility from a discipline standpoint, to maximize mission benefits as quickly as possible

The phased development ultimately defined included a one-year engineering evaluation period beginning shortly after launch, during which about one scene per day of TM would be produced for analysis of systems performance.

[EXERPTED FROM EARLY RESULTS SYMPOSIUM PAPER]

LANDSAT-4 RADIOMETRIC AND GEOMETRIC CORRECTION
AND IMAGE ENHANCEMENT RESULTS

RALPH BERNSTEIN AND JEFFREY B. LOTSPIECH
IBM CORPORATION
PALO ALTO SCIENTIFIC CENTER

KEYWORDS: Radiometric Calibration, Striping, Geometric Correction,
Enhancement, Mapping, Thematic Mapper, Personal Computer

ABSTRACT

Techniques have been developed or improved to calibrate, enhance, and geometrically correct Landsat-4 satellite data. Statistical techniques to correct data radiometry have been evaluated and have been shown to minimize striping and banding. Conventional techniques will cause striping even with perfect calibration parameters. Intensity enhancement techniques have been improved to display image data with large variations in intensity or brightness. Data have been geometrically corrected to conform to a 1:100,000 map reference and image products produced with the map overlay. It is shown that these products can serve as accurate map products. A personal computer has been experimentally used for digital image processing.

DETECTOR CALIBRATION

Figure 1 shows a subimage of San Francisco Bay from Landsat-4 Thematic Mapper scene ID 40168-18143-1 acquired December 31, 1982. Visible in this image are striping defects in spite of NASA gain and bias calibration processing. An experiment was conducted to see what effect the application of standard gain-bias radiometric calibration would have on a random noise image using actual calibration values.

Figure 2 and 3 show the result of this calibration processing applied to the hypothetical, randomly generated data with similar statistical characteristics to the San Francisco Bay sub-image. Figure 2 shows the data as it might come from the satellite, using the actual detector sensitivities

from band 1. Striping is very visible in this figure. Figure 3 shows the data after it has been "ground processed" by multiplying it by the precise inverse of the detector sensitivities. Striping has been reduced, but not completely eliminated. How can striping remain, when the precisely correct calibration factors have been applied? The data is sampled and quantized between the time the radiance is sensed in the satellite and corrected on the ground, which causes a loss of precision and leads to the observed stripes. (Ref. 1).

An alternative to standard calibration is diagrammed in Figure 4. Shown is a probabilistic approach. If a detector's calibrated output of an input 64 count is 64.504, for example, we randomly place 50.4% of the input 64's into the 65 output bucket and 49.6% of the input 64's into the 64 output bucket. The maximum error is greater with the probabilistic approach. However, the expected value of the output counts is exactly equal to the expected value of the radiance. Therefore, the accumulated error over all the pixels evaluates to zero. Thus, no striping can be introduced due to accumulated calibration error. The probabilistic estimating approach was applied to both the randomly generated data and to the actual San Francisco Bay scene. These results are shown in Figure 5 and Figure 6. As can be observed, striping is completely eliminated.

LOCAL INTENSITY ENHANCEMENT

Figure 7 shows a TM band 1 subimage of the San Francisco scene. In general, to produce an image on an output device (such as a display or plotter), the input count $I(i,j)$ must be multiplied by some gain and offset by some bias:

$$I_o(i,j) = b + gI(i,j) \quad (1)$$

Equation 2 can be reformulated:

$$I_o(i,j) = \mu_D + \frac{\sigma_D}{\sigma} (I(i,j) - \mu) \quad (2)$$

where μ is the actual mean of the input pixels, σ is the actual standard deviation, and μ_D and σ_D are the desired mean and standard deviation, respectively. Images can be generated with very dark or light regions that may obscure detail. Wallis and others have observed that μ and σ need not be calculated over the entire image -- that, in fact, the resulting display can be enhanced if each pixel is adjusted based on the mean and standard deviation of its neighborhood. We have parameterized the algorithm to place a weight a , ($0 \leq a \leq 1$) on local versus global statistics:

$$\mu' = a\mu_L + (1-a)\mu_G \quad (3)$$

where μ_L is the local mean in the neighborhood of the pixel and μ_G is the global mean (for the entire image). By including global statistics in the formula, some of the original characteristics of the data can be maintained. We use the concept of "average local standard deviation" to determine the gain:

$$\sigma' = \frac{1}{n} \sum_{i=1}^n \sigma_i \quad (4)$$

where each of the σ_i are local standard deviations of the regions of the image. Figure 7 shows the original subimage, and Figure 8 and 9 with $a = 1$ and 0.5, respectively.

IMAGE GEOMETRIC MODIFICATION

The Landsat-4 TM image was analyzed and a subimage geometrically corrected to conform to a 1:100,000 scale USGS map, such that the two data sets were in registration. The purpose of this processing was to assess the type of processing needed to correct the data to conform to a map reference. In addition, we were interested in determining whether satellite data could serve as a map reference, and what benefits might accrue. We found a bivariate polynomial to be adequate for modeling the image errors. We chose cubic convolution resampling in this experiment. Common geodetic control points were located on the map and on the image, and a mapping function determined:

$$u(xy) = 1818.2 + 0.3515x + 0.0625y \quad (5)$$

$$v(xy) = 1786.9 - 0.0621x + 0.3515y \quad (6)$$

The bivariate polynomials were generated by a mean squared fit to 25 control points. A good fit could be achieved in this case by a bivariate polynomial of first degree. The degree of the polynomial could be greater for a full image. The reference image (map) is shown in Figure 10 and the corrected image in Figure 11. The resultant products can serve as useful map-like materials, in particular when the map is overlain on the corrected Landsat data. Careful comparison shows errors in the map, as the image provides a true representation.

IMAGE PROCESSING ON THE IBM PERSONAL COMPUTER

Because of a concern of users who do not have large computational facilities to process TM data, experiments were conducted to evaluate the utility of the IBM PC to process TM data. Results show that multi-band TM subimages of 320 x 200 can be interactively processed in seconds and displayed with clarity. Functions implemented include image display, enhancement, enlargement, classification, and statistical analysis.

SUMMARY OF RESULTS

Standard radiometric calibration can introduce striping in image data even with precisely known calibration factors. Statistical intensity allocation processing can significantly reduce striping. Local Intensity Enhancement processing can visually enhance images and increase apparent information content. This type of processing will eliminate very dark or light regions which sometimes obscure regions of interest. However, this processing can introduce image artifacts as the algorithm includes some spatial operators. Registration of Landsat Thematic Mapper sensor data to a cartographic map is feasible and provides a user with a new map product that is current and cartographically correct. The correct image can now serve as a cartographic reference for correcting images acquired at a later time.

Personal computers provide a low-cost approach to the processing of sub-image data with adequate function and speed.

RECOMMENDATIONS

Ground calibration processing should use probabilistic radiometric calibration procedures. Operational systems should provide users with a digitized map data set as the eighth "band". If the sensor data is already geometrically corrected to the map, the map than is helpful for location and annotation. If uncorrected, is can be used as a reference for correction, or distorted to conform to the image geometry to support interpretation and analysis.

REFERENCES

R. Bernstein and J. B. Lotspiech, "Landsat-4 Thematic Mapper - Results of Advanced Digital Processing Experiments", 8th Pecora Memorial Remote Sensing Symposium, Oct. 4-7, 1983.

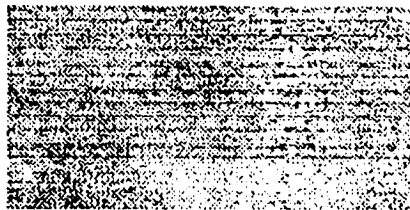


FIGURE 1: SAN FRANCISCO BAY

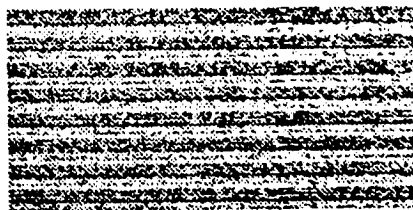


FIGURE 2: HYPOTHETICAL SATELLITE DATA

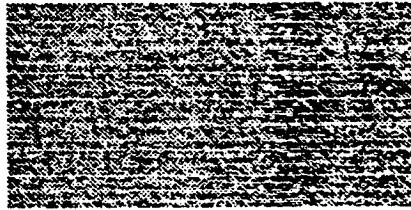


FIGURE 3: HYPOTHETICAL DATA CORRECTED

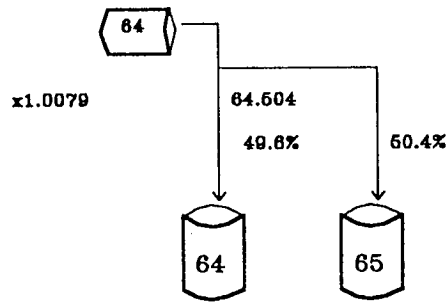


FIGURE 4: PROBABILISTIC CALIBRATION

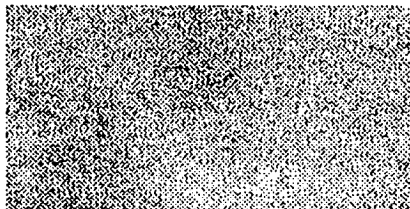


FIGURE 5: SAN FRANCISCO BAY PROBABILISTICALLY DE-STRIPED

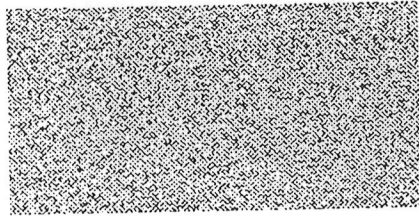


FIGURE 6: HYPOTHETICAL DATA PROBABILISTICALLY DE-STRIPED

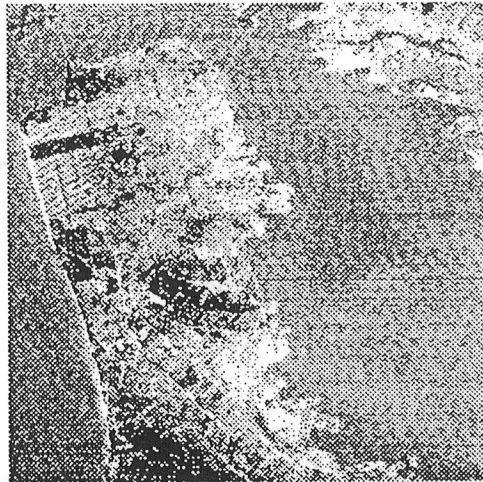


FIGURE 7: SAN FRANCISCO BAND 1

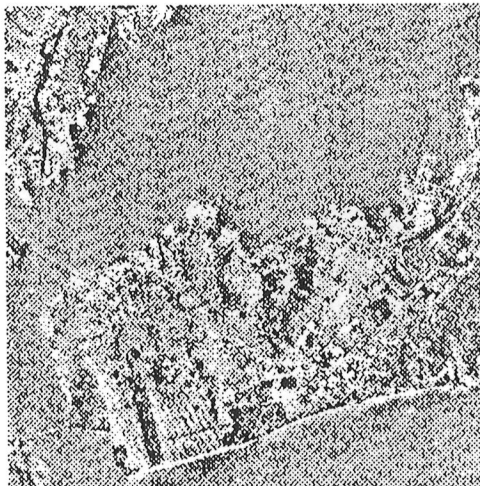


FIGURE 8: LOCAL INTENSITY ENHANCEMENT $a=1.0$



FIGURE 9: LOCAL INTENSITY ENHANCEMENT $a=0.5$

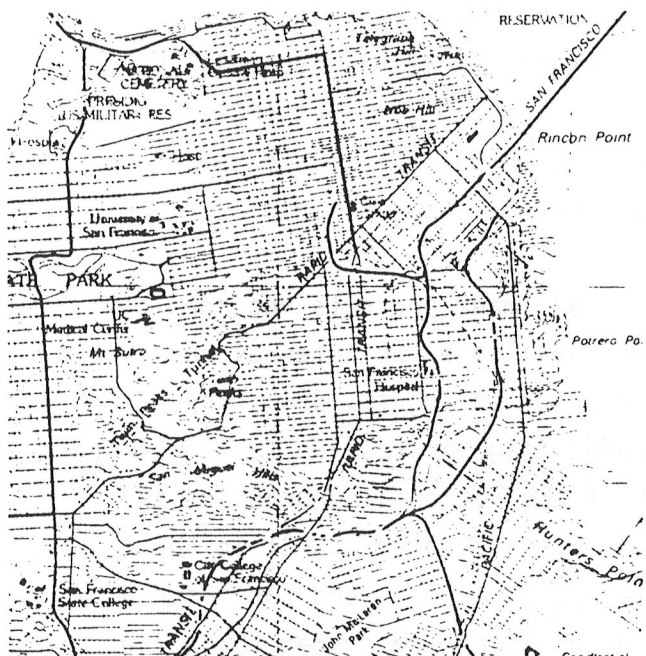
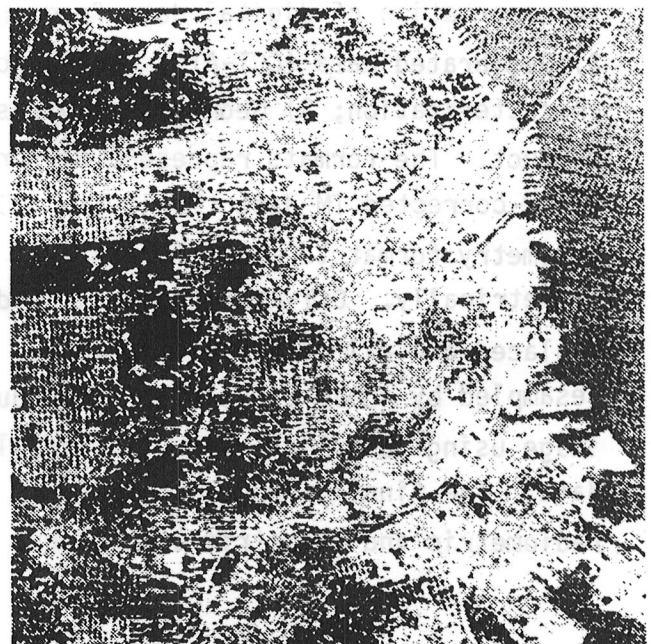


FIGURE 10: DIGITIZED USGS MAP

FIGURE 11: REGISTERED THEMATIC MAPPER IMAGE



TM DIGITAL IMAGE PRODUCTS FOR APPLICATIONS

JOHN L. BARKER
NASA/GODDARD SPACE FLIGHT CENTER

FRED J. GUNTHER
ROCHELLE B. ABRAMS
DAVE BALL
COMPUTER SCIENCES CORPORATION

KEYWORDS: Remote Sensing, Landsat-4, Thematic Mapper, Digital Image Processing, Radiometric Calibration, Geometric Resampling, Interband Registration, Computer Compatible Tapes (CCT), Formats of Tapes, CCT-BT, CCT-AT, CCT-PT, Channel-Correlated Shifts, SCROUNGE-era, TIPS, RLUT (Radiometric Look-Up Table)

Landsat-4 Thematic Mapper (TM) digital image products recorded onto computer compatible tapes (CCTs), which were available for internal research purposes during the SCROUNGE-era processing prior to August, 1983, are reviewed. They were generated by the SCROUNGE image processing system of the Landsat-4 Assessment System (LAS) facility of the National Aeronautics and Space Administration (NASA) at Goddard Space Flight Center (GSFC) in the tape formats: 1) Raw band-sequential data (CCT-BT), generally used for internal transportation of digital data from one ground processing system to another; 2) Calibrated data (CCT-AT), useful for researchers doing radiometric characterization; 3) Geometrically resampled data (CCT-PT), the final product. The formats represent different steps in the process of producing fully-corrected TM data (Table 1). CCT-BT images are re-sequenced from telemetry format to image format, but are uncorrected radiometrically and geometrically. CCT-AT images have had data from two faulty data channels replaced and all data radiometrically calibrated. CCT-PT images have been resampled by cubic convolution procedures to provide a geometrically corrected image using satellite ephemeris and altitude data and scan-mirror correction data. The final product, the CCT-PT, is the one to which all of the radiometric and geometric corrections have been

applied; this is the product that is available to users, who may purchase the set of tapes from NOAA at the EROS Data Center (EDC) in Sioux Falls, SD.

Image files on the three tapes of the CCT-PT set are blocked four image lines per tape record, yielding a blocksize of 28672 bytes. The CCT-AT also has a blocking factor of four but a blocksize of 26624 bytes; the equivalent values for the CCT-BT images are five and 32000 bytes. Some other characteristics of the tapes are summarized in Table 1.

Forward and reverse scans on all products are properly oriented east-west, but the CCT-BT and CCT-AT images have an alignment offset between scans. Original band-6 120m IFOV pixels have been replicated to four 30m IFOV pixels along a line in CCT-BT images, but the lines are not replicated to yield a full 4x4 block of 30m IFOV pixels that are array compatible with the other bands until the CCT-AT image is produced. Production of the CCT-PT involves two sequential steps of geometric resampling to produce 28.5m IFOV pixels.

Image processing artifacts are present in both CCT-AT and CCT-PT products. Application of Radiometric Look-Up Table (RLUT) during radiometric calibration produces discontinuities in the histograms as a result of skipping some gray levels or digital numbers (DN). RLUTs are chosen to cause expansion of original raw data so that it can be recovered by removing the interspersed "empty bins" in CCT-AT digital images. This empty-bin artifact is smoothed over by cubic convolution resampling. However, resampling produces a new artifact when image data and zero-fill data are convolved at the east and west edges of the geocorrected image to produce "fuzzy frame edges."

Channel and scan striping are evident in images in all three image formats. Channel striping in CCT-BT arises from the difficulties in making sensors exactly alike and in CCT-AT images from imperfect radiometric calibration. Scan striping apparently arises from random resetting of the offset to one of two reference states at the start of each scan. It is referred to here as a "channel-correlated shift" since all channels within a band shift at the same time even though the magnitude of their shifts differ. Channels 4, 8, 10 and 12 of Band 1 and Channel 7 of band 7 are the channels

with the largest shifts of between 1 and 2 digital numbers (DN). Cubic convolution resampling to produce the CCT-PT reduces the visual impact of all striping. If resampling was performed to a north oriented column, it would reduce the apparent striping even further, as well as provide a more map-compatible product.

Saturated or very bright isolated pixels in all bands result from apparent specular reflection of small objects on the ground. These pixels have proven to be useful in calculating interband registration coefficients for all CCT formats. The coefficients indicate that the bands are registered to each other within a small fraction of a pixel. The higher spatial resolution of 30m TM imagery as compared to 80m Multispectral Scanner (MSS) imagery has resulted in a dramatic increase in pixels with apparent specular reflection. Higher resolution sensors can expect to see even more specular reflection, especially from man-made objects. New information extraction techniques are needed to utilize these new radiometrically discontinuous data.

Author recommendations call for 1) better documentation, including that on tape files; 2) better calibration procedures and calibrated images; 3) nearest-neighbor resampling option in addition to cubic convolution; 4) computer processing using real-number formats for all intermediate products, to eliminate the effects of integer roundoff; and 5) the use of video laser disk media for recording archival and browse images.

TABLE 1

General Comparisons among Landsat-4 Thematic Mapper Digital Products.

CCT SCROUNGE-ERA FORMATS (prior to August 1983)
LANDSAT-4 TM DIGITAL TAPES

	CCT-BT	CCT-AT	CCT-PT
TAPES	2	2	3
DENSITY	6250 bpi	6250 bpi	6250 bpi
BAND FORMAT	BSQ	BSQ	BSQ
IMAGE RECORDS/FILE	1197 (300—B6)	1497	1493
RECORD LENGTH	32000 BYTES	26624 BYTES	28672 BYTES
LINE LENGTH (FILLED)	6400 (6400)	6176 (6856)	6967 (7168)
BLOCKING FACTOR	5	4	4
PREPROCESSING			
RADIOMETRIC	NONE	YES	RESAMPLED
GEOMETRIC	FLIP REVERSE SCANS	NONE	RESAMPLED
EROS DATA CENTER AVAILABILITY	NO	YES	YES

CCRS EVALUATION OF LANDSAT-4 DATA INVESTIGATION UPDATE

W. MURRAY STROME
CANADA CENTRE FOR REMOTE SENSING

- Multispectral Scanner
- Thematic Mapper

LANDSAT-4 MSS INTERBAND REGISTRATION

- Evaluation of band offset in raw Landsat-4 MSS data
- Method: Statistical comparison between line-pixel locations of uniformly distributed ground control points in the four MSS bands
- Reliability and high accuracy in line-pixel localization is achieved with two different techniques:
 - Manual GCP (lakes, islands, ...) extraction on CCRS DICS System
 - Digital band-to-band correlation (modified one-dimensional stereo correlation algorithm), correlation matrix: 13 lines x 13 pixels
- Image selected: Mistassini scene, path-row 16-24, June 21, 1983

LANDSAT-4 MSS INTERBAND REGISTRATION

BAND "N"

RELATIVE TO

SAMPLE NUMBERS

BAND 1	MANUAL GCP'S	DIGITAL CORRELATION
BAND 2 - BAND 1	98	412
BAND 3 - BAND 1	98	2648
BAND 4 - BAND 1	98	1966

LINE MISREGISTRATION (L \pm σ_L)

	MANUAL GCP'S	DIGITAL CORRELATION
BAND 2 - BAND 1	0.10 \pm 0.03	- - -
BAND 3 - BAND 1	0.10 \pm 0.03	- - -
BAND 4 - BAND 1	0.10 \pm 0.03	- - -

PIXEL MISREGISTRATION (P \pm σ_P)

	MANUAL GCP'S	DIGITAL CORRELATION	POST LAUNCH OFFSET (NASA REV. 7)
BAND 2 - BAND 1	1.91 \pm 0.05	1.92 \pm 0.01	1.95007
BAND 3 - BAND 1	3.97 \pm 0.04	4.01 \pm 0.01	3.89084
BAND 4 - BAND 1	5.77 \pm 0.04	5.74 \pm 0.01	5.84091

LANDSAT-4 MSS INTERBAND REGISTRATION

CONCLUSIONS:

- Possible line misregistration of 0.1 pixel between band 1 and the other bands. No line misregistration between bands 2, 3 and 4.
- Agreement within 1σ between results obtained from the two pixel localization techniques
- Significant divergence (bands 3 and 4) between the experiment pixel misregistration results and the published figures (NASA Rev. 7)

LANDSAT-4 MSS MIRROR VELOCITY PROFILE DEVELOPMENT

BASIC ASSUMPTIONS:

- No orbit or attitude model used
- Independent of line length variations (preadjusted)
- Combine effects of mirror velocity, earth curvature and panoramic distortion
- Development scene has no relief
- Use 200-300 uniformly distributed ground control points (GCPs)

METHOD:

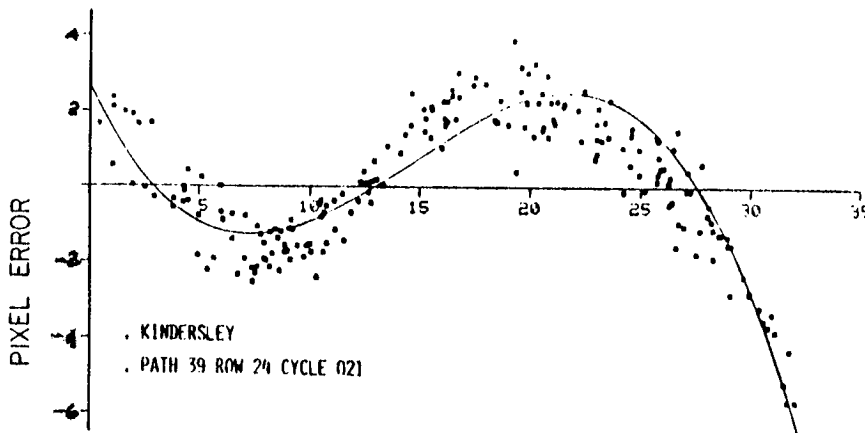
- Find and measure GCPs in uncorrected image
- Do a least squares affine fit of GCP map coords to GCP image coords
- Compute residual errors in the mirror scan direction (pixel #)
- Generate a mirror correction profile by fitting residual pixel errors

LANDSAT-4 MSS MIRROR PROFILE DEVELOPMENT

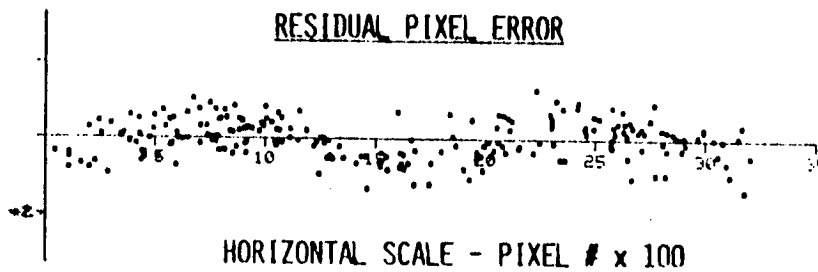
PROFILE FIT: CONVENTIONAL METHOD

- Use a 3rd order polynomial model to fit pixel error to pixel number
- Satisfactory for Landsats 1, 2, 3 but not 4
 - WHY? - Residual error is non-random
 - Model inadequate
- Higher order polynomial fit also unsatisfactory

CUBIC FIT TO PIXEL ERROR



RESIDUAL PIXEL ERROR

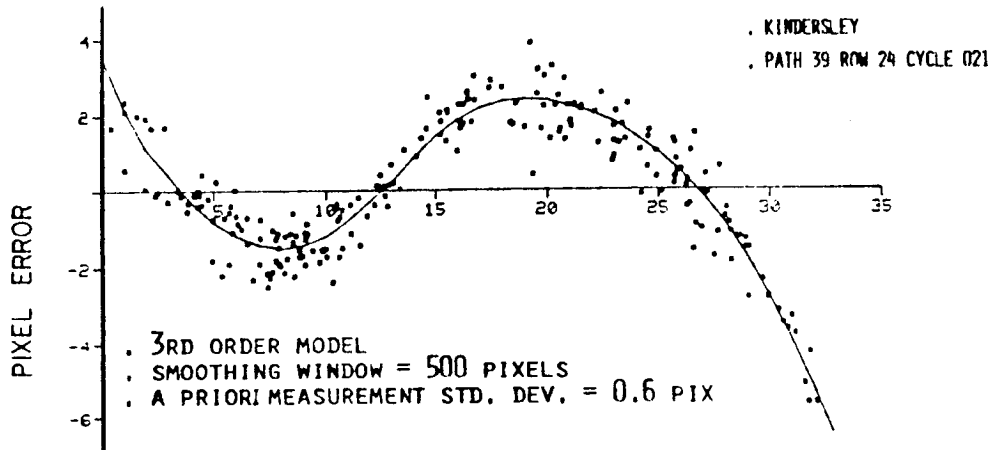


LANDSAT-4 MSS MIRROR PROFILE DEVELOPMENT

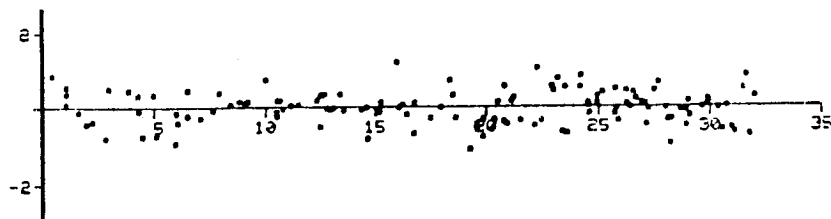
PROFILE FIT: KALMAN SMOOTHING FILTER APPROACH

- Continual updates to a polynomial model
- Incorporates a smoothing window or 'Finite Memory'
- May be 'Tuned' to data
- Tuned filter gave random residual error systematic modelling error removed

KALMAN FILTER SMOOTHED FIT



RESIDUAL PIXEL ERROR



HORIZONTAL SCALE - PIXEL # x 100

SPECTRAL CHARACTERIZATION OF THE LANDSAT THEMATIC MAPPER SENSORS

BRIAN L. MARKHAM AND JOHN L. BARKER
NASA/GODDARD SPACE FLIGHT CENTER

A summary and analysis of data collected by Hughes/SBRC on the spectral characteristics of the Landsat-4 backup Thematic Mapper instruments, the protoflight (TM/PF) and flight (TM/F) models, respectively, is presented. Tests were conducted on the instruments and their components to determine compliance with two sets of spectral specifications: Band-by-band spectral coverage and channel-by-channel within-band spectral matching.

Spectral coverage specifications were placed on: (1) band edges--points at 50% of peak response, (2) band edge slopes--steepness of rise and fall-off of response, (3) spectral flatness--evenness of response between edges, and (4) spurious system response--ratio of out-of-band response to in-band response. Compliance with the spectral coverage specifications was determined by analysis of spectral measurements on the individual components contributing to the overall spectral response: filters, detectors, and optical surfaces. The protoflight and flight model TM's used filter pieces cut from the same substrate and detectors from the same batch (except band 6); any differences between the calculated relative spectral responses (RSR) resulted from optics differences (except band 6).

The RSR's for the reflective bands were similar between PF and F except for the within-band flatnesses. Calculated spectral responses for the reflective bands in both TM/PF and TM/F were within specifications with two exceptions. One was the insufficient spectral flatnesses in bands 2, 3 and 7. The other was the high upper-band edge for band 5, which had a specification of $1750 \pm 20\text{nm}$ and was calculated as 1784nm ; this implies that there will be more contribution from variable atmospheric water vapor absorption.

In the emissive thermal band 6, the TM/PF and TM/F showed fundamentally different spectral responses. The TM/PF upper-band edge was detector limited at a temperature-dependent value of about 11.7m . The TM/F upper-band edge was filter limited at 12.4 m . A specification of 12.5 m for

the upper-band edge was chosen to provide a wide enough window for a radiometric precision of 0.5°C . While the TM/PF upper band was lower than specified, the detectors were sufficiently sensitive that the driving radiometric requirement of 0.5°C was met. In the case of the TM/F, the detectors were less sensitive and had an overall lower signal to noise performance even though both the upper-band edge requirement was met as well as the 0.5°C requirement.

Out-of-band responses for all bands were within specification. Bands 1 and 3 had some sensitivity to near-IR radiation. Band 1 filters had transmission peaks at 800 and 885 nm of 0.5% and 0.7% respectively. When measured on the flight model, an approximately 1 count contribution to band 1 resulted when the radiance between 776 and 905 nm resulted in 100 counts in band 4. Band 3 filters had peaks in out-of-band transmission at 945 and 1000 nm, of 2.8% and 1.2% respectively. The impact of this on the band 3 response has not been determined.

The spectral matching specification stated that "after system calibration, the peak-to-peak signal variations between channels within any of the first five bands and band seven, when all channels are viewing the same scene radiance, shall be less than 0.5 percent of the minimum saturation levels for the two test conditions whose parameters are given in . . . (a linearly varying spectral radiance and a flat spectral radiance)." Initial test plans called for using channel-by-channel relative spectral response curves to determine compliance with the spectral matching specification. As channel-by-channel relative spectral responses were not measured for the TM's, an alternative test was devised to assess the spectral mismatch between channels in a band. This test involved calibrating the individual channels on the 1.2 meter integrating sphere and then recording the mismatch in their outputs to a spectrally different source, the TM calibrator (modified by filters). The protoflight test gave out-of-specification results which appeared to be attributable to spatial non-uniformity of the calibrator source. A refined test was used for the flight model testing, using the calibrator source with and without filters for the two targets. With the exception of band 4, which showed a 1.7% mismatch, all bands were within

specifications. Calculations using the relative spectral response data for the 5 MSS sensors (MSS 1, 2, 3, 4 and 4-backup) showed that the flight model TM had comparable or better spectral matching than the MSS sensors.

An examination for white light leaks in the along-scan line spread function for the flight model TM revealed several minor leaks in the primary focal plane bands (1-4)--i.e., light getting to the detectors without passing through the spectral filters. The magnitude of these light leaks is dependent on the spectral character of the illumination. For the odd channels of band 1 (magnitude of the light leaks comparable for all detectors in a half-band), which was the worst observed, with the TM calibrator 'white' light source, a light leak at 13.1 IFOV off the detector center made about a 1% contribution to the signal. The location and shape of the light leaks suggests they are associated with the slots at the sides of the individual band assemblies. It is believed the protoflight model has comparable light leaks.

PRE-LAUNCH ABSOLUTE RADIOMETRIC CALIBRATION
OF LANDSAT-4 PROTOFLIGHT THEMATIC MAPPER

JOHN L. BARKER
NASA/GODDARD SPACE FLIGHT CENTER

D. L. BALL AND K. C. LEUNG
COMPUTER SCIENCES CORPORATION

J. A. WALKER
SANTA BARBARA RESEARCH CENTER

The Thematic Mapper (TM) sensor is a scanning radiometer for use in land remote sensing on Landsat-4 and Landsat-5. From both scientific and applications perspectives, the usefulness of TM digital imagery is significantly determined by its radiometric characteristics. This includes both the accuracy to which the dynamic range is known and its radiometric reproducibility or precision. This paper summarizes and analyzes results from several pre-launch tests with a 122-cm Integrating Sphere (IS) used as part of the absolute radiometric calibration experiments for the "protoflight" TM sensor carried on the Landsat-4 satellite.

TM RADIOMETRIC CALIBRATION

A radiometric calibration curve for each of the ninety-six reflective channels (detectors) on TM was calculated from a least squares fit of raw radiance, \bar{L}_R , in digital numbers (DN) versus known spectral radiance, L_λ , of the external IS in units of $\text{mWcm}^{-2}\text{ster}^{-1}\text{um}^{-1}$:

$$\bar{L}_R = O_{IS} + G_{IS} * L_{\lambda, IS} \quad (1)$$

where O_{IS} is the offset and G_{IS} is the gain for a specific channel, and

\bar{L}_R is usually averaged over 25 mid-scan values and 100 scans. For example,

on 19 March 1982, such an experiment was run under ambient conditions of temperature and pressure and gave the following results for channel 9 of band 3:

$$\bar{L}_R = (1.53 \pm 0.43) + (10.65 \pm .04) L_{\lambda, IS} \quad (2)$$

where the twenty-one IS spectral radiance levels were those determined in a subsequent recalibration in May 1982. One measure of the linearity of this regression is the $\pm 0.4\%$ coefficient of variation of the gain. This is typical of the linear response to radiance for all channels on TM. Both the gain and the offset of these solid state detectors are more stable with time than the previous generation of photomultiplier tubes used in three bands on the MSS sensor. Because of this stability, fixed electronic components on TM could be selected, in order to obtain nearly identical gains and offsets for all sixteen channels in the band.

The success of this effort is illustrated in Table 1, which summarizes information on gains and offsets for Landsat-4 TM.

Offsets are held at a fixed level by a dark current (DC) restoration circuit which is activated at the end of each scan on TM. Unlike MSS, the offset on TM was set about two counts above zero to increase the ability to measure background noise. Offset values differ by less than a count from the measured background values of radiance where there is no external source. This low uncertainty in the offset is another indication of the degree of linearity of observed raw sensor radiance in DN (0-255) versus known radiance, albeit less significant than the $\pm 0.4\%$ uncertainty in the gain.

A major objective of radiometric calibration in the ground processing of digital imagery from scanners has been to minimize the striping associated with unequal responsivities of the different channels in a specific band. If one could assure that the gains remained constant with time, the standard deviations of the offset and the coefficients of variation of the gains in Table 1 provide a quantitative measure of the degree of striping that could be expected without calibration. The ninety-six individual gains and offsets themselves provide the basis for destriping the image. Since the maximum range of within-band variation is from 3 to 7%, TM imagery may be usable for

TABLE 1

PRE-LAUNCH ABSOLUTE RADIOMETRIC GAIN AND OFFSET BY CHANNEL OF REFLECTIVE BANDS ON LANDSAT-4 PROTOFLIGHT THEMATIC MAPPER SENSOR (TM/PF) FROM LEAST SQUARES OF FIT OF RAW RADIANCE L_R , IN DIGITAL NUMBER (DN) VERSUS KNOWN SPECTRAL RADIANCE L_{λ} , OF EXTERNAL 122cm INTEGRATING SPHERE (IS):

$$\bar{L}_R = O_{IS} + G_{IS} * L_{\lambda, IS}$$

(FROM AMBIENT TEST OF TM WITH IS AT 12 EST ON 19 MARCH 1982 AT GE IN VALLEY FORGE, PA USING SPHERE RECALIBRATION OF MAY 1982 AT SBRC IN SANTA BARBARA, CA)

TM BAND NUMBER	BAND-AVERAGE OFFSET FOR 16 INDIVIDUAL CHANNELS		BAND-AVERAGE GAIN FOR 16 INDIVIDUAL CHANNELS	
	MEAN OFFSET O (DN)	STANDARD DEVIATION σ_O (DN)	MEAN GAIN G (DN PER $mWcm^{-2}ster^{-1}\mu m^{-1}$)	COEFFICIENT OF VARIATION $100\sigma_G/G$ (%)
1	2.58	± 0.18	15.78	± 0.54
2	2.44	± 0.16	8.10	± 0.89
3	1.58	± 0.20	10.62	± 0.76
4	1.91	± 0.22	10.90	± 1.23
5	3.02	± 0.11	77.24	± 0.53
7	2.41	± 0.20	147.12	± 0.72

J. BARKER/D. BALL/JAN 84

some purposes, without radiometric calibration. However, scientific applications such as comparison of radiances from sensors on different satellites, or separate independent information by combination of spectral bands require that radiometric calibration be applied to at least the level of reproducibility of the measurements. Radiometric calibration is also desirable for digital applications such as classification or for creation of stretched enhancements, since individual DN levels are discernible in both cases. Individual values of gain and offset for each reflective channel are given in this paper.

TM RADIOMETRIC SENSITIVITY

Radiometric resolution on TM is greater than that of the Multispectral Scanner (MSS) sensor. Specifications for TM called for minimum signal-to-noise ratios (SNR), as indicated in column 2 of Table 2 (Engle, 1980). While the rms radiometric precision can be no greater than the $\pm 1/\sqrt{12}$ quantization error associated with the 8-bit multiplexer on TM, the measured SNRs were much greater than specified, as summarized in Table 2, especially for the three bands on the cooled focal plane, namely two short-wave infrared (SWIR) bands and one thermal infrared (TIR) band. All channels perform normally with only three exceptions: 1) channel 3 in band 5 is dead, 2) channel 2 in Band 2 is sufficiently noisy to not meet specifications and, 3) channel 4 in Band 2 has a slow electronic response, which resulted in a degraded spatial resolution for boundaries. These three channels were excluded from the SNR averages in Table 2. Band 6 data is only approximate. Individual values for SNR were interpolated at the $\bar{L}_R = 243\text{DN}$ from linear fits of up to 21 measurements of SNR and IS radiance L_λ . Included within the empirical observations of noise are uncertainties associated with unequal bins (intervals) in the analog-to-digital converter on TM, which also contribute to the scatter of the linear fit of SNR versus L_λ . As seen in Table 2, observed rms radiometric precision on TM at full scale is between 3 and 10 parts per thousand, or approximately one digital number for the 256 DN levels, or bins.

TABLE 2

**LANDSAT-4 PROTOFLIGHT THEMATIC MAPPER (TM/PF) POST-LAUNCH RADIOMETRIC BAND CALIBRATION CONSTANTS
(FOR SCRUNGE-ERA PROCESSING PRIOR TO AUGUST, 1983)**

TM BAND NUMBER	DYNAMIC RANGE AFTER GROUND PROCESSING		SPECTRAL RADIANCE TO DIGITAL NUMBER $L_R = 0^\circ(B) + G^\circ(B) * L_\lambda$		DIGITAL NUMBER TO SPECTRAL RADIANCE $L_\lambda = \beta + \gamma * L_R$	
	RMIN AT $LR_{cal} = 0$ DN $\frac{mW}{cm^2 \text{ ster } \mu m}$	RMAX AT $LR_{cal} = 255$ DN $\frac{mW}{cm^2 \text{ ster } \mu m}$	OFFSET $0^\circ(B)$ DN	GAIN $G^\circ(B)$ $\frac{DN}{mW \text{ cm}^{-2} \text{ ster}^{-1} \mu m^{-1}}$	INTERCEPT β $\frac{mW}{cm^2 \text{ ster } \mu m}$	SLOPE γ $\frac{mW}{cm^2 \text{ ster } \mu m \text{ DN}}$
1	-0.152	15.842	2.423	15.943	-0.152	0.06272
2	-0.284	30.817	2.328	8.199	-0.284	0.12197
3	-0.117	23.463	1.265	10.814	-0.117	0.09247
4	-0.151	22.432	1.555	11.298	-0.151	0.08856
5	-0.037	3.242	2.877	77.768	-0.037	0.01286
7	-0.015	1.700	2.230	148.688	-0.015	0.006725
6(CH 4)	0.20	1.564	-37.2	186.0	0.20	0.00535

J. BARKER/JAN 84/GSFC

TM INTERNAL CALIBRATOR

The on-board Internal Calibrator (IC) in the TM sensor is designed to monitor gain and offset of the channels as a function of time (Engel, 1980). There are three IC lamps for the reflective bands which are normally operated in an automatic sequence of eight light levels. These data are collected by intercepting the optical axis of the telescope with a shutter at the end of each scan. Each light level is maintained for about 40 scans in this automatic sequence mode. Following the calibration of each channel by the IS, the automatic sequencer was run to measure the average DN value of the pulses for each level and to calculate an effective spectral radiance for each of these eight IC lamp configurations for all reflective channels. Using Channel 9 of Band 3 as an illustration, the previous IS calibration curve represented by Equation 2 was inverted:

$$L_{\lambda}^{\circ}(\ell, C) = 0.144 + 0.09394 \bar{P}^{\circ}(\ell, C) \quad (3)$$

where $\bar{P}^{\circ}(\ell, C)$ is the observed average pulse value on the date of IC calibration in DN for a particular IC lamp configuration ℓ , and $L_{\lambda}^{\circ}(\ell, C)$ is its effective spectral radiance in $\text{mWcm}^{-2}\text{ster}^{-1}\mu\text{m}^{-1}$. Several transfer tests of this type were run and compared. The final values chosen for post-launch radiometric correction were from a run on March 20, 1982 and are tabulated in this paper.

No correction was attempted in these tables for the "vacuum shift" difference between IC pulse values taken under ambient conditions and pre-launch thermal vacuum (TV) tests. Results of some TV tests are also summarized in this paper. Each time an image is taken in orbit, IC pulses are collected and regressed against these effective spectral radiances to obtain a new value of apparent gain, $G(C)$, and offset, $O(C)$, for each channel:

$$P(\ell, C) = O(C) + G(C) * L_{\lambda}^{\circ}(\ell, C) \quad (4)$$

under the assumption of constant lamp radiance.

Results from the monitoring of apparent changes in gain after launch from IC data are summarized in a companion paper for the three visible (VIS) and near infrared (NIR) bands on the primary focal plane (PFP) and for the two short wave infrared bands (SWIR) on the cooled focal plane (CFP) (Barker, 1984). Such changes in gain over the first year and a half of operation have covered a range of less than 10% for all six reflective bands and are of minimal consequence to users, as long as the radiometric correction performed during "preprocessing" of digital tapes is applied correctly.

For the thermal infrared (TIR) band, a two-point calibration is used to follow changes in gain with time. One point is the temperature of the shutter which is inserted into the optical axis at the end of each scan. This is also the reference for DC restoration on Band 6. The other point is radiance from an internal black body which is reflected to the cooled focal plane (CFP) by a mirror on the shutter. A 30% reduction in the gains for the four TIR channels was observed during the first six months of operation. Gain was restored to pre-launch values by out-gassing, i.e., turning on the TM heaters around the CFP, in January 1983. Results on thermal calibration are reported elsewhere (Lansing and Barker, 1984 and Lansing, 1983).

TM DYNAMIC RANGE AFTER CALIBRATION

One goal of radiometric calibration is to express all calibrated radiance within one band in a common radiance range. The range is called the post-calibration dynamic range of a band and is defined by the values at its two limits, RMIN and RMAX. RMIN is the spectral radiance, L_{λ} , corresponding to a calibrated radiance, L_{cal} , at a DN value of zero. Similarly, RMAX for an 8-bit sensor is the radiance at $L_{cal} = 255$ DN. To convert to in-band radiance, one simply multiplies the spectral radiance by the bandwidth of that band. Spectral response curves for TM bands on Landsat-4 and -5 can be used to compute precise bandwidths and are given elsewhere (Markham and Barker, 1984).

Two equivalent methods of expressing dynamic range can be given in terms of RMIN and RMAX. One is the band offset $O^{\circ}(B)$ and gain $G^{\circ}(B)$ of L_{cal} versus L_{λ} . The other is its linear inverse, namely L_{λ} versus L_{cal} , which

can be quantified by an intercept (β) and a slope (γ) in order to distinguish them from offset and gain. Offset and gain are defined in terms of RMIN and RMAX by two equations:

$$L_{\text{cal}} = \left(\frac{\text{Range} * \text{RMIN}}{\text{RMAX} - \text{RMIN}} \right) + \left(\frac{\text{Range}}{\text{RMAX} - \text{RMIN}} \right) L_{\lambda} \quad (5)$$

or
$$L_{\text{cal}} = O^{\circ}(B) + G^{\circ}(B) * L_{\lambda} \quad (6)$$

where the range is 255 for TM and the symbols $O^{\circ}(B)$ and $G^{\circ}(B)$ are used to provide an explicit difference between the common and constant offset $O^{\circ}(B)$ and gain $G^{\circ}(B)$ for all channels after calibration and the variable pre-calibration offset $O(C)$ and gain $G(C)$ derived from the regression fit of Equation 4. For the numbers in Table 3, $O^{\circ}(B)$ is in units of DN and $G^{\circ}(B)$ in DN per $\text{mWcm}^{-2}\text{ster}^{-1}\text{um}^{-1}$.

In the same way, intercept and slope are defined by:

$$L_{\lambda} = \text{RMIN} + \left(\frac{\text{RMAX} - \text{RMIN}}{\text{Range}} \right) L_{\text{cal}} \quad (7)$$

or
$$L_{\lambda} = \beta + \gamma * L_{\text{cal}} \quad (8)$$

where Equation 8 is one form used for converting DN values into spectral or in-band radiance. For the TM band calibration constants in Table 3, β is in spectral radiance units of $\text{mWcm}^{-2}\text{ster}^{-1}\text{um}^{-1}$ per DN. Numbers in Table 3 were calculated from RMIN and RMAX. Different values may have been inadvertently introduced in the digitally processed tapes distributed to users due to rounding and different choices of bandwidths for calculating in-band radiance. In addition, RMIN values were set to zero and RMAX values to original specifications at the start of processing by TIPS (TM Image Processing System) in August, 1983. This change will be followed by at least two more changes in RMIN and RMAX values during the 1984 TM research period (Barker, 1984). The reason for this is primarily to use observed pre-launch and in-orbit data on Landsat-5 to find a common post-calibration dynamic range for both Landsat-4 and Landsat-5. In addition, recalibration of the absolute

TABLE 3

**LANDSAT-4 PROTOFLIGHT THEMATIC MAPPER (TM/PF) POST-LAUNCH RADIOMETRIC BAND CALIBRATION CONSTANTS
(FOR SCRUNGE-ERA PROCESSING PRIOR TO AUGUST, 1983)**

TM BAND NUMBER	DYNAMIC RANGE AFTER GROUND PROCESSING		SPECTRAL RADIANCE TO DIGITAL NUMBER $L_R = KO + KG * L_\lambda$		DIGITAL NUMBER TO SPECTRAL RADIANCE $L_\lambda = \beta + \gamma * L_R$	
	RMIN AT $L_R = 0$ DN $\left(\frac{\text{mW}}{\text{cm}^2 \text{ ster } \mu\text{m}}\right)$	RMAX AT $L_R = 255$ DN $\left(\frac{\text{mW}}{\text{cm}^2 \text{ ster } \mu\text{m}}\right)$	OFFSET KO (DN)	GAIN KG $\left(\frac{\text{DN}}{\text{mW cm}^{-2} \text{ ster}^{-1} \mu\text{m}^{-1}}\right)$	INTERCEPT β $\left(\frac{\text{mW}}{\text{cm}^2 \text{ ster } \mu\text{m}}\right)$	SLOPE γ $\left(\frac{\text{mW}}{\text{cm}^2 \text{ ster } \mu\text{m DN}}\right)$
1	-0.152	15.842	2.423	15.943	-0.152	0.06272
2	-0.284	30.817	2.328	8.199	-0.284	0.12197
3	-0.117	23.463	1.265	10.814	-0.117	0.09247
4	-0.151	22.432	1.555	11.298	-0.151	0.08856
5	-0.037	3.242	2.877	77.768	-0.037	0.01286
7	-0.015	1.700	2.230	148.688	-0.015	0.006725
6(CH 4)	0.20	1.564	-37.2	186.0	0.20	0.00535

138

5098(6*)/83

J. BARKER/JAN 84/GSFC

radiance values of the integrating sphere is planned as well as possible insertion of temperature-dependent algorithms. Users should therefore refer to values of calibration constants in the ancillary digital data on the tapes to verify the numbers that were actually used in the radiometric processing of the images in each set of tapes.

Errors associated with absolute calibration are discussed. Specifications call for an absolute calibration accuracy within 10% at full scale. An rms averaging of estimated precision in each transfer step from an NBS standard lamp to the IC lamps suggests a rms error of about 6%. Post-launch calibration with ground targets at White Sands, New Mexico are still being evaluated (Slater et al., 1984). Ten tests performed to transfer the channel absolute calibration in the internal calibrator showed a 5% range at full scale, except for Band 5 which showed differences up to 10%. Errors quoted above are associated with random reproducibility and do not include possible systematic errors such as: 1) calibration of NBS lamps, 2) distance dependence of calibration of integrating sphere, 3) temperature dependence of pulses from the internal calibrator (of the order of 5% over 10°C range for some channels), 4) vacuum shift, 5) differences in conditions at times of pre-launch tests and in-orbit observations, 6) random scan correlated shifts, 7) within-scan electronic droop, and 8) within-line bright-target saturation.

ACKNOWLEDGEMENTS

Radiometric calibration up through the SCROUNGE-era for TM has been the result of cooperative efforts of many people over a period of years. A few of those who deserve particular acknowledgment for helping in the designing, gathering and analysis of material for this include: Jack Engel and Jack Lansing from Santa Barbara Research Center (SBRC), Oscar Weinstein from Hughes (formerly at NASA/Goddard), Eric Beyer, Nick Koepp-Baker and Clair Wilda at General Electric in Valley Forge, Loren Linstrom, Hampapuram Ramapriyan and David FischeI for NASA/Goddard, and recent contractor assistance from Yung Lee and Son Truong of Science Applications Research (SAR) and Rochelle Abrams and Fred Gunther of Computer Sciences Corporation (CSC).

RELATIVE RADIOMETRIC CALIBRATION OF LANDSAT
TM REFLECTIVE BANDS

JOHN L. BARKER
NASA/GODDARD SPACE FLIGHT CENTER

INTRODUCTION

The paper summarized herein presents results and recommendations pertaining to characterization of the relative radiometric calibration of the protoflight Thematic Mapper sensor (TM/PF). TM/PF is the primary experiment on the Landsat-4 satellite, launched on July 16, 1982. Some preliminary pre-launch and in-orbit results are also included from the flight model (TM/F) on Landsat-5, which was launched on March 1, 1984. The goals of the paper are:

- Outline a common scientific methodology and terminology for characterizing the radiometry of both TM sensors
- Report on the magnitude of the most significant sources of radiometric variability
- Recommend methods for achieving the exceptional potential inherent in the radiometric precision and accuracy of the TM sensors.

RADIOMETRIC CHARACTERIZATION

The radiometric characteristics of TM digital imagery that are important for scientific interpretation include mean values of absolute and relative calibration constants, and estimates of the uncertainty in the relative and absolute post-calibration radiances. Mean values and uncertainties in the pre-launch absolute radiometric calibration are discussed

elsewhere (Barker, Ball et al., 1984). The subject paper focuses on characterizing variability and uncertainty of TM relative radiometry, including total variability as well as its systematic and random components. Emphasis is placed on identifying the magnitude and types of systematic errors, since these have the potential for being reduced during ground processing. Estimates of innate random variability, such as the standard deviation of a signal or its signal-to-noise ratio, are also important since they place limits on the inferences that can be drawn from single and multiple pixel radiances. However, accurate estimates of random error require the prior removal of all types of systematic variability.

SOURCES OF RADIOMETRIC VARIABILITY

Radiometric variability in the final TM image can be divided into three components, based on origin:

- Scene Variability (the source of potential information)
 - Solar Irradiance
 - Atmospheric Transmission, Absorption and Scattering (Reflection)
 - Transmission, Absorption and Reflection (Scattering) of the Target, including Shadows

- Optical and Electrical Variability of the Sensor
 - Reflected Radiance from the TM Scanning Mirror
 - Radiance from the TM Internal Calibrator (IC)

- Variability Introduced During Processing
 - "Active Scan" Imagery
 - "End-of-Scan" Shutter Calibration Data
 - Housekeeping Telemetry

Once the total variability from all non-information sources is characterized, then an evaluation can be made as to the adequacy of the precision for specific requirements. If the sensor has already been placed in orbit, as with TM/PF and TM/F, then only the systematic errors from the sensor and any possible additional errors introduced by data processing can be reduced.

ORGANIZATION OF PAPER

The table of contents for the paper is given in Table 15 at the end of this summary. Specific objectives of the research effort reported in the paper include:

- Monitoring radiometric performance of TM sensor with time (Sections 2 and 3)
- Characterizing sources of within-scene variability and uncertainty in measuring radiance with the TM sensor (Section 4)
- Outlining possible pre-distribution methodologies for optimizing TM radiometric calibration parameters based on scientific information extraction requirements and on radiometric characteristics of the TM sensor (Section 5)
- Recommending changes in operational or processing procedures and identifying candidates for further calibration, experimentation, and research (Section 6).

APPROACH TO RADIOMETRIC CHARACTERIZATION

The paper concentrates on an analysis of raw TM calibration data from pre-launch tests and from in-orbit acquisitions. A library of approximately one thousand pre-launch test tapes, each of which samples the equivalent of one scene, is currently maintained for characterization. About 25-50% have been examined. Most of the analyses of these tapes, and of data from in-orbit acquisitions, used a software program called TM Radiometric and Algorithmic Performance Program (TRAPP). Required input for TRAPP analyses includes both the raw IC calibration data from the shutter region as well as the raw uncalibrated TM digital imagery. These raw data are not available to the general public. They are used to characterize radiometric characteristics of the sensor rather than performance of the processing system.

The results of the characterization activities reported in the paper (and summarized in the following paragraphs) derive from analyses of raw (IC and image) data only. These results, therefore, pertain to all TM imagery without regard to ground processing system, be it the NASA Scrounge Era (prior to 15 January 1984) system, the TM Image Processing System (TIPS) (effective after 15 January 1984) or other ground processing facilities. Discussion of image processing techniques in response to sensor characteristics will typically reference TIPS but are applicable universally.

CHARACTERIZATION RESULTS

Post Calibration Dynamic Range

Pre-launch absolute radiometric calibrations of the six reflective bands on TM/F were used to identify a pre-calibration range of sensitivity for each of the 96 channels. These results were combined with similar pre-launch calibration ranges of sensitivity for each band in TM/PF to provide a per band post-calibration dynamic range for processing TM imagery on the TIPS. Each post-calibration dynamic range is defined by the minimum spectral radiance, RMIN, and the maximum, RMAX, for the band as given in Table 1. RMIN and RMAX values will be up-dated based on recalibration of the integrating sphere used for pre-launch absolute calibration and on reduction of certain systematic errors in the raw digital data.

Between-Scene Changes in TM/PF Gain

Data on the radiometric stability of the TM/PF with time are recorded for use in future sensor-to-sensor and sensor-to-ground absolute calibration. Figure 1 gives a plot of the band-averaged gain with time for 50 scenes of Band 4. It illustrates the least noisy of the apparent monotonic decreases in IC-determined gain for the four bands on the Primary Focal Plane (PFP). One hypothesis is that this asymptotic drop of 3 to 6% during 300 days in orbit is a long-term "vacuum shift" curve. Vacuum shift has traditionally referred to the difference between IC pulses measured during pre-launch absolute calibration under ambient atmospheric conditions and the IC pulse values observed during pre-launch thermal vacuum testing. This justifies the use of

TABLE 1.

**TM POST-CALIBRATION DYNAMIC RANGE IN
SPECTRAL RADIANCE
($\text{mW cm}^{-2} \text{ster}^{-1} \mu\text{m}^{-1}$)
(FOR TM DIGITAL IMAGERY PROCESSED ON TIPS
AFTER 15 JAN 84)**

	BAND 1	BAND 2	BAND 3	BAND 4	BAND 5	BAND 7
RMIN ^a AT $L_{\text{cal}} = 0$ DN	-0.15	-0.28	-0.12	-0.15	-0.037	-0.015
RMAX ^b AT $L_{\text{cal}} = 255$ DN	15.21	29.68	20.43	20.62	2.719	1.438

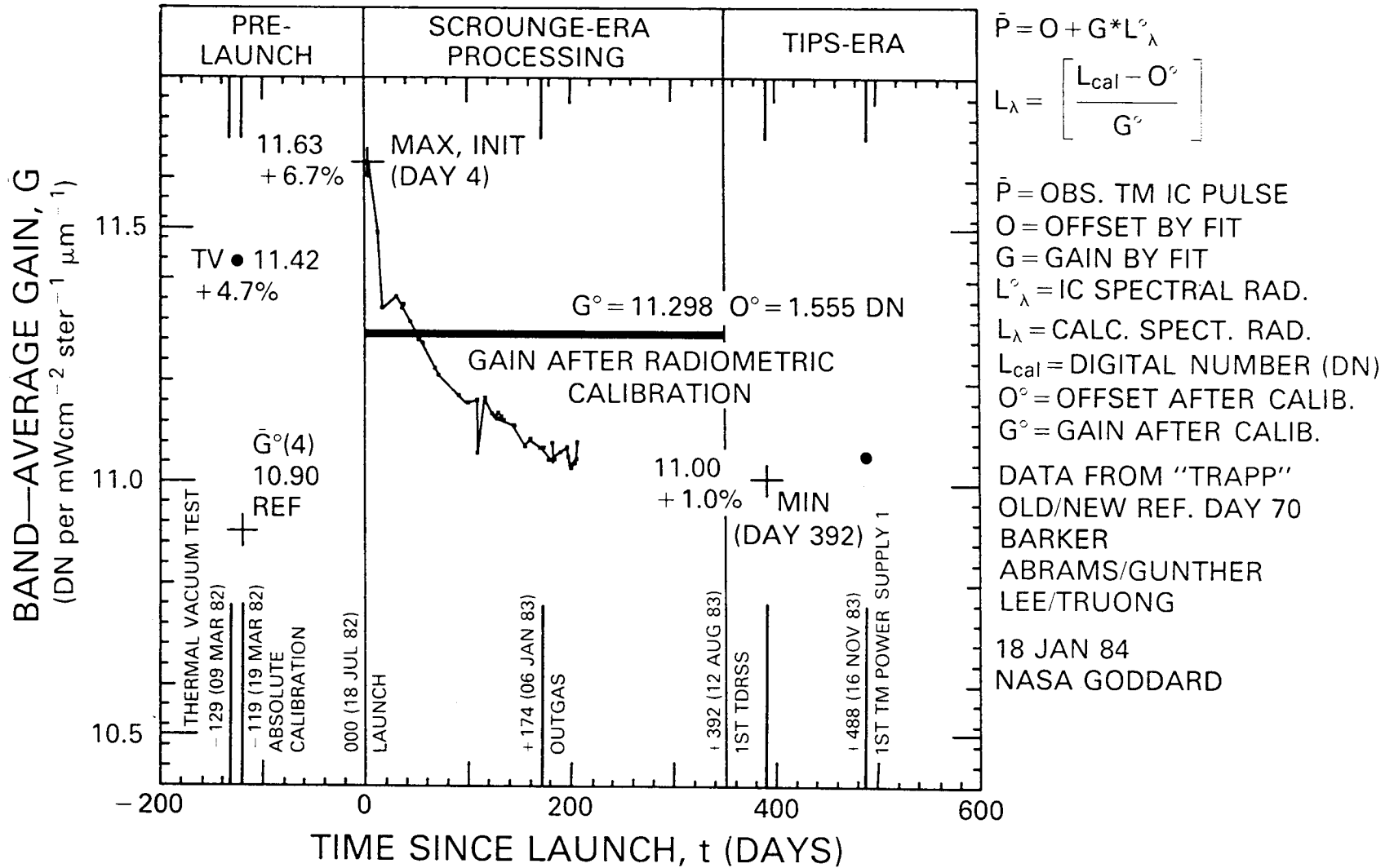
$${}^a\text{RMIN} = \frac{-0^\circ (\text{B})}{G^\circ (\text{B})}$$

$${}^b\text{RMAX} = \frac{\text{RANGE} - 0^\circ (\text{B})}{G^\circ (\text{B})}$$

$$L_\lambda = \frac{L_{\text{cal}} - 0^\circ (\text{B})}{G^\circ (\text{B})} = \text{RMIN} + \left[\frac{\text{RMAX} - \text{RMIN}}{\text{RANGE}} \right] L_{\text{cal}}$$

FIGURE 1.

LANDSAT-4 TM RADIOMETRY, BAND 4 APPARENT GAIN CHANGES FROM INTERNAL CALIBRATOR (IC) PULSES



IC pulses for radiometric calibration of the PFP under the assumption that the "vacuum shift" is due to an optical, physical, or electrical property of the detector and channel itself, rather than to some characteristic of the IC system.

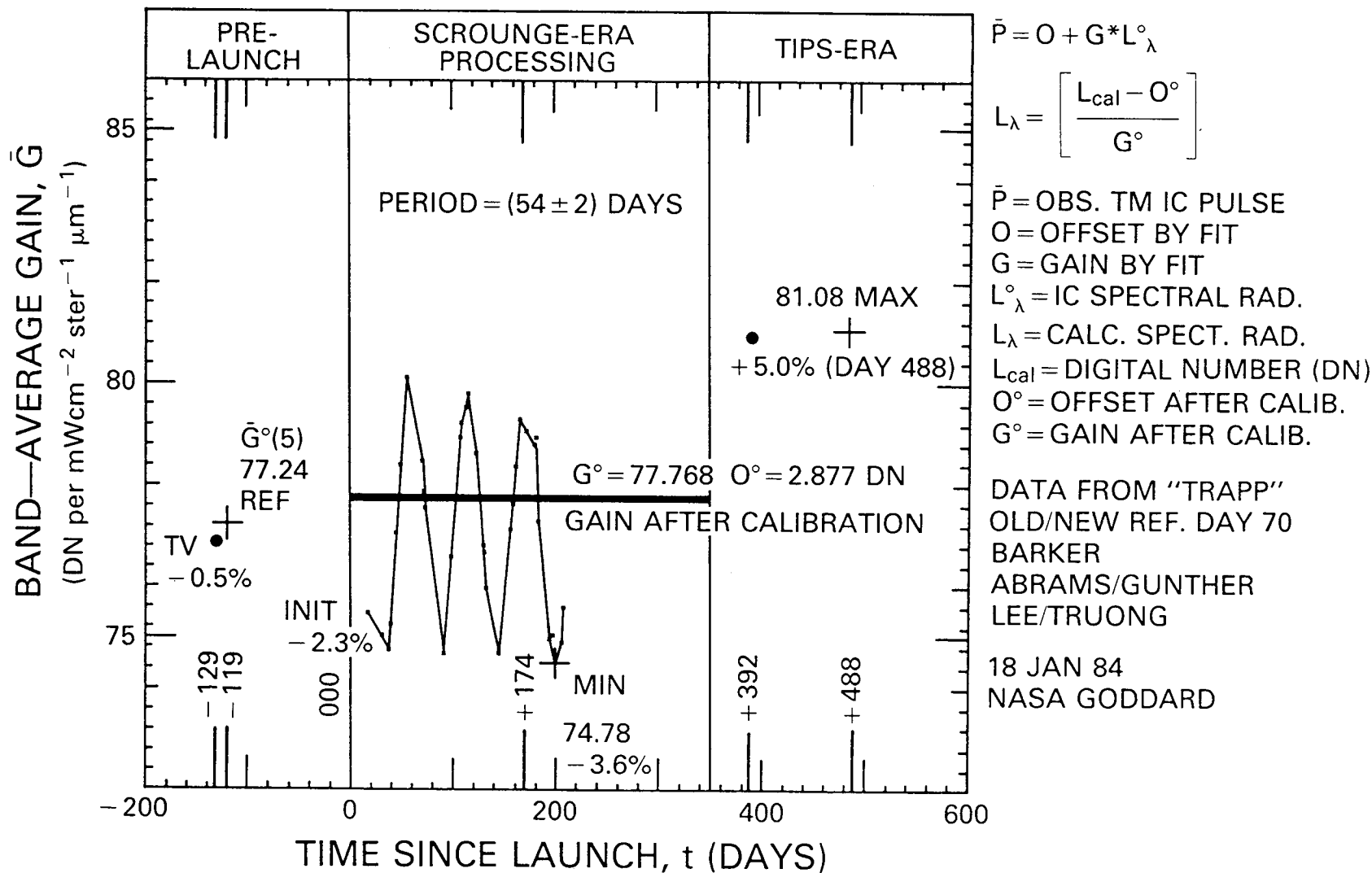
Figure 2 is a plot of the band-averaged gain for Band 5 with time. The cyclic pattern has a period of 54 days, with an rms uncertainty of about 2 days. A similar, although less well defined cyclic pattern is observed in the other shortwave infrared (SWIR) band, i.e., Band 7 has a period of 75 days with a rms error of about 6 days. Differences between peaks and valleys is always less than 9% for both SWIR bands.

The origin of these cyclic patterns on the Cold Focal Plane (CFP) is not known. One hypothesis, based on the apparent direct relationship of the periods and the wavelengths of the SWIR bands, is that the CFP and its optics are moving at a fixed rate of 11 nm/yr relative to the lens on the shutter and the PFP. This hypothesis is possible since the relay optics containing the CFP were designed to be moved in order to bring it into focus with the PFP. Since the velocity of a wave is equal to its wavelength divided by its period, the observed periods for Bands 5 and 7 both imply a velocity of 11 nm/yr. An additional hypothesis is required to explain the amplitude of the cyclic patterns. One such hypothesis is that the amplitude is a function of how close the optics are to the diffraction limit, where it will vary with phase. One test of these hypotheses would be to look for a cyclic pattern in the third band on the CFP, namely the thermal band, and relate its period to its wavelength. Similarly the hypothesized cyclic Band 6 variation in amplitude should depend on the relative sizes and areas of the detectors on the CFP as well as their wavelengths. Proof of this model for the cyclic pattern of the SWIR bands will call for the continued use of the IC to calibrate these bands.

Assuming perfect operation of the IC, all of these slowly varying trends in gain have been corrected out during the calibration of the TM imagery.

FIGURE 2.

LANDSAT-4 TM RADIOMETRY, BAND 5 APPARENT GAIN CHANGES FROM INTERNAL CALIBRATOR (IC) PULSES



There is an approximately 0.5% rms range of variability around these smoothly varying curves of band-averaged gain versus time for bands 4 and 5. While the individual curves of IC-determined gain versus time for each individual channel appear to be even more well defined, the statistical square root of 16 channels indicates that the radiometric predictability of individual channels is at least better than rms error of 0.2%. This radiometric reproducibility of the TM sensor in space suggests that systematic corrections during the ground processing of TM imagery will significantly improve radiometry.

Between-Band Changes in TM/PF Gain

In addition to maintaining scene-to-scene calibration of each band, it is also necessary to maintain band-to-band calibration. Current TIPS procedures do not provide for any within-band or between-band correlation of channels. One limit on the possible between-band variability is change in absolute gain on each of the individual bands. Apparent change in TM/PF gain, relative to the gain determined during pre-launch absolute calibration, are summarized for four specific times in Table 2. The first time was a pre-launch Thermal Vacuum (TV) test, which was designed to duplicate conditions expected in space. The second time was the actual initial (INIT) in-orbit measurement on that band. The difference between these two changes in gain (INIT-TV) was equal to or less than 2% and is a measure of how well the pre-launch TV tests agreed with the first measurements in space. The third and fourth times were upon occurrence of the maximum and minimum values of the IC-determined gain observed over the first year that Landsat-4 was in space. The range of change (MAX-MIN) is an indication of a possible uncertainty of 3 to 9% in the absolute radiometric calibration of the TM/PF reflective bands. The differences between MAX-MIN values for the bands in Table 1 are measures of the limits on possible differences in band-to-band calibrations with time. If the IC system has been working as designed then the radiometric calibration of TM imagery with the IC data will maintain the absolute calibration of the bands, and therefor will also maintain the band-to-band calibration.

TABLE 2.

APPARENT CHANGES IN TM/PF GAIN

BAND	RELATIVE CHANGE IN %, 100 $\left[\frac{\bar{G} - \bar{G}^0}{\bar{G}^0} \right]^*$					
	1	2	3	4	5	7
REF, \bar{G}^0	15.78	8.10	10.62	10.90	77.24	147.12
TV (PRE-LAUNCH)	-1.2	-1.0	3.2	4.7	-0.5	-0.5
INIT (IN-ORBIT)	-1.1	-1.0	3.6	6.7	-2.3	-0.8
(INIT-TV)	0.1	0.0	0.5	2.0	-1.8	-0.3
MAX (IN-ORBIT)	-1.1	-1.0	3.6	6.7	5.0	3.3
MIN (IN-ORBIT)	-8.2	-4.5	-2.8	1.0	-3.6	-2.5
MAX-MIN	7.1	3.4	6.5	5.7	8.5	5.8

*GAINS CALCULATED FROM LANDSAT-4 TM/PF INTERNAL CALIBRATION (IC) PULSES, \bar{P} , REGRESSED AGAINST IC EFFECTIVE SPECTRAL RADIANCE, L_λ^0 :

$$\bar{P} = O + G \cdot L_\lambda^0$$

WHERE O IS FITTED OFFSET AND G IS FITTED GAIN FOR A CHANNEL.

BAND-AVERAGE GAINS, \bar{G} , ARE COMPARED TO AN AMBIENT ABSOLUTE CALIBRATION REFERENCE \bar{G}^0 OF 19 MARCH 1982, WHERE GAINS ARE IN DN per $\text{mWcm}^{-2} \text{ster}^{-1} \mu\text{m}^{-1}$.

Within-Scene Variability in TM Radiometry

If radiometric calibration is done on one scene at a time, as is the case with Scrounge era and TIPS processing, then any sources of systematic variation which occur during the 23 seconds it takes to acquire a scene will remain uncorrected. During initial studies of TM imagery, the following types of within-scene variability have been identified:

- Bin-Radiance Dependence. The mean value of any specific digital number (DN) can be mislocated by up to two levels. Additionally, bin widths vary from nearly zero to 2 DN values. Both effects are due to errors in the analog-to-digital (A/D) converter's bin sizing and location (threshold voltages). Therefore, a calibration which uses more than the 8 bits of the original data can be used to more accurately estimate the mean value of the observed radiance, especially during the calibration, prior to preparing an 8-bit product tape.
- Scan-Correlated Shifts (discussed below).
- Coherent Noise (discussed below).
- Within-Line Droop. "Droop" is one of 3 types of "within-line, sample-location dependent noise." By comparing forward west-to-east scans to reverse east-to-west scans, a systematic droop of up to 1 DN was seen in Band 1 of TM/PF. There is a possibility that droop is actually the same as one of the other types of within-line systematic variation, namely Bright-Target Saturation.
- Bright-Target Saturation (discussed below).
- Forward/Reverse-Scan Difference. Apparent differences between forward and reverse scans may actually be related to the last exposure to a bright target. If an image contains bright objects, which are not symmetric on a scan-by-scan basis

relative to beginning and end of obscuration of the optical axis by the calibration shutter, then bright-target saturation effects will cause an apparent difference in the average values for the forward and reverse scans for the whole scene.

Reference Channels for the TM Sensors

Different channels within a band show different magnitudes for the various sources of within-scene variability. Furthermore, the random noise in the noisiest channel can be as much as a factor of two higher than in the quietest channel. Those channels with the lowest apparent rms noise on the shutter are given in Table 3. Channels with the highest rms noise, highest value for scan-correlated shift, and highest value for coherent noise are also listed. Bright-target saturation appears to have approximately the same effect on all channels in a band, probably because it is a characteristic of the design of the electronics. The high-noise reference channels may be useful for serial stripping of various types of within-scene noise. Magnitudes for these sources of TM radiometric variability are given in Table 4 for each of the reference channels currently identified on Landsat-4 TM/PF and Landsat-5 TM/F.

Scan-Correlated Shifts

Scan-correlated shifts are one of two types of "between-scan line-independent noise"; the other type being differences between forward and reverse scans. These shifts are defined by the observed discontinuity in background level. Three most significant examples are discussed as types 4-1, 4-7 and 5-3 to indicate the satellite and band in which they occur. A procedure for correcting for scan-correlated shifts has been developed and tested as part of this study. Assumptions made include:

- Shifts are constant within a line
- Signed magnitude is consistent within a scene
- Signed magnitude is channel specific

TABLE 3.

TM RADIOMETRIC REFERENCE CHANNELS

	BAND 1	BAND 2	BAND 3	BAND 4	BAND 5	BAND 7	BAND 6
LANDSAT-4 TM/PF							
LOWEST NOISE							
SHUTTER rms	9	14	12	7	2	15	4F
HIGHEST NOISE							
SHUTTER rms	16	2	1	8	7	7	1
SHIFT TYPE 4-1	4	—	1	16	15	—	—
SHIFT TYPE 4-7	—	1	16	—	10	7	—
32 KHz (3.2 mf)	16	6	8	8	[8]	[10]	—
6 KHz (18 mf)	4	1	1	16	[7]	[7]	—
LANDSAT-5 TM/F							
LOWEST NOISE							
SHUTTER rms	15	10	2	1	2	15	4
HIGHEST NOISE							
SHUTTER rms	4	1	12	3	10	9	1
SHIFT TYPE 5-3	10	1	1	1	3	—	—

TABLE 4.

TM RADIOMETRIC VARIABILITY (IN DN)

	BAND 1	BAND 2	BAND 3	BAND 4	BAND 5	BAND 7
LANDSAT-4 TM/PF						
LOWEST NOISE						
SHUTTER rms	± 1.1	± 0.4	± 0.4	± 0.3	± 0.8	± 0.8
HIGHEST NOISE						
SHUTTER rms	± 1.5	± 1.0	± 1.3	± 0.6	± 1.1	± 2.0
SHIFT TYPE 4-1	2.0	—	0.3	0.2	-0.1	—
SHIFT TYPE 4-7	—	-0.2	0.6	—	0.6	0.9
32 KHz (3.2 mf)	2.6	0.3	1.6	0.8	[0.2]	[0.3]
6 KHz (18 mf)	0.4	0.2	0.5	0.3	[0.2]	[0.2]
LANDSAT-5 TM/F						
LOWEST NOISE						
SHUTTER rms	± 0.8	± 0.2	± 0.5	± 0.2	± 0.8	± 0.8
HIGHEST NOISE						
SHUTTER rms	± 1.0	± 0.5	± 0.7	± 0.5	± 1.3	± 1.3
SHIFT TYPE 5-3	-0.3	0.7	0.5	0.4	—	—

- All channels shift together within a scan
- Different shift types can occur in each band
- Backgrounds are not constant within a line or between lines because of effects such as bright-target saturation. In this study, two regions were used on the shutter to monitor background; "shutter background 1" was an average of 24 or 28 pixels before dark current (DC) restoration, and "shutter background 2" was an average of 24 or 28 pixels after DC restore. Forward and reverse scans were separated, giving four sets of backgrounds:

BF-BDC = Background Forward Before DC

BF-ADC = Background Forward After DC

BR-BDC = Background Reverse Before DC

BR-ADC = Background Reverse After DC.

Steps in the procedure for scan-correlated shift correction include:

- Separately process forward and reverse scans
- Use a reference channel for each type of shift:
 - Type 4-1 = Landsat-4, Band 1, Channel 4
 - Type 4-7 = Landsat-4, Band 7, Channel 7
 - Type 5-3 = Landsat-5, Band 3, Channel 1
- Use shutter background to monitor shifts
- Create a binary mask indicating the presence or absence of each type of shift in each scan
- Calculate the averaged signed magnitude of shift in each channel for each type of shift by averaging the differences between backgrounds at each binary transaction
- Apply corrections on a line-by-line basis.

For Landsat-4 TM/PF, the 12 August 1983 scene of San Francisco, CA (40392-18152) was used to illustrate the two most significant types of corrections for scan-correlated shifts. Plots were made of line-averaged background before DC restore, BR-BDC, versus scan number for reverse scans. Plots were made before and after correction for all channels in Band 1 (Figure 3), and for all channels in Band 7 (Figure 4). Signed magnitudes of Type 4-1 shifts, also called "shift 1" or "form 1" shifts, are given in DN units next to the corrected background plots of Band 1 in Figure 3. There were approximately 70 transitions of Type 4-1 in the 380 scans. Type 4-1 shifts are not present in all scenes. Signed magnitudes for Type 4-7 shifts, also called "shift 2" or "form 2" shifts, are given next to the corrected plots of Band 7 in Figure 4. Type 4-1 shifts are as large as 2 DN.

For Landsat-5 TM/F, a 5 March 1984 in-orbit scene of clouds over the Atlantic Ocean (50005-16221) is used to illustrate the single most significant Type 5-3 shift. Plots were made of shutter background BF-BDC, versus scan number before and after correcting all channels in Band 3 (Figure 5). While the magnitude of the largest shifts is lower on TM/F than on TM/PF, shifts are more uniformly present on Landsat-5 TM/F, especially in Bands 2 and 3.

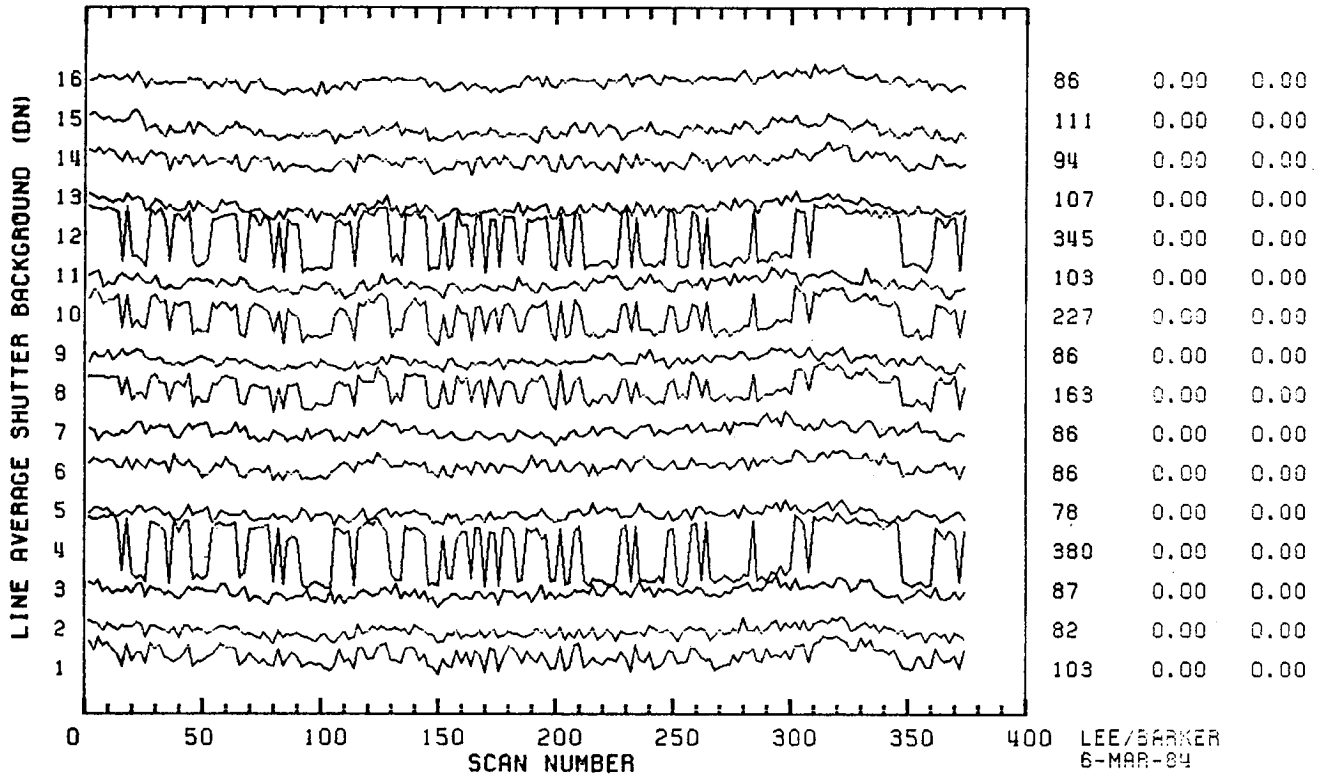
Coherent Noise

Coherent Noise is a "within-scan, sample-location dependent noise", which was made more easily quantifiable in this study by performing a Fast Fourier Transform (FFT) on 512 minor frames (mf) of shutter data from the 3 January 1983 scene of White Sands, NM (approximate ID = 40171-17080; there is no payload correction for this scene so scene ID calculation is approximate). TM/PF exhibits coherent noise in the PFP bands at two frequencies, 32.8 KHz with a period of every 3.2 pixels, and 5.9 KHz with a period of 17.6 pixels. Amounts of coherent noise vary depending on the channel, with the largest integrated area under the 32 KHz peak being about 2.6 DN for Channel 16 of Band 1. Both types of coherent noise in Landsat-4 TM/PF form sharp peaks for PFP bands.

FIGURE 3.

SCENE ID=40392-18152, BAND 1 (REVERSE)
SHUTTER BACKGROUND 1 SPECTRA BEFORE CORRECTION

1000*CV SHIFT1 SHIFT2



SCENE ID=40392-18152, BAND 1 (REVERSE)
SHUTTER BACKGROUND 1 SPECTRA AFTER CORRECTION

1000*CV SHIFT1 SHIFT2

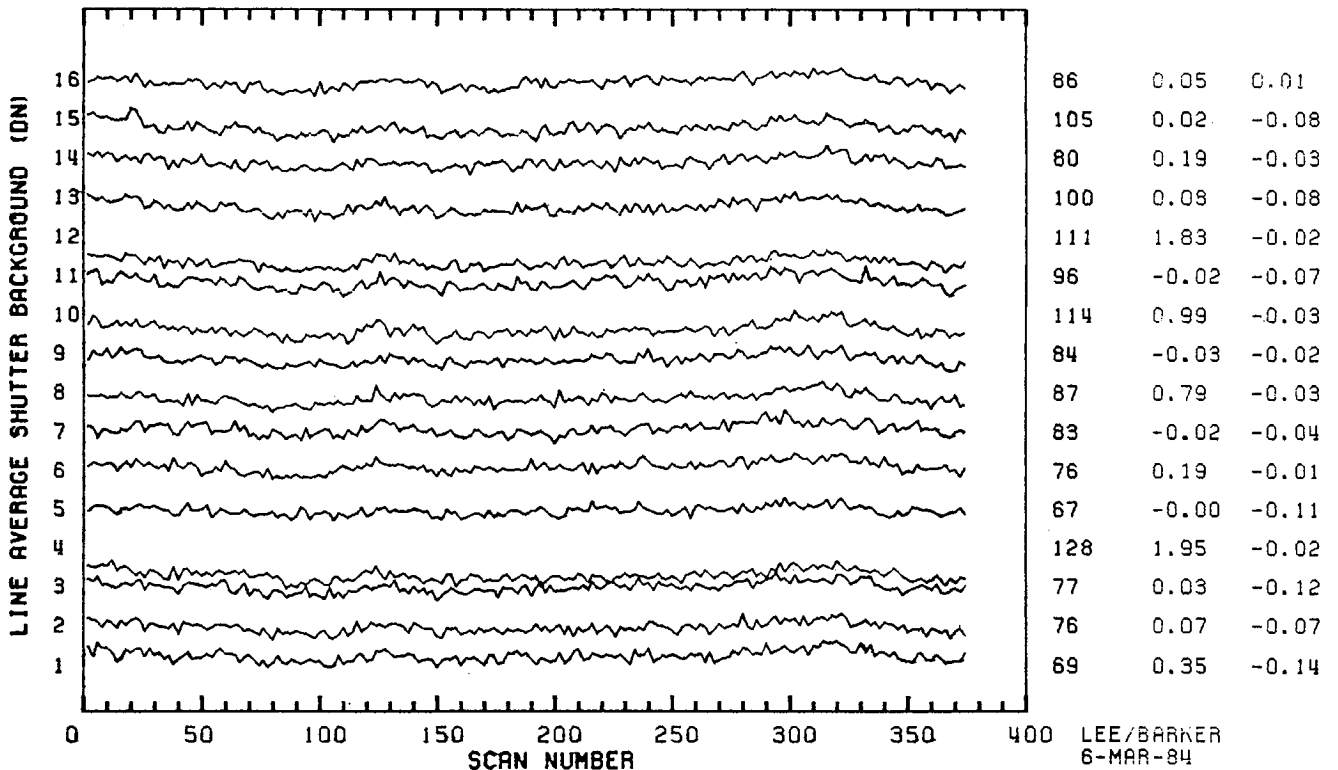
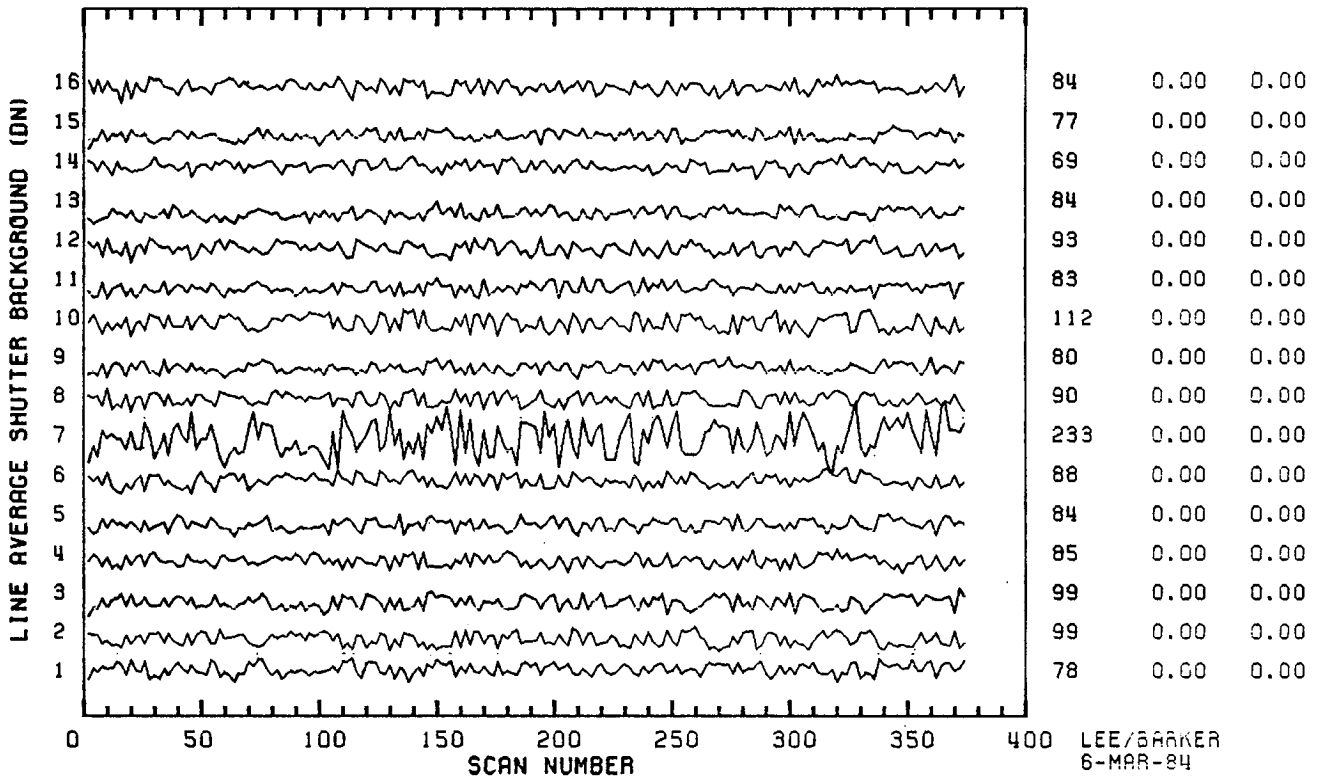


FIGURE 4.

SCENE ID=40392-18152, BAND 7 (REVERSE)
SHUTTER BACKGROUND 1 SPECTRA BEFORE CORRECTION

1000*CV SHIFT1 SHIFT2



SCENE ID=40392-18152, BAND 7 (REVERSE)
SHUTTER BACKGROUND 1 SPECTRA AFTER CORRECTION

1000*CV SHIFT1 SHIFT2

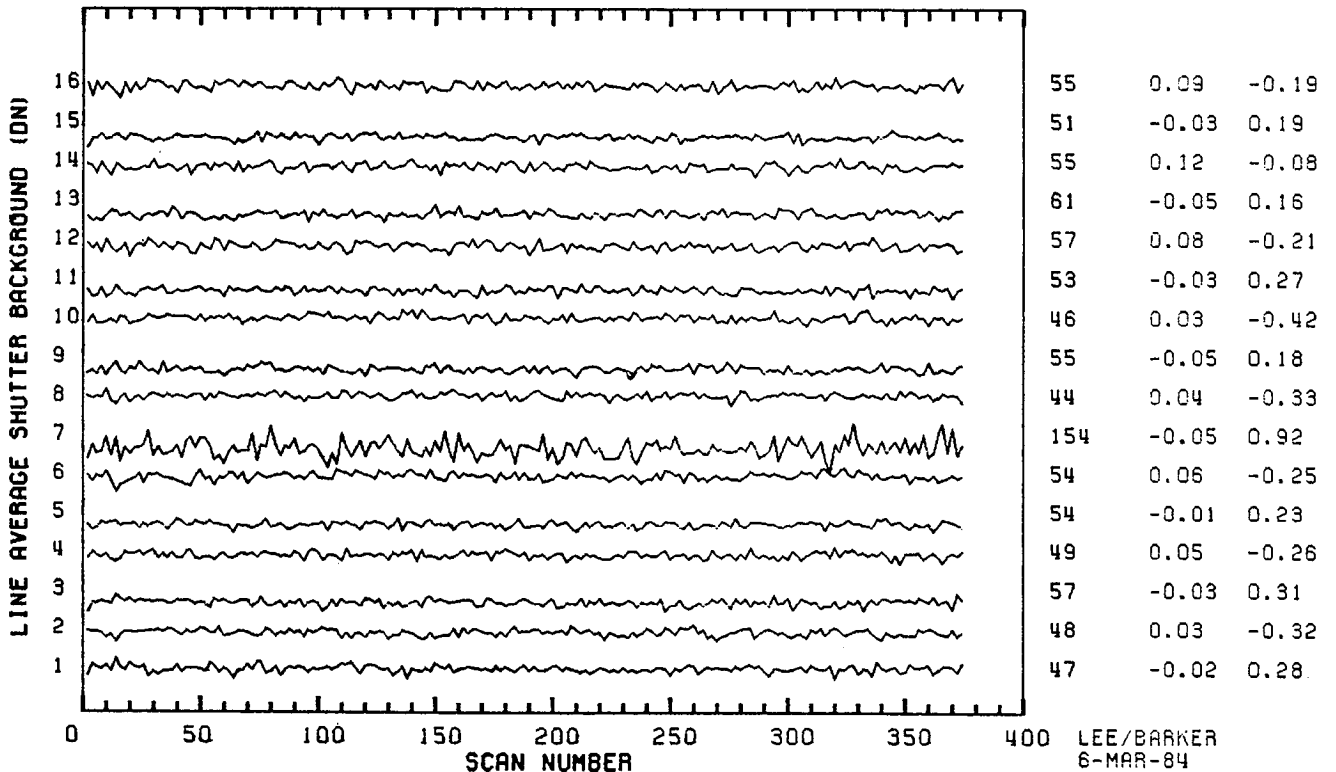
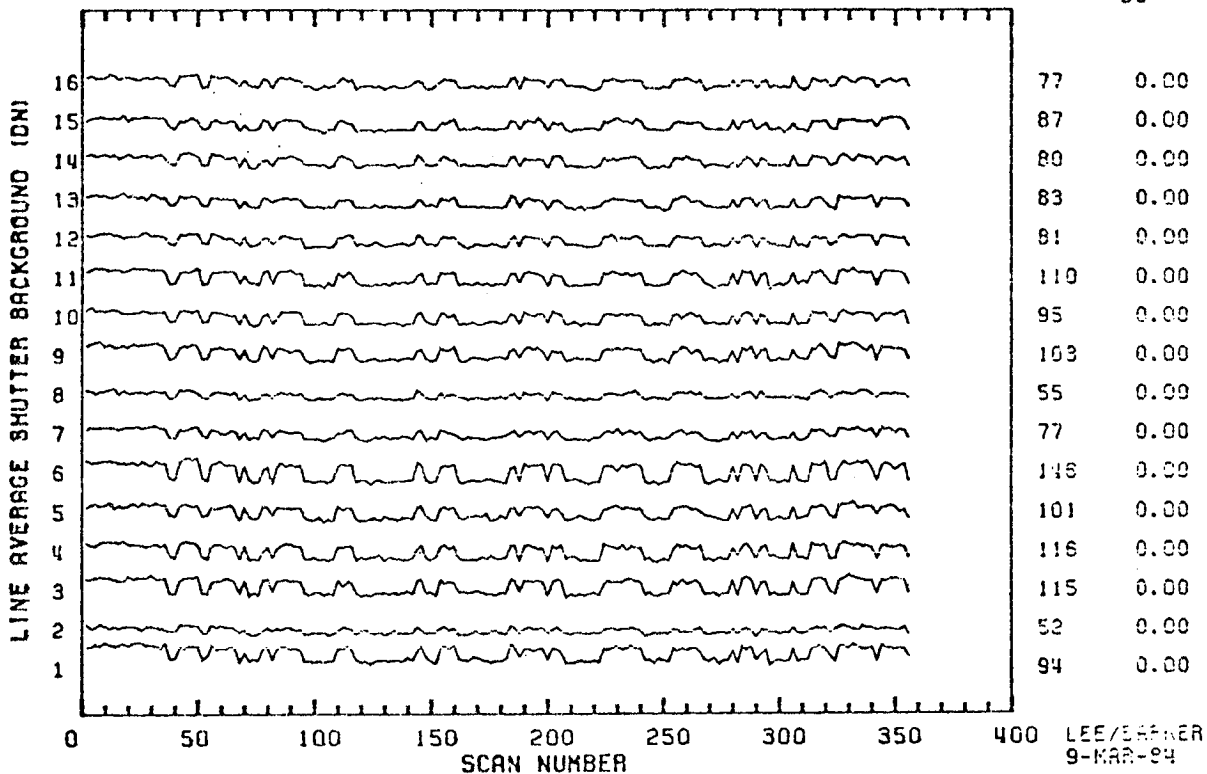


FIGURE 5.

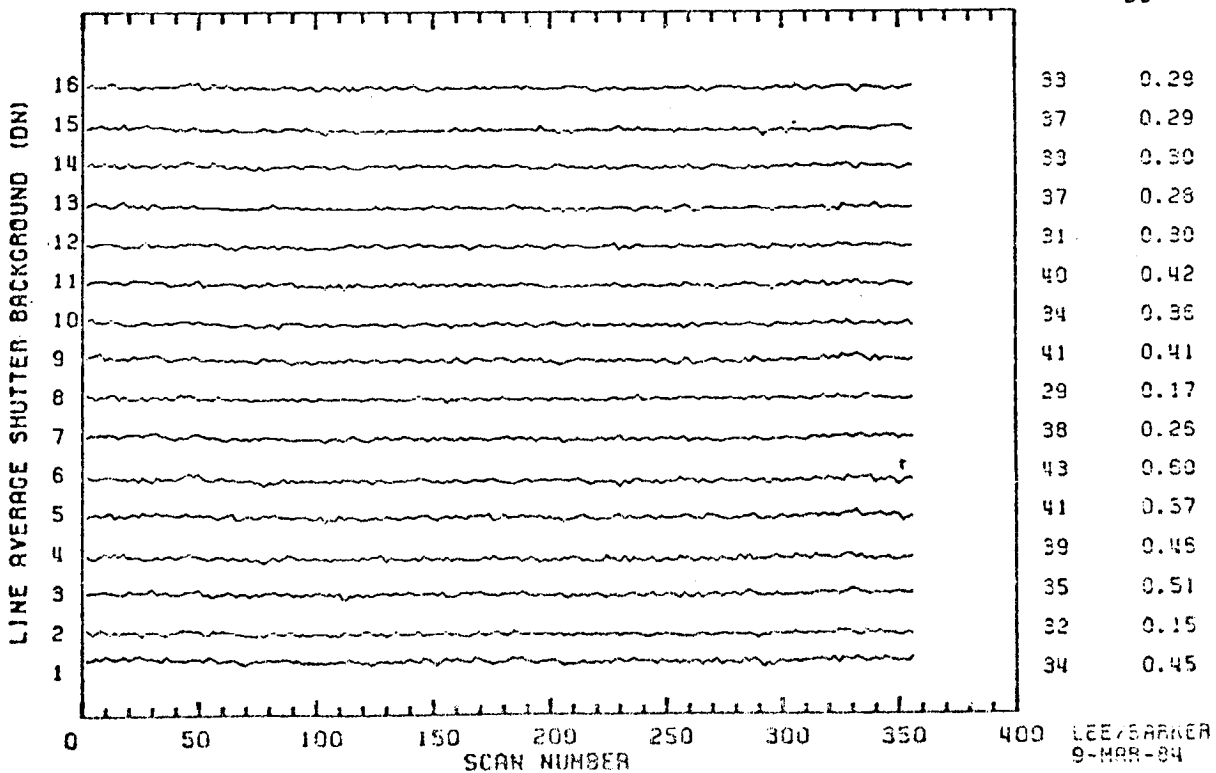
SCENE ID=50005-16221. BAND 3 (FORWARD)
SHUTTER BACKGROUND 1 SPECTRA BEFORE CORRECTION

1000*CV SHIFT
B3



SCENE ID=50005-16221. BAND 3 (FORWARD)
SHUTTER BACKGROUND 1 SPECTRA AFTER CORRECTION

1000*CV SHIFT
B3



Landsat-5 TM/F has a different coherent noise pattern. It does not have a significant peak at 32 KHz. Most channels on the primary focal plane have only one peak, or multiples of it, near 8.5 KHz. This gives spatial periods of every 12.5 pixels, or integer fractions of 12.5 pixels.

Total Within-Scene Variability

An average of the standard deviation of background on the shutter in "quiet scenes" for all channels in a band is given in Table 5 for both TM/PF and TM/F, in units of rms DN. An approximate estimate of the total range of uncertainty for raw radiance values near background can be made by multiplying the total rms noise by six, i.e., ± 3 standard deviations. The uncertainty will be greater at the upper end of the dynamic range. The range of uncertainty is at a low of about 3 DN in Band 4 for both sensors, and at a high of about 7 DN in Band 1 of TM/PF, for these two "quiet" scenes.

The average difference between background in forward and reverse scans in these quiet scenes is less than about 0.2 DN for both sensors. This is part of the justification for suggesting that apparent forward-reverse differences may be related to effects such as bright-target saturation rather than to the direction of scan.

Bright-Target Saturation

Bright-target saturation is like coherent noise and droop in being a "within-line sample-location dependent noise." It is characterized by a memory effect after exposure to a bright target, such as a cloud. The time constant of the hysteresis is such that the effect may last for thousands of samples. There may be two separate physical effects on the detectors, one which has a shorter time constant and decreases the detector sensitivity, and the other which has a longer time constant and increases the sensitivity.

In order to facilitate the interpretation of data in terms of bright-target saturation, a TM scene was chosen which had one "solid" formation of clouds, namely the 12 August 1983 scene of San Francisco, CA (40392-18152). A solid formation of clouds along the coast of the Pacific

TABLE 5.

WITHIN-SCENE VARIABILITY
TM SHUTTER BACKGROUND IN "QUIET" SCENES
TM/PF ON LANDSAT-4 AND TM/F ON LANDSAT-5
 (AVERAGE OF ALL CHANNELS IN A BAND)

BAND	TOTAL VARIABILITY (SD)		(FWD-REV) DIFFERENCE	
	TM/PF ^a (DN)	TM/F ^b (DN)	TM/PF ^a (DN)	TM/F ^b (DN)
1	± 1.24	± 0.89	0.20	0.04
2	± 0.56	± 0.29	0.12	0.06
3	± 0.73	± 0.51	0.13	0.03
4	± 0.41	± 0.37	0.09	0.01
5	± 0.89	± 0.93	0.01	0.08
7	± 1.03	± 0.93	0.03	0.10

^aLANDSAT-4 IN-ORBIT NIGHT SCENE OF BUFFALO, NY (40037-02243, 22 AUG 82)

^bLANDSAT-5 PRE-LAUNCH AMBIENT INTEGRATING SPHERE (5-198-10563, 30 AUG 83)

Ocean is present on the western side of this scene. It starts about scan 80 and then reaches eastward until there is nearly 75% cloud-cover in the lower quarter of the scene. If there were no bright-target saturation effects, then the background in the shutter region may have the same total rms variability as seen in the quiet scene (Table 5), the same near zero values for the difference between forward and reverse scans, and an independence from scan number after correction for scan-correlated shifts. This may in fact be the case for the SWIR bands, however PFP bands show an increase of about 0.5 DN in rms variability on the shutter, and up to a 2.5 DN difference for forward minus reverse background after DC restore in Band 2 (Table 6). This increases the uncertainty in the calibration of the raw radiance to a range of from 6 to 9 DN, and introduces a scene-dependence on this uncertainty. In addition, the four background plots of shutter background versus scan number in Figures 6 and 7 show a direct relationship with the distribution of the clouds.

One model for bright-target saturation effects relates them to the distance from the end of bright target, or cloud. This hypothesis was tested in this study and the results are shown in Figure 8, where the backgrounds from all four regions on the shutter are plotted against the distances from the cloud edge. The initial 1000 mf undershoot and a 6000 mf overshoot suggests that all of this background data can be fit on a single slowly varying curve, thereby justifying the two component model mentioned above.

Within-Scene Variability by Channel

Examples of the magnitudes of the various types of noise in the TM sensors are summarized by channel in Tables 7 through 13.

RECOMMENDATIONS

While the recommendations listed in summary form in Table 14 contain ideas from many people, including scientific investigators on NASA's team for characterizing the quality of the imagery from the sensors on Landsat-4 and Landsat-5, they are the creation and sole responsibility of the author. These recommendations have not been approved by either the Landsat Science Office or

TABLE 6.

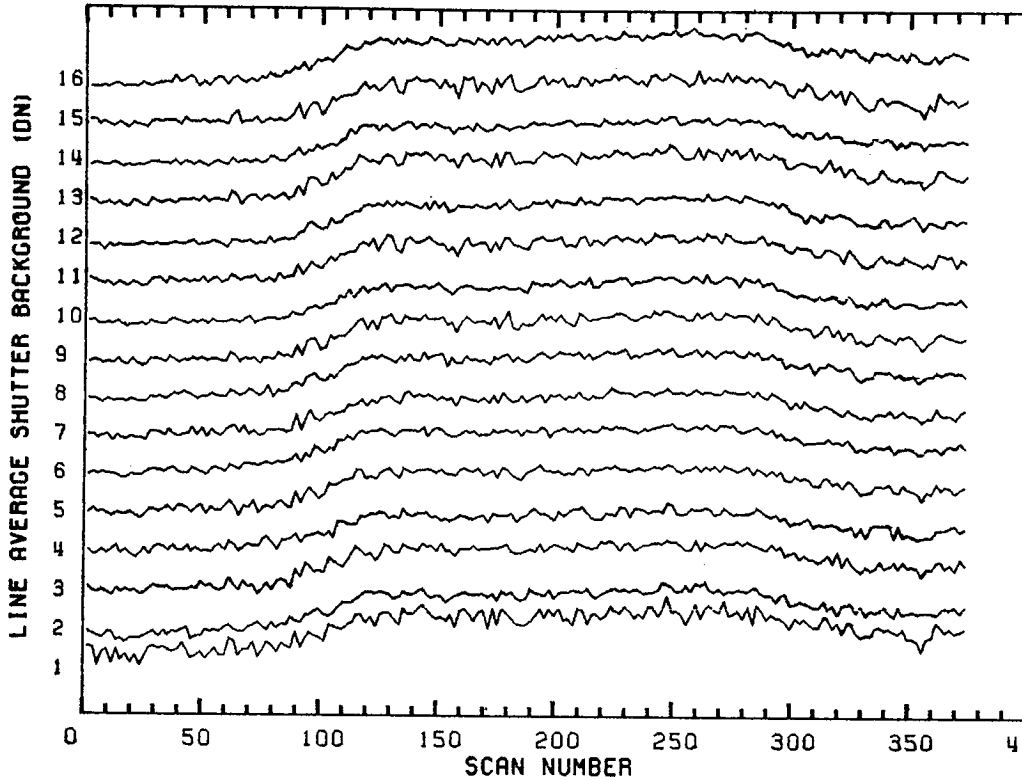
WITHIN-SCENE VARIABILITY
TM SHUTTER BACKGROUND IN CLOUDY SCENE
CLOUDS ON WESTERN EDGE OF SCENE
SAN FRANCISCO, CA (40392-18152, 12 AUG 83)
(AVERAGE OF ALL CHANNELS IN A BAND)

BAND	TOTAL VARIABILITY (SD) BEFORE AND AFTER DC RESTORE		(FWD-REV) DIFFERENCE BEFORE AND AFTER DC RESTORE	
	B-BDC (DN)	B-ADC (DN)	B-BDC (DN)	B-ADC (DN)
1	± 1.45	± 1.42	- 0.54	1.53
2	± 1.11	± 1.51	1.29	2.56
3	± 1.24	± 1.46	1.31	2.44
4	± 0.71	± 1.02	0.39	1.62
5	± 0.93	± 0.89	- 0.21	0.02
7	± 1.05	± 1.01	- 0.15	0.05

FIGURE 6.

SCENE ID=40392-18152, BAND 2 (FORWARD)
SHUTTER BACKGROUND 1 SPECTRA AFTER CORRECTION

1000*CV SHIFT1 SHIFT2

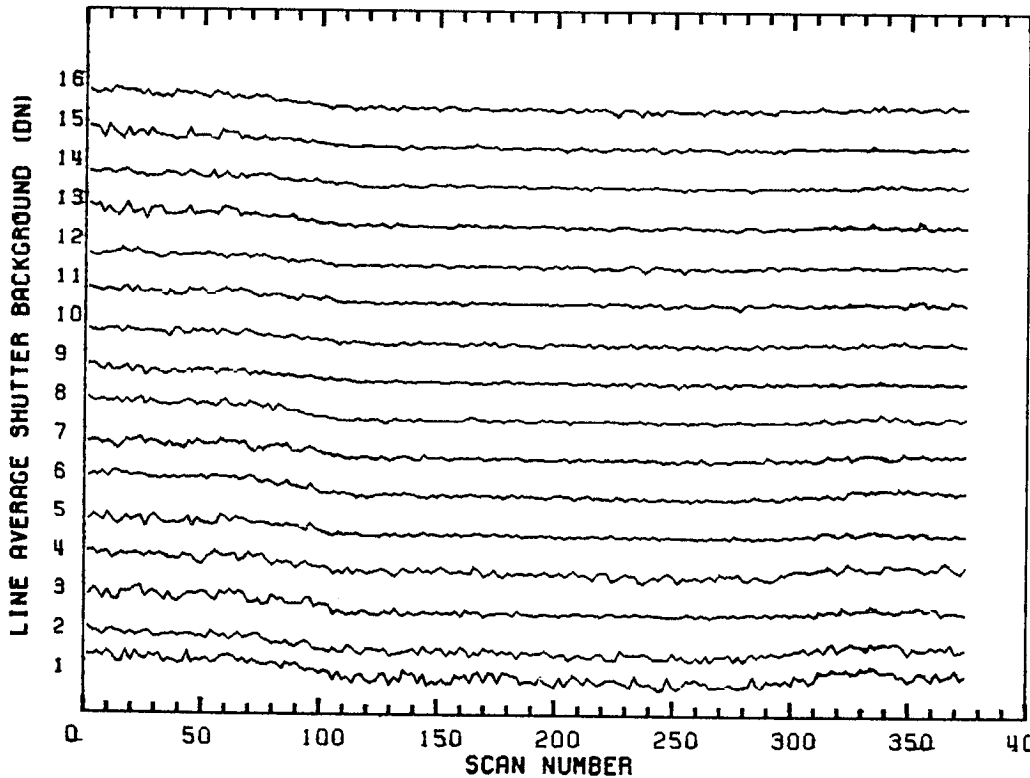


212	-0.00	-0.00
210	0.00	-0.06
204	-0.01	-0.01
219	-0.00	-0.04
219	-0.01	-0.01
207	-0.00	-0.03
206	-0.01	-0.01
217	-0.00	-0.04
205	-0.00	-0.01
193	-0.01	-0.03
193	-0.00	-0.01
192	-0.00	-0.04
178	0.01	-0.01
196	-0.01	-0.06
204	0.00	-0.01
165	0.05	-0.17

LEE/BARKER
6-MAR-84

SCENE ID=40392-18152, BAND 2 (REVERSE)
SHUTTER BACKGROUND 1 SPECTRA AFTER CORRECTION

1000*CV SHIFT1 SHIFT2

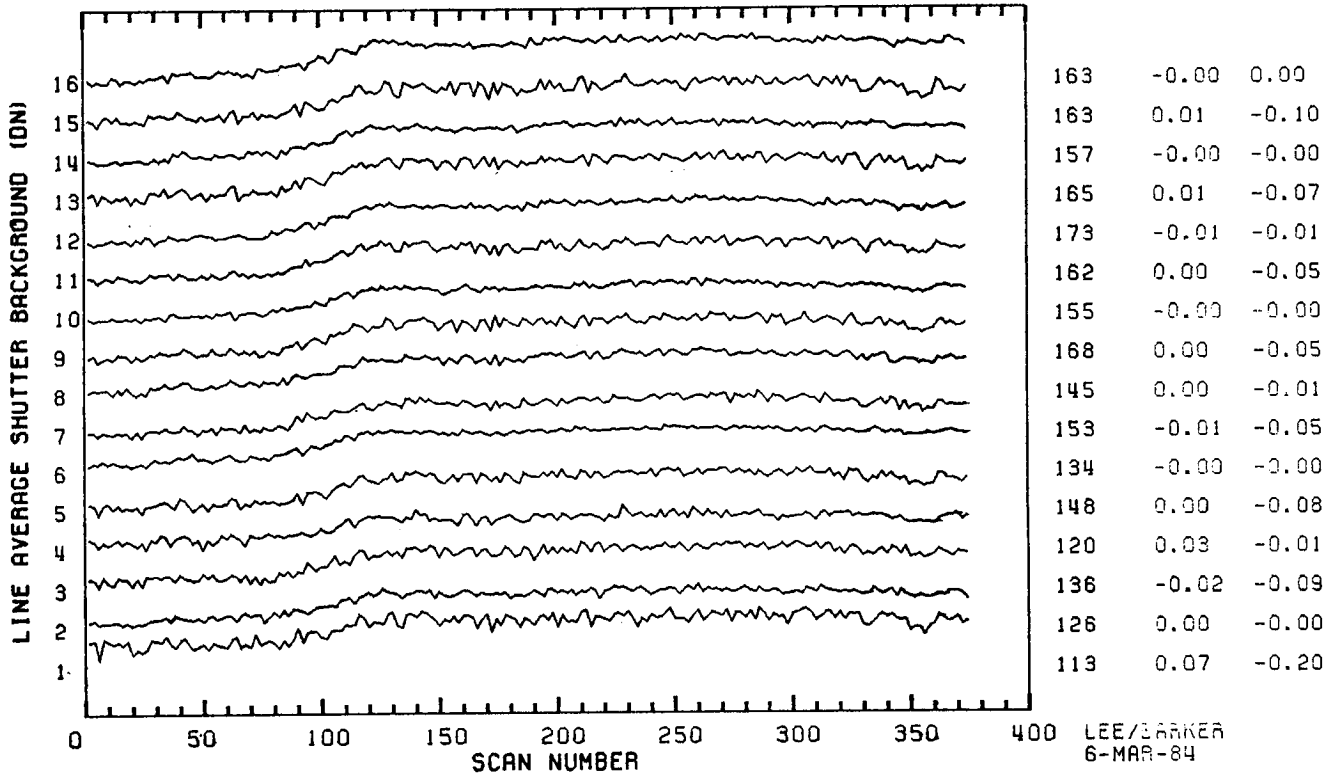


116	0.02	-0.00
108	0.02	-0.03
94	0.01	-0.00
116	0.01	-0.03
93	0.01	-0.01
94	0.01	-0.02
100	0.02	-0.01
96	0.01	-0.02
136	0.02	-0.01
117	0.01	-0.03
145	0.02	-0.00
120	0.02	-0.05
139	0.09	-0.01
140	0.01	-0.06
147	0.08	-0.01
143	0.13	-0.24

LEE/BARKER
6-MAR-84

FIGURE 7.

SCENE ID=40392-18152, BAND 2 (FORWARD)
SHUTTER BACKGROUND 2 SPECTRA AFTER CORRECTION



SCENE ID=40392-18152, BAND 2 (REVERSE)
SHUTTER BACKGROUND 2 SPECTRA AFTER CORRECTION

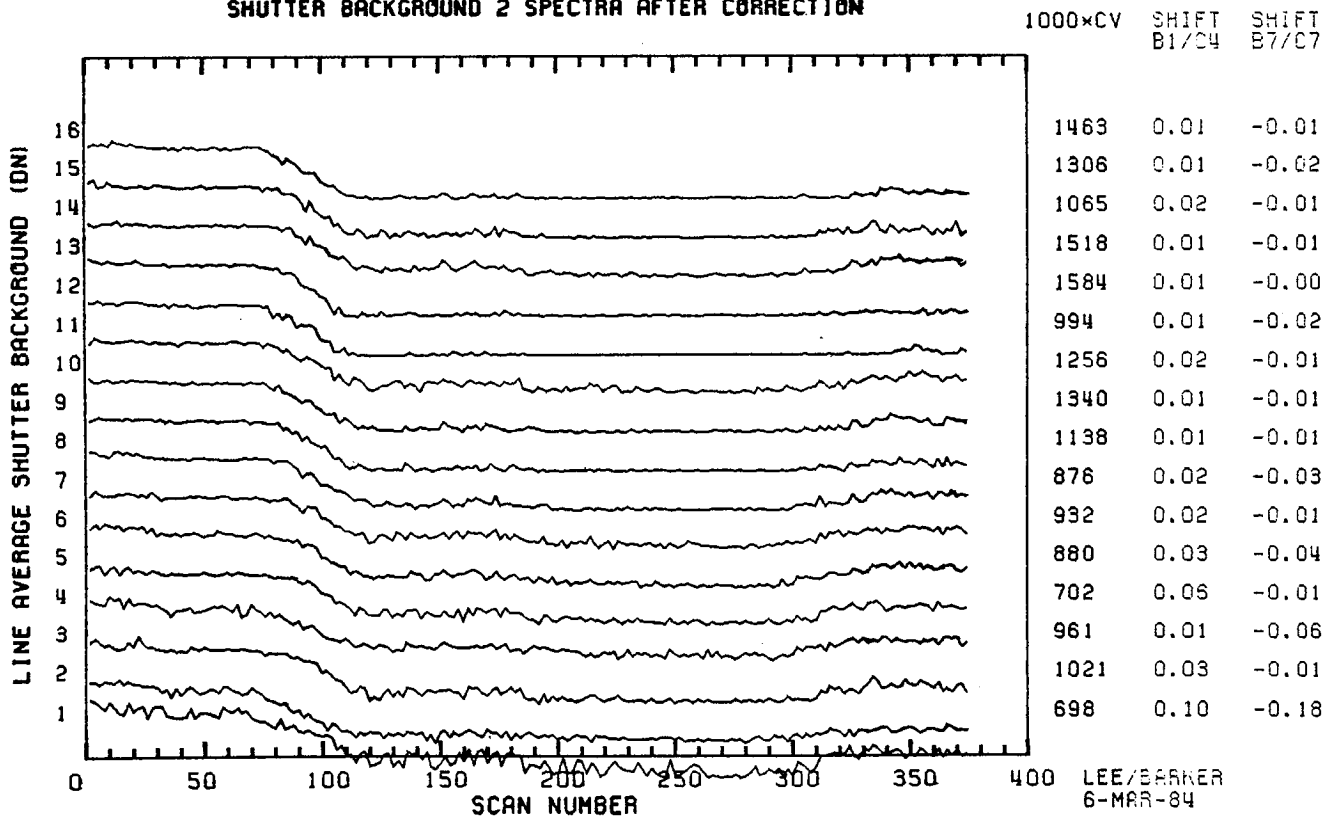


FIGURE 8.

LANDSAT-4 TM RADIOMETRY, BAND 2 CHANNEL 14

BRIGHT TARGET SATURATION OF SCENE 40392-18152

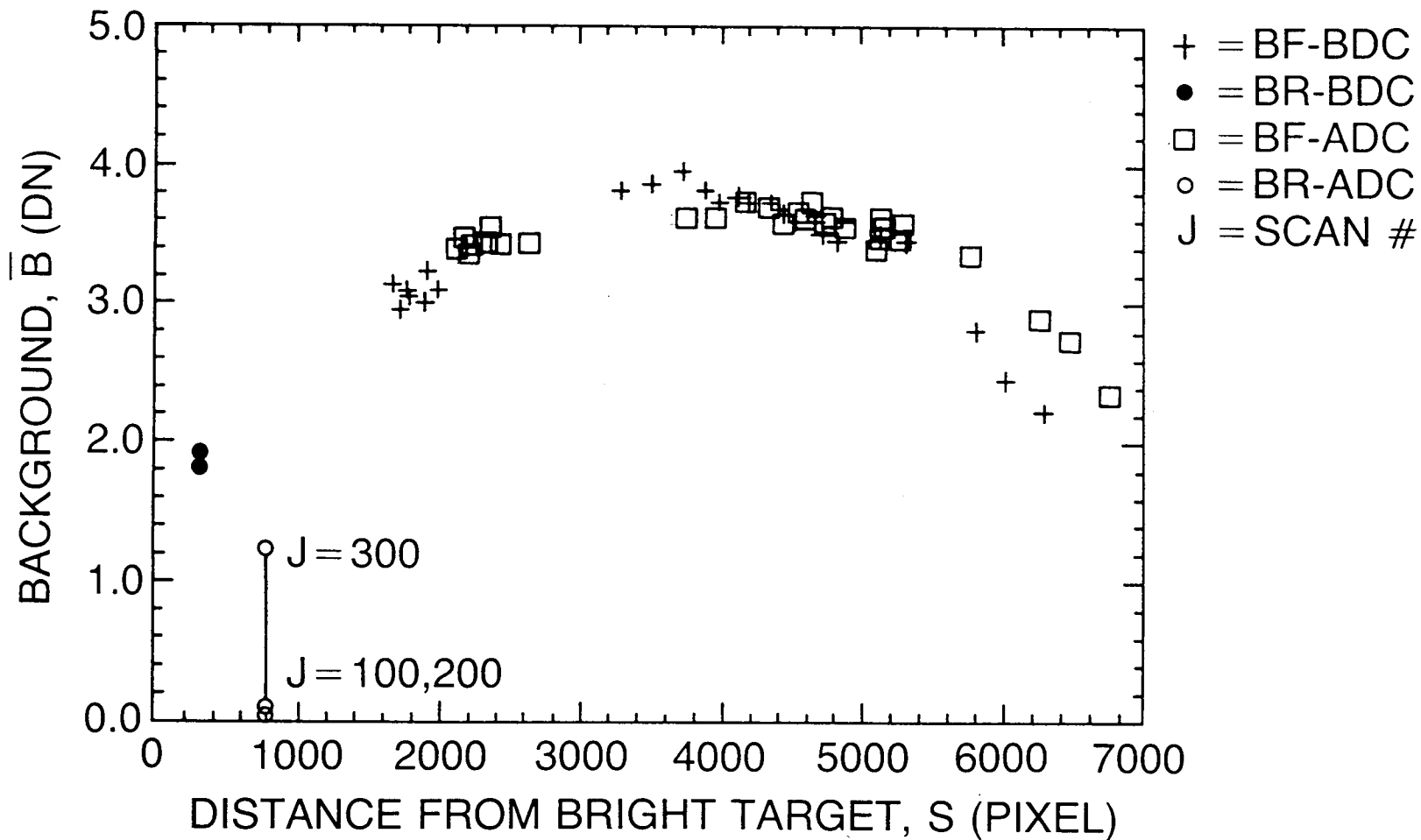


TABLE 7.

BAND 1 ON LANDSAT-4 TM/PF, WITHIN- SCENE VARIABILITY (IN DN)

CHANNEL	TOTAL VARIABILITY STANDARD DEVIATION OF SHUTTER IN AND AROUND DC RESTORATION			(FWD-REV) DIFFERENCE BACKGROUND ON SHUTTER IN AND AROUND DC RESTORATION			SCAN- CORRELATED SHIFTS		COHERENT NOISE	
	PM SCENE ^a SD(B)	CLOUDY SCENE ^b		PM SCENE ^a ΔBFR	CLOUDY SCENE ^b		TYPE 4-1.4 AVERAGE ^b CS(4-1)	TYPE 4-7.7 AVG ^{a,b} CS (4-7)	32 KHz (3.2 mf)	6 KHz (18 mf)
		SD(B-BDC)	SD(B-ADC)		ΔBFR (BDC)	ΔBFR (ADC)			(area ± 2 mf. of peak)	
									CC (32)	CC(6)
16	±1.5	±1.7	±1.7	0.1	-0.6	1.2	0.1	0.0	2.6	0.2
15	±1.4	±1.5	±1.6	0.3	-0.1	2.5	0.0	-0.1	1.0	0.3
14	±1.3	±1.5	±1.4	0.1	-0.6	1.6	0.2	0.0	1.7	0.2
13	±1.3	±1.4	±1.4	0.3	-0.2	2.0	0.1	-0.1	0.8	0.3
12	±1.1	±1.6	±1.4	0.2	-0.4	1.3	1.7	0.0	0.9	0.4
11	±1.3	±1.4	±1.4	0.3	-0.4	2.0	0.0	-0.1	1.0	0.2
10	±1.0	±1.4	±1.4	0.1	-0.6	1.8	1.0	0.0	0.6	0.3
9	±1.1	±1.2	±1.2	0.2	-0.5	1.4	0.0	0.0	0.7	0.2
8	±1.2	±1.5	±1.5	0.1	-1.1	1.3	0.8	-0.1	1.8	0.1
7	±1.3	±1.4	±1.3	0.2	-0.5	1.4	0.0	-0.1	0.6	0.4
6	±1.3	±1.6	±1.5	0.1	-1.3	1.2	0.2	0.0	1.1	0.2
5	±1.1	±1.2	±1.0	0.2	-0.4	1.0	0.0	-0.1	1.1	0.3
4	±1.2	±1.8	±1.6	0.2	-0.5	1.6	2.0	0.0	0.3	0.4
3	±1.1	±1.2	±1.2	0.2	-0.6	1.4	0.0	-0.1	1.2	0.4
2	±1.3	±1.6	±1.6	0.2	-0.7	1.7	0.1	-0.1	1.6	0.1
1	±1.3	±1.4	±1.3	0.2	-0.4	1.3	0.3	-0.1	1.0	0.4

^aPM BUFFALO, NY (40037-02243), ^bSAN FRANCISCO, CA (40392-18152), ^cWHITE SANDS, NM (40171-17080)

TABLE 8.

BAND 2 ON LANDSAT-4 TM/PF, WITHIN- SCENE VARIABILITY (IN DN)

CHANNEL	TOTAL VARIABILITY STANDARD DEVIATION OF SHUTTER IN AND AROUND DC RESTORATION			(FWD-REV) DIFFERENCE BACKGROUND ON SHUTTER IN AND AROUND DC RESTORATION			SCAN- CORRELATED SHIFTS		COHERENT NOISE	
	PM SCENE ^a SD(B)	CLOUDY SCENE ^b		PM SCENE ^a ΔBFR	CLOUDY SCENE ^b		TYPE 4-1.4 AVERAGE ^b CS(4-1)	TYPE 4-7.7 AVG ^{a,b} CS (4-7)	32 KHz (3.2 mf)	6 KHz (18 mf)
		SD(B-BDC)	SD(B-ADC)		ΔBFR (BDC)	ΔBFR (ADC)			(area ± 2 mf of peak)	
									CC (32)	CC(6)
16	±0.5	±1.7	±1.6	0.1	1.5	2.9	0.0	0.0	0.2	0.1
15	±0.6	±1.5	±1.5	0.3	1.3	2.6	0.0	0.0	0.1	0.1
14	±0.4	±1.5	±1.5	0.1	1.2	2.5	0.0	0.0	0.1	0.0
13	±0.6	±1.4	±1.6	0.3	1.5	2.8	0.0	0.0	0.1	0.1
12	±0.5	±1.6	±1.5	0.2	1.3	2.7	0.0	0.0	0.2	0.0
11	±0.5	±1.4	±1.4	0.3	1.3	2.4	0.0	0.0	0.1	0.0
10	±0.4	±1.4	±1.4	0.1	1.2	2.5	0.0	0.0	0.1	0.0
9	±0.5	±1.2	±1.5	0.2	1.3	2.6	0.0	0.0	0.0	0.0
8	±0.5	±1.5	±1.5	0.1	1.3	2.7	0.0	0.0	0.2	0.0
7	±0.5	±1.4	±1.4	0.2	1.2	2.3	0.0	0.0	0.1	0.1
6	±0.5	±1.6	±1.5	0.1	1.3	2.7	0.0	0.0	0.3	0.1
5	±0.5	±1.2	±1.4	0.2	1.3	2.4	0.0	--0.1	0.2	0.1
4	±0.7	±1.8	±1.4	0.2	1.1	2.2	0.1	0.0	0.1	0.1
3	±0.6	±1.2	±1.5	0.2	1.3	2.6	0.0	--0.1	0.2	0.1
2	±1.0	±1.6	±1.7	0.2	1.1	2.6	0.0	0.0	0.3	0.1
1	±0.7	±1.4	±1.5	0.2	1.3	2.6	0.1	--0.2	0.2	0.2

^aPM BUFFALO, NY (40037-02243), ^bSAN FRANCISCO, CA (40392-18152), ^cWHITE SANDS, NM (40171-17080)

TABLE 9.

BAND 3 ON LANDSAT-4 TM/PF, WITHIN- SCENE VARIABILITY (IN DN)

CHANNEL	TOTAL VARIABILITY STANDARD DEVIATION OF SHUTTER IN AND AROUND DC RESTORATION			(FWD-REV) DIFFERENCE BACKGROUND ON SHUTTER IN AND AROUND DC RESTORATION			SCAN- CORRELATED SHIFTS		COHERENT NOISE	
	PM SCENE ^a SD(B)	CLOUDY SCENE ^b		PM SCENE ^a ΔBFR	CLOUDY SCENE ^b		TYPE 4-1.4 AVERAGE ^b CS(4-1)	TYPE 4-7.7 AVG ^{a,b} CS (4-7)	32 KHz (3.2 mf)	6 KHz (18 mf)
		SD(B-BDC)	SD(B-ADC)		ΔBFR (BDC)	ΔBFR (ADC)			(area ± 2 mf of peak) CC (32)	CC(6)
16	±1.0	±1.5	±1.6	0.1	1.3	2.7	0.1	0.6	0.9	0.3
15	±0.9	±1.4	±1.4	0.2	1.4	2.3	0.2	-0.3	0.2	0.3
14	±0.5	±1.2	±1.6	0.0	1.6	2.7	0.0	0.0	0.4	0.1
13	±0.8	±1.3	±1.4	0.2	1.4	2.3	0.1	-0.1	0.2	0.1
12	±0.4	±1.1	±1.6	0.1	1.4	2.8	0.0	0.0	0.1	0.1
11	±0.7	±1.2	±1.4	0.1	1.3	2.3	0.0	-0.1	0.0	0.2
10	±0.5	±1.1	±1.7	0.1	1.4	3.0	0.0	0.0	0.3	0.1
9	±0.8	±1.3	±1.6	0.2	1.5	2.8	0.0	0.0	0.1	0.2
8	±0.9	±1.2	±1.6	0.1	1.2	2.6	0.0	0.0	1.6	0.1
7	±0.7	±1.2	±1.4	0.1	1.2	2.3	0.0	-0.1	0.1	0.2
6	±0.5	±1.0	±1.5	0.1	1.4	2.6	0.0	0.0	0.3	0.2
5	±0.8	±1.2	±1.4	0.2	1.2	2.4	0.1	-0.2	0.1	0.1
4	±0.7	±1.1	±1.4	0.1	1.0	2.2	0.0	0.0	1.2	0.2
3	±0.8	±1.2	±1.2	0.2	1.1	2.0	0.1	-0.2	0.1	0.2
2	±0.6	±1.0	±1.3	0.1	0.9	2.1	0.0	0.1	0.2	0.3
1	±1.3	±1.7	±1.3	0.3	1.4	2.0	0.3	0.5	0.3	0.5

^aPM BUFFALO, NY (40037-02243), ^bSAN FRANCISCO, CA (40392-18152), ^cWHITE SANDS, NM (40171-17080)

TABLE 10.

BAND 4 ON LANDSAT-4 TM/PF, WITHIN- SCENE VARIABILITY (IN DN)

CHANNEL	TOTAL VARIABILITY STANDARD DEVIATION OF SHUTTER IN AND AROUND DC RESTORATION			(FWD-REV) DIFFERENCE BACKGROUND ON SHUTTER IN AND AROUND DC RESTORATION			SCAN- CORRELATED SHIFTS		COHERENT NOISE	
	PM SCENE ^a SD(B)	CLOUDY SCENE ^b		PM SCENE ^a Δ BFR	CLOUDY SCENE ^b		TYPE 4-1.4 AVERAGE ^b CS(4-1)	TYPE 4-7.7 AVG ^{a,b} CS (4-7)	32 KHz (3.2 mf)	6 KHz (18 mf)
		SD(B-BDC)	SD(B-ADC)		Δ BFR (BDC)	Δ BFR (ADC)			(area ± 2 mf of peak)	
								CC (32)	CC(6)	
16	± 0.3	± 0.7	± 0.9	0.0	0.5	1.4	0.2	0.0	0.2	0.3
15	± 0.4	± 0.6	± 1.1	0.1	0.4	1.7	0.1	0.0	0.2	0.1
14	± 0.3	± 0.8	± 1.2	0.1	0.6	1.9	0.0	0.0	0.2	0.0
13	± 0.4	± 0.6	± 0.8	0.1	0.4	1.3	0.0	0.0	0.2	0.1
12	± 0.3	± 0.7	± 1.1	0.1	0.4	1.8	0.1	0.0	0.1	0.1
11	± 0.3	± 0.6	± 0.9	0.1	0.3	1.4	0.1	0.0	0.3	0.1
10	± 0.3	± 0.7	± 1.0	0.1	0.4	1.6	0.0	0.0	0.3	0.0
9	± 0.3	± 0.6	± 1.1	0.1	0.3	1.8	0.0	0.0	0.2	0.1
8	± 0.6	± 0.9	± 1.1	0.1	0.3	1.6	0.0	-0.1	0.8	0.1
7	± 0.3	± 0.6	± 0.9	0.1	0.4	1.5	0.0	0.0	0.2	0.1
6	± 0.5	± 0.7	± 1.1	0.1	0.4	1.8	0.0	0.0	0.3	0.1
5	± 0.4	± 0.7	± 1.0	0.1	0.5	1.7	0.0	0.0	0.3	0.1
4	± 0.5	± 0.8	± 1.0	0.1	0.2	1.6	0.0	-0.1	0.5	0.0
3	± 0.6	± 0.7	± 1.1	0.2	0.4	1.9	0.0	0.0	0.4	0.2
2	± 0.4	± 0.8	± 1.1	0.1	0.3	1.7	0.0	-0.1	0.3	0.1
1	± 0.6	± 0.7	± 0.8	0.1	0.5	1.3	0.2	-0.1	0.6	0.2

^aPM BUFFALO, NY (40037-02243), ^bSAN FRANCISCO, CA (40392-18152), ^cWHITE SANDS, NM (40171-17080)

TABLE 11.

BAND 5 ON LANDSAT-4 TM/PF, WITHIN- SCENE VARIABILITY (IN DN)

CHANNEL	TOTAL VARIABILITY STANDARD DEVIATION OF SHUTTER IN AND AROUND DC RESTORATION			(FWD-REV) DIFFERENCE BACKGROUND ON SHUTTER IN AND AROUND DC RESTORATION			SCAN- CORRELATED SHIFTS		COHERENT NOISE	
	PM SCENE ^a SD(B)	CLOUDY SCENE ^b		PM SCENE ^a Δ BFR	CLOUDY SCENE ^b		TYPE 4-1.4 AVERAGE ^b CS(4-1)	TYPE 4-7.7 AVG ^{a,b} CS (4-7)	32 KHz (3.2 mf)	6 KHz (18 mf)
		SD(B-BDC)	SD(B-ADC)		Δ BFR (BDC)	Δ BFR (ADC)			(area \pm 2 mf of peak) CC (32)	CC(6)
16	± 0.8	± 0.9	± 0.8	0.1	-0.3	0.2	0.0	-0.1	[0.2]	[0.1]
15	± 0.9	± 0.9	± 0.9	0.1	-0.3	0.1	-0.1	-0.1	[0.3]	[0.1]
14	± 0.9	± 0.9	± 0.9	0.0	-0.1	0.0	0.0	-0.1	[0.1]	[0.1]
13	± 0.9	± 0.9	± 0.9	0.0	-0.1	0.0	0.0	0.0	[0.1]	[0.1]
12	± 0.9	± 0.9	± 0.9	0.0	-0.1	0.0	0.0	0.0	[0.0]	[0.1]
11	± 0.9	± 1.0	± 0.9	0.0	-0.1	0.0	0.0	0.0	[0.1]	[0.1]
10	± 0.9	± 1.0	± 0.9	0.0	-0.1	0.0	0.0	0.6	[0.1]	[0.0]
9	± 0.9	± 0.9	± 0.9	0.0	-0.1	-0.1	0.0	0.0	[0.0]	[0.0]
8	± 0.9	± 0.9	± 0.8	0.0	-0.1	0.0	0.0	-0.2	[0.2]	[0.0]
7	± 1.1	± 1.1	± 1.1	0.0	-0.1	0.0	0.0	0.1	[0.2]	[0.2]
6	± 0.9	± 0.9	± 0.9	0.0	-0.1	0.0	0.0	-0.1	[0.2]	[0.0]
5	± 0.9	± 0.9	± 0.9	0.0	-0.1	-0.1	-0.1	0.0	[0.1]	[0.0]
4	± 0.8	± 0.9	± 0.9	0.0	-0.1	0.0	0.1	-0.1	[0.0]	[0.1]
3	—	—	—	—	—	—	0.0	0.0	—	—
2	± 0.8	± 0.9	± 0.8	0.1	-0.7	-0.1	0.1	-0.1	[0.1]	[0.1]
1	± 0.8	± 0.9	± 0.9	0.0	-0.7	-0.1	0.0	0.1	[0.2]	[0.0]

^aPM BUFFALO, NY (40037-02243), ^bSAN FRANCISCO, CA (40392-18152), ^cWHITE SANDS, NM (40171-17080)

TABLE 12.

BAND 7 ON LANDSAT-4 TM/PF, WITHIN- SCENE VARIABILITY (IN DN)

CHANNEL	TOTAL VARIABILITY STANDARD DEVIATION OF SHUTTER IN AND AROUND DC RESTORATION			(FWD-REV) DIFFERENCE BACKGROUND ON SHUTTER IN AND AROUND DC RESTORATION			SCAN- CORRELATED SHIFTS		COHERENT NOISE	
	PM SCENE ^a SD(B)	CLOUDY SCENE ^b		PM SCENE ^a Δ BFR	CLOUDY SCENE ^b		TYPE 4-1.4 AVERAGE ^b CS(4-1)	TYPE 4-7.7 AVG ^{a,b} CS (4-7)	32 KHz (3.2 mf)	6 KHz (18 mf)
		SD(B-BDC)	SD(B-ADC)		Δ BFR (BDC)	Δ BFR (ADC)			(area ± 2 mf of peak)	
									CC (32)	CC(6)
16	± 1.0	± 1.0	± 1.0	0.1	-0.2	0.2	0.1	-0.2	[0.2]	[0.1]
15	± 0.8	± 0.8	± 0.8	0.1	-0.2	0.1	0.0	0.2	[0.1]	[0.2]
14	± 1.1	± 1.1	± 1.1	0.0	-0.1	0.0	0.1	-0.1	[0.0]	[0.1]
13	± 0.8	± 0.9	± 0.8	0.0	-0.1	0.0	0.0	0.2	[0.1]	[0.1]
12	± 1.0	± 1.0	± 1.0	0.0	0.0	0.0	0.1	-0.2	[0.2]	[0.1]
11	± 1.0	± 1.0	± 0.9	0.0	0.0	0.0	0.0	-0.2	[0.1]	[0.0]
10	± 1.1	± 1.1	± 1.1	0.0	0.0	0.0	0.1	-0.4	[0.3]	[0.0]
9	± 1.0	± 1.0	± 1.0	0.0	-0.1	0.0	-0.1	0.2	[0.1]	[0.0]
8	± 1.0	± 1.0	± 0.9	0.0	-0.1	0.0	0.0	-0.3	[0.1]	[0.1]
7	± 2.0	± 1.8	± 1.8	0.0	-0.2	0.2	-0.1	0.9	[0.1]	[0.2]
6	± 1.0	± 1.0	± 1.0	0.0	0.0	0.0	0.1	-0.3	[0.1]	[0.1]
5	± 0.9	± 1.0	± 0.9	0.0	0.0	0.0	0.0	0.2	[0.0]	[0.1]
4	± 1.0	± 1.0	± 1.0	0.0	-0.1	0.0	0.1	-0.2	[0.2]	[0.1]
3	± 0.9	± 0.9	± 0.9	0.0	-0.1	0.0	-0.1	0.3	[0.1]	[0.0]
2	± 1.0	± 1.0	± 1.0	0.1	-0.6	0.1	0.0	-0.3	[0.2]	[0.1]
1	± 1.0	± 1.0	± 1.0	0.0	-0.6	0.1	0.0	0.3	[0.1]	[0.1]

^aPM BUFFALO, NY (40037-02243), ^bSAN FRANCISCO, CA (40392-18152), ^cWHITE SANDS, NM (40171-17080)

TABLE 13.

LANDSAT-5 TM/F WITHIN-SCENE VARIABILITY (IN DN)

CHANNEL	BAND 1		BAND 2		BAND 3		BAND 4		BAND 5	BAND 7
	TOTAL SHUTTER NOISE ^a SD(B)	SHIFT TYPE 5-3.1 AVERAGE ^b CS (5-3)	TOTAL SHUTTER NOISE ^a SD(B)	SHIFT TYPE 5-3.1 AVERAGE ^b CS (5-3)	TOTAL SHUTTER NOISE ^a SD(B)	SHIFT TYPE 5-3.1 AVERAGE ^b CS (5-3)	TOTAL SHUTTER NOISE ^a SD(B)	SHIFT TYPE 5-3.1 AVERAGE ^b CS (5-3)	TOTAL SHUTTER NOISE ^a SD(B)	TOTAL SHUTTER NOISE ^a SD(B)
16	±0.9	-0.2	±0.3	0.7	±0.5	0.3	±0.5	0.0	±0.8	±0.9
15	±0.8	0.0	±0.3	0.3	±0.4	0.3	±0.3	0.1	±0.8	±0.8
14	±1.0	-0.3	±0.2	0.2	±0.4	0.3	±0.4	0.0	±0.8	±0.9
13	±0.8	0.0	±0.3	0.4	±0.5	0.3	±0.3	0.2	±0.9	±0.8
12	±0.9	-0.2	±0.2	0.1	±0.7	0.3	±0.3	0.0	±1.0	±1.0
11	±0.9	0.0	±0.3	0.3	±0.5	0.5	±0.4	0.1	±0.8	±0.9
10	±0.9	-0.3	±0.2	0.0	±0.4	0.4	±0.3	0.0	±1.3	±1.0
9	±0.8	0.0	±0.3	0.2	±0.6	0.4	±0.4	0.1	±1.0	±1.3
8	±1.0	-0.1	±0.2	0.1	±0.5	0.2	±0.4	0.0	±0.9	±1.0
7	±0.8	0.0	±0.3	0.3	±0.5	0.3	±0.3	0.1	±1.3	±0.9
6	±0.9	-0.1	±0.2	0.1	±0.4	0.6	±0.4	0.0	±0.8	±0.9
5	±0.8	0.0	±0.3	0.3	±0.6	0.4	±0.3	0.1	±0.9	±0.8
4	±1.0	-0.1	±0.3	0.0	±0.5	0.5	±0.4	0.3	±0.9	±0.9
3	±0.9	0.0	±0.4	0.4	±0.6	0.5	±0.5	0.1	±0.9	±0.9
2	±1.0	-0.1	±0.4	0.0	±0.5	0.2	±0.4	0.1	±0.8	±1.0
1	±1.0	0.0	±0.5	0.7	±0.6	0.5	±0.2	0.4	±0.8	±0.9

^aPRE-LAUNCH "IS GOLDEN TAPE" (5-198-10563, 16:14 30 AUG 83)

^bAVERAGED (5-596-13285), (5-198-10563) AND (50005-16221)

the Landsat Project. Evaluation, and possible implementation, of the recommendations will pose significant difficulties both during the research period before the transition of the TIPS from NASA to NOAA near the end of 1984, and afterwards, during the operational period.

TABLE 14
RECOMMENDATIONS
TM RADIOMETRIC CHARACTERIZATION

6.1 ENGINEERING CHARACTERIZATION

6.1.1 RECALIBRATE INTEGRATING SPHERE USED IN PRE-LAUNCH CALIBRATION

- 48" TM Integrating Sphere
 - SBRC
 - GSFC
 - NBS
- Two 30" MSS Spheres
- MMR 8-Band Field Radiometer

6.1.2 ANALYZE RELATIVE RADIOMETRY OF PRE-LAUNCH DATA ON 42 TRACK TAPES

6.1.3 EMPLOY ENGINEERING MODEL TM TESTS TO INVESTIGATE SOURCE OF

- Bin-Radiance Dependence (Unequal Bins)
- Coherent Noise (Stationary and Time-Dependent)
- Within-Line Droop
- Bright Target Saturation (Recovery)
- Scan-Related Shifts
- IC Pulse Temperature-Dependence
- "Secondary" Light Pulse in Calibration Region
- Apparent Gain Changes with Time

6.1.4 PRODUCE FINAL REPORT DESCRIBING TM PERFORMANCE CHARACTERISTICS

6.2 FLIGHT SEGMENT OPERATIONS

6.2.1 INSTITUTE CHANGES IN OPERATIONAL PROCEDURES

- Stop Routine Operation of IC Automatic Sequencer
- Alternate Black Body Temperatures "T2" and "T3"
- Set Outgassing Strategy at 20% Band 6 Gain Loss

6.2.2 PERFORM IN-ORBIT CALIBRATION TESTS

- Calibrate Temperature-Dependence of IC Pulses

6.2.3 PERFORM IN-ORBIT CHARACTERIZATION TESTS

- Redundant Power Supply Noise
- Manual IC Operation with Automatic Sequencer Off
- "Override" Back-up IC Operation
- Coherent Noise Phasing Relative to Midscan Pulse
- Noise with DC Restoration Off

6.2.4 PERFORM IN-ORBIT SCIENTIFIC MISSION TESTS

- Subsampled Extension of Swath Width, No Shutter
- Bidirectional Reflectance by Off-Nadir Pointing
- Intensive Single Site Acquisition by Pointing
- TM/F and TM/PF Stereo by Pointing
- TM/F and MSS/F (High Gain) Bathymetry
- TM Single S/C Stereo
 - Fore/Aft
 - Side-to-Side

6.3 TIPS GROUND PROCESSING

6.3.1 PROVIDE FOR FUTURE CHANGE IN RADIOMETRIC CALIBRATION PARAMETERS

- Post-Calibration Dynamic Range (RMIN, RMAX)
- Spectral Radiance for each IC Lamp Level
- Averaged Pulse for each IC Lamp Level
- Pre-Launch Gains and Offsets
- Calculated Pre-Launch Nominal IC Pulses

6.3.2 PROVIDE FOR CHANGES IN IC SYSTEMATIC RADIOMETRIC CORRECTION PROCEDURES INVOLVING

- Two Background Shutter Collects (avoid DC Restore)
- Within-Scene Corrections
 - Bin-Radiance Dependence
 - Coherent Noise
 - Scan-Related Shifts
- Background Outliers (Incomplete Obscuration)
- "Secondary" Light Pulses in Calibration Region
 - Search 80 of 148 mf Collect Window
- Pulse Integration Parameters
 - Optimize Integration Width (near 39 mf)
- Pulse Averaging
 - Separate Forward and Reverse Scans
- Lamp State Options
 - Reject 111 State for any Regression
 - Omit 000 State when possible
 - Omit Shutter Background when possible
 - Permit any States and Background
- IC Pulse Temperature-Dependence
- Between-Channel Correlations
 - Between-Band Absolute Radiometry
 - Quality Assurance Redundancy Check
- Within-Pass Smoothing
- Between-Date Smoothing
- Reference Channels or Variance Weighting
- Statistical Quality Indices

6.3.3 MODIFY HISTORGRAM EQUALIZATION PROCEDURE TO PROVIDE FOR

- Optional 1st Pass HDT-RT Histogram
- Line-by-Line Systematic Correction
- 2nd Pass HDT-RT 11-Bit Histogram
- HDT-AT 11-Bit Histogram and File
- Histogram Reference to "Quiet" Channel
- Histogram Monitoring of IC quality
- Weighting of IC and Histogram Constants
- HDT-PT Histogram File for each Band

- 6.3.4 MODIFY GEOMETRIC PROCESSING PROCEDURES TO PROVIDE FOR
- Single Pass Image Rectification (Geodetic) Product
 - Geocoded Map Compatibility
 - UTM Resampling as Standard
 - Single Pass Cubic Spline Resampling
 - Image Coordinate File for GCPs
 - Relative GCPs
 - Alternative Global GCP Library Build
- 6.3.5 PROVIDE THREE-SECTIONED POST-CALIBRATION DYNAMIC RANGE
- 6.3.6 MODIFY IMAGE CALIBRATION PROCEDURE TO PROVIDE FOR
- Non-Adjacent Channel Replacement Algorithm
 - Probabilistic Approach
- 6.3.7 PROVIDE THE FOLLOWING PRODUCTS
- Semi-weekly Tapes of Raw Calibration Data
 - Semi-weekly "Unity" CCT-AT
 - Special "Unity" CCT-AT of Calibration Region
 - Reprocessed "Reference" Scenes
 - History Tapes of Calibration Constants
 - Selected HDT-RT Copies
 - Extra Band(s) of Binary Data
 - Extra Band(s) of 8-Bit Data
 - Tapes at Reduced Resolution
 - Cloud-free Global TM Archive by Season
 - "Unity" HDT-AT and CCT-AT as Standard, with PDC
- 6.3.8 RESEARCH AND DEVELOP PROCEDURES FOR
- Within-Line Processing
 - Band 6 Processing
 - Ingestion of Foreign TM Tapes
 - Full Interval Radiometric Processing
 - Creation and Processing of Pre-Launch Data
 - GPC Test to Reduce Control Point Neighborhood Size

6.4 DEVELOP PROCEDURES FOR POSSIBLE CONTINGENCY EXPERIMENTS

- SCIENTIFIC EXPERIMENTS
 - Lunar Radiometric Calibration
 - Stereo and Bidirectional Reflectance
 - Time-of-Day Orbital Changes
 - Revisit Frequency Requirements
 - Utility of Mixed Spatial Resolution

- ENGINEERING EXPERIMENTS
 - Band 6 Sensitivity at 70K
 - Focus Test on Inchworms over GCPs
 - Tests of Global Position System Utility
 - Tests of On-Board Computer Options
 - Alternative Lamp and Power Supply Tests
 - Recalibration Before and After In-Orbit Repair

TABLE 15
TABLE OF CONTENTS

SECTION 1 - INTRODUCTION

- 1.1 TM Radiometric Calibration
- 1.2 Approach to Characterization

SECTION 2 - BETWEEN-SCENE CHANGES IN TM GAIN

SECTION 3 - BETWEEN-BAND CHANGES IN TM/PF GAIN

SECTION 4 - WITHIN-SCENE VARIABILITY IN TM RADIOMETRY

- 4.1 Bin-Radiance Dependence
- 4.2 Within-Line Droop
- 4.3 Bright-Target Saturation
- 4.4 Coherent Noise
- 4.5 Scan-Related Shifts
- 4.6 Forward/Reverse-Scan Differences
- 4.7 Total Noise
- 4.8 Within-Scene Error Models

SECTION 5 - PROCESSING EFFECTS OF RADIOMETRY

5.1 Calibration and Internal Calibrator

- 5.1.1 Background Calculation
- 5.1.2 Pulse Window Locations
- 5.1.3 Pulse Integration Parameters
- 5.1.4 Pulse Averaging Parameters
- 5.1.5 Regression Strategy
- 5.1.6 Within-Scene Smoothing
- 5.1.7 Within-Path Smoothing
- 5.1.8 Between-Date Smoothing

5.2 Image Calibration

- 5.2.1 Histogram Equalization
- 5.2.2 Replacement of Channels
- 5.2.3 Post-Calibration Dynamic Range
- 5.2.4 Unbiased Pixel Calibration
- 5.2.5 Geometric Resampling

5.3 Radiance-To-Reflectance Conversion

- 5.3.1 Irradiance Normalization
- 5.3.2 Atmospheric Peeling

5.4 Information Extraction

- 5.4.1 Spectrometry
- 5.4.2 Radiometry
- 5.4.3 Geometry

SECTION 6 - RECOMMENDATIONS

6.1 Engineering Characterization

- 6.1.1 Absolute Radiometric Calibration
- 6.1.2 Relative Radiometric Calibration
- 6.1.3 Modeling of Systematic Variabilities
- 6.1.4 TM Sensor Report

6.2 Flight Segment Operations

- 6.2.1 Changes in Operational Procedures
- 6.2.2 In-Orbit Calibration Tests
- 6.2.3 In-Orbit Characterization Tests
- 6.2.4 In-Orbit Scientific Mission Tests

6.3 TIPS Ground Processing

- 6.3.1 Absolute Radiometric Calibration Parameters
- 6.3.2 IC Systematic Radiometric Corrections
- 6.3.3 Histograms Equalization
- 6.3.4 Geometric Processing
- 6.3.5 Three-Sectioned Post-Calibration Dynamic Range
- 6.3.6 Image Calibration
- 6.3.7 Products
- 6.3.8 Research and Development

6.4 Contingency Experiments

SECTION 7 - ACKNOWLEDGMENT

SECTION 8 - SELECTED BIBLIOGRAPHY

SECTION 9 - APPENDICES

- 9.1 TIPS Post-Calibration Dynamic Range
- 9.2 Integrating Sphere Spectral Radiances
- 9.3 TM/F Gains
- 9.4 TM/F Offsets
- 9.5 Landsat-4 TM/PF Gain Changes with Time, by Band
- 9.6 Catalog of Landsat-4 Images Processed by TRAPP
- 9.7 TM/PF Plots of "Shifted" Background Versus Scan
- 9.8 TM/PF Plots of Shutter Background Versus Scan
- 9.9 TM/PF Plots of "Shifted" Background Versus Scan
- 9.10 TM/F Plots of "Shifted" Background Versus Scan
- 9.11 TM/F Tables of Scan-Related Shifts
- 9.12 Shutter Backgrounds
- 9.13 Recommendations
- 9.14 Key Words

EVALUATION OF THE RADIOMETRIC INTEGRITY OF LANDSAT-4
THEMATIC MAPPER BAND 6 DATA

JOHN R. SCHOTT
ROCHESTER INSTITUTE OF TECHNOLOGY

INTRODUCTION AND BACKGROUND

The data from the thermal infrared channel (Band 6) aboard the thematic mapper represent the highest spatial resolution thermal information yet available from space. The radiometric response function of the thermal sensor must be carefully evaluated to permit proper interpretation of these unique data. Probably the most generally accepted method for processing radiometric data from space is to correct the observed radiance or apparent temperature to a surface radiance or temperature value using atmospheric propagation models. For example using radiosonde data from the study area at the time of an overpass the atmospheric transmission and path radiance terms (τ and W_A) can be computed using AFCRL's LOWTRAN code. These terms can be used to compute the surface radiance from

$$W_S = (W - W_A) / \tau. \quad (1)$$

Where; W is the observed radiance and W_S is the surface radiance which can be associated with an equivalent black body temperature (T_S).

As part of NASA's Heat Capacity Mapping Mission (HCMM) experiment the atmospheric propagation models were used in reverse in an attempt to evaluate the post launch radiometric response of the Heat Capacity Mapping Radiometer (HCMR). Bohse et al 1979, described how surface radiometric readings were used in conjunction with radiosonde data to predict the radiance at the top of the atmosphere using atmospheric propagation models. Surface data taken with a point radiometer viewing a lake were averaged to define W_S and the atmospheric propagation models were used to define and W_A at the time of the overpass. Therefore the radiance observed by the spacecraft sensor W' and the radiance calculated from the model ($W = \tau W_S + W_A$) should be identical. In fact for the five dates studied the difference in observed and predicted

values ranged from 4.15 to 6.14⁰C with an average difference of 5.24⁰C (radiance values have been converted to equivalent blackbody temperatures). As a result of these analysis, NASA offset the prelaunch calibration values for the sensor by -5.5⁰C and applied this offset to all standard HCMM products (Ref. 4).

This offset was based on the assumption that the sensor response and/or the calibration standard had somehow changed since the prelaunch calibration. Subsequent studies five months later conducted in an identical fashion indicated that the offset should be moved back toward the original value by 3.3 to 7.7⁰C (Ref. 5). This would essentially nullify the original offset. If we accept the initial premise of a shift in the HCRM response function we must now speculate on the possibility of long term drift in the sensor calibration. An alternative and perhaps more acceptable hypothesis is that the atmospheric propagation models are inadequate and part or all of the variance is associated with changes in the atmosphere insufficiently accounted for by the models.

Since nearly all users have a requirement for surface radiance data it is also essential that the atmospheric propagation models be more carefully evaluated and refined as preprocessing algorithms. This effort is designed to experimentally evaluate the radiometric calibration of the Landsat-4 band 6 data. This approach draws on a method employed by Schott and Schimminger, 1981 as part of the HCMM experiment to radiometrically calibrate the HCRM data. Schott and Schimminger 1982 successfully utilized an approach to radiometric calibration of HCRM data that involved underflying the satellite with an infrared line scanner. This approach enabled calibration of the satellite sensor to within 1⁰C of surface temperature values. By extending this technology to higher altitudes experimental radiance data suitable for radiometric calibration of the TM band 6 sensor can be generated. Repetition of this experiment will permit evaluation of long term drift in the sensor and provide a data base for the second phase of the program.

The second phase of the experiment involves evaluation of the atmospheric propagation models for radiation transfer. Along with the underflight data from phase one, radiosonde data (suitable for input to the propagation models) will be available. The propagation models can be used to predict atmospheric transmission and path radiance values as a function of altitude and at slant paths to the satellite. These same values are derivable from the empirical data gathered during the underflight. By comparing these values it should be possible to begin to evaluate any systematic errors in the models. During this phase modifications to the models based on systematic errors and/or additional surface truth data will be evaluated. If sufficiently accurate models can be defined then underflight data would not be required for continued evaluation of sensor performance. In addition satellite data could be preprocessed to produce direct surface radiance or equivalent temperature images.

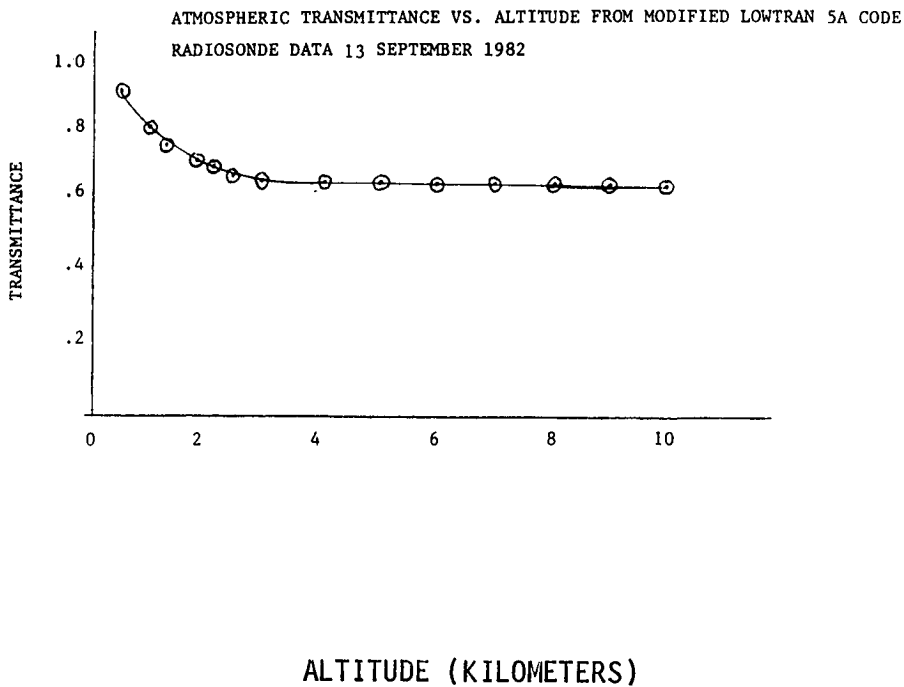
To date, efforts have concentrated on modification of the infrared line scanner to match the spectral response of the TM band 6 sensor. In addition, the LOWTRAN code corresponding to a satellite overpass of September 1982 has been run to yield a plot of transmission and path radiance as a function of altitude as shown in Figure 1. When underflight data is available, the empirically observed values would be compared to these modeled values. The computed values would be compared to these modeled values. The computed values of transmission and path radiance ($0.6293, 6.005\text{wm}^{-2}\text{sr}^{-1}$) are used to compute water surface temperature for Lake Ontario assuming unit emissivity. Future efforts will incorporate correlation with underflight empirical measurements and corrections for the emissivity and reflected sky radiance of the water. The major data collection thrust is scheduled for the spring of 1983 when the large temperature gradients in the Laurentian Great Lakes will insure the availability of properly dispersed data.

REFERENCES

1. Selby et al, 1978. "Atmospheric Transmittance". Radiance Computer Code Lowtran 4, AFGL-TR-78-0053.

2. Rangaswamg, S., Subbaragudu, J. 1978. RADTRA Program developed under contract NAS5-2-4272.
3. Bohse, J. R., Bewtra, M. and Barnes, W. L. 1979. "Heat Capacity Mapping Radiometer (HCMR) Data Processing Algorithm, Calibration, and Flight Performance Evaluation". NASA Technical Memorandum 80258.
4. . 1980. Heat Capacity Mapping Mission (HCMM) Data User Handbook prepared by NASA Goddard.
5. Subbaragudu, J. 1979. "Heat Capacity Mapping Mission (HCMM) Validation Study". Systems and Applied Sciences Corporation Report #R-SAG-3/79-01 to NASA Goddard.
6. Schott, J. R. and Schimminger, E. W. 1981. "Data Use Investigations For Applications Explorer Mission A (HCMM)". CAL #6175-M-1, NASA Accession #E81-10079.
7. Schott, J. R. 1979. "Temperature Measurement of Cooling Water Discharged from Power Plants". Photogrammetric Engineering and Remote Sensing, Vol. 45, NO6.

ATMOSPHERIC TRANSMITTANCE VS. ALTITUDE FROM MODIFIED
 LOWTRAN 5A CODE RADIOSONDE DATA 13 SEPTEMBER 1982



ATMOSPHERIC PATH RADIANCE VS. ALTITUDE FROM MODIFIED
 LOWTRAN 5A CODE RADIOSONDE DATA 13 SEPTEMBER 1982

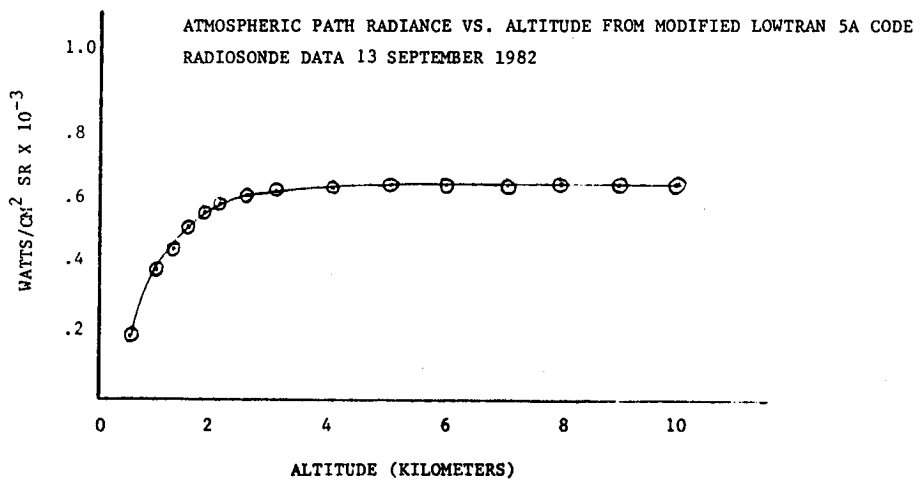


FIGURE 1. PREDICTED TRANSMISSION AND PATH RADIANCE VALUES FROM LOWTRAN CODE

THERMAL BAND CHARACTERIZATION OF LANDSAT-4 THEMATIC MAPPER

JACK C. LANSING
SANTA BARBARA RESEARCH CENTER

JOHN L. BARKER
NASA/GODDARD SPACE FLIGHT CENTER

OBSERVATIONS WITH TIME

A quick-look monitor in the spacecraft control center was used to measure the Thematic Mapper (TM) Band 6 shutter background and the 34.7°C internal blackbody signal on over 50 dates. Variability of the shutter background temperature varied from 7°C to 11°C. The digital counts of the calibration data were measured for ten specific images, and the average pulse value of the blackbody peak, Q_{cb} , decreased from 174 to 149 counts while the shutter background counts, Q_{sh} , varied as a function of shutter temperature, T_{sh} , from 77 to 85 [$Q_{sh} = 3.05 T_{sh} (^{\circ}C) + 53.27$]. The net calibration peak, $Q_{cb} - Q_{sh}$, decreased from 95 to 64 between August 22nd and December 20th. Relative internal gains between the four channels were calculated and compared to prelaunch values; they showed changes over 9 months of up to 5%, while 512 x 512 subsections of the original 10 daytime scenes showed scene counts, Q_{sc} , that ranged from 135 down to 62. This included a range of standard deviations from as low as ± 0.5 for a pure water scene off Boston to as high as ± 4.1 for an August 22nd scene over Arkansas.

IMAGE DESTRIPIING

Frequency histograms of numbers of pixels versus digital counts from a night scene of the Buffalo area of 22 August 1982 were used to determine channel gain relative to the mean and to discern a systematic along-scan pattern in a difference between forward and reverse scan counts of up to 0.5.

These results were used to produce a corrected digital image which, in turn, exposed minor adjustments necessary to further correct the channel gains and offsets. Individual gains and offsets were calculate for the four channels; the final values may be used to produce a destriped image of Band 6.

AT-SATELLITE RADIANCE

An illustrative thermal band radiometric calibration graph was produced to relate known spectral radiance to digital counts. Calibration lines were calculated for initial turn-on of the cold focal plane in August through the 40% gain loss in Band 6 over 5 months until outgassing of the cooler in early January, when the gain was restored to its original value.

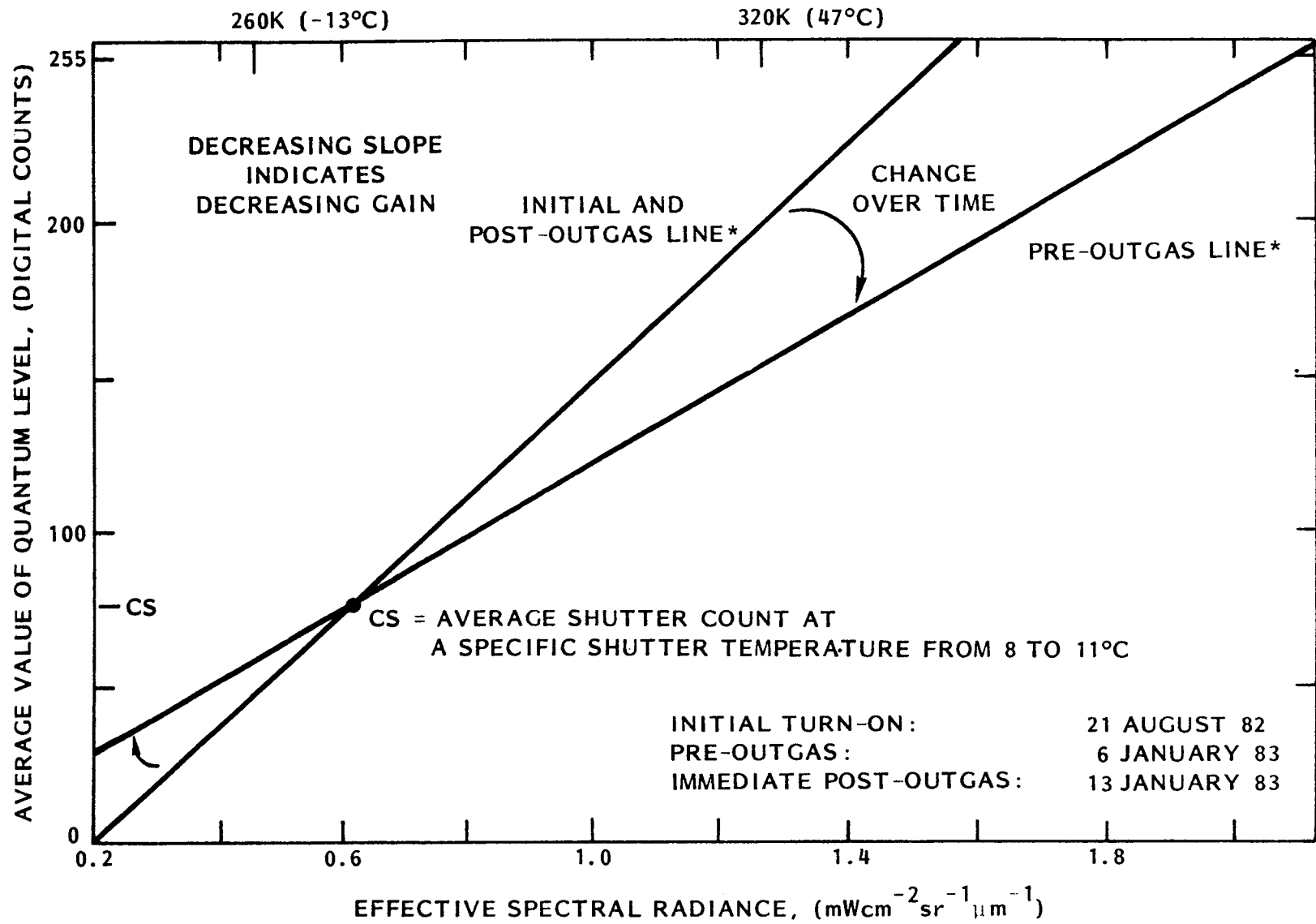
The specified range of 260K to 320K corresponds to a range of approximately 50 to 195 counts, which is centered in the 0 to 255 counts available.

NOISE EQUIVALENT TEMPERATURE

An area of 600 120m pixels in Lake Erie was used to calculate noise equivalent temperature difference, which was 0.10K at 300K, neglecting the forward to reverse scan difference.

TARGET TEMPERATURE AFTER ATMOSPHERIC CORRECTION

The calibration data and the Buffalo scene, with the corrections mentioned and estimates of the atmospheric transmission and radiance, were used to make a temperature estimate for an area of Lake Erie of 21⁰C to 27⁰C. Local records of the temperature showed 21⁰C.



Thermal Band Gain Change with Time

A PRELIMINARY ASSESSMENT OF LANDSAT-4
THEMATIC MAPPER DATA

D. G. GOODENOUGH, E. A. FLEMING, K. DICKINSON
DEPARTMENT OF ENERGY, MINES AND RESOURCES, CANADA

The results of a preliminary assessment of both raw and NASA-processed Thematic Mapper (TM) data will be discussed.

Geometric correction of NASA-processed TM data has been carried out. Correction was possible to within 3 pixels in the along track direction and 2 pixels in the across track direction.

A preliminary evaluation of TM imagery provided by the NASA LANDSAT Assessment System for geometric accuracy and map information content has been carried out on samples of imagery. The initial indications were that bands 3, 5 and 7 contain the most useful cartographic information. The resolution of rural and urban detail as well as the fit to plotted map detail was found to be improved over LANDSAT MSS, and such images may provide adequate revision information for 1:250,000 maps in areas where it is not currently profitable to use LANDSAT MSS.

As part of a study of the radiometric correction of TM data, the relative gains and offsets for each detector in each band of raw data were calculated. This was done for different subscenes as well as a full scene and the variation of the results with direction of scan and position of subscene were studied.

REVISED RADIOMETRIC CALIBRATION TECHNIQUE FOR LANDSAT-4
THEMATIC MAPPER DATA BY THE CANADA CENTRE FOR
REMOTE SENSING

J. MURPHY, T. BUTLIN, P. DUFF AND A. FITZGERALD
CANADA CENTRE FOR REMOTE SENSING

KEYWORDS: Remote Sensing, Landsat-4, Thematic Mapper, Radiometric
Calibration

INTRODUCTION

A technique for the radiometric correction of LANDSAT-4 Thematic Mapper (TM) data was proposed by the Canada Centre for Remote Sensing (CCRS) in 1982, and two reports defining the method and discussing preliminary results were presented by CCRS at the LANDSAT-4 Scientific Characterization Early Results Symposium. Subsequent detailed observations of raw image data, raw radiometric calibration data and background measurements extracted from the raw data stream on High Density Tape have highlighted in the proposed method, major shortcomings, which if left uncorrected, can cause severe radiometric striping in the output product. Results presented here correlate measurements of the DC background with variations in both image data background and calibration samples. The effect on both raw data and on data corrected using the earlier proposed technique is explained, and the correction required for these factors as a function of individual scan line number for each detector is described. It is shown how the revised technique can be incorporated into an operational environment.

RADIOMETRIC CORRECTION OVERVIEW

The radiometric correction method has three separate steps.

- i) For a reference detector in each spectral band, the corrections required to place the data from this detector on an absolute scale are calculated, using in-flight calibration data.

- ii) The relative differences between all other detectors in each band and the reference detector are calculated, using the means and standard deviations of the raw data values, which are derived from the raw data histograms. In order to ensure that the histograms correspond only to pixels with radiance values for which the response of each detector is linear, all those pixels which saturate any one detector within a band are removed from the histogram of each detector within that band.

- iii) Absolute and relative corrections are combined, to give absolute gains and offsets for all detectors of all bands.

RAW DATA OBSERVATIONS

Calibration Data Extraction

The absolute calibration procedure using in-flight calibration data relies on extracting and averaging calibration pulses from within the raw data stream, for each detector, for each scan line in turn. The internal calibration steps through eight unique calibration states, with approximately 40 consecutive scans at each level, as shown in Figure 1. An average digital number (DN) for each of the eight states (after ignoring overshoot, warm-up time and cool-down time), is then combined with the corresponding prelaunch DN and radiance level.

Calibration Data Variability

Detailed observations of averaged calibration pulse values within the stable area of each calibration state have shown variations of magnitudes from one to four DN from line to line for the same detector, which are uncorrelated with scan direction. Moreover, it has been observed that for many detectors, the averaged calibration pulse values are quantized into either the high or low extremes of the range of variability, rather than being randomly distributed throughout the range. This is exemplified in Figure 4 for detector 4 of band 1.

Image Data Variability

Using a scene (Path 48, Row 28, November 11, 1982) consisting of only a large water body with nominally very small scene content variability from scan line to scan line, an estimate of the variation of detector response both within one spectral band and from swath to swath was obtained. This was achieved by selecting a strip 100 pixels wide by 320 swaths long, and by plotting the average of each of these 100 pixels as a function of scan line number.

Detailed observations have shown, in addition to the 16-line periodicity, due to differences in absolute calibration of each of the 16 detectors, variations of magnitudes from one to four DN for those lines corresponding to particular detectors. As is the case with the calibration data, the variations are uncorrelated with scan direction, and show the same quantization effects. This is exemplified in Figure 3, Plot 1, for detector 4 of band 1.

(This detector has been chosen for illustrative purposes only. At least seven other detectors in the reflective bands have shown similar quantization effects, and many others have shown random variations of approximately 2 DN).

Background Level Observations

In order to define the procedure for extracting calibration pulse averages and for estimating DC reference levels, the raw data stream from the end of one scan line to the start of the next scan line was investigated in detail. Sample plots were marked up with the nominal locations of calibration pulse centre, and with three nominal regions characterizing the background level, one before DC restore (BDC), one during DC restore (DDC), and one after DC restore (ADC).

Observations of the BDC values revealed very close correlation with the observed image data background level for the scan line immediately preceding the background level measurement. This is exemplified for detector 4, of band 1 in Figure 3, Plot 2.

A similar high correlation was observed between the appropriate DC (ADC for forward scans, and BDC for reverse scans) measurement for the calibration pulses. This is exemplified for detector 4 of band 1 in Figure 4.

However, there was no correlation between ADC of the previous line and the observed image data background level at the start of the next scan line. Plots of BDC, DDC and ADC as a function of line number show that there is little change in DC level during this entire region. The example shown in Figure 2 for detector 4 of band 1 indicates the change in DC level, for each scan line independently, by connecting with straight lines the BDC, DDC and ADC measurements appropriate to that line. The discontinuity between the background level measurement immediately prior to the start of scan line N (ADC from scan line N-1) and the background level measurement immediately after scan line N (BDC for scan line N) is clearly evident.

DEFICIENCIES IN THE EARLIER PROPOSED TECHNIQUE

The effects on TM data radiometrically corrected using the earlier proposed technique will be three-fold. Firstly, the variations in calibration samples will decrease the accuracy of the absolute calibration of the reference detector. Secondly, the random variations in background reference level within a scene for some detectors means that the detector responses cannot be characterized by a fixed, scene-dependent, gain and offset. Relative gains and offsets calculated from raw data histograms will therefore be inaccurate. Thirdly, the application of a fixed gain and offset over an entire scene will not remove the observed background variations of up to 4 DN which occur randomly from line to line throughout the scene.

REVISED OPERATIONAL PROCEDURE

Revisions to the earlier proposed technique are therefore required.

- i) The in-flight calibration data will be accumulated for the reference detector, but the relevant line-by-line background level measurement (corresponding to BDC or ADC) will be subtracted before including it in the calibration state average.

- ii) The sums and sums of squares of the raw data will be accumulated for a full scene, as follows. However, histograms will be accumulated a swath at a time, such that any saturated values can be removed. A background level, corresponding to BDC, will be subtracted from the truncated histogram before the sums and sums of squares are accumulated.
- iii) The absolute and relative correction parameters will be combined to yield scene-dependent absolute gains and offsets for all detectors.
- iv) The data will be calibrated line by line, by applying offsets and gains to each pixel in turn. However, the scene-dependent offset must first be modified by the line-dependent offset, corresponding to BDC, before being subtracted from the raw data value.

If pixel-dependent corrections are required, these will be calculated and applied before modifying each pixel in the line by the scene-dependent gain.

All these operations can be conveniently performed in floating-point notation before geometric correction and conversion to the final 8-bit form.

CONCLUSION

Detailed observations of background reference levels have shown that line-dependent variations in raw TM image data and in the associated calibration data can be measured and corrected within an operational environment, by applying simple offset corrections on a line-by-line basis. The radiometric calibration procedure defined by CCRS has been revised accordingly.

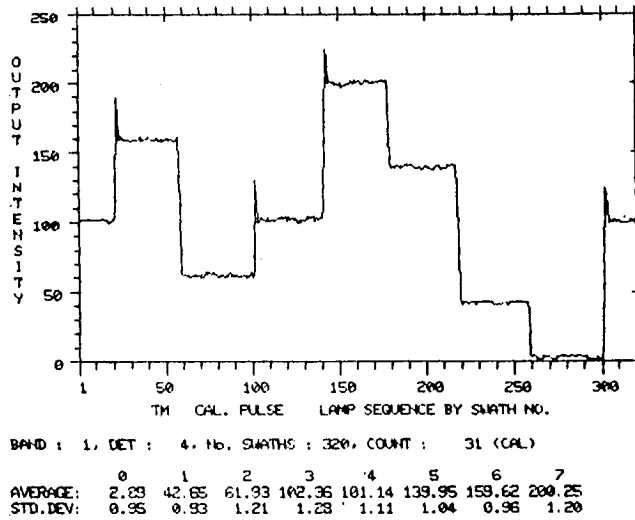
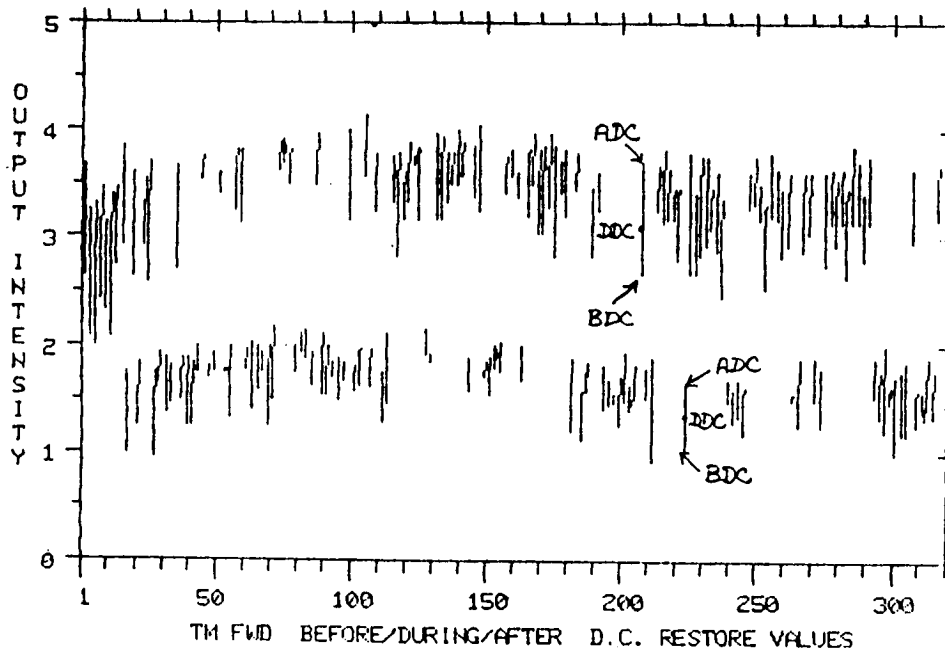


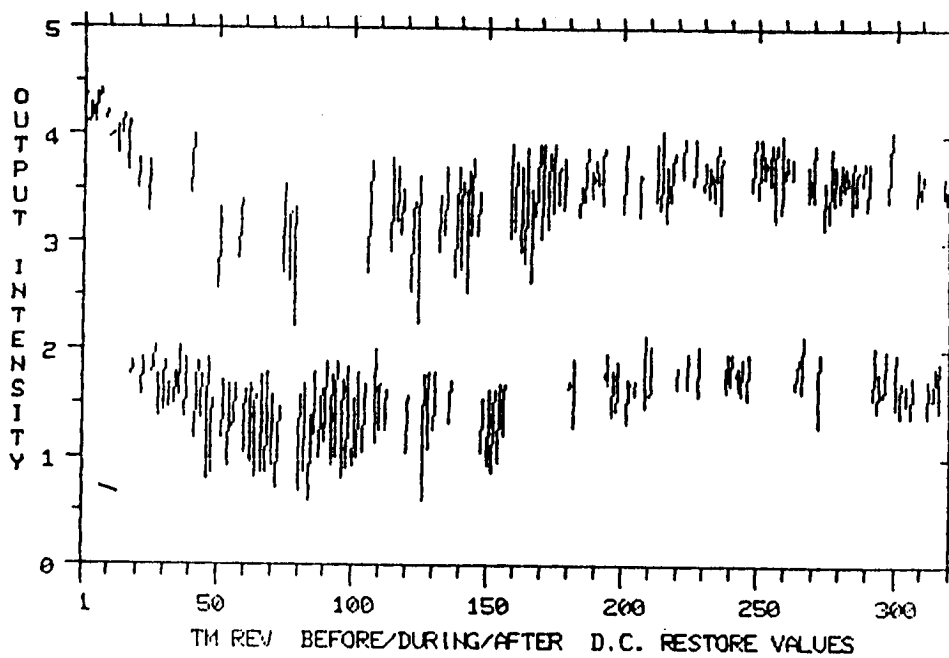
FIGURE 1
 REPRESENTATIVE CALIBRATION LAMP STATE SEQUENCE
 FOR DETECTOR 4 OF BAND 1



BAND	DET	NO. SWATHS	COUNTS		
			BDC	DDC	ADC
1	4	320	24	100	28

FORWARD

Forward Scans Only



BAND	DET	NO. SWATHS	COUNTS		
			BDC	DDC	ADC
1	4	320	28	100	24

REVERSE

Reverse Scans Only

FIGURE 2

PLOTS OF BDC, DDC AND ADC AS A FUNCTION OF LINE NUMBER
FOR DETECTOR 4 OF BAND 1

TM IMAGE-MEAN AND D.C. RESTORE VARIATION

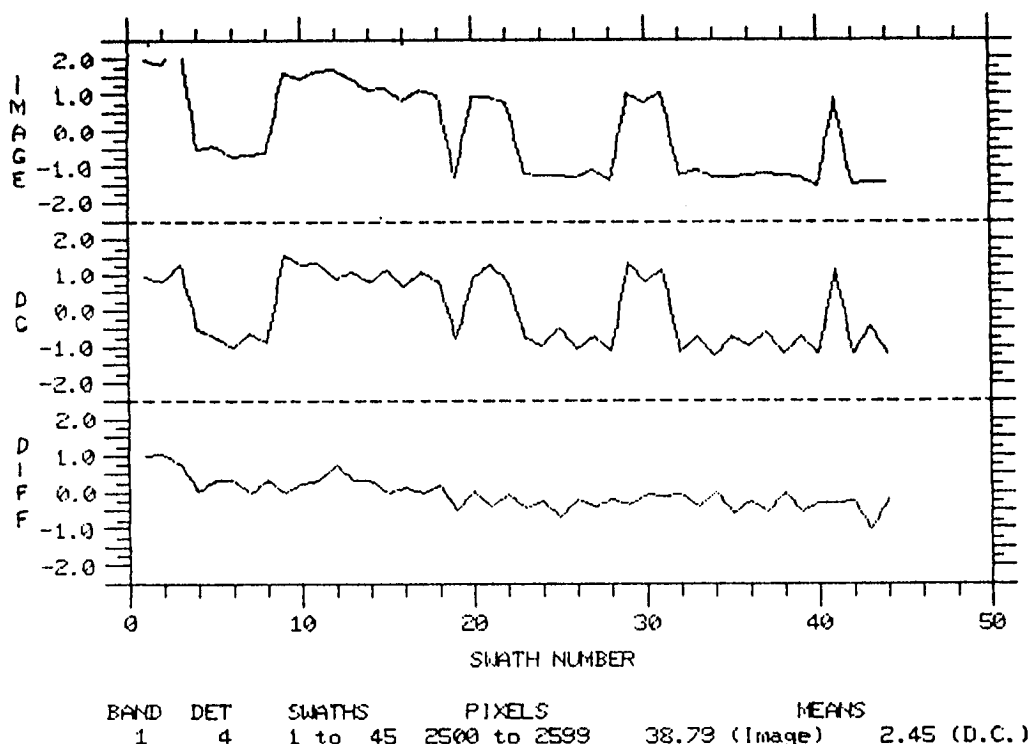


FIGURE 3

Variations in image data background level as a function of scan line number for detector 4 of band 1.

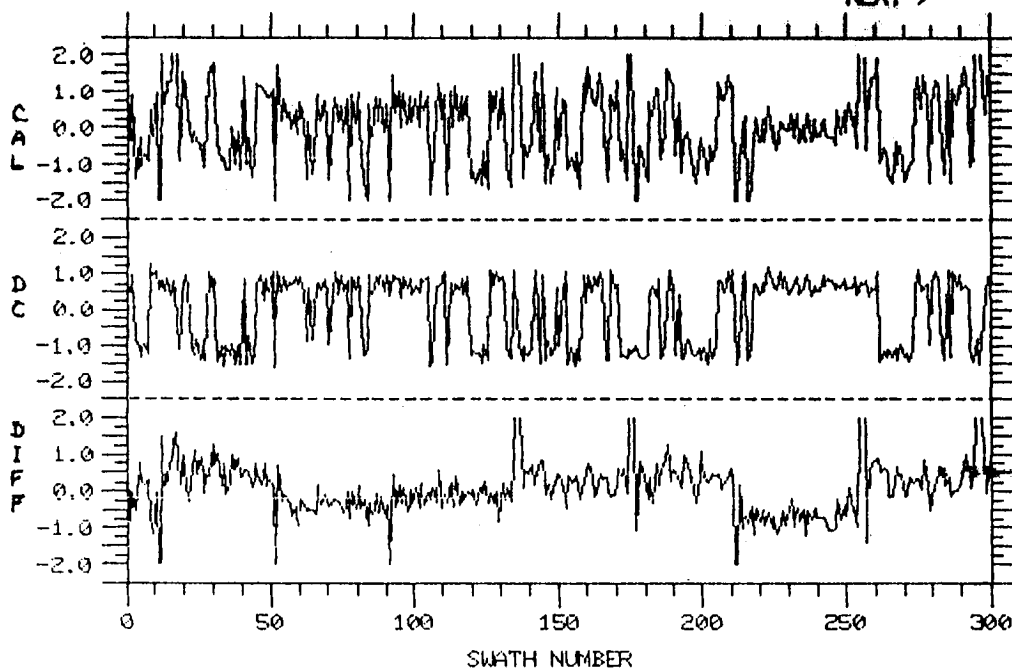
Plot 1 shows changes in raw image data background level (RAW) represented as a deviation from the mean value averaged over all 320 scans.

Plot 2 shows changes in DC reference level before DC restore (BDC).

Plot 3 shows changes in RAW after BDC has been subtracted.

TM CALIBRATION AND D.C. RESTORE VARIATION

NEXT >



BAND	DET	No. SWATHS	COUNTS
1	4	300	31 (CAL), 28 (D.C.)

FIGURE 4

Variations in averaged calibration pulse values as a function of scan line number for detector 4 of band 1. Plot 1 shows changes in averaged calibration pulse values (CALSAM) represented as a deviation from the mean value for the appropriate calibration state average. Plot 2 shows changes in DC reference level using ADC for forward scans and BDC for reverse scans. Plot 3 shows changes in CALSAM after BDC (or ADC) has been subtracted.

A PRELIMINARY ANALYSIS OF LANDSAT-4 THEMATIC
MAPPER RADIOMETRIC PERFORMANCE

C. JUSTICE AND L. FUSCO
EUROPEAN SPACE AGENCY/EARTHNET PROGRAMME OFFICE

W. MEHL
COMMISSION OF THE EUROPEAN COMMUNITIES/JOINT RESEARCH CENTRE

INTRODUCTION

Analysis was performed to characterize the radiometry of three Thematic Mapper (TM) digital products of a scene acquired on August 22, 1982 of Arkansas, USA (Track 23, Frame 35). The three digital products examined were the NASA raw (BT) product, the radiometrically corrected (AT) product and the radiometrically and geometrically corrected (PT) product. The scene was one of the first seven band images made available for analysis as part of the Landsat Image Data Quality Assessment (LIDQA) program. The objective of the analysis was to examine the frequency distribution of the digital data; the statistical correlation between the bands; and the variability between the detectors within a band. The analyses were performed on a series of image subsets from the full scene. The results presented in this paper are from one 1024 x 1024 pixel subset of Reelfoot Lake, Tennessee which displayed a representative range of ground conditions and cover types occurring within the full frame image. Bands 1, 2 and 5 of the sample area are presented as Figure 1, 2, and 3 respectively. The subsets were extracted from the three digital data products to cover the same geographic area. The following analysis was undertaken within the first few weeks of obtaining the TM data and provides the first step towards a full appraisal of the TM radiometry being performed as part of the ESA/CEC contribution to the NASA/LIDQA program.

1. Report No. NASA CP-2326		2. Government Accession No.		3. Recipient's Catalog No.	
4. Title and Subtitle LANDSAT-4 SCIENCE INVESTIGATIONS SUMMARY Including December 1983 Workshop Results VOLUME I				5. Report Date July 1984	
				6. Performing Organization Code 923	
7. Author(s) John Barker, Editor				8. Performing Organization Report No.	
9. Performing Organization Name and Address NASA Goddard Space Flight Center Greenbelt, Maryland 20771				10. Work Unit No.	
				11. Contract or Grant No. NAS5-28033	
12. Sponsoring Agency Name and Address National Aeronautics and Space Administration Washington, D.C. 20546				13. Type of Report and Period Covered Conference Publication	
				14. Sponsoring Agency Code	
15. Supplementary Notes					
16. Abstract This document presents a series of brief summaries of the results of individual investigations of Landsat-4 image data characteristics. The results were reported at the Landsat-4 Early Results Symposium, February 1983, and at the Landsat Science Characterization Workshop held in December 1983.					
17. Key Words (Suggested by Author(s)) Landsat-4, imagery, results, radiometry, geometry, remote sensing, Multispectral Scanner, Thematic Mapper, applications			18. Distribution Statement Unclassified-Unlimited STAR Category 42		
19. Security Classif. (of this report) Unclassified		20. Security Classif. (of this page) Unclassified		21. No. of Pages 212	22. Price A10

National Aeronautics and
Space Administration

SPECIAL FOURTH CLASS MAIL
BOOK

Postage and Fees Paid
National Aeronautics and
Space Administration
NASA-451



Washington, D.C.
20546

Official Business
Penalty for Private Use, \$300

NASA

POSTMASTER: If Undeliverable (Section 158
Postal Manual) Do Not Return
